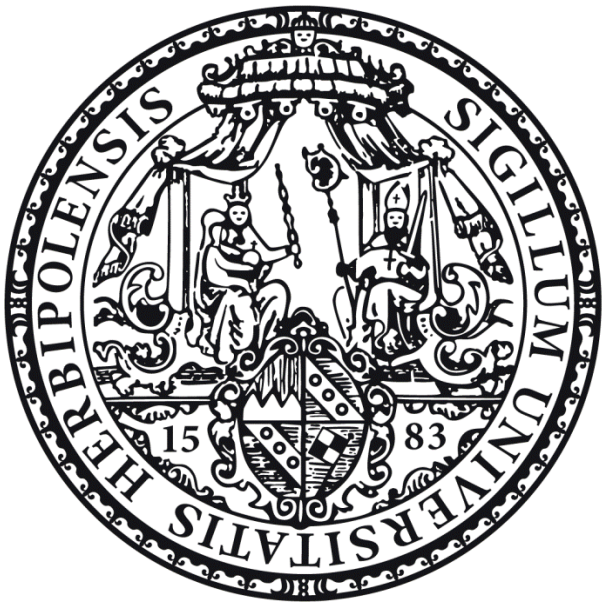

Determination of the hypertrophic potential of Oncostatin M on rat cardiac cells and the characterisation of the receptor complexes utilised by rat Oncostatin M

Erforschung des hypertrophen Potentials von Oncostatin M auf Ratten-Herzzellen und die Charakterisierung der Rezeptorkomplexe, welche von Ratten-Oncostatin M genutzt werden

Doctoral thesis for a doctoral degree
at the Graduate School of Life Sciences,
Julius-Maximilians-Universität Würzburg,
Section Biomedicine

submitted by

Johannes Drechsler

from

Würzburg

Würzburg, September 2012

Submitted on: 11th September 2012

Members of the *Promotionskomitee*:

Chairperson: Prof. Dr. Thomas Müller

Primary Supervisor: PD Dr. Heike Hermanns

Supervisor (Second): Prof. Dr. Stefan Engelhardt

Supervisor (Third): Prof. Dr. Manfred Lutz

Date of Public Defence: ……

Date of receipt of Certificates: ……

For my parents

A man who dares to waste one hour of life has not discovered the value of life. – Charles R. Darwin

Table of Contents

Table of Contents

Index of Abbreviations

A	Absorbance
ADP	Adenosine diphosphate
Akt	Protein kinase B (PKB)
Amp^R	Ampicillin resistance
Approx.	Approximately
APS	Ammonium persulfate
ATP	Adenosine triphosphate
BSA	Bovine serum albumin
°C	Degree Celsius
CBM	Cytokine binding module
CD	Cluster of differentiation
C/EBP	CCAAT/enhancer binding protein
CIS	Cytokine inducible SH2 domain containing protein
CLC	Cardiotrophin-like cytokine
cm	Centimetre
CNTF	Ciliary neurotrophic factor
CT-1	Cardiotrophin-1
DAPI	4´,6-Diamidino-2-phenylindole
DMEM	Dulbecco's Modified Eagle Medium
DMSO	Dimethyl sulfoxide
DNA	Deoxyribonucleic acid
dNTP	Deoxyribonucleotide triphosphate
E. coli	*Escherichia coli*
ECL	Enhanced chemiluminescence
EDTA	Ethylenediaminetetraacetic acid
ELISA	Enzyme linked immunosorbent assay
ERK	Extracellular signal regulated kinase
FDU	FastDigest unit
FCS	Fetal calf serum (also called fetal bovine serum, FBS)
FERM	Four-point-one protein, ezrin, radixin and moesin
for	Forward
GAPDH	Glyceraldehyde 3-phosphate dehydrogenase
GDP	Guanosine diphosphate
gp	Glycoprotein
GTP	Guanosine triphosphate
h	Hour
h*	Human
Hepes	4-(2-hydroxyethyl)-1-piperazineethanesulfonic acid
HPRT	Hypoxanthine phosphoribosyl-transferase
HRP	Horseradish peroxidase

Hyg^R	Hygromycin resistance
IFN	Interferon
Ig	Immunoglobulin
IL	Interleukin
JAK	Janus kinase
JH	Janus homology domain
kDa	Kilodalton
KIR	Kinase inhibitory region
l	Litre
LB	Lysogeny broth
LIF	Leukaemia inhibitory factor
LPS	Lipopolysaccharide
M	Molar
m*	Murine
MAPK	Mitogen-activated protein kinase
MAP2K	Mitogen-activated protein kinase kinase
MAP3K	Mitogen-activated protein kinase kinase kinase
MEK/MKK	MAP/ERK kinase
mg	Milligram
µg	Microgram
min	Minute
ml	Millilitre
µl	Microlitre
mM	Millimolar
µM	Micromolar
mm	Millimetre
µm	Micrometre
MMP	Matrix metalloproteinase
mRNA	Messenger ribonucleic acid
Neo^R	Neomycin resistance
nM	Nanomolar
nm	Nanometre
NRCM	Neonatal rat cardiomyocytes
NRCFB	Neonatal rat cardiofibroblasts
OSM	Oncostatin M
P	Cell passage number
PAA	Polyacrylamide
PAGE	Polyacrylamide gel electrophoresis
PAMP	Pathogen associated molecular pattern
PBS	Phosphate buffered saline
PCR	Polymerase chain reaction
PE	Phenylephrine
PIAS	Protein inhibitor of activated STATs
PKC	Proteinkinase C
PMSF	Phenylmethylsulfonyl fluoride

Index of Abbreviations

pY	Phospho-tyrosine
R	Receptor
r*	Rat
rcf	Relative centrifugal force
rev	Reverse
rpm	Revolutions per minute
RT	Room temperature
RT-PCR	Reverse transcription PCR
SDS	Sodium dodecyl sulfate
SDS-PAGE	Sodium dodecyl sulfate polyacrylamide gel electrophoresis
sec	Second
SEM	Standard error of mean
SH	Src homology domain
Shc	SH2 and collagen homology domain containing protein
SHP	SH2 domain containing tyrosine phosphatase
siRNA	Small interferring RNA
SOCS	Suppressor of cytokine signalling
SOS	Son of sevenless
STAT	Signal transducer and activator of transcription
TEMED	Tetramethylethylenediamine
TF	Transcription factor
TNF	Tumor necrosis factors
Tris	Tris(hydroxymethyl)aminomethane
U	Unit
UV	Ultraviolet

* Letter in front of a gene, mRNA, oligonucleotide or protein defining the species.

1 Introduction

1.1 The IL-6-type cytokine family and their appending receptor complexes

The family of interleukin-6 (IL-6)-type cytokines represents a group of pleiotropic cytokines which share a similar four α-helix bundle architecture[1]. At present nine members of the family are known: IL-6 itself, IL-11, leukaemia inhibitory factor (LIF), oncostatin M (OSM), ciliary neurotrophic factor (CNTF), cardiotrophin-1 (CT-1), cardiotrophin-like cytokine (CLC), IL-27 (consisting of p28 and EBI-3) and neuropoietin (NP)[1-4]. In addition to the comparable structure of these polypeptides, organised in a bundle consisting of four helices linked with flexible loops, they share the common property to bind to glycoprotein 130 (gp130) serving as receptor subunit. IL-6-type cytokines play important roles in inflammation and the acute phase response[5-10]. However, they also contribute to various biological processes including cardiovascular remodelling, neuronal differentiation, haematopoiesis, cell differentiation and proliferation[11]. Recently IL-35, that consists of p35 and EBI-3, was found to bind to gp130-IL-12Rβ2 receptor complexes[12]. Therefore, the cytokine fulfils the criteria to be added to the family of IL-6-type cytokines.

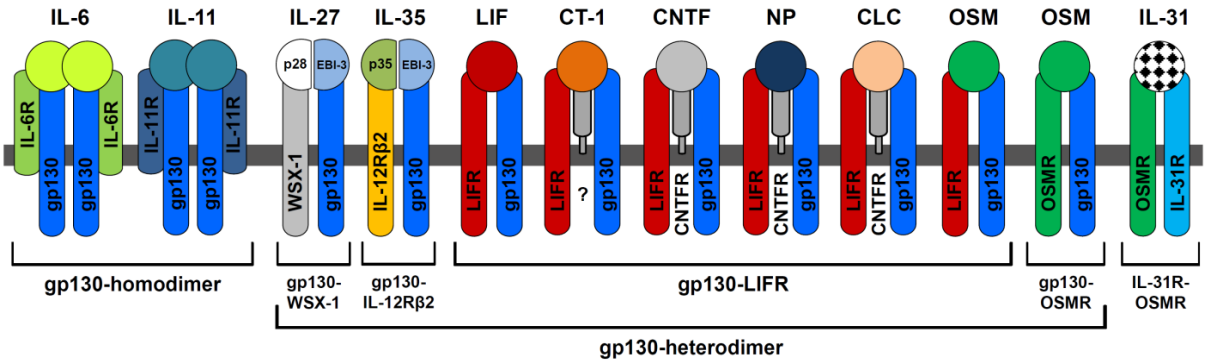

Figure 1: The IL-6-type cytokine family and its receptor complexes

IL-6-type cytokines signal via gp130 homo- or heterodimers. IL-6 and IL-11 use IL-6R/gp130 and IL-11R/gp130 receptor complexes, respectively, for their signalling. Structural data propose hexameric complexes for these two cytokines bound to their receptors. IL-27 utilises a gp130/WSX-1 heterodimer for signalling. IL-35 signals via binding of gp130/IL-12Rβ2 complexes. LIF, CT-1, CNTF, NP, CLC and OSM signal through gp130/LIFR-heterodimers. The CNTFR (α-receptor for CNTF, NP and CLC) is a non-signalling receptor chain lacking intracellular domains. Human OSM can additionally bind to gp130/OSMR receptor complexes. The OSMR connects the IL-6-type cytokine family to the closely related cytokine IL-31, that signals through OSMR/IL-31R heterodimeric receptor complexes.

Due to the heterodimeric organisation of the cytokines, IL-27 and IL-35 appear to mark evolutionary bridges between the IL-6 and IL-12 family of cytokines. The IL-6-type cytokine receptors belong to the haematopoietic receptor superfamily. Referring to their architecture, including an extracellular N-terminus and a single transmembrane region, they are further classified as type I membrane receptors[13]. Only the CNTF-receptor (CNTFR) does not fulfil this criterion, because it contains a glycosylphosphatidylinositol anchor instead of the transmembrane domain[14].

The initialisation step of a target cell signalling cascade, by which cytokine signals are transduced from the extra- to the intracellular compartments, is the cytokine binding to its receptors. Receptors can directly participate in this signalling process or only be involved in the cytokine binding. Therefore, the IL-6-type cytokine receptors can be classified into non-signalling receptors (IL-6R(α), IL-11R(α) and CNTFR(α)) and the signal-transducing receptor subunits (gp130, LIFR, OSMR, WSX-1 and IL-12Rβ2)[11, 12, 15] (Fig. 1). Initially gp130 was thought to serve exclusively as signalling receptor for IL-6 mediated signalling[16]. Only later it became evident, that this receptor functions as a common signalling receptor to many cytokines. Physiologically active cytokine/receptor complexes appear to function as trimers, tetramers or hexamers. After low affinity binding of IL-6 to its α-receptor, the IL-6Rα, the resulting IL-6/IL-6R complex binds to gp130 with high affinity. This interaction causes dimerisation of two gp130 molecules resulting in a hexameric complex containing two molecules each of gp130, IL-6R and IL-6[16-20]. IL-11 is believed to function in an analogous fashion also resulting in a hexameric receptor complex[21, 22]. For both cytokines the α-receptors are not directly involved in the signal transduction. In contrast to IL-6 and IL-11, LIF and OSM utilise signalling receptor heterodimers, in which one of the signalling chains is represented through gp130. LIF first binds to the LIFR(α) with low nanomolar affinity, but no signalling occurs until binding of the initial LIF/LIFR complex to gp130[23-25]. Human OSM that is very closely related to LIF also binds the LIFR to form OSM/LIFR/gp130 complexes. But in contrast to LIF the cytokine additionally uses OSMR/gp130 heterodimers to induce its signalling cascades. Unlike the LIF/LIFR interactions, OSM first binds to gp130 and the resulting OSM-gp130 complex subsequently interacts with the LIFR or the OSMR. The gp130/LIFR(β) complex is classified as type I receptor complex and the gp130/OSMR(β) complex is called type II receptor complex[26, 27]. In this scenario both receptor subunits are able to initiate signalling cascades, provided OSMR and LIFR proteins were actually

expressed in a particular human cell type. CNTF, CLC and NP bind to yet another α-receptor, the CNTF-receptor (CNTFR), although signalling occurs via LIFR/gp130 heterodimers[14, 28]. However, it was shown recently that the NP induced STAT3 activation occurs independent of LIFR phosphorylation[29]. For CT-1 that also binds to LIFR/gp130 heterodimers[30], a specific α-receptor subunit was proposed several years ago[31], but no concrete evidence for the existence of the receptor was found until now. IL-27 uses a heterodimer consisting of gp130 and the specific receptor WSX-1 for inducing its signalling[32]. IL-31, that is closely related to the IL-6-type cytokine family and sometimes even included into this family, binds to heterodimers of the specific IL-31-receptor (IL-31R) and the OSMR[33, 34].

Interactions of the cytokines with their cognate receptors appear to follow a similar pattern which was first determined for the IL-6 receptor complex. The binding of IL-6-type cytokines to their receptors is mainly achieved through interaction of the cytokine with the cytokine-binding module (CBM) of the receptor. The presence of this 200 amino acid encompassing motif defines IL-6-type cytokine receptors as class I cytokine receptors. The CBM is characterised by an N-terminal domain of 100 amino acids including four conserved cysteine residues and a C-terminal domain containing a specific WSXWS motif[35]. Structurally, both domains of the CBM can be characterised as FnIII (fibronectin type III)-like domains. Each of the IL-6-type cytokine receptors contains at least one CBM. With exception of WSX-1, IL-12Rβ2 and IL-31R, an additional immunoglobulin (Ig)-like domain is found in all IL-6 family receptors which is located N-terminally to the membrane-proximal CBM. In sharp contrast to the non-signalling receptors, the signalling receptors possess three additional FnIII-like domains located C-terminally of the membrane-proximal CBM[1]. For some IL-6-type cytokines the exact molecular binding mechanisms to their cognate receptors were determined within the last two decades. Various mutagenesis studies and binding assays identified the interfaces on the surface of the IL-6-type cytokines and receptors. For the cytokines these are characterised as site I, site II and site III and are the hot spots for the receptor interaction. The site II of all IL-6-type cytokines, except IL-27, interacts with the CBM of gp130. The second signalling receptor (e.g. gp130, LIFR, OSMR) is interacting with site III of the cytokine via its Ig-like domain[1, 36-40]. The CBM of the non-signalling receptor (e.g. IL-6R) binds to the site I of the cytokine[1]. However, the heterodimeric cytokine IL-27 (composed of

p28 and EBI-3) uses its site III for gp130 interaction and site II for WSX-1 binding. The site I of p28 is important for interaction with EBI-3[41, 42].

1.2 Receptor and cross-species specificity of OSM and LIF

OSM was initially described as an IL-6-type cytokine able to inhibit the growth of melanoma cells[43]. Studies within the last decade, however, have shown that OSM has pleiotropic properties. The cytokine plays important roles in haematopoietic progenitor cell homeostasis[44, 45], extrathymic T cell development[46, 47], suppression of fetal liver haematopoiesis[48, 49], liver development[50, 51] and regeneration[52], angiogenesis[53] and most notably in inflammatory processes. Various articles describe elevated levels of human OSM during arthritis, psoriasis and atherosclerosis[54-58]. Moreover, OSM is capable of inducing inflammatory genes like chemokines[59-63] or P-selectin[64]. The human polypeptide is mainly produced by activated macrophages, dendritic cells, neutrophils and T-cells[43, 58, 65, 66]. The translated, unprocessed protein is a 252 amino acid long precursor[67]. The highest bioactivity of the protein is found after cleavage of an N-terminal 25 amino acid signal peptide and the last 32 amino acids of the C-terminus[68].

During the last two decades the human (hOSM), bovine (bOSM), murine (mOSM) and rat OSM (rOSM) orthologs have been cloned[51, 69, 70]. Comparison of the gene organisation of OSM with that of IL-6, LIF and granulocyte-colony stimulatory factor indicates evolutionary relation and descent from a common ancestral gene[71]. In the human, the bovine as well as the rodent system the genes encoding OSM and LIF are located on the same chromosome as a tight tandem possibly resulting from a gene duplication[72]. Until today only the murine and the human OSM receptor complexes have been characterised. Interestingly and in contrast to other IL-6-type cytokines the composition of the receptor systems for OSM are different in man and mouse. Human OSM is able to bind and signal via two receptor complexes: the type I receptor complex (LIFR/gp130 heterodimer) and the type II receptor complex (OSMR/gp130 heterodimer)[26, 27, 73]. This is in sharp contrast to murine OSM which only signals via the type II OSMR/gp130 receptor complex, since it lacks high affinity binding sites for the LIFR[74, 75]. Thus, *in vivo* studies using mice cannot correctly address the physiological response to human OSM. Further information was gained by studies treating human and murine cells with OSM originating from both species.

Thereby it was found that hOSM is able to efficiently induce signalling in murine cells, but it exclusively activates the murine LIFR/gp130 (type I) complex[74, 75]. Hence, reconstitution studies using human OSM in mouse models of human diseases only mimic the actions of LIF, because no OSMR signalling is involved. On the other hand, mOSM is not capable of stimulating human cells, a characteristic shared by many other IL-6-type cytokines[74].

Comparable to OSM, LIF is a pleiotropic cytokine expressed by embryonic stem cells, megakaryocytes, osteoblasts and neuronal cells[76]. The LIF-LIFR system is identical in both mouse and man[23-25]. Human and mouse LIFR share 76% amino acid identity, while human and murine LIF contain 78% identical amino acids. Despite this high degree of homology species specific signalling characteristics can be observed. Binding and signalling activity of mouse LIF is highly restricted, since it cannot stimulate human cells. Human LIF, on the other hand, is capable of binding the human and the murine LIFR/gp130 complex with high affinity[36]. Impressively, human LIF binds to the foreign mouse LIFR with a 100-500-fold higher affinity than murine LIF itself[36].

1.3 Cell-type specific expression of IL-6 family receptors and trans-signalling

While the common IL-6-type cytokine signalling receptor subunit, gp130, is ubiquitously expressed on most cell types, the distribution of the other IL-6-type cytokine associated receptors is much more restricted. This allows an adequate cell response and distinct cellular function for most IL-6-type cytokines. However, recently an additional mechanism was identified which allows cells to respond to a specific cytokine in the absence of a membrane-bound alpha-receptor. This mechanism was called ‘trans-signalling’. In contrast to classical signalling which depends on membrane-bound receptors, cells normally devoid of receptor subunits (e.g. the IL-6R) can react to IL-6 molecules in their vicinity when soluble IL-6R is present. The soluble IL-6-receptors (sIL-6R) lack a cytoplasmic and transmembrane part, but the extracellular portion is comparable to their membrane-bound counterparts. These soluble forms can be generated either by alternative splicing or by regulated extracellular proteolysis (shedding) of the membrane-anchored receptor[1, 77-79]. The shedding of the IL-6R is mediated through extracellular metalloproteinases. While

ADAM17 (a disintegrin and a metalloproteinase 17, also known as tumor necrosis factor-α converting enzyme, TACE) mediates induced shedding of the IL-6R, ADAM10 accomplishes constitutive shedding of the receptor[80].

Cells expressing gp130 but no IL-11R can be activated by IL-11 combined with recombinant soluble IL-11R (sIL-11R)[22, 81]. In contrast to sIL-6R, however, no naturally occurring sIL-11R has been detected so far. A soluble form of the CNTFR[82] might be generated by cleaving the glycosylphosphatidylinositol anchor from the peptide part of the receptor. This reaction can be experimentally mediated by addition of phosphatidylinositol specific phospholipase C to astrocytes[83]. Within the last decade also soluble forms of WSX-1[84], gp130[78], OSMR[85] and the LIFR[86, 87] were analysed and characterised. However, while the soluble forms of the non-signalling receptor subunits (IL-6R, IL-11R and CNTFR) act agonistically and allow trans-signalling, the soluble forms of gp130 (sgp130)[78, 88], OSMR[85], LIFR[24, 86] and WSX-1[84] are able to inhibit the actions of receptor-cytokine-complexes (e.g. sIL-6R-IL-6). Furthermore, the correlation between sIL-6R, sgp130 and IL-6 can be understood as a natural buffer system. Therefore, under normal conditions sgp130 might buffer the trans-signalling capacity of sIL-6R and IL-6 within certain ranges. Interestingly, during infections and inflammatory conditions sIL-6R serum levels proportionally increase much stronger than IL-6 serum levels[89, 90]. As only a minor fraction of free IL-6 dimerises with sIL-6R, this effect might actually increase the pool of active IL-6/sIL-6R complexes[91]. Depending on the ratio of sIL-6R and IL-6, the classical IL-6 signalling can be partially inhibited as well, representing a further role of sgp130, as the soluble receptor was previously thought to exclusively antagonise trans-signalling[91].

1.4 IL-6-type cytokine induced signalling pathways

Once the IL-6-type cytokine has bound its receptor subunits (e.g. LIF to LIFR and gp130), the signalling transduction to the intracellular milieu occurs. With exception of IL-27 and IL-35, all other IL-6-type cytokines signal via homo- or heterodimerisation of gp130 with a second gp130, the LIFR or OSMR. Interactions within the cytoplasmic regions of the signal transducing chains induced through the cytokine/receptor complex formation initiate the intracellular signalling cascades. Conformational changes in the receptor chains and the recruitment of additional

cellular proteins (e.g. kinases) are the driving forces that allow all following steps. The most prominent signalling pathway activated by IL-6 type cytokines is the JAK/STAT (Janus kinase/signal transducers and activators of transcription) pathway. The MAPK (mitogen-activated protein kinase) cascade leading to activation of ERK1/2 (extracellular signal-regulated kinase) is the second key pathway. Depending on the cell type, the respective IL-6-type cytokine, concentration of the cytokine and the expression rates of receptor(s), the PI3K (phosphatidylinositol 3-kinase)/Akt (protein kinase B (PKB), encoded by *AKT1*, *AKT2* and *AKT3*) cascade can also be activated[11]. To avoid overshooting cytokine responses it is necessary to inhibit cytokine induced signalling cascades after certain periods of time. To facilitate this inhibition, 'cellular brakes' are transcribed or their activity is induced. Therefore, the SOCS (suppressors of cytokine signalling) and/or the PIAS (protein inhibitors of activated STATs) proteins as well as distinct phosphatases are recruited to disable the signalling machinery.

1.4.1 Activation of the JAK/STAT pathway

Once the IL-6-type cytokine is bound to its receptors, the signalling machinery is started. The first exclusively cytoplasmic proteins that allow signal transduction into the cytosol are tyrosine kinases of the JAK (Janus kinase) family. This step is essential, because the IL-6-type cytokine family receptors are devoid of an intrinsic kinase activity. Unlike receptor tyrosine kinases like the FGFR (fibroblast growth factor receptor) or insulin receptors, they need the support of additional kinases for the phosphorylation of distinct amino acid residues. In mammalians there are four members of the JAK proteins known: JAK1, JAK2, TYK2 ((non-receptor) tyrosine-protein kinase 2) and JAK3[92-95] with molecular weights between 120 to 140 kDa. JAK1, JAK2 and TYK2 are ubiquitously expressed and all JAK members show an extraordinary homology. JAK3 is mainly expressed in haematopoietic cells and mutations of JAK3 are therefore associated with severe combined immunodeficiency syndrome[96, 97].

The domain architecture of the JAKs is highly unique, because they contain two kinase domains in series. This circumstance was crucial for naming these kinases after the two-faced Roman god Janus[98]. While the JH1 (JAK homology domain 1) has functional tyrosine kinase activity, the JH2 domain, which is also called

pseudokinase domain, is thought to possess no catalytic activity[99] (Fig. 2). However, it has to be noted that a recent article from Ungureanu and colleagues provides evidence, that the pseudokinase domain of JAK2 has catalytic activity and plays an important role in the negative regulation of the protein[100]. The N-terminal FERM (four-point-one protein, ezrin, radixin and moesin) domain, located between JH4 and JH7, is important for the interaction of JAKs with the cytokine receptors and can be found in many proteins with membrane proximal localisation, since it is able to bind to peptides and phospholipids[101]. Although the FERM domain is crucial for receptor binding, staurosporine induced conformational change of the JAK3 kinase domain is able to inhibit binding to the common γ-chain[102]. This indicates an involvement of the kinase domain in receptor binding. The JAKs bind to the box1 and box2 motifs of corresponding IL-6-type cytokine receptors (Fig. 3). Mutation of only two proline residues in the box1 or deletion of the entire box1 completely abrogates the JAK binding to gp130, LIFR or OSMR[103-105]. The box2 is characterised by various hydrophobic amino acids followed by positively charged residues and seems to increase the binding affinity of the receptor to the JAKs. Hence, a recombinant gp130 with a box2 deletion can only be coprecipitated with JAK1, if the kinase was overexpressed[106]. The interbox region between box1 and box2 also participates in binding to the JAK proteins. Mutation of Trp666, localised between box1 and box2, abrogates JAK binding to gp130[105]. Experiments investigating the role of the potential SH2 domain located between JH3 and JH4 could not identify a classical SH2 domain function[107].

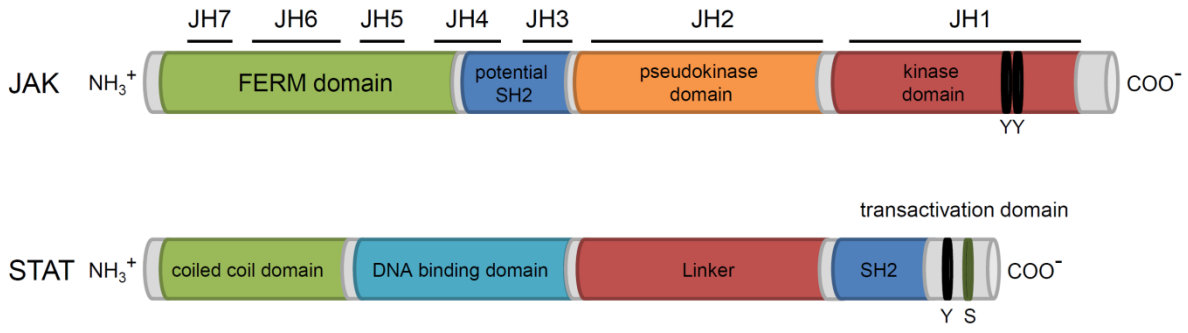

Figure 2: Domain organisation of JAK and STAT proteins

JAK proteins possess an N-terminal FERM domain that is important for receptor interaction, a putative SH2 domain (without classical SH2 function), a pseudokinase domain (without classical catalytic activity) and an active tyrosine kinase domain with an important double tyrosine (Y) motif in the activation loop. The STAT proteins consist of an N-terminal coiled coil domain, a DNA binding domain (important for promoter binding), a linker region, a C-terminal SH2 domain and phosphorylatable tyrosine (Y) and serine (S) residues.

To initiate the activity of the JAKs, the receptor chains have to dimerise, which is the case after cytokine binding. Through dimerisation of the receptors and the induced conformational changes, the JAK proteins are brought in close contact and become phosphorylated (probably autophosphorylated)[98, 101, 108-110]. The activated JAKs subsequently phosphorylate specific tyrosine residues in the receptor chains. Thereby these sites are transformed into docking sites for SH2 domain-containing proteins like the SH2 domain-containing protein tyrosine phosphatase (SHP2) or the STATs, which recognise these phosphorylated tyrosine residues[111].

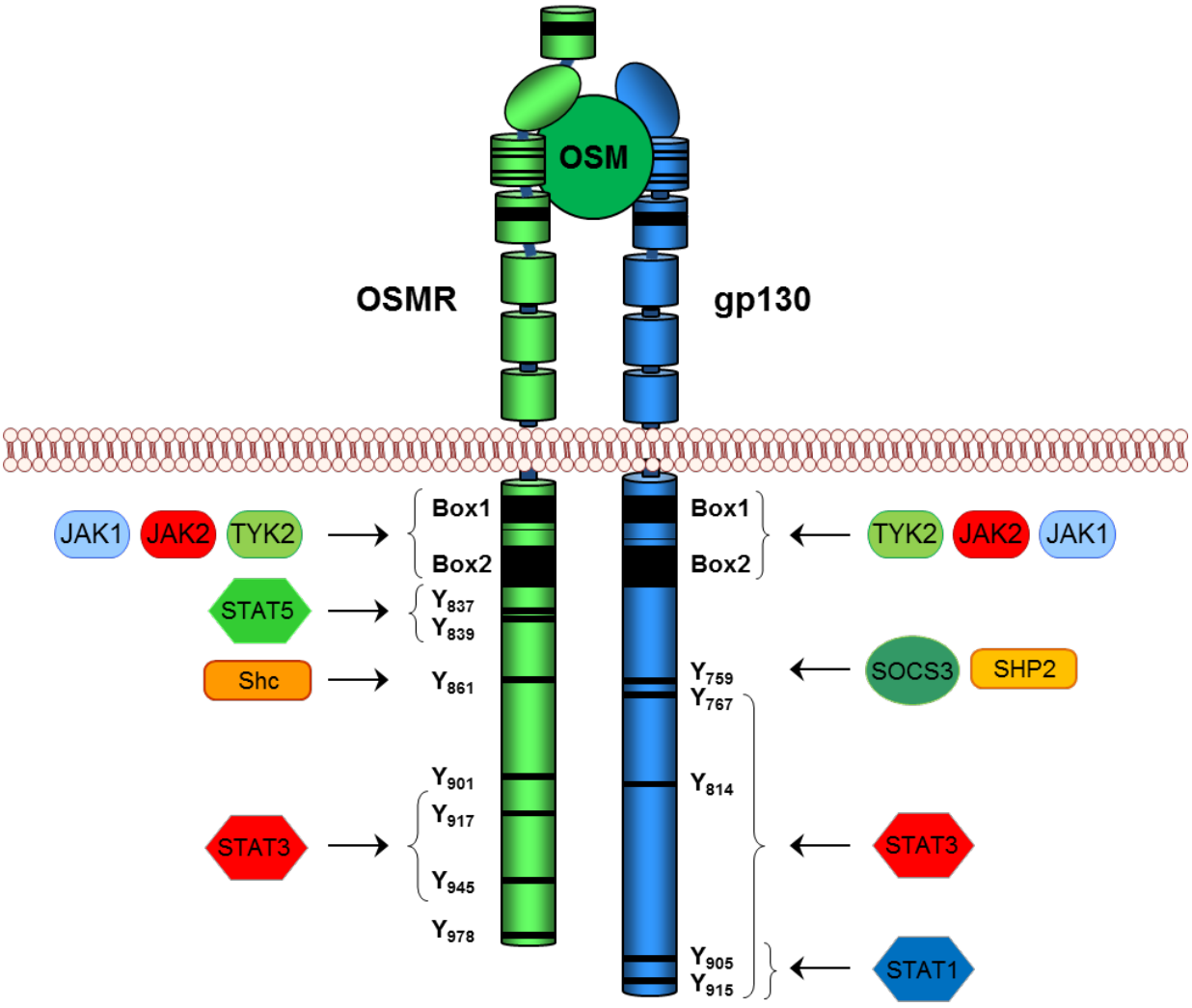

Figure 3: The OSMR-gp130-complex: a junction for several signalling pathways and networks

After OSM binding, the receptor chains of gp130 and OSMR dimerise and initiate the JAK dependent phosphorylation of the indicated tyrosine residues. The box1 and box2 regions are important for JAK recruitment. The STATs, SOCSs and SHP2 are recruited to their respective docking sites (phospho-tyrosine residues, see above). SHP2 as well as the STATs are subsequently phosphorylated by JAKs. While the STATs translocate into the nucleus upon phosphorylation, SHP2 serves as adaptor protein for the activation of the Ras-Raf-MAPK cascade. Thus the transcription of various genes is induced or repressed. One of the STAT3 induced genes is the feedback inhibitor SOCS3.

JAK1, JAK2, TYK2, but not JAK3, can be immunoprecipitated with gp130 and are tyrosine phosphorylated in response to IL-6-type cytokine binding[112-115]. JAK1 appears to be the most important kinase for IL-6 signalling[116]. Cells from JAK1 knockout-mice are no longer responsive to IL-6, LIF, CT-1, OSM or CNTF[117], indicating the importance of this kinase also for other IL-6-type cytokines.

After phosphorylation of specific tyrosine residues in the cytoplasmic region of the receptors, the STAT proteins are recruited and become tyrosine phosphorylated themselves (Fig. 3 and 4). After homo- or heterodimerisation, the STATs translocate into the nucleus, where they bind their respective promoter regions to induce specific target gene transcription[111].

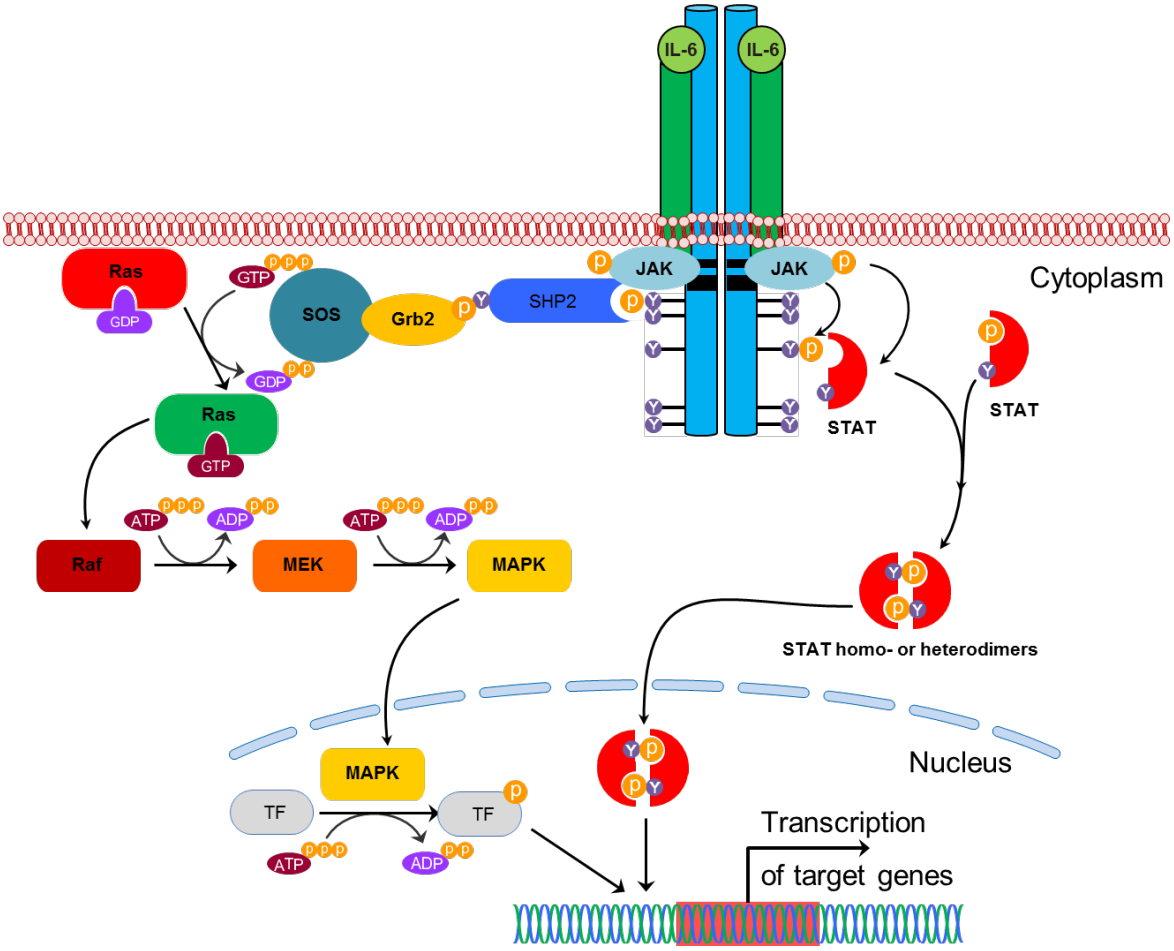

Figure 4: IL-6 activates the JAK/STAT pathway and the MAPK cascade

IL-6 binds to its α-receptor, the IL-6 receptor, thus generating a high affinity complex for gp130. After formation of the hexameric receptor complex (homodimerisation of the signalling gp130 chains), two major pathways are initiated, the JAK-STAT pathway and the Ras-Raf-MAPK cascade. Before STAT dimers can translocate into the nucleus, where they induce IL-6-responsive gene transcription, they are recruited to specific phospho-tyrosine residues in gp130 (intracellular) and phosphorylated via JAKs. Another protein that is recruited to a specific phospho-tyrosine is the phosphatase SHP2. Serving as an adaptor, SHP2 interacts with additional proteins and induces the Ras-Raf-MAPK pathways. At the end of the cascade MAPKs like ERK1/2 are phosphorylated resulting in the activation of specific transcription factors (TF).

In mammals, the STAT family comprises seven genes that code for STAT1, STAT2, STAT3, STAT4, STAT5A, STAT5B and STAT6. Depending on the analysed cell system, the used cytokine and the applied cytokine concentration, STAT1, STAT3 and STAT5 can be activated by IL-6-type cytokines[118-123]. The common STATs that are activated by all known IL-6-type cytokines are STAT1 and STAT3 (originally termed acute phase response factor, APRF)[113]. Not all STATs can be recruited to each phospho-tyrosine of the IL-6-type cytokine receptors. Today many details of this complex regulatory mechanism are known. The tyrosine (Y) residues Y_{767}, Y_{814}, Y_{905} and Y_{915} of gp130 can serve as docking sites for STAT3, while Y_{905} and Y_{915} are additionally able to recruit STAT1[114, 124]. STAT1 and STAT3 can be also recruited by the OSMR[125, 126]. Although not all details of the exact phospho-tyrosine binding are solved yet, the box1/box2 region seems to be sufficient for the STAT1 activation. STAT3 is suggested to interact with Y_{917} und Y_{945} of the OSMR. In addition to STAT3 and STAT1, activation of STAT5 can be observed after OSM induced signalling[127]. The recruitment of STAT5 to the human OSMR is dependent on Y_{837} and Y_{839}[128]. The tyrosine phosphorylation of the STATs is very important both for their dimerisation and translocation. STAT1, STAT3 and STAT5 have similar tyrosine residues located at the C-terminus. Phosphorylation occurs at Y_{701} of STAT1, Y_{705} of STAT3 and Y_{694} of STAT5. Once the STATs are phosphorylated at these sites, they homo- or heterodimerise. The SH2 domains play major roles for the dimerisation through binding to the newly phosphorylated tyrosine[129, 130]. After dimerisation STATs are able to dock to and regulate specific promoter regions of various genes.

Besides the well determined tyrosine phosphorylation, STATs can additionally be serine (S) phosphorylated in their transactivation domain. The serine phosphorylation in STAT1 (S_{727}) can be observed after type I interferon stimulation and is mediated by protein kinase C-delta[131]. In contrast, STAT5A/B serine phosphorylation (STAT5A at S_{726} and STAT5B at S_{731}) observed after erythropoietin treatment is dependent on the activity of the MAPKs ERK1/2 (extracellular signal-regulated kinase 1/2) and p38[132]. For STAT3, phosphorylation of S_{727} has been described[133]. Interestingly, the tyrosine and serine phosphorylations can act synergistically, but also antagonistically. In STAT3 for example, the ERK2 induced phosphorylation of S_{727} decreases the transcriptional activity of STAT3[134]. In spite of other reports showing that for maximal transcriptional activity of STAT3 and STAT1 S_{727} has to be phosphorylated, this residue seems not to be important for the DNA binding of the transcription factors[135,

[136]. On the other hand, for mitochondrial localisation the serine phosphorylation of STAT3 seems to be of major importance[137].

1.4.2 Activation of the MAPK cascade

While the JAK/STAT pathway represents the most prominent pathway triggered by IL-6-type cytokines, most family members additionally activate the MAPKs ERK1/2 and some also the SAPK (stress-activated protein kinases), p38 and JNK1/2/3 (c-Jun N-terminal kinase)[11] (Fig. 3 and 4). This is achieved through receptor recruitment of the phosphatase SHP2 which serves as adaptor protein. SHP2 uses its SH2 domains to bind to the previously phosphorylated tyrosine residues of gp130 and LIFR[138, 139]. The essential residues for this recruitment are Y_{759} of gp130 and Y_{974} of the LIFR[114, 140]. In contrast to gp130 and the LIFR, the OSMR does not utilise SHP2 for activating the Ras-Raf-MAPK pathway. It has been shown that the adaptor protein Shc (SH2 and collagen homology domain-containing protein) is recruited to the OSMR via tyrosine residue 861[141].

The MAPK cascade is initiated after gp130 becomes tyrosine phosphorylated by JAK activity. SHP2 is rapidly recruited to the receptor and afterwards phosphorylation of SHP2 occurs in a JAK1 mediated manner[142]. Phosphorylated SHP2 subsequently interacts with the adaptor protein Grb2 (growth factor receptor-bound protein 2)[138]. Grb2 contains a SH2 and a SH3 (Src homology 3) domain, but no catalytic activity. Shc that is recruited to the OSMR also binds Grb2 allowing Ras-Raf-MAPK cascade initiation[141]. Grb2 is constitutively associated with the guanine nucleotide exchange factor SOS (son of sevenless). SOS thereby migrates from cytoplasm to the plasma membrane and is able to exchange GDP to GTP in the GTPase Ras thus activating the serine/threonine kinase Raf. Raf, a MAP kinase kinase kinase (MAP3K), subsequently activates the dual specificity kinases MEK1/2 (MAP2K)[143]. As dual specificity kinases, MEK1/2 phosphorylate ERK1/2 on an important tyrosine and threonine residue. JNK1/2/3 are phosphorylated by the dual specificity kinases MKK4/7 and p38 by MKK3/6[144]. Afterwards ERK1/2, p38 and JNK1/2/3 can modify the activity of various transcription factors[143].

1.4.3 Activation of the PI3K cascade

IL-6-type cytokines are able to activate additional pathways besides the JAK/STAT and the MAPK pathway. The most frequently described one is the PI3K cascade. This enzyme modifies certain phosphatidylinositides thus inducing the recruitment of the serine/threonine kinase Akt/PKB to the cell membrane. Akt itself is phosphorylated at T_{308} by the phosphoinositide dependent kinase-1 (PDK1) and at S_{473} by mTOR (mammalian target of rapamycin)[145-147]. Typical substrates of Akt are forkhead transcription factors (e.g. FOXO1) and the important pro-apoptotic protein Bad (Bcl-2/Bcl-X_L antagonist). The phosphorylation of Bad results in its cytoplasmic retention and is therefore associated with increased/prolonged survival and cell growth. In cardiomyocytes, for instance, gp130 signalling mediates the activation of this pathway leading to the prevention of apoptosis induced by the cytostatic doxorubicin[148]. Moreover, PI3K is deeply involved in the IL-6 mediated prevention of apoptosis which coincides with the upregulation of the anti-apoptotic protein Mcl-1 in basal cell carcinoma[149] and multiple myeloma cells[150-152]. Interestingly the PI3K activation upon IL-6-type cytokine stimuli is a cell-type specific phenomenon. For example, no elevated Akt activation can be observed in IL-6-treated human HepG2 hepatoma cells[153]. The exact mechanism by which the PI3K/Akt pathway is activated after gp130 dimerisation is not completely clear. After IL-6-type cytokine receptor binding, the adaptor protein Gab1 (Grb2-associated binding protein 1) interacts with PI3K finally resulting in an activation of Akt[139, 154].

1.4.4 Termination of IL-6-type cytokine induced signalling pathways

To prevent an overshoot of cellular responses upon IL-6-type cytokine stimulation, various molecular brakes have evolved. The protein tyrosine phosphatases (PTP), for example SHP2, represent one side of the signalling suppressing machinery. As described above, SHP2 is recruited to phospho-Y_{759} of the cytoplasmic tail of gp130[114, 155] or to phospho-Y_{974} of the LIFR. SHP2 is a ubiquitously expressed phosphatase with two N-terminal SH2 domains in series and a catalytic phosphatase domain in the C-terminal half of the protein. Based on the crystal structure of SHP2 it is assumed that the N-terminal SH2 domain masks the active site of the enzyme and thereby inhibits the catalytic activity in the absence of a tyrosine phosphorylated

substrate protein. The interaction of the SH2 domains with phosphorylated tyrosine motifs of binding partners such as receptors (e.g. gp130) or free cytoplasmic proteins (e.g. STAT3) leads to the opening of the protein structure resulting in the restoration of enzymatic activity[156-159]. A further regulatory mechanism of SHP2 is its own phosphorylation on amino acids Y_{542} and Y_{580} close to the C-terminus of the protein. These phospho-tyrosines behave 'self-reactive' to the two SH2 domains of SHP2 and induce the unmasking of the phosphatase domain by releasing it from the N-terminal SH2 domain[160]. Thus, tyrosine phosphorylated proteins of the gp130/OSMR/LIFR induced signalling pathways are potential SHP2 phosphatase substrates. Overexpression of dominant-negative SHP2 mutants leads to strongly increased gp130, JAK, STAT and SHP2 phosphorylation indicating the harmful potential of a lack of functional SHP2[161].

The second important arm of the cellular signal silencing machinery is the induced expression of the SOCS proteins. These proteins are indispensable components for the termination of the IL-6-type cytokine induced signalling. There are eight members of the SOCS family known at present. They are called CIS (cytokine-inducible SH2 protein) and SOCS1-7. Partially already expressed under basal conditions, their expression can be strongly increased through cytokine mediated signalling. Thus they act as inducible feedback inhibitors[162-164]. The SOCS proteins have a central SH2 domain and a so called SOCS box at the C-terminus. While CIS and SOCS1 expression levels are upregulated by the actions of IL-6, LIF and OSM, SOCS3 transcription is strongly increased after stimulation with IL-6, IL-11, LIF and OSM. IL-6 and its related cytokines are also able to induce increased levels of SOCS2[162, 165-167]. The exact inhibitory mechanisms by which SOCS proteins suppress signalling seem to differ within the SOCS family members. Hence, it is not possible to draft one mechanistic blueprint for all eight proteins. CIS, for example, was shown to be recruited to the erythropoietin receptor (EpoR) and to compete with STAT5 for its docking site at the receptor[168, 169]. The most important SOCS members for inhibiting IL-6-type cytokine signalling are SOCS1 and SOCS3, which are structurally closely related. Both were shown to directly influence the activity of the Janus kinases thus inhibiting phosphorylation of JAKs themselves and consequently of gp130 and STATs[162, 166]. SOCS1 is able to inhibit JAK/STAT signalling by binding to the phosphorylated activation loop within the kinase domain of JAKs via its SH2 domain. The N-terminal KIR (kinase inhibitory region) domain and the extended SH2

subdomain, which is located N-terminally of the SH2 domain, play the crucial role in the inhibition process. The KIR of SOCS1 is thought to inhibit the catalytic activity of the JAK kinase domain by blocking the substrate binding pocket[170]. Although SOCS3 has a comparable KIR domain and is able to bind the JAKs[171-173], it appears to mainly interact with phospho-tyrosine motifs of activated cytokine receptors, such as gp130, the EpoR, the leptin receptor and the granulocyte colony-stimulating factor receptor[172-179]. Referring to IL-6-type cytokine signalling it was discovered that SOCS3 binds to the same docking site of gp130 as SHP2, namely phospho-Y_{759}[125, 174]. Moreover, SOCS proteins are implicated in the destabilisation of their interacting partners. This is achieved by their function as substrate-recruiting component for ubiquitin ligases. Thus SOCS proteins are not only affecting the STAT activation, but also the amount of functional protein[180].

In addition to these major signalling suppressors, further proteins are described to be involved in the inhibition process for gp130 mediated signal transduction. The PIAS proteins, for instance, are able to negatively influence cytokine induced signalling. The PIAS family comprises 5 members: PIAS1, PIAS3, PIASy, PIASxα and PIASxβ. PIASxα and PIASxβ are identical with exception of their C-Termini. In contrast to the SOCS proteins, the constitutively expressed PIAS proteins have to be phosphorylated before associating with their corresponding STATs. The molecular details of the inhibition mechanism of the PIAS proteins are not completely understood to date. But it has been shown that PIAS1 specifically interacts with STAT1, while PIAS3 interacts with STAT3. PIAS1 and PIAS3 exert their inhibitory actions by blocking the DNA binding activity of STATs and thus suppressing the STAT mediated transcription[181, 182].

1.5 The role of IL-6-type cytokines in cardiac remodelling and hypertrophy

Cardiac remodelling is defined as a compensatory reaction of heart tissue to sudden physiological or pathophysiological changes resulting from pregnancy, exercise, aging or pathophysiological injuries (i.e. myocardial infarction, pressure overload, exposure to cardiotoxic agents and infections). It is characterised by modified cardiomyocyte size and changes in vasculature, extracellular matrix composition, cytoskeleton composition, myosin chains, cardiac energetics, metabolism and

inflammatory status. On the cellular level three different processes can contribute to cardiac remodelling: Cell growth of cardiomyocytes, apoptosis/necrosis of cardiac myocytes and fibrosis (infiltration of interstitial cells). In some situations these changes are reversible and also important for compensating transient physiological requirements (e.g. pregnancy, adaptive hypertrophy). However, under many pathophysiological conditions these alterations proceed and become irreversible contributing to an abnormal phenotype and function of the left ventricle and subsequently heart failure[183, 184]. The most frequently studied modification is the cardiomyocyte growth (cardiomyocyte hypertrophy). This unique cell type represents the major component of the myocardium and is responsible for the contractility of the heart tissue. As described above, several conditions can induce a compensatory increase of heart muscle weight and size. Since adult cardiomyocytes hardly proliferate under such conditions[185], they only grow in size to replace inoperable tissue parts (e.g. after myocardial infarction) or to compensate altered requirements. On the molecular level this reaction is achieved through sarcomeric addition in responding cardiomyocytes. Sarcomers represent the contractile units of the muscle tissue and can be assembled in parallel or in series. Assembly in series causes eccentric hypertrophy (elongation of the cardiac myocyte), while parallel assembly leads to concentric hypertrophy (increase of the entire cell diameter)[186].

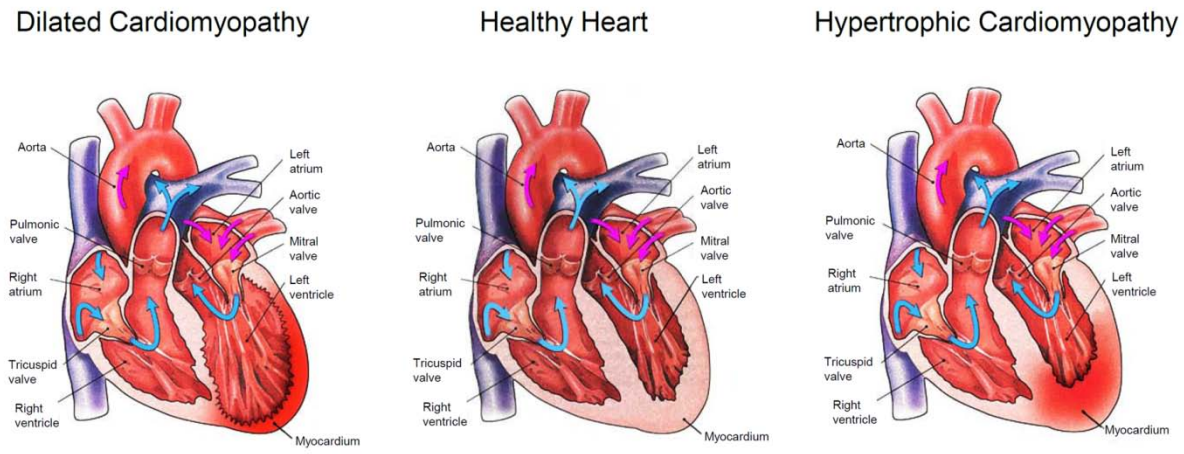

Figure 5: Schematic view of dilated and hypertrophic cardiomyopathy

Dilated cardiomyopathy (left side) is characterised by stretched muscle fibres leading to enlargement of one or two ventricles. The septum and the ventricular walls are thinned and the heart becomes insufficient to pump adequate volumes of blood. Often a correlation with a decreased left ventricular ejection fraction is observed. Hypertrophic cardiomyopathy (right side) displays thickened ventricular walls causing an increased left ventricular ejection fraction. The electrical function of the heart can be negatively affected and sudden heart death can be a direct consequence of such alterations. The scheme is modified after http://www.cts.usc.edu.

One has to distinguish the anatomic and physiological consequences of the two kinds of hypertrophies. Concentric hypertrophy is the cellular basis for a thickened ventricular wall (hypertrophic cardiomyopathy) that is followed by diastolic dysfunction (Fig. 5). Eccentric hypertrophy is attended by dilatation of the ventricle (dilated cardiomyopathy) and is associated with systolic dysfunction (Fig. 5). During the progression of cardiac hypertrophy a remarkable number of dying myocytes can be observed. Apoptosis as well as necrosis play important roles in provoking this process[187]. Fibroblasts are subsequently infiltrating the tissue to replace dead cells thus finally decreasing the contractility and flexibility of the heart to an additional severe extent[188, 189].

Besides their roles in inflammation, acute phase, neuronal differentiation, haematopoiesis etc., IL-6-type cytokines play a role in cardiac hypertrophy, remodelling and survival, which is not fully understood. First of all they are fundamental for the developing heart. LIF and CT-1 are highly expressed during cardiogenesis and contribute to proliferation and survival of embryonic cardiac myocytes[190]. The role of the cytokine family in the adult heart exposed to pathogenesis is, however, far more cryptic. On the one hand, various previous studies unambiguously demonstrated that IL-6-type cytokines induce cardiac hypertrophy, on the other hand it remains unclear if their activity is more protective or rather harmful for the adapting heart[191-193]. From all family members, IL-6, CT-1, LIF, OSM and IL-11 have been identified so far to have cardio-remodelling activities. On the cellular level, CT-1, IL-6, LIF, IL-11 and OSM mediate eccentric hypertrophy by addition of new sarcomeric units in series, as described above[194-201]. It was also shown, that IL-6 serum concentrations are elevated after myocardial infarction[202]. Moreover, increased blood concentrations of IL-6 and sIL-6R were found in patients with congestive heart failure, hypertrophic and dilative cardiomyopathy[203, 204]. Furthermore, the severity of left ventricular dysfunction correlates with systemic IL-6 levels. Therefore, IL-6 may serve as indicator in patients with heart failure and myocardial infarction[202, 203, 205-208]. However, complete genetic ablation of the *Il6* gene does not influence remodelling, survival, left ventricular function or infarct size in mice[209]. Besides the IL-6 and sIL-6R expression, severity based elevations of LIF and soluble gp130 plasma levels were found in heart failure patients[210]. Another study analysing failing hearts of patients suffering from dilative cardiomyopathy, however, found all gp130 protein levels and CT-1 expression levels unaltered[211].

Therefore, this study is in sharp contrast to an article by Zolk and colleagues who analysed patients with ischemic and dilative cardiomyopathy. Here, CT-1 levels were elevated, while gp130 protein levels were reduced and, even more controversially, gp130 mRNA levels were increased[212]. Podewski and colleagues have also shown that expression levels or phosphorylation status of several proteins of the IL-6 and LIF signalling pathways including IL-6, LIF, LIFR, JAK1, JAK2, TYK2, gp130, SOCS1 and SOCS3 are significantly altered in end-stage heart failure[211]. Furthermore, the study indicates that IL-6 levels are impaired in failing hearts, while LIF expression is elevated. Because of these rather controversial data and the relatively small number of articles dealing with human cardiomyocytes in combination with IL-6-type cytokines, it is difficult to correctly address the role of these cytokines during hypertrophic development.

The IL-6-type cytokine induced cardiac remodelling is mainly mediated via three major pathways (JAK/STAT, MAPK cascade and PI3K/Akt)[11, 191, 213-216]. Recent publications also demonstrated that ERK5 phosphorylation might play an important role in inducing eccentric hypertrophy upon LIF and CT-1 stimulation[217, 218]. Furthermore, metabolic changes upon IL-6-type cytokine signalling are described including a switch to anaerobic catabolism[219, 220] and the generation of reactive oxygen species (ROS)[221]. The latter seem to have a beneficial role in cardioprotection by blocking the IL-6-type cytokine induced STAT3 activity. Indeed, it has been suggested for several years that systemically elevated IL-6-type cytokine signalling may contribute to the progression of heart failure[222]. Conversely, a large number of experimental work over the last decade has implicated that the signalling induced by these cytokines contributes to compensatory hypertrophy, promotes cardioprotection and neovascularisation[214, 223-226].

Indeed, STAT3 plays a key role in gp130 mediated cardiac hypertrophy and is sufficient to induce cardiomyocyte hypertrophy *in vitro*[227] and *in vivo*[214], when overexpressed in heart cells. Moreover, the augmented STAT3 activation induced by overexpression of IL-6 and IL-6R without any further stimulus is sufficient to induce cardiac hypertrophy *in vitro* and *in vivo*[199]. Besides their functions during pressure overload or ischemia induced cardioprotection, the involvement of IL-6-type cytokines in inflammatory diseases of the heart should be mentioned. It has been shown that heart specific gp130 knockout-mice or mice overexpressing SOCS3 develop an elevated susceptibility to viral infections of cardiomyocytes suggesting a role of

STAT3 in protecting these cells from viral pathogens by promoting survival[228]. STAT3 seems to mediate not only viral-protective effects, but it also plays a role in pathogen-associated molecular pattern (PAMP) induced myocardial inflammation. Cardiac specific deletion of STAT3 negatively influences the sensitivity of myocytes to lipopolysaccharide (LPS) induced inflammation. As consequences of this attenuated immune status, extensive fibrosis and augmented apoptosis of cardiac myocytes can be observed[225]. However, these beneficial properties of IL-6 and the related cytokines can turn into harmful actions over time. Continuous and excessive secretion of IL-6 during viral myocarditis can destroy viral clearance and the activation of cytokine networks[229]. To prevent the heart from myocardial injury, a well triggered regulation of the gp130 downstream signalling, therefore, is obviously essential.

Driven by the partially beneficial effects, proteins of the gp130-JAK-STAT axis were thought to be appropriate targets for pharmaceutical interventions. The treatment with combined hIL-6 and sIL-6R, for example, was shown to suppress myocyte apoptosis and to limit infarct size after experimental ischemia and subsequent reperfusion[230].

1.6 C/EBP beta and delta: IL-6 inducing/induced transcription factors

CCAAT/enhancer binding proteins (C/EBP) represent a well analysed family of transcription factors. The six known members (C/EBPα, C/EBPβ, C/EBPγ, C/EBPδ, C/EBPε and C/EBPζ) contain a highly conserved C-terminal basic leucine zipper that is important for dimerisation and DNA binding[231]. C/EBPβ was initially described as nuclear factor (for) IL-6 (NF-IL-6). It was shown that C/EBPβ expression is inducible through IL-6 stimulation and that the transcription factor itself is able to upregulate *IL6* transcription[232, 233]. Moreover C/EBPβ can form homodimers or heterodimers with C/EBPα, δ and γ. The protein specifically binds to promoter regions of immunity- and inflammation-associated genes including IL-6 as well as other cytokines and acute-phase proteins. C/EBPs also play a role in adipocyte differentiation and liver regeneration. There are two protein variants of C/EBPβ that are generated through alternative translation start sites, the transcriptional active LAP (liver activating protein) and the inhibitory LAP antagonising LIP (liver inhibitory protein)[231]. The ratio of both polypeptides can alter and LIP expression has been shown to be increased under some conditions, like oncogenic transformation of breast epithelial cells[234]. In

contrast to C/EBPβ, only one transcriptionally active version of C/EBPδ is known. Originally called NF-IL6b, C/EBPδ was shown to form heterodimers and to act with C/EBPβ synergistically[235]. Comparable to C/EBPβ, the expression of the transcription factor can be induced by multiple stimuli including IFN-γ, IL-1, IL-6, insulin, LPS and TNF-α[231].

The IL-6 induced C/EBPβ induction during acute phase response is based on STAT3 activity and binding to cAMP-response element (CRE)-like sequences[236]. The transcription of C/EBPδ can also be induced by STAT3. Strong upregulation of both transcription factors in response to STAT3 was found in growth-arrested mammary epithelial cells and the involuting mammary gland[237, 238], but also in hepatocytes during the acute-phase response[239, 240]. While STAT3 tyrosine phosphorylation is a rather transient event, the thereby initiated C/EBPδ activity can be a state of clearly longer duration[239, 240]. This extremely prolonged and enhanced expression seems to be achieved via autoinduction representing a feed forward mechanism that can be maintained by the IL-6-STAT3-C/EBPδ axis[235, 241-243].

A further level of C/EBP regulation is the phosphorylation of the transcription factors at different serine or threonine residues. For example, the trans-activation potential of C/EBPβ can be enhanced by phosphorylation of T_{235} through an activated MAPK pathway[244, 245]. Moreover, trans-activation can be induced by phosphorylation of S_{195} via protein kinase C (PKC)[246] or S_{276} by Ca^{2+}/calmodulin dependent protein kinase[247]. There are also additional phospho-sites in the protein known that are able to suppress the DNA-binding activity of C/EBPβ, once they were phosphorylated[248]. In the case of C/EBPδ no phosphorylation sites have been identified so far, but its trans-activation potential is decreased in hepatocytes that are treated with phosphatase inhibitors (okadaic acid or sodium orthovanadate)[249], a condition that, of course, alters several other kinase/phosphatase dependent effects in those cells.

Furthermore, C/EBPs can interact with other transcription factors, such as NF-κB (nuclear factor-kappa B), CREB/ATF (cAMP-response-element-binding protein/ activating transcription factor) and AP-1 (activator protein 1) indicating that different target genes can be induced by altering the composition of transcription factor complexes that translocate to specific promoters[250-252].

1.7 Aims of the study

The study of numerous published articles describing the influence of IL-6-type cytokines on the heart highlights one obvious discrepancy: The classification of the cytokine family within the context of cardiac disease ranges from protective to harmful. The role of these cytokines in the development and persistence of cardiac hypertrophy/dilated cardiomyopathy is of central interest, since several members of the cytokine family seem to be capable of inducing cardiomyocyte hypertrophy[194-201]. While the hypertrophic potentials of IL-6, CT-1 and LIF were already partly shown, the influence of OSM on heart cells (especially cardiomyocytes) has not been determined at this stage. Therefore, the present study was designed to compare the hypertrophic potentials of heart relevant IL-6-type cytokines, with particular regard to OSM. Furthermore, redundant and specific activities of the various IL-6-type cytokines should be clarified with focus on their activated signalling pathways and selected target genes. Hypertrophy development and persistence is not only dependent on cardiomyocytes, but it is supported by the cardiac fibroblasts. Therefore, the cellular responses to IL-6-type cytokine stimulation will be evaluated in neonatal rat cardiomyocytes (NRCM) as well as neonatal rat cardiac fibroblasts (NRCFB).

Adrenergic pathways and the renin-angiotensin system were described to cross-talk with IL-6-type cytokines. The molecular mechanisms, however, are not fully understood to date. Hence, as second aim of this thesis the regulation of several members of the renin-angiotensin system in response to IL-6-type cytokines will be analysed. Vice versa, it will be examined whether α_1-adrenergic stimuli (e.g. phenylephrine (PE)) or ATII are able to influence/induce the expression of IL-6-type cytokines or their receptors.

Differential activation of signalling pathways and induction of target genes in the course of the study prompted us to analyse the receptor usage of mOSM and hOSM on NRCM and NRCFB. The central question of this examination was which receptor complexes were utilised by mOSM and hOSM on rat cells. Upon availability of recombinant rat OSM, the third major aim of this thesis will be the characterisation of the receptor complex(es) used by rat OSM on cells of rat origin. In addition, cross-species activities of rOSM on murine and human cells will complete the comparison of the three OSM variants.

2 Materials

2.1 Antibodies

2.1.1 Antibodies for immune fluorescence

Antibody	Epitope species	Host species	Dilution/final concentration	Manufacturer
Alexa488-anti-mouse IgG (polyclonal)	mouse	goat	1:200/10 µg/ml	Life Technologies (Carlsbad, USA)
α-actinin, sarcomeric (monoclonal)	mouse	mouse	1:1000	Sigma-Aldrich (Taufkirchen)

2.1.2 Primary and secondary antibodies for flow cytometry

Antibody	Epitope species	Host species	Dilution/final concentration	Manufacturer
anti-mouse/rat IL-6Rα (monoclonal)	mouse/rat	rat	1:50-1:100	BioLegend (San Diego, USA)
anti-mouse gp130 (monoclonal)	mouse	rat	1:50-1:100	MBL International (Woburn, USA)
Diaclone™ anti-human gp130 (monoclonal)	human	mouse	1:50-1:100	Gen-Probe Incorporated (San Diego, USA)
Diaclone™ anti-human IL-6R (monoclonal)	human	mouse	1:50-1:100	Gen-Probe Incorporated (San Diego, USA)
anti-mouse OSMRβ (monoclonal)	mouse	rat	1:50-1:100	MBL International (Woburn, USA)
Alexa488-anti-mouse IgG (polyclonal)	mouse	goat	1:200	Life Technologies (Carlsbad, USA)
Alexa488-anti-rat IgG (polyclonal)	rat	goat	1:200	Life Technologies (Carlsbad, USA)
R-Phycoerythrin-anti-mouse IgG (polyclonal)	mouse	goat	1:200	Dianova (Hamburg)
R-Phycoerythrin-anti-rat IgG (polyclonal)	mouse	goat	1:200	Dianova (Hamburg)

2.1.3 Antibodies for Western blotting

Antibody	Epitope species	Host species	Dilution	Manufacturer
anti-mouse IgG-HRP (polyclonal)	mouse	horse	1:2000-1:3000	Cell Signaling (Frankfurt)
anti-rabbit IgG-HRP (polyclonal)	rabbit	goat	1:2000-1:3000	Cell Signaling (Frankfurt)
anti-biotin-HRP		goat	1:3000	Cell Signaling (Frankfurt)
anti-mouse IgG-HRP (polyclonal)	mouse	rabbit	1:2000-1:3000	DAKO (Hamburg)
anti-rabbit IgG-HRP (polyclonal)	rabbit	goat	1:2000-1:3000	DAKO (Hamburg)
anti-goat IgG-HRP (polyclonal)	goat	rabbit	1:2000-1:3000	DAKO (Hamburg)
anti-mouse OSMRβ (polyclonal)	mouse	goat	1:500	R&D Systems (Minneapolis, USA)
anti-human OSMRβ (polyclonal)	human	goat	1:1000	R&D Systems (Minneapolis, USA)
anti-human gp130 (monoclonal)	human	mouse	1:1000	R&D Systems (Minneapolis, USA)
anti-murine IL-6R (monoclonal)	mouse	rat	1:500-1:1000	R&D Systems (Minneapolis, USA)
anti-human LIFR (monoclonal)	human	mouse	1:500-1:1000	Santa Cruz Biotechnology (Heidelberg)
anti-ph-JAK1 (Y_{1022}/Y_{1023}) (polyclonal)	human	rabbit	1:1000	Cell Signaling (Frankfurt)
anti-JAK1 (polyclonal)	human	rabbit	1:1000	Cell Signaling (Frankfurt)
anti-ph-JAK2 (Y_{1007}/Y_{1008}) (monoclonal)	human	rabbit	1:1000	Cell Signaling (Frankfurt)
anti-JAK2 (monoclonal)	human	rabbit	1:1000	Cell Signaling (Frankfurt)
anti-ph-STAT5 (Y_{694}) (monoclonal)	mouse	mouse	1:1000	Cell Signaling (Frankfurt)
anti-STAT5 (polyclonal)		rabbit	1:1000	Cell Signaling (Frankfurt)
anti-ph-STAT5A (Y_{694}) (polyclonal)	human	rabbit	1:1000	Signalway Antibody (Pearland, USA)

Antibody	Epitope species	Host species	Dilution	Manufacturer
anti-STAT5A (polyclonal)	human	rabbit	1:1000	Signalway Antibody (Pearland, USA)
anti-ph-STAT3 (Y_{705}) (monoclonal)	mouse	mouse	1:1000	Cell Signaling (Frankfurt)
anti-STAT3 (monoclonal)	mouse	rabbit	1:1000	Cell Signaling (Frankfurt)
anti-STAT3 (polyclonal)	mouse	rabbit	1:1000	Cell Signaling (Frankfurt)
anti-STAT3 (monoclonal)	mouse	mouse	1:1000	Cell Signaling (Frankfurt)
anti-ph-STAT1 (Y_{701}) (polyclonal)	human	rabbit	1:1000	Cell Signaling (Frankfurt)
anti-hSTAT1 (monoclonal)	human	rabbit	1:1000	Cell Signaling (Frankfurt)
anti-STAT1 (polyclonal)	human	rabbit	1:1000	Cell Signaling (Frankfurt)
anti-ph-ERK1/2 (T_{202}/Y_{204}) (monoclonal)	human	mouse	1:1000	Cell Signaling (Frankfurt)
anti-ERK1/2 (polyclonal)	rat	rabbit	1:1000	Cell Signaling (Frankfurt)
anti-ph-p38 (T_{180}/Y_{182}) (monoclonal)	human	mouse	1:1000	Cell Signaling (Frankfurt)
anti-p38 (polyclonal)	human	rabbit	1:1000	Cell Signaling (Frankfurt)
anti-ph-Akt (S_{473}) (polyclonal)	mouse	rabbit	1:1000	Cell Signaling (Frankfurt)
anti-Akt (polyclonal)	mouse	rabbit	1:1000	Cell Signaling (Frankfurt)
anti-ph-SHP2 (Y_{542}) (polyclonal)	human	rabbit	1:1000	Cell Signaling (Frankfurt)
anti-SHP2 (monoclonal)	human	mouse	1:1000	Santa Cruz Biotechnology (Heidelberg)

2.2 Recombinant cytokines, receptors and other ligands

Peptide	Activity	Concentrations	Manufacturer/source
recombinant human IL-6	$1x10^7$ U/mg	20-100 ng/ml	Peprotech (Rocky Hill, USA)
recombinant rat IL-6	$1x10^8$ U/mg	20-100 ng/ml	Peprotech (Rocky Hill, USA)
recombinant human sIL-6Rα		500 ng/ml	A. Küster und M. Kauffmann (Aachen), Weiergraber *et al.*[253]
recombinant human LIF	$1x10^8$ U/mg	1-10 ng/ml	Sigma-Aldrich (Taufkirchen)
recombinant human CT-1	$1x10^6$ U/mg	10 ng/ml	Peprotech (Rocky Hill, USA)
recombinant human OSM	$5x10^5$ U/mg	10-100 ng/ml	Peprotech (Rocky Hill, USA)
recombinant rat OSM		10-100 ng/ml	Peprotech (Rocky Hill, USA)
recombinant murine OSM	$5x10^6$ U/mg	10-20 ng/ml	R&D Systems (Minneapolis, USA)
Phenylephrine (PE)		50 µM	Sigma-Aldrich (Taufkirchen)
LIF-05		5-50 ng/ml	Prof. Dr. J. Heath (Birmingham, UK), Vernallis *et al.*[254]

2.3 Small interfering RNAs (siRNAs)

siRNA targeting rOSMR	ON-TARGET*plus* SMARTpool from Dharmacon (Chicago, USA), purchased from Thermo Fisher Scientific Inc. (Waltham, USA)
siRNA targeting mOSMR	ON-TARGET*plus* SMARTpool from Dharmacon (Chicago, USA), purchased from Thermo Fisher Scientific Inc. (Waltham, USA)
siRNA targeting hOSMR	Silencer® Select siRNA from Ambion (Austin, USA), purchased from Life Technologies (Carlsbad, USA)
nonsilencing control siRNA	AllStars Negative Control siRNA from QIAGEN (Hilden, Germany)

2.4 Plasmids for cloning and generation of stably transfected cells

pBO

Eukaryotic expression vector was derived from pBI (Clontech, Mountain View, USA), that contains a tetracycline responsive bidirectional promoter and *Amp*^{R} (ampicillin resistance gene). *Hyg*^{R} (hygromycin resistance gene) was inserted and both MCS were modified generating restriction sites for NotI, PacI, NheI, AgeI and AscI in MCSII and for SbfI, SgrAI, FseI and SwaI in MCSI[255].

pTet-On®

pTet-On® (Clontech, Mountain View, USA) expresses the reverse tet-responsive transcriptional activator (rtTA) and contains *Neo*^{R} (neomycin resistance gene) and *Amp*^{R}. The rtTA is induced by doxycycline.

2.5 Oligonucleotide primers for semi quantitative RT-PCR

mRNA	Name	Sequence (5´→3´)	Amplicon length
hGAPDH	h/r GAPDH for h/r GAPDH rev	TGATGACATCAAGAAGGTGG TTACTCCTTGGAGGCCATGT	244 nt
hOSMR	hOSMR for hOSMR rev	GACACTGCCTTGGGGTGGTC CATCTCCAGGTTGGGGTTTC	877 nt
rGAPDH	h/r GAPDH for h/r GAPDH rev	TGATGACATCAAGAAGGTGG TTACTCCTTGGAGGCCATGT	244 nt
rgp130	rat gp130 for rat gp130 rev	CATGGTCAACTTGTGGAACCATG TCCCACTGACACAGCATGTTC	380 nt
rgp130	rat gp130 for II rat gp130 rev II	GTCAGAGTGGGCAACAGAGA GTCTTCCATATGAGCCGTGC	573 nt
rOSMR	rat OSMR for II rat OSMR rev II	ATATACCAGCGCTGGCCAGG AATAGTCCGAGTTGGTGCGG	504 nt
rLIFR	rat LIFR for rat LIFR rev	ACTGACTGAATAGCACGGAC TTACTCTGAAAGCCGTTTTGG	380 nt
rLIFR	rat LIFR for II rat LIFR rev II	GGACCAGATACTTGGCGAGA GGTGCGACAATTGGAGCTAA	573 nt
rIL-6R	rat IL-6R for rat IL-6R rev	TCACAGAGCAGAGAATGGACT GTATGGCTGATACCACAAGGT	481 nt
mGAPDH	m GAPDH for m GAPDH rev	CTACTGGTGTCTTCACCACC GTGGCAGTGATGGCATGGAC	259 nt
mOSMR	mOSMR for mOSMR rev	GGCATCCCGAAGCGAAGTCTT GACGTCCTGCGGAGCCTTTG	952 nt

2.6 Oligonucleotide primers for quantitative real time RT-PCR

mRNA	Name	Sequence (5´→3´)	Amplicon length
hGAPDH	hGAPDH for hGAPDH rev	AGCCACATCGCTCAGACAC GCCCAATACGACCAAATCC	66 nt
hgp130	hgp130 for hgp130 rev	AGGACCAAAGATGCCTCAAC GAATGAAGATCGGGTGGATG	69 nt
hOSMR	hOSMR72 for hOSMR72 rev	TGTCTGGAGAATTGTGAGCTTG CATGCAGTTTTGATAATGGCTTC	77 nt
hLIFR	hLIFR for hLIFR rev	GGCCCGGAGAAGAGTATGTA TCACCACTCCAACAATGACAG	103 nt
rGAPDH	rGAPDH for rGAPDH rev	TGGGAAGCTGGTCATCAAC GCATCACCCCATTTGATGTT	78 nt
rgp130	rgp130 for rgp130 rev	TGTGTATGGAATCACCATACTTTCA CCCTCATTCACAATGCAACTC	75 nt
rOSMR	rOSMR for rOSMR rev	CCTTCATCAAGTGACCTTCCTT GTAAAGGCTCCCCCAAGACT	77 nt
rLIFR	rLIFR for II rLIFR rev II	AAGCTAATTCCAAGAAAGAAGTGC CACAGCAACATGGTAGGTTGA	74 nt
rIL-6R	rIL-6R for rIL-6R rev	CACGAAGGCTGTGATGTTTG GGCACCTGGAAGTCACTCTT	66 nt
rIL-6R*	r msIL-6R for r msIL-6R rev	GCCCACATTCCTGGTAGCTGGAGG CCCAAGGGATACGGTGGGGGAG	141 nt
rOSM	rOSM for III rOSM rev III	TGGCTGCTCCAGCTCTTC GAGCGTGTTCAGGTTTTGGT	118 nt
rLIF	rLIF for rLIF rev	TGCCAATGCCCTCTTTATTT CCGATACAGCTCGACCAACT	148 nt
rIL-6	rIL-6 for III rIL-6 III	TCTCGAGCCCACCAGGAACGA ACTGGCTGGAAGTCTCTTGCGGA	88 nt
rACE	rACE for rACE rev	TCTGCTTCCCCAACAAGACT AGGAAGCCAGGATGTTGGT	69 nt
rAT1α (Agtr1a)	rAT1A for rAT1A rev	CACCCGATCACCGATCAC CAGCCATTTTATACCAATCTCTCA	110 nt
rSOCS1	rSOCS1 for rSOCS1 rev	CAGCCGACAATGCGATCT CGAGGACGAAGACGAGGAC	77 nt
rSOCS3	rSOCS3 for rSOCS3 rev	AATCCAGCCCCAATGGTC GGCCTGAGGAAGAAGCCTAT	65 nt
rC/EBPβ	rC/EBP b for rC/EBP b rev	TCTACTACGAGCCCGACTGC GGTAGGGGCTGAAGTCGAT	120 nt

mRNA	Name	Sequence (5´→3´)	Amplicon length
rC/EBPδ	rC/EBP d for rC/EBP d rev	CCTCCGGCAGTTCTTCAA CGGTCGTTCGGAGTCTCTAA	105 nt
rC/EBPδ	rC/EBP d for II rC/EBP d rev II	CATCAGCGTGTGGAGCAG GCTGGGCAGCTCTTTGAA	69 nt
rSTAT3	rSTAT3 for rSTAT3 rev	CCAGACAGAAGATGCAGCAG CTCGCTCACGATGCTCCT	74 nt

*Oligonucleotide primers that exclusively recognise the membrane bound variant of the IL-6R, because primers anneal in the corresponding cDNA region of the intracellular part of the IL-6R. Thus alternatively spliced sIL-6R is not detected.

2.7 Oligonucleotide primers for cloning rgp130, rOSMR and rLIFR

cDNA	Name	Site for	Sequence (5´→3´)	Product length
rgp130	rgp130 AgeI	AgeI	ATAAT**ACCGGT**TGCAAG*ATG*TCCGC ACTAAGGATCTGG[#]	2791 nt complete
	rgp130 NotI	NotI	TAATTAAT**GCGGCCGC**GGTCCC*TCA* CTGTGGCATGTAGCCACC[#]	
rOSMR	rOSMR SbfI	SbfI	AATATT**CCTGCAGG**GCCACC*ATG*GC TTTCTCTGTGGTCCTTCATCAAG[#]	2925 nt complete
	rOSMR FseI	FseI	TAGGTT**GGCCGGCC**CCTTGGC*CTA*A GAAGTCAAGTTGTTCTCCTTC[#]	
rLIFR	rLIFR SbfI	SbfI	AATATT**CCTGCAGG**CGGACA*ATG*GG AGCTTTCTCATGGTGG[#]	3323 nt complete
	rLIFR FseI	FseI	TTAATT**GGCCGGCC**GACCTGG*TTA*G TCATTTGGTTTGTTCTGG[#]	

[#]Printed in bold: Restriction sites for the corresponding enzymes. Printed in italics/underlined: Start codon or stop codon, respectively

2.8 Sequencing primers

Target	Name/Orientation	Sequence (5´→3´)	Position 5´ of the ATG
rgp130	1rgp130 rev	TCCAAACCTGAATTGACCCA	747 nt
	2rgp130 for	GAAACCCAGCCCACCTCATA	657 nt
	3rgp130 for	TCCCAGACTGGCAGCAAGAA	1397 nt
	4rgp130 for	CATCTCCAGCAGTGAGGAGA	2217 nt
rOSMR	1rOSMR rev	GTTGCTCTCCACGGATTGGC	571 nt
	2rOSMR for	GTTGGAAGAAGGTTCCAATG	471 nt
	3rOSMR for	GTGCGAGTGCCAACCACTTC	1211 nt
	4rOSMR for	CAGCGACTTCCAGTCTGGCT	1941 nt
	5rOSMR for	ACACACCGCACCAACTCGGA	2621 nt
rLIFR	1rLIFR rev	TCAGCACTGTGTTGAGTGAC	571 nt
	2rLIFR for	CCAATGCCACCTGGGAGGTT	491 nt
	3rLIFR for	TGCTCGCAATCCACTGGGCC	1221 nt
	4rLIFR for	AGCCCTGCCTCCTGGACTGG	1991 nt
	5rLIFR for	ACCCATCATTGAGGAGGAAA	2841 nt

2.9 Reaction kits

The following reaction kits were used following the manufacturer´s instructions:

Name of the kit	Manufacturer
QIAGEN Plasmid Mini Kit	(QIAGEN, Hilden)
HiSpeed Plasmid Maxi Kit	(QIAGEN, Hilden)
QIAquick Gel Extraction Kit	(QIAGEN, Hilden)
RNeasy Mini Kit, combined with QIAshredder and RNase-Free DNase Set	(QIAGEN, Hilden)
QIAGEN OneStep RT-PCR Kit	(QIAGEN, Hilden)
Verso 1-Step RT-PCR Kit	Thermo Fisher Scientific Inc. (Waltham, USA)
Transcriptor First Strand cDNA Synthesis Kit	Roche (Basel, Switzerland)
FastStart Universal SYBR Green Master (Rox)	Roche (Basel, Switzerland)

Name of the kit	Manufacturer
PCR Extender System	5 PRIME (Hamburg)
Thermo Scientific Pierce Enhanced Chemiluminescence Kit	Thermo Fisher Scientific Inc. (Waltham, USA)
WST-1 Cell Proliferation Assay Kit	(Clontech, Mountain View, USA)
Rat IL-6 Quantikine ELISA Kit	R&D Systems (Minneapolis, USA)

2.10 Restriction enzymes

Restriction endonucleases	Recognised palindrome	Manufacturer
FastDigest® AgeI (BshTI)	5´…A$^{\vee}$ CCGGT…3´ 3´…TGGCC$_{\wedge}$ A…5´	Fermentas (St. Leon-Rot)
FastDigest® NotI	5´…GC$^{\vee}$ GGCCGC…3´ 3´…CGCCGG$_{\wedge}$ CG…5´	Fermentas (St. Leon-Rot)
SbfI	5´…CCTGCA$^{\vee}$ GG…3´ 3´…GG$_{\wedge}$ ACGTCC…5´	New England Biolabs (Ipswich, USA)
FseI	5´…GGCCGG$^{\vee}$ CC…3´ 3´…CC$_{\wedge}$ GGCCGG…5´	New England Biolabs (Ipswich, USA)

2.11 Enzymes

Used enzyme	Method	Manufacturer
Difco Trypsin 250	NRCM isolation	BD (Heidelberg)
DNAse	NRCM isolation	Sigma-Aldrich (Taufkirchen)
0.05% Trypsin-EDTA (1X), Phenol Red	Cell Culture	GIBCO (Karlsruhe)
T4 DNA Ligase	Ligation	New England Biolabs (Ipswich, USA)
T4 DNA Ligase	Ligation	Fermentas (St. Leon-Rot)

2.12 Protein and DNA ladder

1) Ladder used for SDS-Gels and Western blotting:

-PageRuler™ Plus Prestained Protein Ladder (10-250 kDa) from Fermentas (St. Leon-Rot)
-Biotinylated Protein Ladder (9-200 kDa) from Cell Signaling (Frankfurt)

2) Ladder used for DNA-Agarose-Gels:

-GeneRuler™ 100 bp DNA Ladder (up to 1 kbp) from Fermentas (St. Leon-Rot)
-GeneRuler™ 1 kb DNA Ladder (up to 10 kbp) from Fermentas (St. Leon-Rot)

2.13 Eukaryotic cells

Ba/F3	Non adherent murine pre-B cell line, cultured in RPMI (10% FCS) + 10 ng/ml mIL-3
Ba/F3 hOSMR/hgp130	Ba/F3 cells expressing hOSMR and hgp130, cultured in RPMI (10% FCS) + 10 ng/ml hOSM or mIL-3; the cells were a kind gift form Prof. Dr. J. Heath (Birmingham, UK)[256]
Ba/F3 @164 (pBO-rOSMR/rgp130)/pTet-On	Ba/F3 cells expressing the rOSMR and rgp130, selected and cultured in RPMI (10% FCS) + 200 ng/ml hygromycin B, 200 ng/ml geneticin (G418), 500 ng/ml doxycycline, 10 ng/ml rOSM
Ba/F3 @166 (pBO-rLIFR/rgp130)/pTet-On	Ba/F3 cells expressing the rLIFR and rgp130, selected and cultured in RPMI (10% FCS) + 200 ng/ml hygromycin B, 200 ng/ml geneticin (G418), 500 ng/ml doxycycline, 10 ng/ml hLIF
JTC-27	Adherent rat hepatoma cells, cultured in RPMI 1640 (10% FCS), purchased from the DSMZ (Braunschweig)
HepG2	Adherent human hepatoma cells, cultured in DMEM (10% FCS), purchased from the DSMZ (Braunschweig)

Hepa1c1c7	Adherent murine hepatoma cells, cultured in MEMα without nucleosides (10% FCS), purchased from Sigma-Aldrich (Taufkirchen)

All cell lines mentioned were cultured according to the instructions of the supplier at 5% CO_2 and 37°C in water-saturated atmosphere.
NRCM and NRCFB were isolated from ≤ 24 h old neonatal Sprague Dawley rats (Janvier, Saint-Berthevin Cedex, France), as described in the methods section. While NRCM were cultured in self-made NRCM culture medium (as described in chapter 2.16) at 1% CO_2 and 37°C in water-saturated atmosphere, NRCFB were cultured using Medium 199 (10% FCS) at 5% CO_2 and 37°C in water-saturated atmosphere.
All culture media were purchased from GIBCO (Karlsruhe).

2.14 *E. coli* strain for cloning

XL10-Gold Ultracompetent Cells from Agilent (Santa Clara, USA) were used for cloning.

2.15 Chemicals

Acrylamide solution (30%) - Mix 37, 5:1	AppliChem (Darmstadt)
Agar	AppliChem (Darmstadt)
Agarose	Peqlab (Erlangen)
Aminocaproic acid	AppliChem (Darmstadt)
Ampicillin	Roth (Karlsruhe)
Ammonium persulfate (APS)	AppliChem (Darmstadt)
Aprotinin	AppliChem (Darmstadt)
Bromodeoxyuridine (BrdU)	Sigma-Aldrich (Taufkirchen)
Bromophenol blue	AppliChem (Darmstadt)
Bovine serum albumin (BSA), blotting grade	AppliChem (Darmstadt)
DharmaFECT 4 Transfection Reagent	Dharmacon (Chicago, USA)
4´,6-Diamidino-2-phenylindole (DAPI)	AppliChem (Darmstadt)
Dimethyl sulfoxide (DMSO)	AppliChem (Darmstadt)

Disodium hydrogen phosphate (Na_2HPO_4)	AppliChem (Darmstadt)
Disodium hydrogen phosphate heptahydrate (Na_2HPO_4 x 7 H_2O)	Merck (Darmstadt)
Doxycycline	AppliChem (Darmstadt)
Ethanol	Roth (Karlsruhe)
Ethanol absolute	AppliChem (Darmstadt)
Ethidium bromide	AppliChem (Darmstadt)
Fetal calf serum (FCS)	PAA (Pasching, Austria)
Fibronectin solution, bovine (1 mg/ml)	PromoCell (Heidelberg)
Ficoll® 400	AppliChem (Darmstadt)
Geneticin (G418)	GIBCO (Karlsruhe)
Glucose	Merck (Darmstadt)
Glycerol	AppliChem (Darmstadt)
Glycine	AppliChem (Darmstadt)
Halt™ Phosphatase Inhibitor Cocktail	Thermo (Waltham, USA)
HEPES	AppliChem (Darmstadt)
Hydrogen chloride (HCl)	AppliChem (Darmstadt)
Hygromycin B	Life Technologies (Carlsbad, USA)
Isopropyl alcohol	Roth (Karlsruhe)
Leupeptin	AppliChem (Darmstadt)
Lipofectamine™ 2000	Life Technologies (Carlsbad, USA)
Magnesium chloride ($MgCl_2$)	AppliChem (Darmstadt)
Magnesium sulphate ($MgSO_4$)	AppliChem (Darmstadt)
2-Mercaptoethanol	AppliChem (Darmstadt)
Methanol	AppliChem (Darmstadt)
Minimum Essential Eagle (MEM), powder	Sigma-Aldrich (Taufkirchen)
Non-essential amino acids	GIBCO (Karlsruhe)
Non-fat dry milk powder, blotting grade	AppliChem (Darmstadt)
Nuclease free H_2O	QIAGEN (Hilden)
N-Z-Amine®	Sigma-Aldrich (Taufkirchen)
Opti-MEM®	GIBCO (Karlsruhe)
Paraformaldehyde	AppliChem (Darmstadt)
Penicillin (5000 U/ml)/Streptomycin (5 mg/ml)	GIBCO (Karlsruhe)
Pepstatin A	Merck (Darmstadt)

Phenylmethylsulfonyl fluoride (PMSF)	AppliChem (Darmstadt)
Potassium chloride (KCl)	AppliChem (Darmstadt)
Potassium dihydrogen phosphate (KH_2PO_4)	AppliChem (Darmstadt)
Sodium acetate	AppliChem (Darmstadt)
Sodium chloride (NaCl)	AppliChem (Darmstadt)
Sodium dihydrogen phosphate (NaH_2PO_4)	Roth (Karlsruhe)
Sodium dodecyl sulfate (SDS)	AppliChem (Darmstadt)
Sodium fluoride (NaF)	AppliChem (Darmstadt)
Sodium hydrogen carbonate ($NaHCO_3$)	Sigma-Aldrich (Taufkirchen)
Sodium hydroxide (NaOH)	AppliChem (Darmstadt)
Sodium orthovanadate (Na_3VO_4)	AppliChem (Darmstadt)
50x TAE buffer	AppliChem (Darmstadt)
Tetramethylethylenediamine (TEMED)	AppliChem (Darmstadt)
Triton X-100	AppliChem (Darmstadt)
Tris(hydroxymethyl)aminomethane (Tris)	AppliChem (Darmstadt)
Trypan blue for Countess®	Life Technologies (Carlsbad, USA)
Trypan blue	AppliChem (Darmstadt)
Tryptone	Roth (Karlsruhe)
Tween 20	AppliChem (Darmstadt)
Vitamin B12	Sigma-Aldrich (Taufkirchen)
Xylene cyanol FF	AppliChem (Darmstadt)
Yeast extract	Roth (Karlsruhe)

2.16 Buffers, solutions and prepared culture media

All buffers and solutions were prepared using H_2O of Millipore-quality. Solutions, self-made media and buffers used for cell culture and primary cell extraction/culture were sterile-filtered. Heat inactivated FCS was always added to self-made medium after sterile filtration.

10x PBS:

1.37	M	NaCl
27	mM	KCl
100	mM	Na_2HPO_4
20	mM	KH_2PO_4
	pH	7.4

1x PBS:

137	mM	NaCl
2.7	mM	KCl
10	mM	Na_2HPO_4
2	mM	KH_2PO_4
	pH	7.4

2x Laemmli sample buffer/lysis buffer:

125	mM	Tris-HCl (pH 6.8)
20	%	Glycerol
10	%	2-Mercaptoethanol
4	%	SDS
0.005		Bromophenol blue

Triton X-100 lysis buffer:

20	mM	Tris-HCl pH 7.5
150	mM	NaCl
10	mM	NaF
1	%	Triton X-100

Applied protease and phosphatase inhibitors for Triton X-100 lysis buffer:

Final concentration	Inhibitor
1mM	Na_3VO_4
1mM	PMSF
5 µg/ml	Aprotinin
5 µg/ml	Leupeptin
3 µg/ml	Pepstatin
10µl/ml	Halt™ Phosphatase Inhibitor Cocktail

Tris-buffered saline Tween 20 (TBS-T):

137	mM	NaCl
20	mM	Tris
0.1	%	Tween 20
	pH	7.6

Running buffer for SDS-PAGE:

25	mM	Tris
192	mM	Glycine
35	mM	SDS

10% Separating gel:

5.9 ml	H_2O (Millipore)
5.0 ml	30% Acrylamide solution
3.8 ml	1.5 M Tris-HCl (pH 8.8)
150 µl	10% SDS
12 µl	TEMED
75 µl	APS

3% Stacking gel:

3.4 ml	H_2O (Millipore)
830 µl	30% Acrylamide solution
630 µl	2.0 M Tris-HCl (pH 6.8)
50 µl	10% SDS
5 µl	TEMED
40 µl	APS

Anode I buffer for Western blot:

300	mM	Tris
20	%	Methanol
	pH	10.4

Anode II buffer for Western blot:

25	mM	Tris
20	%	Methanol
	pH	10.4

Cathode buffer for Western blot:

40	mM	Aminocaproic acid
20	%	Methanol

Stripping buffer:

62.5	mM	Tris
2	%	SDS
0.78	%	2-Mercaptoethanol (freshly added)
	pH	6.7

London Stripping buffer:

2	M	Glycin
	pH	2.5

6x DNA sample buffer:

15	%	Ficoll® 400
0.25	%	Bromophenol blue
0.25	%	Xylene cyanol FF

Paraformaldehyde (4% solution):

-20 g PFA solved in 480 ml 1x PBS

-Solution heated up to 60°C and pH adjusted to pH 7.2 (NaOH)

-Filled up to 500 ml with 1x PBS

10 mM BrdU:	230	mg	BrdU
	74.8	ml	H_2O (sterile)
			5 ml aliquots, frozen at -20°C

DNase solution:	100	mg	DNase
	50	ml	0.9% NaCl (sterile)
			2 ml aliquots, frozen at -20°C

Calicum- and bicarbonate free Hanks with HEPES (CBFHH):

NaCl (3 M)	40 ml
KCl (0.5 M)	10 ml
$MgSO_4$ x 7 H_2O (8.1 M)	10 ml
KH_2PO_4 (0.05 M)	10 ml
Na_2HPO_4 x 7 H_2O (0.03 M)	10 ml
HEPES	4.76 g
Glucose	1 g
	pH 7.3 (NaOH)
H_2O	ad 1 l and sterile filtration
Penicillin/Streptomycin	5 ml
	Storage at 4°C

Trypsin solution for enzymatic heart digestion:

Difco Trypsin 250	300 mg
CBFHH	200 ml
DNase	2 ml
	Sterile filtration

Vitamin B12 solution:	100	mg	Vitamin B12
	50	ml	H_2O (sterile)
			2 ml aliquots, frozen at -20°C

NRCM basis medium (uncomplete):

MEM (powder)	10.8 g
Vitamin B12 solution	1 ml
$NaHCO_3$	350 mg
H_2O	ad 1 l
	pH 7.3 and sterile filtration

NRCM culture medium (ready to use):

FCS	0.5 ml – 25 ml (0.1 - 5.0%), see methods
Penicillin/Streptomycin	5 ml
BrdU solution (10 mM)	5 ml
NRCM basis medium	ad 500 ml

Preplating medium:

FCS	25 ml (5%)
Penicillin/Streptomycin	5 ml
NRCM basis medium	ad 500 ml

Freezing medium:

Respective medium (e.g. DMEM)	40 %
FCS	50 %
DMSO	10 %

LB-medium:

Tryptone	10	g
Yeast extract	5	g
NaCl	10	g
		pH 7.0
H_2O		ad 1 l

LB-agar:

Agarose	15	g
LB-Medium		ad 1 l

NZY$^+$-broth:

N-Z-Amine	10	g
Yeast extract	5	g
NaCl	5	g
		pH 7.5
H_2O		ad 1 l

12.5 ml of 1 M $MgCl_2$, 12.5 ml of 1 M $MgSO_4$ and 10 ml of 2 M glucose were freshly added to the NZY$^+$-broth.

2.17 Consumables

Consumables as culture plates, dishes, flasks and tubes, disposable pipettes, tips, 15 or 50 ml tubes, cryotubes, Eppendorf tubes, cell culture pipettes, well plates, filter tips and cuvettes were purchased from Sarstedt (Nümbrecht). Syringes, injection needles and scalpels were obtained from B. Braun Melsungen AG (Melsungen). Cell strainers and 12 well plates were purchased from BD (Heidelberg). Western blot consumables as PVDF-membrane and whatman paper were received from Whatman (Kent, UK). Medium bottles and filters for sterile filtration and medium storage were obtained from Corning Incorporated (Corning, USA). All other used consumables were purchased from Hartenstein (Würzburg), Eppendorf (Hamburg), Serva (Heidelberg) or Millipore (Billerica, USA).

2.18 Laboratory equipment (technical instruments, machines and robotic systems)

Apparatus	Manufacturer
ABI PRISM® 7900HT, real time PCR cycler	Life Technologies (Carlsbad, USA)
Adjustable casting chamber (JustCast)	Peqlab (Erlangen)
Agarose gel electrophoresis chambers	Peqlab (Erlangen)
AxioObserver.Z1, fluorescence microscope	Zeiss (Jena)
Bacteria incubator	Memmert (Schwabach)
Benchtop shakers, magnetic stirrers and overhead stirrers	Heidolph (Schwabach)
BioPhotometer plus	Eppendorf (Hamburg)
Benchtop centrifuges	Eppendorf (Hamburg)
Biometra Multigel and Maxigel, protein gel electrophoresis systems	Analytik Jena (Jena)

Apparatus	Manufacturer
Countess®, automated cell counter	Life Technologies (Carlsbad, USA)
FluorChem Q, Western blot Imager	PoteinSimple (Santa Clara, USA)
Freezer and refrigerators	Liebherr (Bulle, Switzerland)
Gel documentation system	Herolab (Wiesloch)
Heraeus HERAcell 240®, cell incubator	Thermo Fisher Scientific Inc. (Waltham, USA)
Heraeus HERAfreeze, -80°C freezer	Thermo Fisher Scientific Inc. (Waltham, USA)
High performance centrifuges (Avanti™ J-25 and Avanti™ J-20XP)	Beckmann Coulter (Brea, USA)
Incubator shaker, Kühnershaker ISF-W1	Adolf Kühner AG (Basel, Switzerland)
Mastercycler® pro, thermal PCR cycler	Eppendorf (Hamburg)
Microwave oven	Privileg (Stuttgart)
Multiskan EX Microplate Photometer	Thermo Fisher Scientific Inc. (Waltham, USA)
NanoPhotometer® P 300	Implen (Westlake Village, USA)
4D-Nucleofector™ System, nucleofection system	Lonza (Basel, Switzerland)
Single channel and multichannel pipettes	Eppendorf (Hamburg)
pH sensor, FE20 - FiveEasy™ pH	Mettler-Toledo (Giessen)
Pipetus®, electronic pipette controller	Hirschmann Laborgeräte (Eberstadt)
Power supplies for electrophoresis	Consort (Turnhout, Belgium)
QIAgility, automated pipetting robot	QIAGEN (Hilden)

Apparatus	Manufacturer
Sterile benches for cell culture, BDK-S 1200	BDK Luft- und Reinraumtechnik (Sonnenbühl)
Thermomixer compact/comfort	Eppendorf (Hamburg)
Transmitted light microscope, Leica DMIL	Leica (Wetzlar)
Vortex-Genie® 2; vortex mixer	Scientific Industries (Bohemia, USA)
Water bath	GFL - Gesellschaft für Labortechnik (Burgwedel)
Western blot chamber, semi-dry blotting	Peqlab (Erlangen)

3 Methods

3.1 Cell-biological Methods

3.1.1 Cultivation of eukaryotic cell lines

Cells were cultured under water-saturated atmosphere at 5% CO_2 and 37°C. All used culture media contained 10% FCS. For Ba/F3 (stably transfected with rOSMR/rgp130 or rLIFR/rgp130) selection, the antibiotics hygromycin B (200 ng/ml) and geneticin (G418, 200 ng/ml) were freshly added to the medium. When Ba/F3 cells were cultured without mIL-3 (10 ng/ml), they received 500 ng/ml doxycycline to induce the expression of the respective receptors, for at least 24 h. When rLIFR/gp130 expression was initiated, cell proliferation was induced by treatment with 10 ng/ml hLIF. When rOSMR/rgp130 expression was initiated, rOSM (10 ng/ml) was added to the medium.

For longer cultivation of cell lines, continuous passaging of confluent or nearly confluent cells was performed. Therefore, suspension cells, as Ba/F3 cells, were first centrifuged at 1000 rpm, RT for 5 min. Old medium was removed and cells were diluted in fresh medium. The cells were then seeded using the respective passage ratio (e.g. one 10 cm dish of confluent cells was passaged 1:2, when the cells were seeded on two new 10 cm dishes). Adherent cells were washed with sterile PBS and treated with Trypsin/EDTA (e.g. 1 ml for a confluent 10 cm dish). To support the process of trypsination, cells were incubated in the incubator at 37°C. The time of incubation was dependent on the respective cell line (0.5-3 min). To stop the enzymatic reaction and to re-culture the cells, medium with 10% FCS was added and cells were seeded applying the particular dilution/passage ratio.

3.1.2 Freezing and thawing eukaryotic cells

For long term storage, non-adherent or adherent cells were removed from the cell dishes as described above and centrifuged at 1000 rpm (105 rcf), 4°C for 5 min. Medium or PBS was discarded and cells were resuspended in 1 ml cold DMSO-containing freezing medium (see materials, 2.14). Cells were pipetted into cryotubes

and a slow freezing process was achieved by using a Cryo-freezing device (Hartenstein, Würzburg). The Isopropyl alcohol filled device allows a slow and gentle freezing procedure, as it was cooled down with a rate of -1°C/min. After 24 h, the cryotubes were transferred to the liquid nitrogen tank for long term storage.
Thawing cells was performed by first warming the cryotubes in the water bath at 37°C. The almost thawed cell suspension was diluted using warm medium containing 10% FCS. The Falcon tubes were centrifuged at 1000 rpm (105 rcf), RT for 5 min, medium was discarded and cells were resuspended in the relative volume of prewarmed medium.

3.1.3 Isolation and culture of NRCM and NRCFB

One day before preparation NRCM culture medium and CBFHH (see materials, 2.14) were freshly prepared and all instruments (e.g. scissors) as well as beakers with agitators were autoclaved. Immediately before the neonatal heart excision, the trypsin solution was prepared (see materials, 2.14) and four 50 ml Falcon tubes were filled each with 7.5 ml FCS. These tubes, the trypsin solution, the preplating medium, the NRCM culture medium and the Medium 199 (10% FCS) were prewarmed in the water bath. A further 50 ml Falcon tube with 25-30 ml CBFHH was precooled on ice. The newborn rat was cleaned with 70% Ethanol, the head was rapidly cut off using biopsy scissors and the rat chest was opened utilizing round scissors. The heart was excised via tweezers and transferred into the Falcon tube containing cold CBFHH. These steps were repeated with all remaining newborn rats (approximately 22-26 pups, if two pregnant rats were ordered). The hearts together with a portion of CBFHH were transferred into a 10 cm dish on ice. Using the pike scissors and small tweezers, the atria were cut off and discarded and the ventricular parts of the hearts were gently squeezed to remove residual blood. The hearts were cut into small pieces and the tissue pieces were divided into two beakers with agitators using 10 ml trypsin solution. Then 5 ml of solution were added to each beaker and the tissue solution was incubated for 15 min at RT under the sterile bench while stirring. The supernatant was carefully removed and discarded. 20 ml new trypsin solution was added to each beaker and they were again incubated at RT while stirring for 10 min. Using wide-mouth pipettes, cells were pipetted up and down several times and transferred into the FCS containing Falcons. This step was repeated until the trypsin

solution was used up. The heart cells were subsequently pelleted via centrifugation at 800 rcf for 10 min (RT). The supernatants were discarded and the cells were suspended in 10 ml (per Falcon) preplating medium. The suspension was filtered into a new Falcon tube by use of a cell strainer (40 µm pore size) and 10 ml of the filtrate were seeded in a 10 cm culture dish, allowing four 10 cm dishes to be filled. For preplating the dishes were incubated for 1 hour in the cell incubator at 1% CO_2 and 37°C under water-saturated atmosphere. During this time period fibroblasts adhered to the bottom of the dishes, while cardiac myocytes remained in the supernatant. Meanwhile, cell dishes or plates were coated with fibronectin. For this purpose, CBFHH containing 10 µl/ml fibronectin solution (10 µg fibronectin per ml CBFHH) was added to the dishes or plates (e.g. 2 ml solution for wetting of a 6 cm dish) and incubated at RT for at least 15 min. The fibronectin solution was immediately removed before seeding NRCM.

After 1 hour the NRCM containing supernatant was transferred into a new tube. NRCFB were vigorously washed with PBS or Medium 199 (twice) and 10 ml Medium 199 containing 10% FCS was added. NRCFB were incubated at 37°C and 5% CO_2.

After reaching 90% confluency a few days later, the cells were counted (Countess®), passaged once at appropriated dilutions and seeded on new plates or dishes.

The NRCM suspension was mixed well and counted using the Countess® following the manufacturer`s instructions. The cells were diluted and the desired amount of cells (usually 1.5 - 2.0 x 10^6 cells per 6 cm dish for protein lysates or RNAs, 4 x 10^4 cells per 96 well for the hypertrophy assay) was seeded on fibronectin coated dishes or plates. NRCM designated for lysates or RNAs were diluted with medium containing 5% FCS and were incubated at 1% CO_2 at 37°C for 24 h. After 24 h the medium was replaced by NRCM culture medium containing 1% FCS. NRCM designated for the 96 well plate based hypertrophy assay were diluted in medium containing 1% FCS and incubated at 1% CO_2 at 37°C for 24 h. Afterwards the culture medium was replaced by NRCM medium containing 0.1% FCS to prevent serum based hypertrophic influences.

All NRCM were processed at day 3 after isolation to ensure reproducibility of the performed experiments. The cells were stimulated with the indicated cytokines for the indicated time periods.

3.2 Microscopic techniques to determine NRCM cell size

3.2.1 Immune fluorescence staining on NRCM

For performing hypertrophy assays with microscopic cell size determination, NRCM were seeded on 96 well plates (4.0 x 10^4 cells/well). 72 h after PE or IL-6-type cytokine treatment, supernatants were removed and cells were treated with 100 µl/well 4% PFA that was added dropwise. The fixation process was performed incubating the cells for 5 min on ice. Afterwards cells were washed thrice with PBS. The fixed cells were permeabilised with 0.2% Triton X-100 in PBS (100 µl/well) for 5 min at RT. NRCM were again washed 3 times with PBS. The primary antibody staining with the cardiomyocyte specific α-actinin antibody (1:1000 in PBS) was the next step of the immune fluorescence staining procedure. The cells were incubated for 30 min at 37°C followed by three further washing steps. The secondary antibody (Alexa488 conjugated anti-mouse IgG, 1:200 in PBS) was mixed with the DNA staining agent DAPI (1:100 dilution of a 20 mg/ml stock solution in PBS). 100 µl of the mixture was added to each well and the plates were incubated at 37°C for 30 min. After 3 additional washing steps, the cells were covered with a 50% Glycerol solution (200 µl/well). Afterwards cells were either used for the automated cell size measurement described in the next chapter, or for manual fluorescence microscopy with the AxioObserver.Z1 (20x objective) microscope.

3.2.2 Automated measurement of NRCM hypertrophy (hypertrophy assay): High content screening (HCS)

Cell size analysis was performed using an automated microscopy method acquiring determination of cell size and quantity. This method was previously established and published by Jentzsch *et al.*[257]. Since the working group of Stefan Engelhardt was our former lab neighbour, we had access to the original microscopic equipment and were kindly instructed by Claudia Jentzsch and Simon Leierseder. The above described immune fluorescence method for the staining of NRCM was the cellular base of the automated cell size determination. The following microscopic setup was used: The AxioObserver.Z1 (10x objective) microscope, a motorised scanning stage

(Märzhäuser, Wetzlar), the Retiga™ 4000DC CCD camera (QImaging, Surrey, Canada) and the Lumen200 fluorescence illumination unit from Prior (Cambridge, UK). Image acquisition was automated utilizing the so-called Journal record mode (Makro functions) of the MetaMorph Basic Imaging Software Package (Molecular Devices, Sunnyvale, USA). A main journal consisting of three sub journals was generated. The first sub journal coordinates the accurate positioning of the 96 well plate to the objective, the focusing of the 10x objective and the image acquisition of four images per well (the well is separated into four segments). The acquisition was performed consecutively for both fluorescence channels. The second sub journal coordinates the 384 images (per 96 well plate) from one fluorescence channel and copies them to one stack. A third stack is generated by merging both previously generated stacks and can be used for later illustrations. The next subjournal determines cell size and quantity via the MetaMorph plug-in “Cell Scoring” that was adjusted to the expected diameters and fluorescence intensities. This mode was terminally applied to the previously generated stacks.

3.3 Molecular biological methods

3.3.1 Proliferation assay using Ba/F3 cells and the WST-1 Cell Proliferation Assay Kit

Proliferation assay was performed using stably transfected Ba/F3 cells expressing hgp130/hOSMR, a kind gift from Prof. Dr. J. Heath (Birmingham, UK)[256]. The cells were thawed as described above. Cells were cultured in culture flasks in the presence of RPMI containing 10% FCS and 10 ng/ml mIL-3. After several days of culture cells were counted via the Countess®, diluted in the appropriate amount of medium and seeded on a 96 well plate. Cells were seeded at a concentration of $1x10^4$ cells per 96 well and treated with different concentrations of hOSM or rOSM (0, 0.0064, 0.032, 0.16, 0.8, 4, 20 and 100 ng/ml) for 48 h (incubation at 37°C and 5% CO_2 in water-saturated atmosphere). The experiment was performed in triplicates, as every experimental group existed thrice. After the incubation period, 10 µl premixed WST-1 reagent were added to every well. The cells were incubated for four additional hours at 5% CO_2 and 37°C. Subsequently the plates were vortexed gently to

disperse the reagent, and the absorbance of the wells was measured at 450 nm and 660 nm (reference wavelength) using the Multiskan EX Microplate Photometer. The results of the assay were calculated by subtracting the A660 reference value from the A450 value.

3.3.2 Rat IL-6 ELISA using the Rat IL-6 Quantikine ELISA Kit

NRCFB (P1) were seeded at a density of $3x10^4$ cells per 24 well. The cells were stimulated for the indicated time and supernatants were collected subsequently. The samples were stored at -80°C until use. The rat IL-6 Quantikine ELISA Kit was purchased from R&D Systems (Minneapolis, USA) and the experimental protocol was performed according to manufacturer`s recommendations. Absorbance was measured using the Multiskan EX Microplate Photometer according to the recommendation of the Quantikine ELISA protocol.

3.3.3 Reverse transcription of rgp130, rOSMR and rLIFR for subsequent cloning

RNA was isolated from JTC-27 rat hepatoma cells using the RNeasy mini Kit according to the manufacturer's instructions. 5 µg RNA were used for every reverse transcription reaction performed with the Transcriptor First Strand cDNA Synthesis Kit. The following approach was pipetted: 5 µg RNA (in 50 µl final volume) were mixed with 5 µl anchored-oligo$(dT)_{18}$ primers, 10 µl random hexamer primers, 20 µl 5x Transcriptor RT reaction buffer, 2.5 µl protector RNase inhibitor, 10 µl dNTP-Mix and 2.5 µl Transcriptor reverse transcriptase. The 100 µl samples were gently mixed using the pipette. The samples were shortly centrifuged (short spin) and transferred to the Eppendorf Mastercycler® pro. The reverse transcription run was performed according to the following steps: 60 min at 50°C (reverse transcription) and 5 min at 85 °C (inactivation). The resulting cDNA samples were subsequently cooled to 4°C.

3.3.4 PCR amplification of long cDNA products (rgp130, rOSMR and rLIFR)

To generate PCR products containing specific restriction enzyme sites, the cDNA templates were used to amplify the complete coding sequence of each receptor with

specific primers containing restriction sites flanking the start or stop codon (see 2.7) and the PCR Extender System. The kit was used according to the manufacturer`s instructions and the following pipetting scheme was applied: Mastermix I (total volume: 10 µl): 2.0 µl of each primer (10 µM stock), 100-500 ng template cDNA and nuclease free H_2O, Mastermix II (total volume: 40 µl): 5 µl 10x tuning buffer, 2.5 µl dNTP mix (10 mM each), 0.4 µl PCR Extender polymerase mix and 32.1 µl nuclease free H_2O. Final concentrations were: 400 nM of each primer, 500 µM of each dNTP and 2 U polymerase mix in the entire reaction. Both solutions were mixed shortly before transferring the resulting mixture to the Mastercycler® pro. The run was performed using the following conditions: 2 min initial template denaturation at 94°C, 45 cycles of template denaturation (20 sec at 94°C), primer annealing (20 sec at 56°C for rgp130 and rOSMR, 20 sec at 66°C for rLIFR) and product elongation (4 min at 68°C) followed by a final extension step (6 min at 68°C) and cooling down to 4°C. After gel extraction (see 3.3.4 and 3.3.5), the products were subsequently exposed to restriction enzyme digestion (described in 3.3.6). After additional gel extraction, the processed fragments served as inserts for ligation with linearised pBO (see 3.3.7).

3.3.5 Horizontal Agarose Gel Electrophoresis (DNA electrophoresis)

DNA fragments were separated according to their size using agarose gel electrophoresis. 0.8-1.0% agarose gels were used to separate larger DNA fragments (2 kb to ≥ 12 kb), while 1.5-2.0% agarose gels were applied to separate DNA fragments up to a size of 1 kb. Gels were produced solving the appropriate amount of agarose in 1x TAE buffer (diluted from 50x TAE buffer) and heating the solution several times in a microwave. The gel was allowed to cool down for 5 min and ethidium bromide (0.3-0.5 µg/ml) was added. Ethidium bromide intercalates between both DNA strands thus visualising a DNA band under UV light (λ=312 nm). The agarose gel was cast using the adjustable casting chamber and the appropriate combs (Peqlab, Erlangen). The DNA samples were diluted with 6x DNA loading buffer and the resulting stained samples as well as the appropriate DNA ladder (see materials, 2.11) were loaded onto the gel. The electrophoresis chamber was filled with 1x TAE buffer and electrophoresis performed at 80-120 V.

3.3.6 Purification of separated DNA fragments from agarose gels

To regain PCR products or restricted DNA fragments from an agarose gel, the respective gel slice was cut out using a fresh disposable scalpel and purified using the QIAquick Gel Extraction Kit according to the instructions of the manufacturer. The DNA fragment was eluted with nuclease free H_2O and the amount and purity were determined using the NanoPhotometer® P 300. PCR products were further used for restriction enzyme digestion, whereas already digested and purified DNA fragments were ligated to an appropriate vector.

3.3.7 Digestion of DNA using restriction enzymes

The purified inserts as well as the plasmid (pBO) were digested with matching restriction enzymes, whose recognition sequences are present in the MCS of pBO and the designed receptor primers. The rgp130 amplicon (1.5 ng) and 1.6 ng pBO (MCS I) were digested with 1 µl AgeI (1 FDU) and 1 µl NotI (1 FDU) fast digest enzymes for 30 minutes at 37°C (total reaction volume was 10 µl including the template, the enzymes, 1 µl FD buffer (10x) and nuclease free H_2O). The rOSMR (1.5 ng), rLIFR (1.5 ng) amplicon and 1.5 ng pBO-rgp130 (MCS II) were digested with 2 µl SbfI (20 U) for 4 h at 37°C. For the last hour, 5 µl FseI (10 U) was added to the solution (total reaction was 50 µl including enzymes, template, 5 µl NEB buffer 4 (5x) and nuclease free H_2O). The completeness and success of the reaction were determined via agarose gel electrophoresis, as described above. The desired fragment was subsequently extracted and purified, as described in 3.3.5.

3.3.8 Ligation of inserts and vector with T4 DNA Ligase

Purified AgeI/NotI restricted rgp130 was ligated with purified AgeI/NotI restricted pBO using T4 DNA ligase. The following pipetting scheme was used: 2 µl 10x T4 DNA ligase buffer, 50 ng vector DNA (6210 bp), 4-8-fold molar excess of insert DNA (e.g. 135 ng of rgp130 DNA corresponds to a 4 molar excess of insert; rgp130 DNA consisted of 2780 bp after digestion), 1 µl T4 DNA ligase and nuclease free water to a total volume of 20 µl. A stepwise ligation was performed, because rgp130 was first

inserted into pBO. Then the generated vector (pBO-rgp130) was transformed into XL10-Gold bacteria and purified with the QIAGEN Plasmid Mini Kit according to the manufacturer´s instructions (see next chapters). pBO-rgp130, the rOSMR and the rLIFR were subsequently restricted with FseI and SbfI, as described above. The resulting fragments were again ligated, thus generating pBO-rgp130-rOSMR (@164) and pBO-rgp130-rLIFR (@164). Portions of the ligation mixtures were subsequently transformed into XL10-Gold (see 3.3.8).

3.3.9 Transformation of ligated vectors into XL10-Gold

Before transformation, XL10-Gold cells were thawed on ice. Cells were gently mixed and aliquoted in prechilled culture tubes (50 µl per transformation). 2 µl β-mercaptoethanol (provided with the cells) were added to the bacteria solutions, the tubes were gently swirled and the cells were incubated on ice for 10 min. During this incubation period an additional swirling step was performed every 2 min. 5 or 10 µl of the respective ligation product were added to an aliquot of ultracompetent cells and the tubes were incubated for 30 min on ice. After this, the tubes were rapidly transferred to a water bath (42°C) for 40 sec. Thus, a heat-shock was induced which initiated the uptake of the vectors. The cells were incubated on ice for 2 min and 450 µl of NZY^+ (preheated) were added. The culture tubes were transferred to the incubator shaker and incubated for 1 h at 37°C at 250 rpm. 250 and 50 µl, respectively, of the transformed bacteria were plated on LB agar plates containing 100 µg/ml ampicillin. The bacteria were incubated over night at 37°C. The next day, colonies were counted and used for plasmid purification and determination of correct insertion (see 3.3.9).

3.3.10 Plasmid purification using the QIAGEN Plasmid Mini Kit

After bacterial colonies were grown on petri dishes over night, clones were picked and inoculated in 4 ml LB-medium (containing 100µg/ml ampicillin) for further over night culture in the incubator shaker at 37°C and 225 rpm. 2 ml of these cultures were utilised for small scale purification of the plasmid DNA. Cells were pelleted through centrifugation at 6000 g for 3 min. Lysis of the bacteria and plasmid isolation

were achieved using the QIAGEN Plasmid Mini Kit according to the manufacturer´s instructions. The DNA was eluted in 50 µl EB buffer (provided with the kit). The correct insertion of the inserts was analysed using appropriate restriction enzymes and gel electrophoresis. At last samples were sent to Eurofins MWG (Ebersberg) for sequencing the generated finished construct.

3.3.11 Plasmid purification using the QIAGEN Plasmid Maxi Kit

For large scale purification of plasmids, over night cultures were inoculated, as described in 3.3.9. For this purpose, 5 ml LB-medium (containing 100 µg/ml ampicillin) were inoculated with a swipe of a glycerol stock (mixture of 200 µl bacteria culture + 800 µl glycerol, used for long term storage at -80°C) using the inoculation loop. After over night culture (as described above), 250 ml LB-medium (containing 100 µg/ml ampicillin) were inoculated with 1 ml of the first small over night culture. Cells were incubated in the incubator shaker over night at 37°C and 225 rpm. The next day, bacteria were pelleted through centrifugation at 4°C and 6000 g for 15 min. Lysis of the cells and plasmid purification was performed using the HiSpeed Plasmid Maxi Kit according to the instructions of the manufacturer. The purified DNA was eluted in 1 ml TE buffer provided with the kit.

3.3.12 DNA sequencing

The sequencing of the purified plasmid/construct DNA was performed by Eurofins MWG (Ebersberg). For this purpose, 15 µl (per sequencing reaction) of a 75-100 ng/µl DNA solution and the appropriate sequencing primers were shipped to Eurofins MWG. The sequencing data were verified through alignment analysis using the GENtle software (Magnus Manske, Köln, http://gentle.magnusmanske.de).

3.3.13 Stable transfection of murine Ba/F3 cells

First, Ba/F3 cells were transfected with the 2.5 µg of the pTet-ON (neo) plasmid using the 4D-Nucleofector® according to the manufacturer’s instruction. For approximately 2 weeks, positive cells were selected using geneticin (G418 (200

ng/ml)) that was freshly added every day together with fresh RPMI medium (10% FCS and 10 ng/ml mIL-3). Cells without the neomycin cassette from the pTet-On were dying during selection. The remaining neomycin resistant pool of cells was then transfected with 2.5 µg of the pBO-rgp130/rLIFR (@166) or the pBO-rgp130/rOSMR (@164) plasmid again using the 4D-Nucleofector® according to the manufacturer`s instructions. As described above, cells were again selected for several days using 200 ng/ml hygromycin and 200 ng/ml geneticin (G418). A hygromycin/neomycin-resistant pool of cells was then used to induce the respective receptor combination expression through treatment with 0.5 µg/ml doxycycline. Now the cells were able to proliferate in the presence of hLIF (Ba/F3-rgp130/rLIFR) or rOSM (Ba/F3-rgp130/rOSMR) and in the absence of mIL-3. For Western blot analysis cells were treated over night with 0.5 µg/ml doxycycline. The next day, they were stimulated with 10 ng/ml hLIF, 20 ng/ml hOSM, mOSM or rOSM for 15 min and lysed subsequently.

3.3.14 Semiquantitative RT-PCR using the QIAGEN OneStep RT-PCR Kit

Semiquantitative reverse transcription polymerase chain reaction (RT-PCR) for the analysis of mRNA expression was performed using the QIAGEN OneStep RT-PCR Kit. Total RNA from transfected and/or stimulated cells was isolated using the RNeasy Mini Kit according to the manufacturer's protocol. RNA concentration and purity was determined using the Implen NanoPhotometer. Reverse transcription and following PCR were performed with 1 µg isolated total RNA, aforementioned oligonucleotide primers (material section) and the kit. The following pipetting scheme was applied: Mix I: 1 µl of each primer (4 µM, 200 nM final concentration), 4 µl RT-PCR reaction buffer (5x), 0.8 µl dNTP-Mix (10 mM of each, 400 µM final concentration), 0.4 µl nuclease free H_2O and 0.8 µl RT-PCR enzyme-mix, Mix II: 1 µg RNA was diluted with nuclease free H_2O to a final volume of 10 µl. Both solutions were gently mixed, shortly centrifuged (short spin) and transferred to the cycler. The RT-PCR run was performed on a Mastercycler® pro as follows: reverse transcription at 50°C for 30 minutes, 15 minutes initial activation of the HotStartTaq DNA polymerase and denaturation of reverse transcriptase at 95°C, 32-35 cycles of 94°C for 30 seconds (denaturation), 58°C for 30 seconds (primer annealing) and 72°C for 1 minute (elongation). The program was finalised by 10 minutes at 72°C (finale

elongation). As described above, DNA products were separated via a 1.5% agarose gel electrophoresis. DNA bands were detected using ethidium bromide staining.

3.3.15 Semiquantitative RT-PCR using the Verso 1-Step RT-PCR Kit

RT-PCR analysing the existence of the rat receptor mRNAs in the stably transfected Ba/F3 cells (3.3.13) were performed using the Verso 1-Step RT-PCR Kit. Total RNA was isolated from Ba/F3 cells ("empty", rgp130/rOSMR, rgp130/rOSMR + 0.5 µg/ml doxycycline (24 h), rgp130/rLIFR, rgp130/rLIFR + 0.5 µg/ml doxycycline (24 h)) using the RNeasy Mini Kit according to the instructions of the manufacturer. The following pipetting scheme was applied: Mix I (5 µl): 100 ng RNA in 5 µl total volume. Mix II (25 µl): 1.25 µl of each primer (4 µM, 200 nM final concentration), 12.5 µl Verso 1-Step RT-PCR Master Mix (2x), 1.25 µl RT-Enhancer, 3.25 µl nuclease free H_2O and 0.5 µl RT-PCR enzyme-mix. Mix I and II were gently mixed, shortly centrifuged (short spin) and transferred to the cycler. The run was performed on a Mastercycler® pro as follows: reverse transcription at 50°C for 15 minutes, 2 minutes initial activation (of the Thermo-Start *Taq* DNA polymerase) and denaturation of reverse transcriptase at 95°C, 45 cycles of 95°C for 20 seconds (denaturation), 53°C for 30 seconds (annealing) and 72°C for 1 minute (elongation). The program was finalised by 72°C for 5 minutes (final elongation). DNA products were separated via a 2.0% agarose gel. DNA bands were detected using ethidium bromide staining.

3.3.16 Quantitative real time RT-PCR (qPCR)

Quantitative analysis of gene expression was assessed by real time RT-PCR (qPCR) analysing the mRNA expression levels. Total RNA was isolated by use of the RNeasy Mini Kit and RNase-Free DNase Set according to the manufacturer's protocol. An initial reverse transcription PCR was performed using the Transcriptor First Strand cDNA Synthesis Kit according to the recommendations of the manufacturer. The following pipetting scheme was used: 1 µg RNA (in 10 µl final volume) were mixed with 1 µl anchored-oligo$(dT)_{18}$ primers, 2 µl random hexamer primers, 4 µl Transcriptor RT reaction buffer, 0.5 µl Protector RNase inhibitor, 2 µl dNTP-Mix and 0.5 µl Transcriptor reverse transcriptase. The 20 µl reactions were gently mixed with a pipette. The samples were shortly centrifuged (short spin) and

transferred to the Eppendorf Mastercycler® pro. The reverse transcription run was performed according to the following steps: 60 min at 50°C (reverse transcription) and 5 min at 85 °C (inactivation). The cDNA samples were subsequently cooled to 4°C. The resulting cDNA was used to perform real time PCR with the FastStart Universal Sybr Green Master (Rox), as instructed by the manufacturer. Primers applied in qPCR experiments are mentioned in the material section, chapter 2.6 (Oligonucleotide primer for quantitative real time RT-PCR). Serial dilutions of template cDNAs were used to verify primer efficiencies. For each target mRNA to be analysed, 5 µl of Sybr Green master mix, 400 nM of each primer (0.4 µl of a 10 µM stock), 2.2 µl nuclease free H_2O and 2 µl of the respective cDNA were mixed on 384 well plates in duplicates using the automated liquid handling robot QIAgility. Real time PCR was performed on a real time PCR cycler (ABI PRISM 7900HT) under the following conditions: initial activation of 10 minutes at 95˚C, followed by 40 cycles of 15 seconds denaturation at 95˚C, 20 seconds hybridisation at 60˚C, 20 seconds elongation at 60C and a final elongation at 65˚C for 15 seconds. The additional recording of the melting curves for determining the exclusiveness of the amplicons and the right melting temperature consisted of 15 seconds at 95˚C and 15 seconds at 60˚C (last step of the PCR run). Quantification of target messages was performed by applying the mathematical model described by Pfaffl[258].

3.3.17 Cell stimulation and lysis

Stimulated and/or transfected cells were lysed for use in SDS-PAGE and Western blotting procedure. At first, cells were stimulated with the cytokines mentioned in the figure legends, for the indicated times. While hsIL-6R was directly added before stimulation with hIL-6, indicated concentrations of the LIFR specific antagonist LIF-05 were preincubated 30 min before cells were stimulated with additional cytokines. After stimulation periods, cells were instantly washed with cold PBS and lysed with either Triton X-100 lysis buffer at 4°C (containing 1 mM Na_3VO_4, 3 µg/ml pepstatin, 1 mM PMSF, 5 µg/ml aprotinin, 5 µg/ml leupeptin and 10 µl/ml Halt Phosphatase Inhibitor Cocktail), or with 1x Laemmli buffer (63 mM Tris HCl, 10% Glycerol, 2% SDS, 0.0025% Bromophenol blue and 5% β-mercaptoethanol, pH 6.8) for all protein lysates from siRNA transfected cells. After addition of Triton X-100 lysis buffer, adherent cells were scraped using a rubber cell scraper. The solution was transferred

to an Eppendorf reaction tube and incubated on ice for 30 min. Lysed cells were subsequently centrifuged in a cooled Eppendorf centrifuge at 15000 rpm (21130 rcf) for 15 min at 4°C. Supernatants were transferred into new 1.5 ml reaction tubes. Lysates were stored at -20°C and gently thawed before further use. Prior to loading to a protein gel, equal protein portions of the samples were diluted with Laemmli buffer and heated for 5 min at 95°C. Cells were centrifuged (short spin) and loaded. Cells directly lysed in Laemmli were detached from the plates/dishes utilizing a polyethylene cell scraper. After cell lysis, lysates were incubated for 15 min on ice and heated at 95°C for 5 min before loading. They were kept at -20°C for long term storage.

3.3.18 SDS-PAGE (Sodium dodecyl sulfate polyacrylamide gel electrophoresis)

The separation of polypeptides according to their mass was performed using the denaturating SDS-PAGE under reducing conditions, as described by Laemmli[259]. SDS gels were cast applying the above mentioned gel formula (see 2.14) and the Biometra Multigel or Maxigel system. First the separating gel was cast between both glass plates (provided with the Biometra gel systems) and covered with isopropyl alcohol. After polymerisation of the gel, the isopropyl alcohol was discarded and the plates were dried. Then the stacking gel was cast and the appropriate comb was immediately inserted. After polymerisation of the stacking gel the pockets were washed and the gel chamber filled with 1x running buffer. For the experiments described in this work, only 10% separation gels and 3% stacking gels were produced. After loading the samples, electrophoresis was performed at 25-50 mA amperage for 2-3 h. Besides the samples, the PageRuler™ Plus Prestained Protein Ladder and the Biotinylated Protein Ladder were loaded to the gel. The anionic part of the detergent SDS binds to side chains of proteins after constant distances and thus masks the electrical charges of the protein. By addition of SDS, proteins can be separated according to their size irrespective of their own charges. Moreover, SDS interrupts hydrogen bonds and, in combination with β-mercaptoethanol, denatures polypeptides.

3.3.19 Semi-dry Western blot

After proteins were separated according to their size via 10% SDS-polyacrylamide gel electrophoresis, they were transferred to a PVDF (polyvinylidene fluoride) membrane via semi-dry Western blotting. The membrane and 12 layers of whatman paper were cut to the required gel size. The PVDF-membrane was activated through immersion in 100% methanol for a few seconds. Afterwards the membrane was shortly washed in H_2O (Millipore) and equilibrated in anode II buffer. Meanwhile, the gel was extracted from the glass plates and equilibrated in cathode buffer. The whatman papers were equilibrated in the appropriate buffer and the assembly was performed according to the following conditions (from the bottom (anode) to the top (cathode)): 5 whatman paper soaked in anode I buffer, 2 whatman paper soaked in anode II buffer, the PVDF-membrane soaked in anode II buffer, the gel soaked in cathode buffer and 5 whatman paper soaked in cathode buffer. The blotting chamber was gently closed and electric current was applied. The applied amperage was defined as follows: 0.8 x area of the membrane (cm^2) = used amperage (mA) (e.g. 50 cm^2 area of the membrane x 0.8 = 40 mA). The procedure was operated for 65 min. After protein transfer, membranes were blocked using 10% Western blot grade BSA (in TBS-T) for 50 minutes. Membranes were subsequently incubated over night with indicated primary antibodies at 4°C on a shaker. The next day, membranes were washed thrice for 10 minutes each in 1x TBS-T, incubated with the respective horseradish peroxidase (HRP) conjugated second antibody for 1 h at room temperature, followed again by three washing steps. Western blot analysis was finalised by using an enhanced chemiluminescence Kit according to the manufacturer's instructions. For detecting the chemiluminescence signal, a quantitative Western blot imager from ProteinSimple, the FluorChem Q, was used. Before washing, blocking and reprobing of the blots to detect the unphosphorylated protein loading controls and/or independent α-tubulin detection, the membranes were incubated in stripping buffer (at 70°C for 20 min) to remove primary and secondary antibodies. When a second phospho-protein was detected on the same membrane, the blots were incubated in London stripping buffer supplemented with a point of a spatula of SDS. After incubating the membranes for 2 h on a shaker and additional 3 h without shaking, blots were washed three times, blocked and reprobed with the respective antibody. These procedures were performed as described above.

3.3.20 Small interfering RNA (siRNA) transfection

For siRNA transfections, JTC-27 cells were seeded on 6 cm plates at a density of 3.0 x 10^5 cells/plate, while HepG2 and Hepa1c1c7 were cultured on 6 wells at a density of 2.0 x 10^5 cells/well. After 24 h incubation (37°C, 5% CO_2), growth media were removed and replaced by Opti-MEM®. DharmaFECT 4 was used as transfection reagent for transient JTC-27 transfections and Lipofectamine 2000 was chosen for transient HepG2 and Hepa1c1c7 transfections. Both transfection reagents were applied according to the manufacturer´s instructions. The respective siRNA as well as the transfection reagent were each prediluted in Opti-MEM® without FCS. Then both solutions were mixed and incubated for 30 minutes. JTC-27 cells were transfected with a final concentration of 100 nM siRNA, whereas HepG2 and Hepa1c1c7 were transfected with 50 nM siRNA final concentration. After the incubation period the mixtures were added dropwise and cells were incubated for 5 h at 37°C and 5% CO_2 without serum. After 5 h incubation, Opti-MEM® containing excessive FCS for adjustment of a final concentration of 10% FCS was added. Cells were incubated for 28 h (Hepa1c1c7) or 48 h (HepG2 and JTC-27). After incubation, cells were stimulated as mentioned in the figure legends and further investigated. The transfection efficiencies were analysed on RNA level using RT-PCR or qPCR. In Hepa1c1c7 and HepG2 cells the protein levels were additionally analysed performing Western blots.

4 Results

4.1 Analysis of IL-6-type cytokine induced hypertrophy

Previous studies have indicated that stimulation of the LIFR/gp130 receptor complex via LIF[196, 217] or CT-1[194, 195, 201, 218] as well as of the IL-6R/gp130 receptor complex via IL-6[199, 260] induces hypertrophy and morphological changes in neonatal rat cardiomyocytes (NRCM). One of the central questions in this first part of the thesis was, which kind of hypertrophy IL-6-type cytokines induce in comparison to the α_1-adrenergic agonist PE and whether different IL-6-type cytokines act in a comparable manner, particularly since for OSM only limited information is available. The currently best established model for the analysis of cardiomyocyte hypertrophy uses neonatal rat cardiomyocytes. However, not for all IL-6-type cytokines rat recombinant proteins were available. Therefore, cross-species activities have to be taken into account. Previous publications have demonstrated that human OSM (hOSM) exclusively utilises LIFR/gp130 heterodimers (type I receptor complex) on murine cells[74], while murine OSM (mOSM) utilises the murine type II (OSMR/gp130) receptor complex[74, 75]. Moreover, human IL-6 (hIL-6) has been shown to stimulate murine and rat cells as potent as murine IL-6[261]. Human LIF (hLIF) that was used for many studies with cells of rat and murine origin has been demonstrated to strongly activate rodent cells by utilising the heterodimeric LIFR/gp130 complex[23-25, 36]. Human Cardiotrophin-1 (hCT-1) has been shown to stimulate murine and rat cells equally potent as murine CT-1[262]. In contrast to all other mentioned IL-6-type cytokines, the murine variant of CT-1 is also able to signal through the human receptor complex[262].

Therefore, we decided to analyse the hypertrophic potential of hOSM, mOSM, hLIF, hIL-6 with and without human soluble IL-6R (hsIL-6R) and of hCT-1. Since IL-6 signal transduction is achieved via g130 homodimerisation requiring two IL-6 molecules for the activation of one gp130 homodimer[18-20], we used the twofold amount of IL-6 (20 ng/ml) in comparison to all other cytokines (10 ng/ml hOSM, mOSM, hLIF and hCT-1). The latter cytokines utilise gp130/LIFR heterodimers or gp130/OSMR heterodimers, respectively, requiring only one cytokine molecule for the activation of one receptor heterodimer[23-27, 30, 31]. The induced hypertrophic phenotype was

determined regarding hypertrophy type and cytokine capacity 72 h after stimulation of NRCM via fluorescence microscopy/automated cell size measurement.

4.1.1 Hypertrophy assay of IL-6-type cytokine treated NRCM

Upon isolation of NRCM as described in the methods section, the cells were cultured for three days prior to treatment with the mentioned IL-6-type cytokines for 72 h.

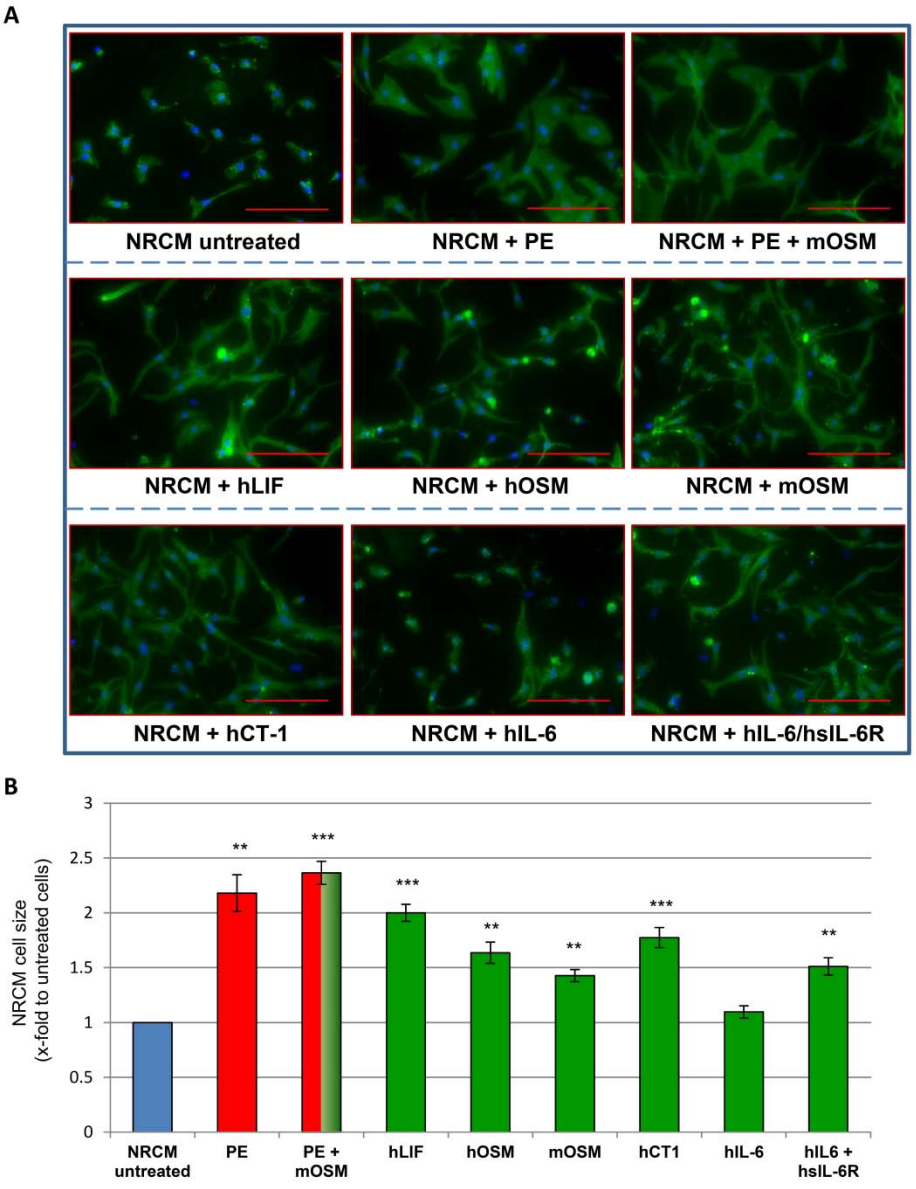

Figure 6: Hypertrophic properties of IL-6-type cytokines on NRCM

NRCM (cultured for three days) were treated for 72 h with 50 µM PE, 50 µM PE + 10 ng/ml mOSM, 10 ng/ml hLIF, hOSM, mOSM, hCT-1 or 20 ng/ml hIL-6 (± 0.5 µg/ml hsIL-6R). **A**, Representative immunostainings of NRCM using a sarcomere specific α-actinin antibody and DAPI for visualisation of nuclei (stimuli as indicated, scale bar: 100 µm, 20x objective). **B**, The diagram represents cell size values corresponding to the immunostainings shown in A. Mean values of four experiments with standard error of mean (SEM) are displayed. Statistical significance was calculated against untreated NRCM using a two-tailed, paired Student's t-test, ** $p<0.01$, *** $p<0.001$.

A clear but differentially strong hypertrophic answer of the analysed NRCM has been observed (Fig. 6). While PE predominately mediates a concentric type of hypertrophy (cells increase in length and width), all used IL-6-type cytokines induce a more eccentric type of hypertrophy (cell length, but not width, is critically increased). Human LIF is the strongest inducer of hypertrophy among the tested IL-6-type family members and has a hypertrophic potential comparable to PE (induction od twofold cell size increase).

All other IL-6-type cytokines cause 1.4- to 1.8-fold cell size increases (hOSM 1.6-fold, mOSM 1.4-fold, hCT-1 1.8-fold and hIL-6/hsIL-6R 1.5-fold cell size enlargement). Although hIL-6 together with its soluble α-receptor (trans-signalling) is able to induce hypertrophy comparable to mOSM, pure hIL-6 mediates no measureable cell growth stimulatory effect providing first evidence for a lack of IL-6R on the NRCM cell surface.

4.1.2 IL-6-type cytokines induce changes of the sarcomeric assembly

The fluorescence microscopy was additionally used for analysis of sarcomeric changes that are induced by IL-6-type cytokines. Alpha-actinin staining allows optical visualisation of the Z-lines of sarcomers. Thus degradation, reorganisation or addition of sarcomers can be detected after treatment of NRCM with hypertrophic stimuli.

The enlarged immunostainings clearly show that PE treated NRCM possess perfectly organised Z-lines, and the sarcomeric architecture seems to be retained (Fig. 7, left).

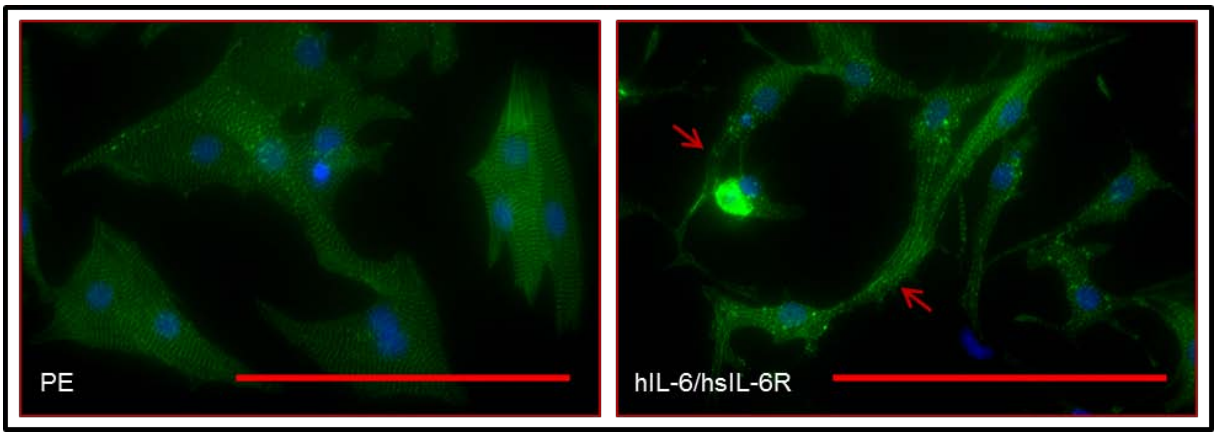

Figure 7: Partial loss of the Z-line pattern in IL-6-type cytokine treated NRCM
Detailed section (scale bar: 100 µm, 20x objective) of PE (left) and hIL-6/hsIL-6R (right) treated NRCM (for details see Fig. 6) stained with an α-actinin-FITC antibody (green) and DAPI (blue).

In contrast, IL-6-type cytokine treated NRCM (e.g. hIL-6/hsIL-6R) show a lack of Z-lines in some locations (Fig. 7, right, marked by red arrows). In these regions the typical T-shaped structure of the sarcomers is interrupted indicating strong remodelling of sarcomeric proteins in the contractile units of the cardiomyocytes or the cardiac muscle, respectively.

4.1.3 Time dependent analysis of IL-6-type cytokine induced signalling in NRCM

One major part of this study is describing the IL-6-type cytokine induced signalling pathways in NRCM. To understand the hypertrophic actions and differences in the potential of hypertrophy initiation, the known relevant pathways activated in response to hLIF, hOSM, mOSM, hCT-1, hIL-6 (with and without hsIL-6R) were analysed in detail. Hence, the time kinetics (up to 60 min) of the cytokine mediated phosphorylations of STAT3, STAT1 and the MAPK ERK1/2 were analysed in NRCM (Fig. 8). pY705-STAT3 and STAT3 are detected at 79, 86 kDa (α and β isoform, respectively), pY701-STAT1 and STAT1 at 84, 91 kDa (α and β isoform, respectively), pT202-pY204-ERK1 and -ERK2 at 44 and 42 kDa, respectively.

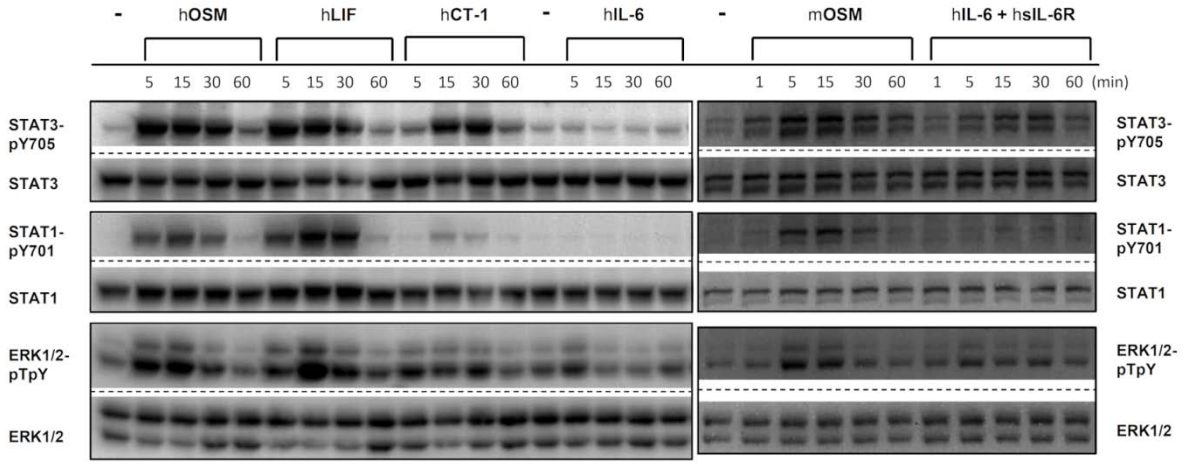

Figure 8: IL-6-type cytokines induce phosphorylation of STATs and ERK1/2 in NRCM with different strength and duration

NRCM (cultured for three days) were stimulated for the indicated time periods with 10 ng/ml hOSM, hLIF, hCT-1, mOSM, 20 ng/ml hIL-6 or 20 ng/ml hIL-6 + 0.5 µg/ml hsIL-6R. Phosphorylation levels of STAT3 (pY705) and STAT1 (pY701) as well as ERK1/2 (pT202/pY204) were detected via Western blot analysis. The blots were stripped and reprobed with antibodies recognising the proteins irrespective of their activation status (STAT3, STAT1 and ERK1/2). Blots shown are representative for three independent experiments.

As shown in figure 8, hOSM and hLIF are potent activators of STAT3, STAT1 and ERK1/2 phosphorylation. The signalling pathways are activated in a time dependent manner with phosphorylation maxima at 15 min past stimulation. 60 min after cytokine treatment, the observed pathways are hardly stimulated above basal status. While hCT-1 is also able to strongly induce activation of STAT3, only a weak ERK1/2 and STAT1 phosphorylation can be observed after treatment of NRCM with the cytokine. The signalling pathway composition and kinetics induced by mOSM are highly comparable to those initiated by hOSM and hLIF. IL-6 on its own is not able to induce STAT activation, however a very transient ERK1/2 phosphorylation is observed. Nevertheless, IL-6 together with its soluble α-receptor (sIL-6R) induces a moderate STAT3 phosphorylation. However, it has to be mentioned that responses to hIL-6/hsIL-6R were variable between different experiments regarding the phosphorylation intensities.

4.1.4 Receptor preference of hOSM and mOSM on NRCM

Up to now, the receptor usage of mOSM and hOSM on cells of rat origin was not definitely clarified. Detailed information from murine cells demonstrated that mOSM, unlike hOSM, exclusively signals via the type II OSMR/gp130 receptor complex[74]. Treatment of murine cells with hOSM activates the type I LIFR/gp130 complex, but not the type II receptor complex[74, 75]. To analyse the receptor complexes used by hOSM and mOSM on rat cells (NRCM), the cells were pretreated with various concentrations of the LIFR specific antagonist LIF-05[254] (30 min, indicated concentrations) followed by 15 min hOSM or mOSM stimulation (Fig. 9). LIF-05 pretreatment strongly reduces the hOSM induced activation of various signalling pathways (phospho-STAT3, phospho-STAT1, phospho-STAT5 and ERK1/2) in a concentration dependent manner (Fig. 9, compare lanes 3-6). For STAT1, STAT5 and ERK1/2 activation, 5ng/ml LIF-05 were sufficient to completely abolish the hOSM mediated activation, while application of 20 ng/ml LIF-05 was required to achieve complete inhibition of STAT3 activation (Fig. 9, first panel). In contrast, mOSM induced activation of all analysed signalling proteins remains mostly unaffected upon LIF-05 pretreatment (Fig. 9, compare lanes 7-10). This strongly suggests that hOSM signals via the type I LIFR/gp130 complex on NRCM, as it does on murine cells, and that mOSM exclusively utilises the type II OSMR/gp130 complex. Higher

concentrations of LIF-05 (≥20 ng/ml) have a weak influence on the mOSM induced STAT phosphorylations, however, this might be due to the observation that the basal phosphorylation levels of STAT3 and STAT1 are decreased as well by LIF-05 (compare lanes 1 and 2). In chapter 4.4 the examined receptor preferences of hOSM, mOSM and rOSM on rat, murine and human cells will be further described in detail.

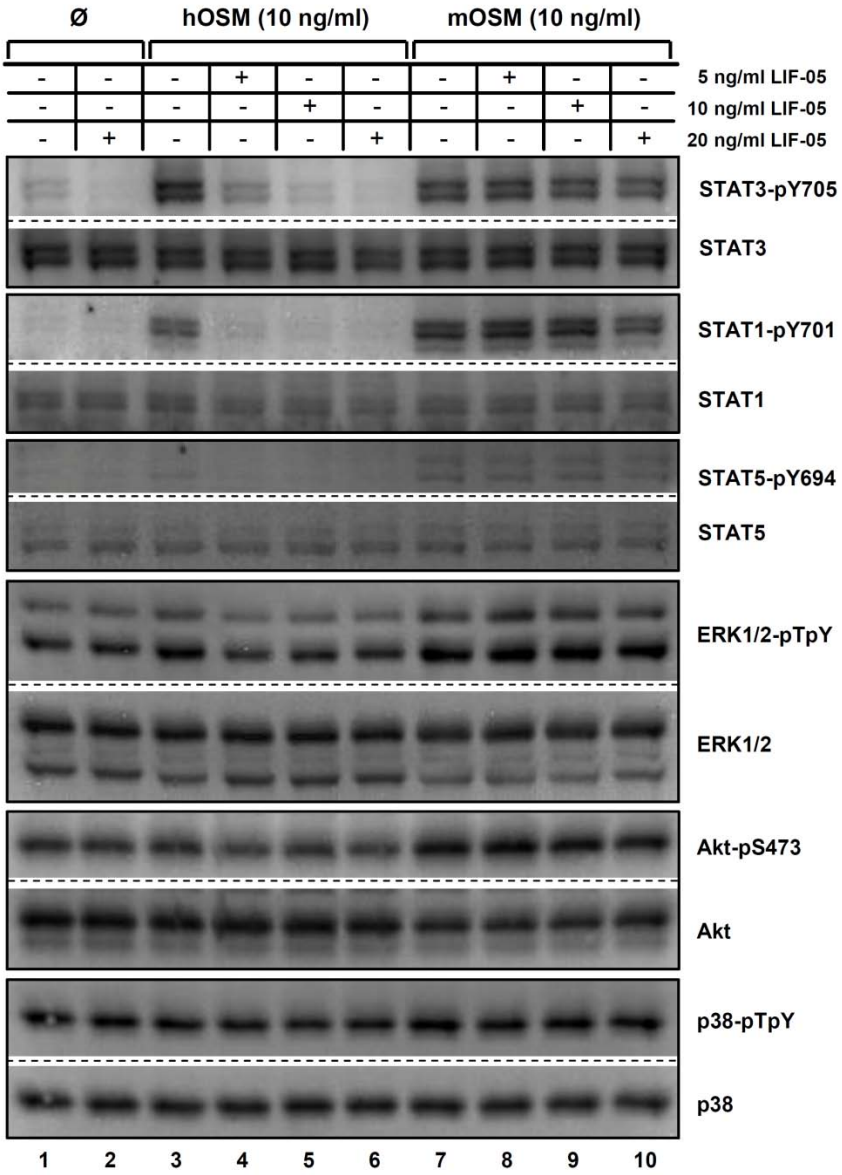

Figure 9: LIF-05 suppresses hOSM but not mOSM mediated signalling on NRCM

NRCM (cultured for three days) were pretreated with the indicated concentrations of LIF-05. 30 min later, cells were stimulated with 10 ng/ml hOSM or mOSM for 15 min. Phosphorylation levels of STAT3 (pY705), STAT1 (pY701), STAT5 (pY694), ERK1/2 (pT202/pY204), Akt (pS473) as well as p38 (pT180/pY182) were detected via Western blot analysis. The blots were stripped and reprobed with antibodies recognising the proteins irrespective of their phosphorylation status. Blots shown are representative for three independent experiments.

4.1.5 Comparison of the IL-6-type cytokine mediated signalling pathways

After determining the signalling peaks of the IL-6-type cytokines in NRCM (Fig. 8) and the receptor preferences of hOSM and mOSM on NRCM (Fig. 9), all induced signalling pathways were compared 15 min post stimulation, since most pathways were found to be stimulated most strongly at this time point. The rationale for these experiments was to determine if the strength, lack or presence of one pathway correlates with the distinguishable hypertrophic potential of the tested IL-6-type cytokines (compare 4.1.1). As mentioned in the introduction, the phosphorylations of STAT3, ERK1/2 and Akt are most frequently described to promote cardiomyocyte hypertrophy. Because the hypertrophic actions of hCT-1 have already been extensively described, we decided to analyse the signalling activities of mOSM, hOSM and hIL-6 ± hsIL-6R in comparison to hLIF, which has been the most potent hypertrophic cytokine in the hypertrophy assay. OSM was not yet characterised in the cardiac context when the presented work was started.

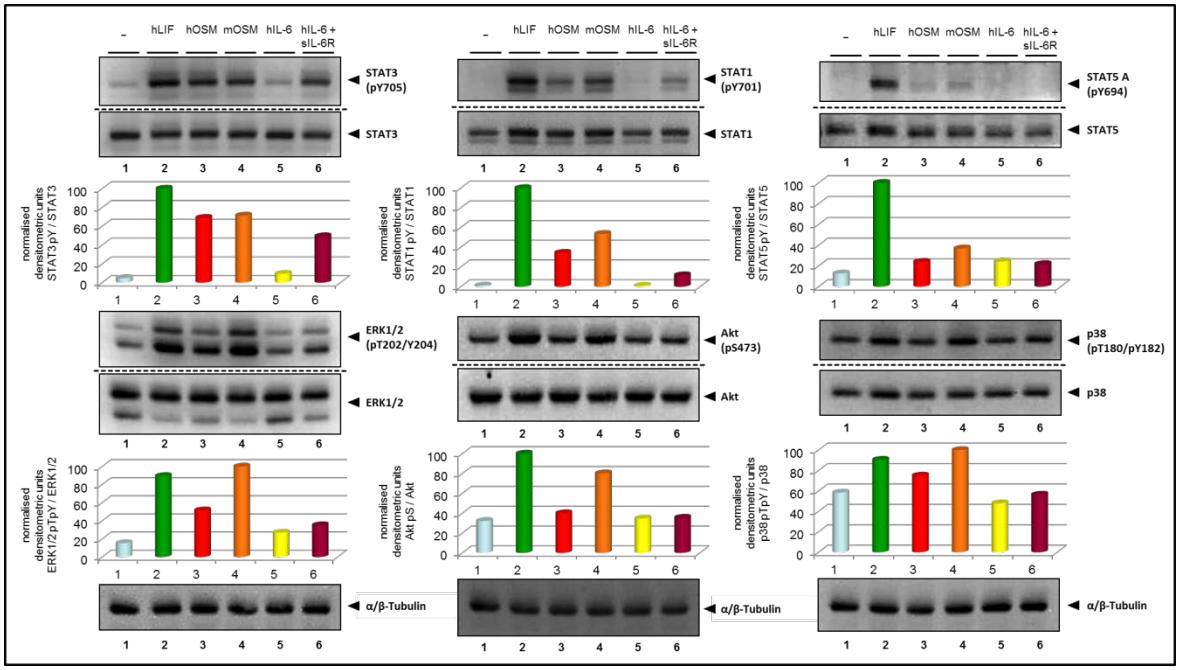

Figure 10: LIF, hOSM and mOSM are inducers of STAT, MAPK and Akt pathways in NRCM

NRCM (cultured for three days) were stimulated with 10 ng/ml hLIF, hOSM, mOSM or 20 ng/ml hIL-6 ± 0.5 µg/ml hsIL-6R for 15 min. Phosphorylation levels of STAT3 (pY705), STAT1 (pY701), STAT5 (pY694), ERK1/2 (pT202/pY204), Akt (pS473) as well as p38 (pT180/pY182) were detected via Western blot analysis. The blots were stripped and reprobed with antibodies recognising the proteins irrespective of their activation status (STAT3, STAT1, STAT5, ERK1/2, Akt, p38). The detection of α/β-tubulin served as additional loading control. Phosphorylation signals were quantified by determination of chemiluminescence intensities and normalisation to loading controls (strongest signal is set to 100%). Depicted blots and quantifications are representative for three independent experiments.

Human LIF, hOSM, mOSM and hIL-6 in combination with hsIL-6R are capable of inducing STAT3 and STAT1 phosphorylation with different intensities (Fig. 10, compare lanes 2, 3, 4 and 6 of upper left and middle panel). While LIF additionally induces strong STAT5 tyrosine phosphorylation (Fig. 10, upper right panel, lane 2), hOSM and mOSM provoke only very weak phosphorylation of STAT5 (lanes 3 and 4). Moreover, hLIF, hOSM and mOSM cause ERK1/2 phosphorylation, while hIL-6/hsIL-6R stimulation has only minor influence on the activation of this pathway (Fig. 10, lower left panel). In addition, distinct phosphorylations of Akt and p38 are observed after stimulation of NRCM with hLIF and mOSM, while activation of these pathways cannot be detected upon hIL-6 + hsIL-6R (Fig. 10, lower middle and right panels).

4.1.6 Expression of IL-6-type cytokine family receptors on NRCM

The differences of hOSM, mOSM and hLIF induced signal intensities in NRCM, mainly regarding STAT1, STAT5, ERK1/2, p38 and Akt phosphorylation (Fig. 10), led to the question whether the LIFR and the OSMR are expressed in similar amounts. Clearly distinguishable expression ratios of the two receptors could explain the observed differences in hOSM, mOSM and hLIF signalling strength. We also wanted to analyse the IL-6R expression levels, because we did not find any effect of IL-6 on its own in NRCM. First, we tried to determine IL-6R, gp130 and OSMR levels on NRCM via flow cytometry. For this purpose, we applied a monoclonal rat/mouse specific IL-6R antibody (anti-mouse/rat CD126 (IL-6Rα chain), clone D7715A7) from BioLegend, a monoclonal mouse specific gp130 antibody (anti-mouse gp130, clone RMβ1) and a monoclonal mouse specific OSMR antibody (anti-mouse OSMR, clone 30-1) from MBL International. Labelled (phycoerythrin- or Alexa488-conjugated) secondary antibodies were used to detect the primary antibodies. Since these initial stainings failed, we tried to determine gp130 and IL-6R levels again performing flow cytometry, using a monoclonal anti-human gp130 antibody (clone B-R3) and a monoclonal anti-human IL-6R antibody (B-R6) from Diaclone^{TM} (Gen-Probe Incorporated). Furthermore, different antibodes were used to detect whole protein levels of IL-6R (monoclonal anti-mouse IL-6R, MAB1830, R&D systems), gp130 (monoclonal anti-human gp130, MAB228, R&D Systems), LIFR (monoclonal anti-human LIFR, clone AN-E1, Santa Cruz Biotechnology) and OSMR (polyclonal anti-

human OSMR, AF4389, R&D systems and polyclonal anti-murine OSMR, AF662, R&D systems) via Western blot analysis. Unfortunately, due to the lack of cross-species reactivity of the tested antibodies, IL-6R, gp130, LIFR and OSMR protein levels could not been detected by Western blot analysis or flow cytometry.

Thus, the mRNA expression of gp130, OSMR, LIFR and IL-6R was analysed performing semiquantitative RT-PCR and additionally quantitative real time RT-PCR. The results of the RT-PCR clearly show that NRCM express high levels of gp130 and OSMR mRNA (Fig. 11A).

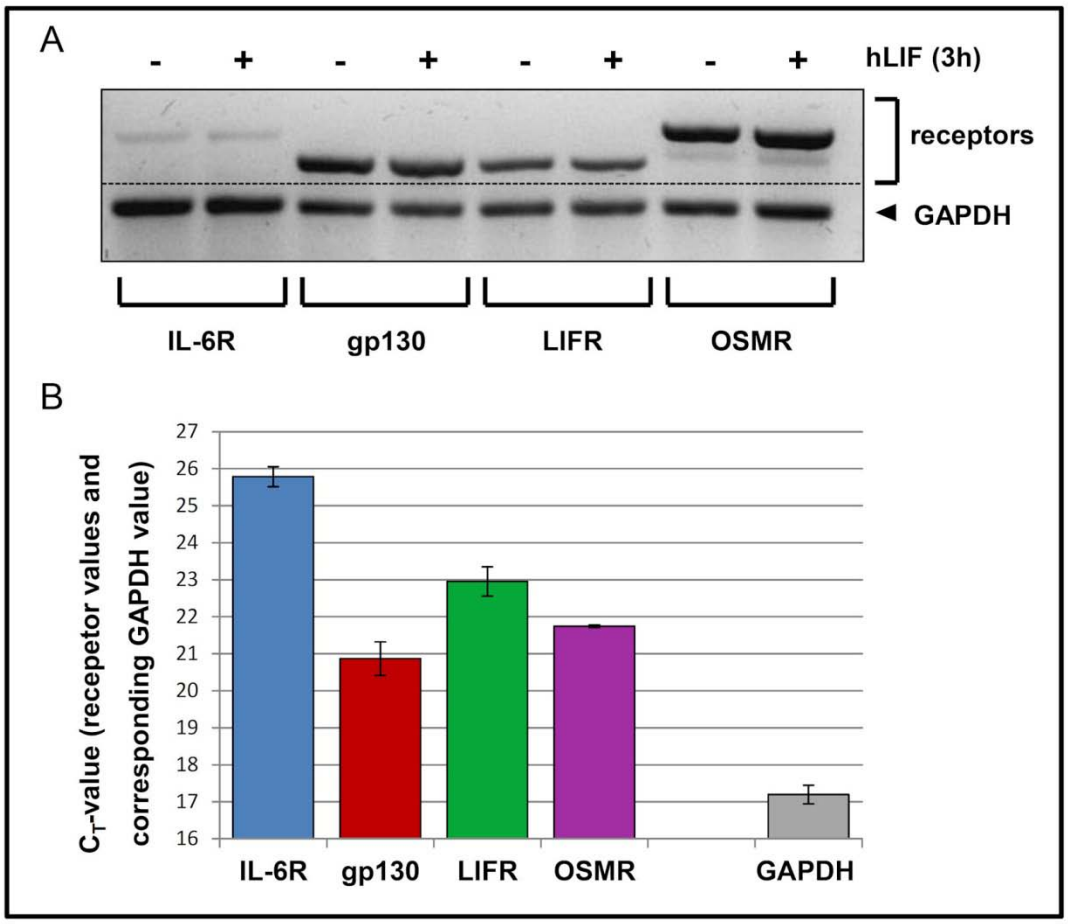

Figure 11: NRCM express gp130, OSMR and LIFR

A, NRCM (cultured for three days, untreated or 3 h hLIF (10ng/ml) treated) were lysed and total RNA was isolated. Semiquantitative RT-PCR was performed using the OneStep RT-PCR Kit (reverse transcription and 30 cycles of denaturation, annealing, elongation, as described in the method section) and resulting cDNA was separated by 2% agarose gel electrophoresis. Receptors are represented by the upper bands, while the lower bands show GAPDH serving as housekeeping gene. **B**, Total RNA of untreated NRCM (cultured for three days) was isolated and mRNA levels of the indicated receptors and GAPDH were determined by quantitative real time RT-PCR (reverse transcription, 40 cycles of denaturation, annealing, elongation). Shown are the C_T-value means with standard error of mean (SEM) of three independent experiments. Lower C_T-values correlate with higher mRNA amounts.

While the LIFR is strongly expressed (compare LIFR mRNA levels in NRCFB, chapter 4.2.1, Fig. 15) too, only very low mRNA levels of the IL-6R are found in NRCM (weak bands after 30 PCR cycles) correlating with the unresponsiveness of NRCM to pure IL-6 stimulation (see Fig. 10). This would also explain why the IL-6R was not detected in flow cytometry using the rat/mouse specific IL-6R antibody from BioLegend.

As shown in figure 11B, the real time RT-PCR results confirm that gp130, OSMR and LIFR (gp130 C_T: 20.9, OSMR C_T: 21.7, LIFR C_T: 23.0) mRNAs are highly expressed. Since the C_T-value (cycle threshold) indicates the PCR cycle number which is required for the fluorescent signal to cross the background threshold level, a higher C_T-value indicates a lower amount of mRNA (i.e. the C_T-value is inversely proportional to the amount of target mRNA). The IL-6R has been found to pass the background fluorescence level five cycles later than gp130 (IL-6R C_T: 25.8, gp130 C_T: 20.9). This means that in case of a theoretical mRNA duplication within each cycle and comparable oligonucleotide primer efficiencies, the IL-6R is expressed only 0.03-fold the amount of gp130. Later results of receptor expression in cardiac fibroblasts and hepatoma cells will substantiate the suspicion, that IL-6R expression is not sufficient to promote IL-6-signalling in the absence of soluble α-receptor in NRCM. Hence, in the next chapter the hIL-6 stimulation of the rat hepatoma cell line JTC-27 and its IL-6R expression levels are shown as a direct comparison.

4.1.7 IL-6R expression levels and IL-6 signalling in rat hepatoma cells – a comparison of IL-6-non-responsive cells

The unresponsiveness of NRCM to stimulation with IL-6 (see chapters 4.1.5 and 4.1.6) and the correlating low level expression of the IL-6R mRNA elicited the question, if other cells from rat origin expressing similar low levels of the IL-6R are also not responsive to the cytokine. Therefore the rat hepatoma cell line JTC-27, that we also utilised for the characterisation of the rat OSM receptor complexes (chapter 4.4), was used to determine IL-6R expression levels and the correlating responsiveness to hIL-6 (with and without sIL-6R) as well as to rIL-6 stimulation. As shown in figure 12, JTC-27 cells are strongly responding to 10 ng/ml hLIF (15 min), a feature they share with NRCM. Again, STAT3 is potently phosphorylated at tyrosine

705 and the double phospho-motif of ERK1/2 (pT202-pY204) is phosphorylated after LIF treatment (Fig. 12A). Neither a concentration of 20 ng/ml nor of 100 ng/ml hIL-6 is

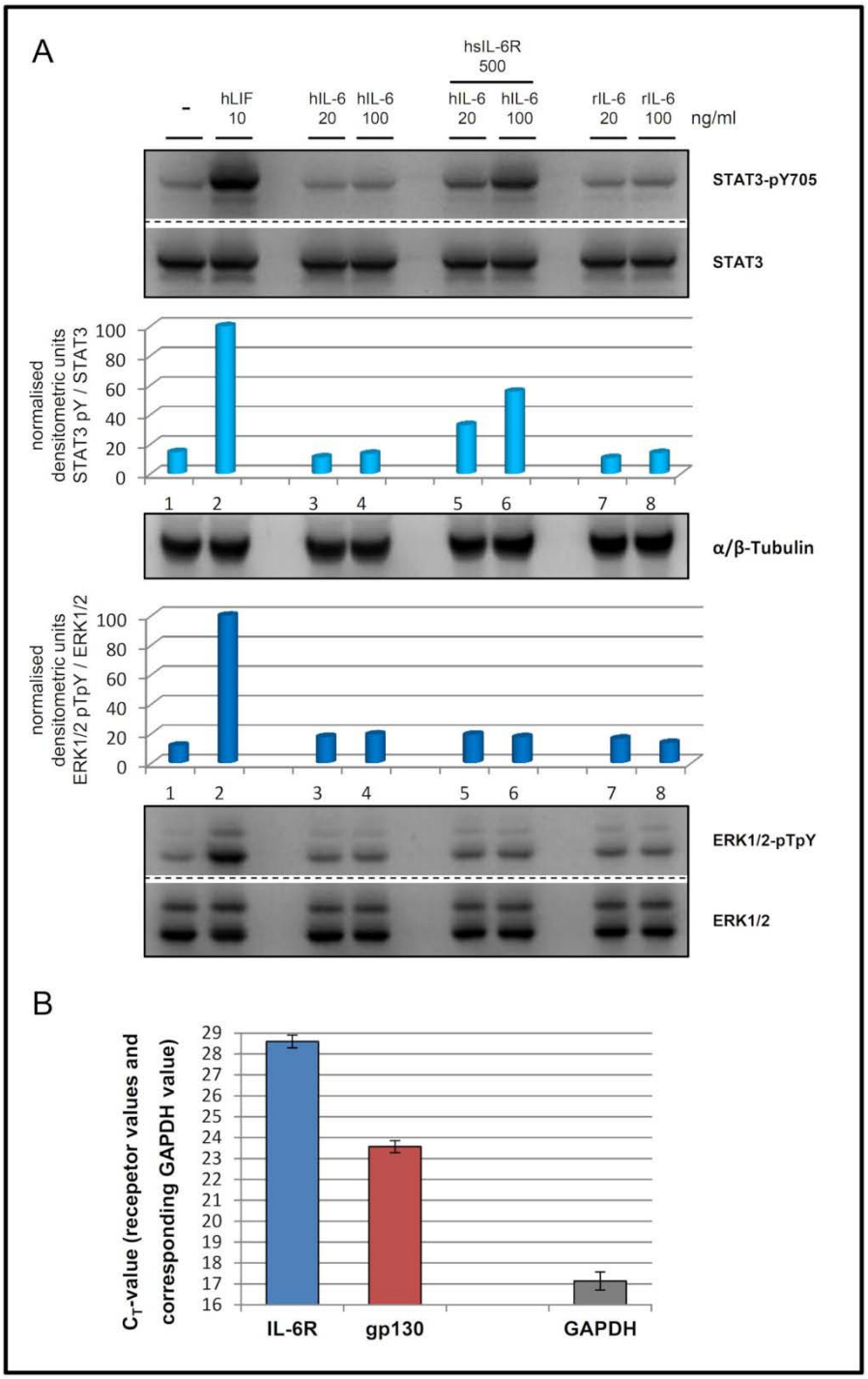

Figure 12: Rat hepatoma cells (JTC-27) exhibit NRCM-like IL-6R expression and corresponding IL-6 unresponsiveness to pure IL-6 stimulation

A, JTC-27 cells were treated with hLIF (10 ng/ml), hIL-6 (20 ng/ml or 100 ng/ml) ± hsIL-6R (0.5 µg/ml) or with rIL-6 (20 ng/ml or 100 ng/ml) for 15 min. Phosphorylation levels of STAT3 (pY705) and ERK1/2 (pT202/pY204) were detected via Western blot analysis. The blots were stripped and reprobed with antibodies recognising the proteins irrespective of their activation status. **B**, RNA from JTC-27 cells was isolated and used for real time RT-PCR (reverse transcription, 40 cycles of denaturation, annealing, elongation). Using specific primers, IL-6R and gp130 and GAPDH mRNA levels were detected. Shown are the C_T-value means with standard error of mean (SEM) of three independent experiments.

able to induce a measureable phosphorylation of STAT3 or ERK1/2 (compare lanes 1, 2, 3 and 4). In contrast, hIL-6 together with hsIL-6R is capable of mediating the phosphorylation of STAT3 in a concentration dependent manner, but no distinct phosphorylation of ERK1/2 can be observed upon hIL-6/hsIL-6R stimulation (lanes 1, 5 and 6).

As a precaution, JTC-27 were also stimulated with 20 and 100 ng/ml rIL-6 to exclude the possibility of cross-species problems with human IL-6 on cells of rat origin (lanes 1, 7 and 8). Comparable to hIL-6 treatment, stimulation of JTC-27 with rIL-6 also does not induce any detectable STAT3 or ERK1/2 activation. To analyse the mRNA amounts of rIL-6R and rgp130 in the hepatoma cell line, again quantitative real time RT-PCR was performed to determine the C_T-values of both receptors. As shown in figure 12B, similar gp130 and IL-6R expression rates as in NRCM (Fig. 11B) have been found. While both receptors elicit later C_T-values (IL-6R C_T: 28.6 and gp130 C_T: 23.6), the ratio of the rgp130 C_T to the IL-6R C_T is equal to the ratio of both receptors in NRCM. Notably, the gp130 expression levels measured in JTC-27 cells are fully sufficient to mediate incoming LIF signals (lane 1 and 2 in Fig. 12A).

4.1.8 IL-6-type cytokines partially induce enhanced transcription of their own cytokine as well as receptor genes prolonging their hypertrophic potential and cytoprotection

Time course experiments have shown that most of the immediately activated signalling pathways following IL-6-type cytokine stimulation are suppressed back to basal levels after approximately one hour (Fig. 8). However, for the hypertrophy assay NRCM were treated once per day with each tested IL-6-type cytokine. In order to determine how the cytokines can maintain their activity over longer time periods finally resulting in the observed dramatic phenotypical change of NRCM, we first analysed the expression of a number of genes known to be involved in the hypertrophic response (angiotensinogen (*Agt*), renin (*Ren1*), angiotensin II receptor 1 alpha (*At1α*) and angiotensin I converting enzyme (*Ace*)). No obvious alterations of the corresponding mRNA levels were detected. Next the transcriptional regulation of OSM, LIF, IL-6 and their receptors (OSMR, LIFR, gp130, IL-6R) following stimulation with hLIF, mOSM and hIL-6/hsIL-6R was analysed. No significant alterations of gp130, LIFR, IL-6R or OSM mRNA levels are detectable using real time RT-PCR. In

contrast, significantly increased transcription of the *Osmr* gene is found in response to mOSM, hLIF and hIL-6R/sIL-6R stimulation (Fig. 13, upper panel). Elevated mRNA levels can be detected between 3 h and 24 h post stimulation. OSM itself mediates the strongest upregulation of its own receptor (3.7 ± 0.4-fold induction after 24 h stimulation). Interestingly, no subsequent decrease of OSMR mRNA levels can be observed up to 24 h after NRCM treatment.

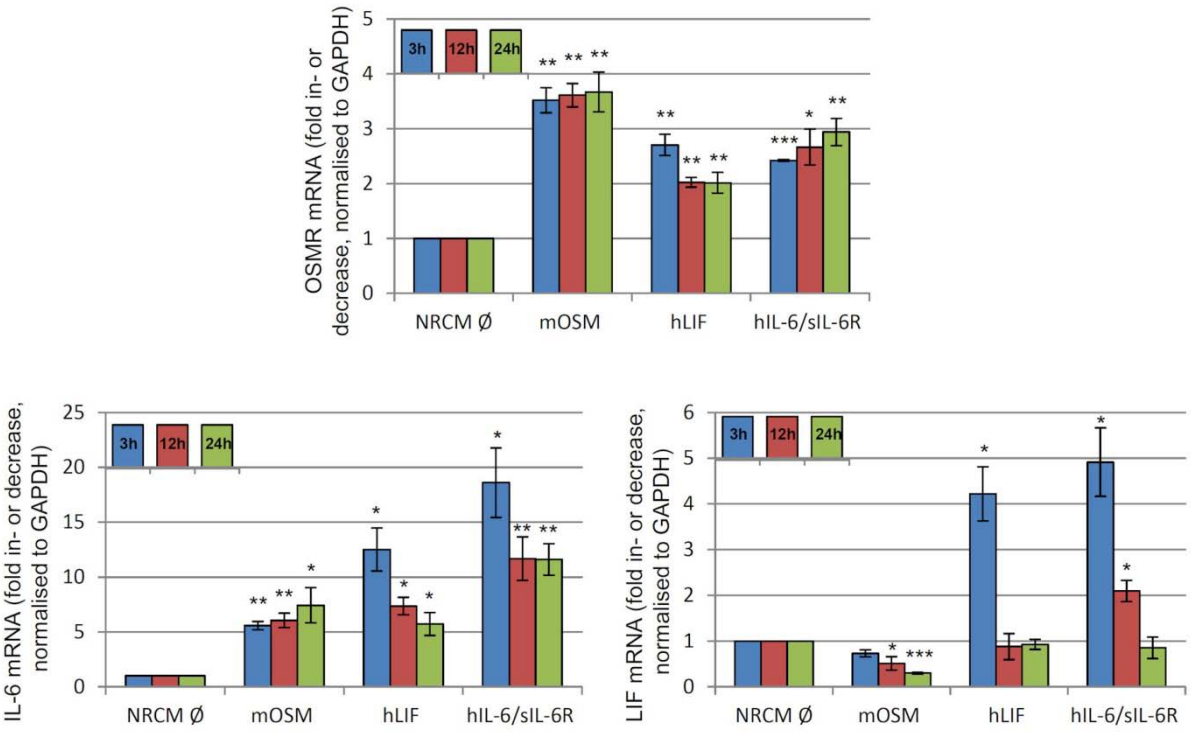

Figure 13: IL-6-type cytokines strongly increase OSMR, IL-6 and LIF expression in NRCM

NRCM (cultured for three days) were treated with 10 ng/ml hLIF, mOSM or 20 ng/ml hIL-6 plus 0.5 µg/ml hsIL-6R for the indicated time (3 h, 12 h and 24 h). Total RNA from NRCM was isolated, reverse transcribed and the resulting cDNA used for real time PCR (40 cycles of denaturation, annealing and elongation). Shown are the means (± SEM) of three or more independent experiments. Means represent x-fold mRNA increase or decrease, respectively, normalised to GAPDH mRNA levels. Statistical significance was calculated using a paired, two-tailed Student's t-test, * $p<0.05$, ** $p<0.01$, *** $p<0.001$.

Moreover, a strong increase of IL-6 mRNA levels is observed in response to mOSM (5.6 ± 0.4-fold induction after 3 h), hLIF (12.5 ± 2.0-fold induction after 3 h) and hIL-6/sIL-6R (18.6 ± 3.2-fold mRNA induction after 3h, Fig. 13). Also after 12 and 24 h stimulation elevated levels of IL-6 mRNA can be detected indicating a permanent effect. Especially between 12 and 24 h no decrease of IL-6 mRNA levels is observed. Interestingly, IL-6 induces the strongest transcription of its own gene. While mOSM also leads to enhanced *Il6* gene transcription, it negatively influences the expression

levels of LIF mRNA (Fig. 13, 0.3 ± 0.02 LIF mRNA expression rate compared to unstimulated cells, after 24 h). In contrast, hLIF and hIL-6/sIL-6R treatment results in a distinct, but transient upregulation of LIF mRNA levels (4.2 ± 0.6-fold LIF mRNA upregulation after 3 h LIF and 4.9 ± 0.8 LIF mRNA upregulation after 3 h IL-6/sIL-6R stimulation). However, after 24 h only basal expression levels of the cytokine mRNA can be detected (Fig. 13).

4.1.9 The hypertrophic potential of hIL-6/sIL-6R and mOSM seems to be supported by the lower induction of feedback inhibition when compared to LIF

The discrepancy between the extremely strong initial signalling of hLIF on NRCM (Fig. 8 and 10) and the rather intermediate gene induction of *Il6*, *Lif* and *Osmr* compared to mOSM and hIL-6/sIL-6R (Fig. 13) is obvious. On the other hand, mOSM and hIL-6/sIL-6R are able to deliver an almost equivalent hypertrophic signal to hLIF (Fig. 6), although their initial induction of hypertrophic pathways is clearly less potent. In detail, hIL-6/sIL-6R treatment causes lower STAT3 and STAT1 phosphorylation than hLIF (Fig. 10). Moreover, phosphorylations of ERK1/2 and Akt are not detectable in response to hIL-6/sIL-6R stimulation. While mOSM induces ERK1/2 and Akt phosphorylation equivalent to hLIF, STAT1 and STAT3 are, however, less strongly phosphorylated (Fig. 10). Furthermore, hIL-6/sIL-6R induces an increase of LIF mRNA levels equivalent to hLIF, and the highest gene induction levels of *Il6* are also mediated by IL-6 trans-signalling (Fig. 13). The strongest induction of *Osmr* gene transcription is observed after mOSM treatment and the cytokine significantly increases IL-6 mRNA levels as well (Fig. 13).

To solve this enigma, we analysed the induction of SHP2 phosphorylation, SOCS1 and SOCS3 expression following IL-6-type cytokine treatment. Although operating through absolutely different mechanisms, these three proteins represent the most important and mostly examined inhibitors of IL-6-type cytokine based signalling. As shown in figure 14A, SOCS3 and SOCS1 mRNA levels are increased by the activity of all used IL-6-type cytokines. The highest increase of mRNA levels has been found 1 h after cytokines were applied. As direct targets of STAT3 or STAT1 activity, respectively, their expression rate directly correlates with the potency of STAT phosphorylation and translocation to the nucleus. Hence, hLIF induces the highest expression levels of SOCS3 and SOCS1 (Fig. 14A) by most strongly activating

STAT3 and STAT1 (Fig. 14B). The expression of SOCS mRNAs is an extremely transient cellular event. This is due to the feedback inhibitory function of the proteins and their short-lived mRNAs. Hence the increased transcription is ceased already after 3 h cytokine treatment. 24 or 48 h after NRCM stimulation, only marginally elevated mRNA levels of SOCS3 and basal SOCS1 levels can be observed.

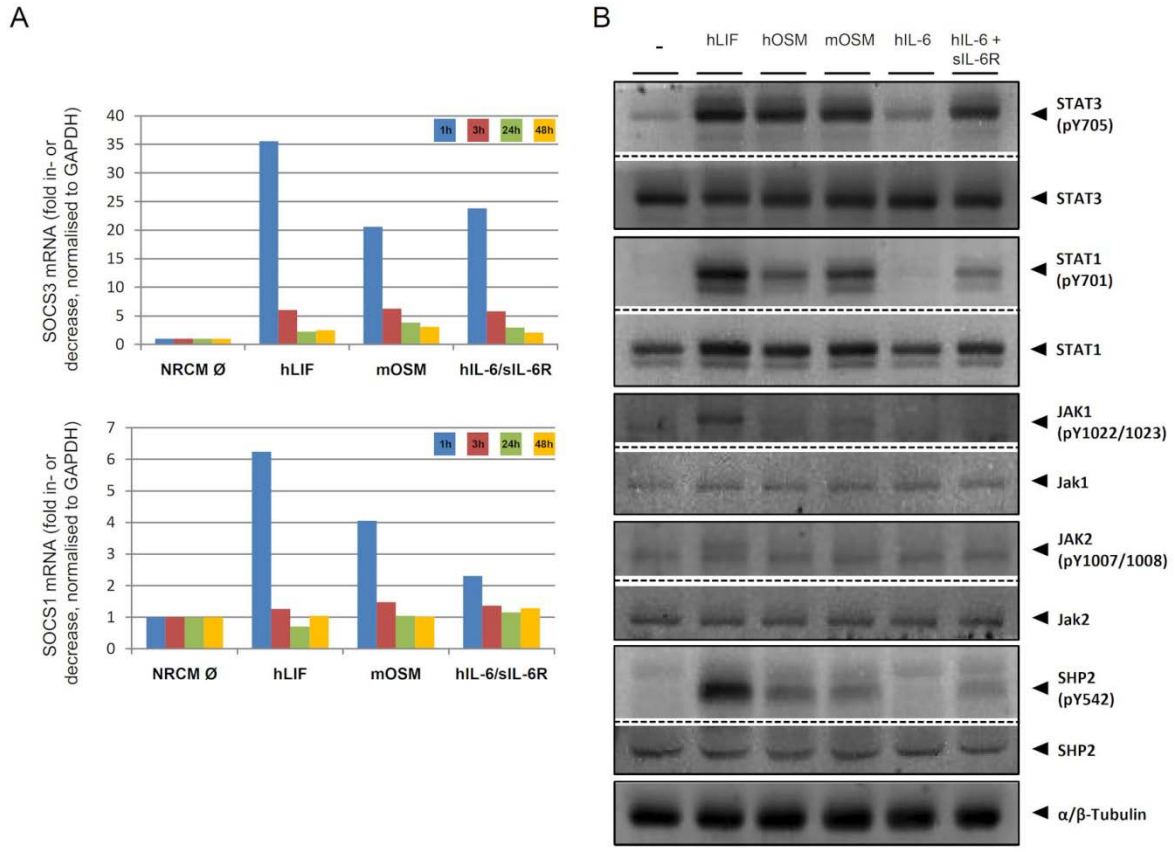

Figure 14: hIL-6/sIL-6R and mOSM mediate less SOCS1 and SOCS3 mRNA increase and weaker SHP2 phosphorylation in NRCM than hLIF

A, NRCM (cultured for three days) were treated with 10 ng/ml mOSM, hLIF or 20 ng/ml hIL-6 plus 0.5 µg/ml hsIL-6R for the indicated time (1 h, 3 h, 24 h and 48 h). Total RNA from NRCM was isolated and used for real time RT-PCR (reverse transcription, 40 cycles of denaturation, annealing and elongation). Shown values represent x-fold mRNA increase or decrease, respectively, normalised to GAPDH mRNA levels (n=1). **B**, NRCM (cultured for three days) were stimulated with 10 ng/ml hLIF, hOSM, mOSM or 20 ng/ml hIL-6 ± 0.5 µg/ml hsIL-6R for 15 min. Phosphorylation levels of STAT3 (pY705), STAT1 (pY701), JAK1 (pY1022/pY1023), JAK2 (pY1007/pY1008) and SHP2 (pY542) were detected via Western blot analysis. The blots were stripped and reprobed with antibodies recognising the proteins irrespective of their activation status. As an additional and independent loading control, α/β-tubulin was detected.

The JAK1 dependent phosphorylation of SHP2 in response to hLIF, mOSM and hIL-6/sIL-6R (additional stimuli are hOSM and pure hIL-6) was also analysed and is shown in figure 14B. Corresponding to the other phosphorylations, SHP2 activation was analysed 15 min after cytokines were applied. Interestingly double tyrosine

phosphorylations in the activation loop of the kinase domains of JAK1 and JAK2 are only detectable following hLIF stimulation. SHP2 phosphorylation is observed in response to all applied cytokines (with the exception of pure IL-6 as explained before), but it is obvious that hLIF mediates the strongest phosphorylation of this phosphatase. Altogether, it is likely that mOSM and hIL-6/sIL-6R are amplifying the observed gene inductions and their hypertrophic potential by weaker induction of SOCS3 mRNA, SOCS1 mRNA and SHP2 phosphorylation. Nevertheless, this seems to be a rather transient mechanism, because the SOCS3 and SOCS1 mRNA levels are very similar at later time points (Fig. 14A). Further experiments analysing the signalling at later time points in response to cytokine treatment will substantiate this hypothesis (chapter 4.3.2).

4.2 Analysis of IL-6-type cytokine induced signalling in cardiac fibroblasts: Expression of hypertrophy supporting targets

While the role of cardiomyocytes in the development and progression of hypertrophic diseases like hypertrophic cardiomyopathy was described in countless studies, the involvement of the underrepresented cardiac fibroblasts has been started to be determined only recently. Doubtless, cardiac myocytes that respond to hypertrophic stimuli like adrenergic agonists, IL-6-type cytokines or angiotensin II (ATII) represent the main cell type in the heart responsible for morphological changes and thus causing cardiac hypertrophy. As described in the introduction, cardiac fibroblasts represent a second cell type in the heart that is able to support hypertrophic changes of heart tissue, for example by replacing dead cardiomyocytes. While the consequences of fibroblast tissue invasion, fibroblast proliferation and progressing fibrosis, causing decreased contractility and flexibility of the heart, were shown in several articles, cardiac fibroblast based cytokine production and cross talk with cardiomyocytes were rarely determined. Therefore, the signalling pathways of IL-6-type cytokines on neonatal rat cardiac fibroblasts (NRCFB) and the corresponding induction of cytokine mRNAs, cytokine receptor mRNAs and additional hypertrophic targets were analysed. One of our main goals was to compare receptor availability and the resulting receptor preference of the IL-6-type cytokines on NRCFB with those of NRCM.

4.2.1 Receptor availability and resulting consequences for hOSM and mOSM signalling in NRCFB

Synchronously to the experiments in NRCM, the receptor expression levels of gp130, OSMR, LIFR and IL-6R and the resulting signalling properties of mOSM, hOSM, hLIF and hIL-6 on NRCFB have been determined. As shown in figure 15A, the basal receptor C_T-values indicate that the expression levels of the IL-6R (C_T-value: 26.3 ± 0.2) are similar to those in NRCM (C_T-value: 25.8 ± 0.5) suggesting that classical IL-6 signalling would also not be supported by these cells. While the C_T-value of the OSMR (22.8 ± 0.3) in untreated cells is comparable to that observed in NRCM (21.7 ± 0.0), NRCFB clearly express lower levels of the LIFR (C_T-value: 26.2 ± 0.2) in comparison to NRCM (C_T-value: 23.0 ± 0.4).

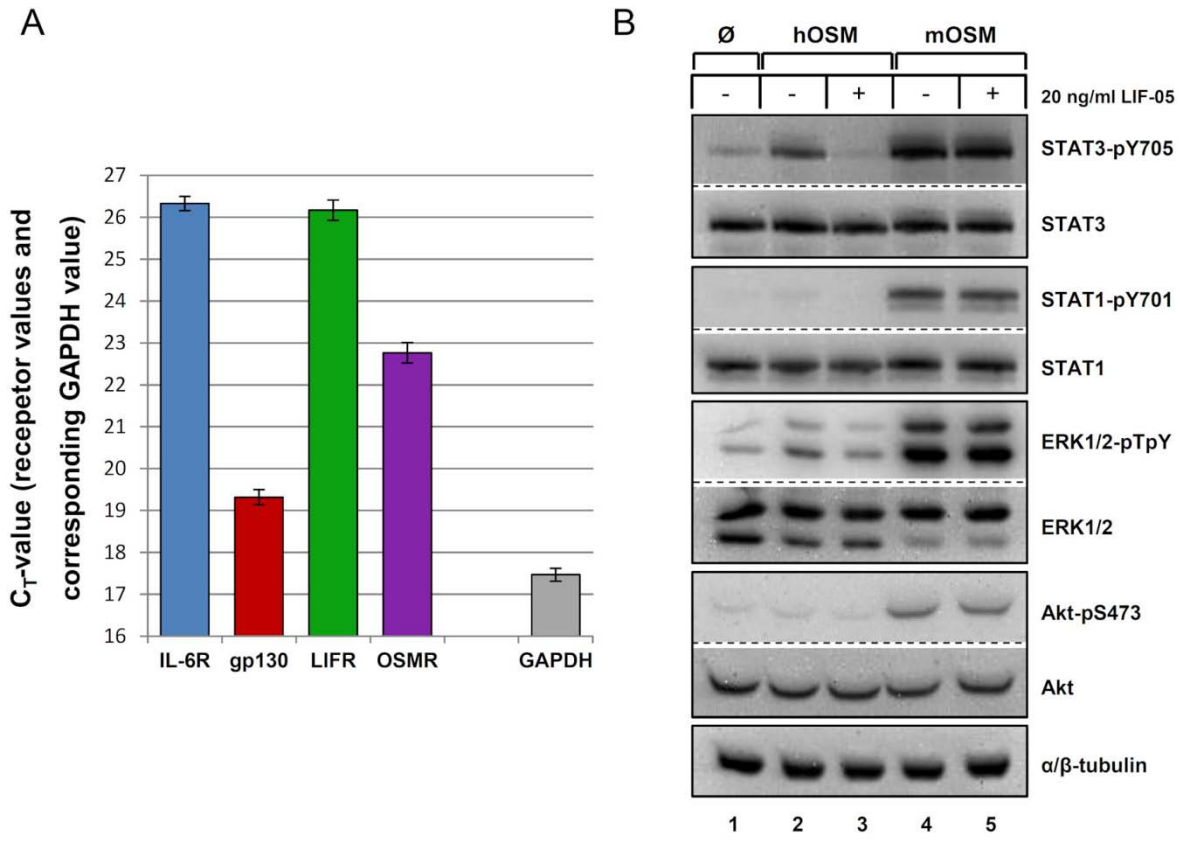

Figure 15: NRCFB are producing high levels of gp130 and OSMR mRNA, while IL-6R and LIFR are weakly expressed

A, Total RNA from untreated NRCFB (P1) was isolated and used for real time RT-PCR (reverse transcription, 40 cycles of denaturation, annealing and elongation). Shown are the C_T-value means with standard error of mean (SEM) of four independent experiments. Lower C_T-values correlate with higher initial mRNA-amounts. **B**, NRCFB were pretreated with 20 ng/ml LIF-05 for 30 min and afterwards stimulated with 10 ng/ml hOSM or mOSM for further 15 min. Phosphorylation levels of STAT3 (pY705), STAT1 (pY701), ERK1/2 (pT202/pY204) and Akt (pS473) were detected via Western blot analysis. The blots were stripped and reprobed with respective total protein recognising antibodies. Depicted blots are representative for three independent experiments.

The fibroblasts from cardiac origin show remarkably strong expression of gp130 (C_T-value: 19.3 ± 0.2) that is clearly still higher than in NRCM (C_T-value: 20.9 ± 0.3). In other words, when GAPDH mRNA would be set to 100%, cells would produce 30% gp130 mRNA in comparison. The strong *Il6st* (encoding for gp130) transcription in NRCFB could have a severe influence on the IL-6 trans-signalling. Further indications supporting this hypothesis as well as the signalling analysis of the remaining cytokines (hLIF, hIL-6 without sIL-6R) are described in chapter 4.2.2. In line with the LIFR, OSMR and gp130 real time RT-PCR data (Fig. 15A), hOSM induces extremely weak phosphorylation of STAT3, STAT1 and ERK1/2 (Fig. 15B), since NRCFB only express low levels of LIFR mRNA. As shown before in NRCM (Fig. 9) and in line with results from murine cells[74, 75], hOSM is able to exclusively activate LIFR/gp130 heterodimers (type I receptor complex) on NRCFB. Therefore, hOSM signalling (Fig. 15B, lanes 2 and 3) is completely abrogated by the antagonist LIF-05, which blocks LIFR downstream signalling[254]. In contrast, mOSM mediated phosphorylations of STAT3, STAT1, ERK1/2 and Akt (lanes 4 and 5) remain entirely unaffected by the presence of LIF-05. This indicates again that mOSM, unlike hOSM, uses the type II receptor complex on rat cells, as it does on murine cells. Final proof for this proposed receptor binding of mOSM and hOSM on rat cells will be described in chapter 4.4.

4.2.2 LIF, OSM and IL-6 mediated signalling on NRCFB

To analyse the signalling potentials of hLIF, hOSM, mOSM, hIL-6 (± sIL-6R) in NRCFB, the phosphorylation intensities of STAT3, STAT1, STAT5, ERK1/2, Akt and p38 were determined 15 min after stimulation. In contrast to the previously described signalling of these cytokines in NRCM, NRCFB are only poorly responsive to the LIFR utilising cytokines hLIF and hOSM (Fig. 16, lanes 2 and 3 of each panel). However, the LIFR agonists hOSM and hLIF are capable of inducing measureable phosphorylations of STAT3, STAT1 and ERK1/2, while STAT5, p38 or Akt phosphorylations cannot be detected. On the other hand, mOSM strongly induces phosphorylations of STAT3, STAT1, STAT5, ERK1/2, Akt and p38 (Fig. 16, lane 3 of each panel). As anticipated by the extremely low level of mRNA for the IL-6R (Fig. 15), hIL-6 on its own (lane 5) provokes no detectable activation of any analysed signalling pathway. However, hIL-6 combined with its soluble receptor (sIL-6R) mimicking trans-signalling is able to induce potent phosphorylations of STAT3,

STAT1 and ERK1/2 (lane 6), while no distinct phosphorylations of p38, Akt or STAT5 are detected.

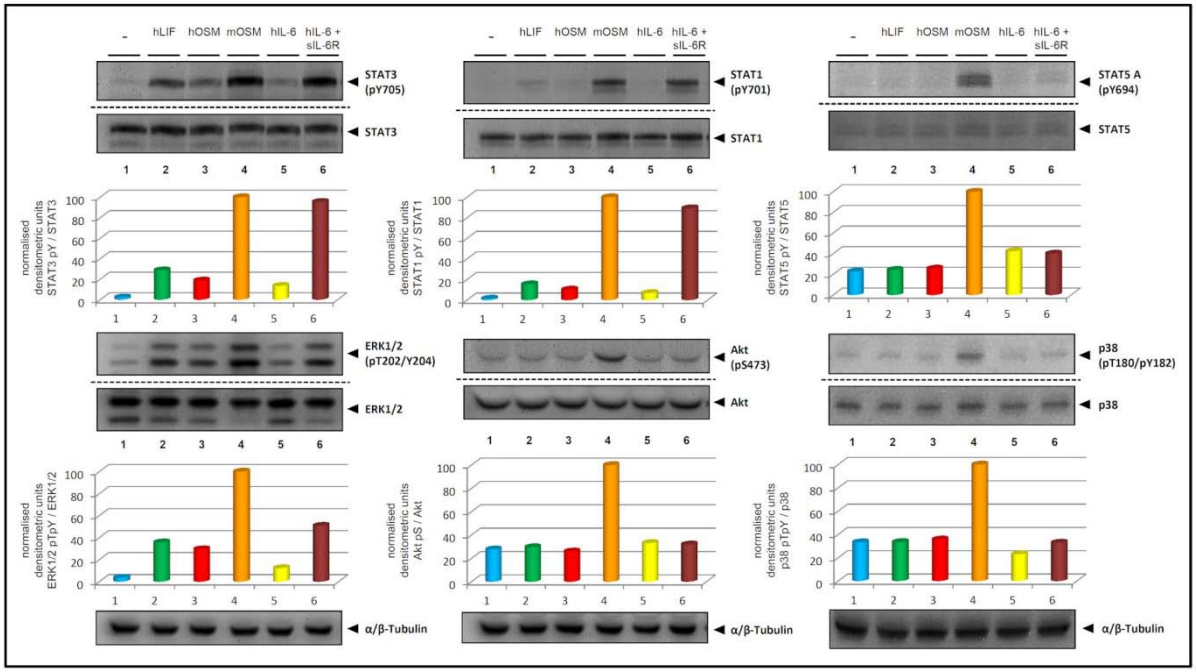

Figure 16: mOSM and hIL-6/sIL-6 are potent promoters of NRCFB signalling

NRCFB (P1) were stimulated with 10 ng/ml hLIF, hOSM, mOSM or 20 ng/ml hIL-6 ± 0.5 µg/ml hsIL-6R for 15 min. Phosphorylation levels of STAT3 (pY705), STAT1 (pY701), STAT5 (pY694), ERK1/2 (pT202/pY204), Akt (pS473) as well as p38 (pT180/pY182) were detected via Western blot analysis. The blots were stripped and reprobed with antibodies recognising the proteins irrespective of their activation status (STAT3, STAT1, STAT5, ERK1/2, Akt, p38 and α/β-tubulin). The shown Western blots are representative for three independent experiments. Phosphorylation intensities were quantified by chemiluminescence analysis and normalised to loading controls (mOSM signal is set to 100%).

Because LIFR-based signalling in NRCFB was rather weak and OSM as well as IL-6 are typical cytokines described to elicit fibroblast responses, following experiments in NRCFB were carried out as comparisons between mOSM and hIL-6/sIL-6R stimulation.

4.2.3 Cytokine and cytokine receptor expression by NRCFB in response to OSM and IL-6 trans-signalling

In line with the described experiments from NRCM, NRCFB were stimulated with mOSM or hIL-6/sIL-6R for 3 h or 18 h, respectively. The isolated RNA was used to perform real time RT-PCR using specific oligonucleotide primers for the detection of gp130, IL-6R, OSMR, LIFR, LIF and IL-6 mRNA levels. Furthermore, the mRNA

levels of endogenous OSM were analysed, but cytokine induced alterations could not be detected (data not shown) and the corresponding C_T-values indicated that OSM is not produced from NRCFB, neither under basal conditions nor in response to mOSM or hIL-6/sIL-6R treatment.

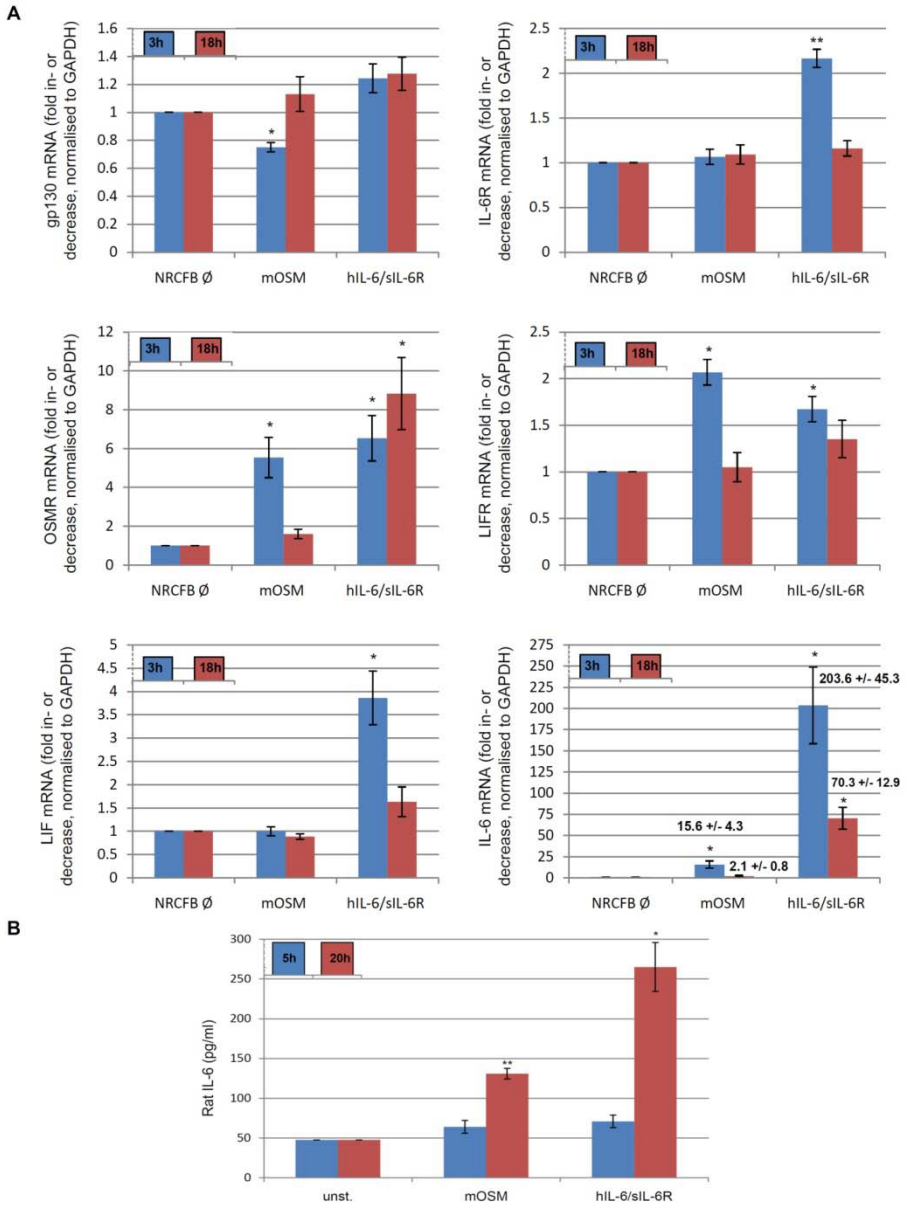

Figure 17: IL-6-type cytokines induce upregulation of IL-6R, OSMR, LIFR, LIF and IL-6 in NRCFB

A, NRCFB (P1) were treated with 10 ng/ml mOSM or 20 ng/ml hIL-6 plus 0.5 µg/ml hsIL-6R for the indicated time (3 h and 18 h). Afterwards total RNA was isolated and used for real time RT-PCR (reverse transcription, 40 cycles of denaturation, annealing, elongation). Shown are means (± SEM) of three or more independent experiments. Means represent x-fold mRNA increase or decrease, respectively, normalised to GAPDH mRNA levels. Statistical significance was calculated using a paired, two-tailed Student's t-test, * $p<0.05$, ** $p<0.01$, *** $p<0.001$. **B**, NRCFB (P1) were stimulated as described in A for 5 or 20 h, respectively. Rat IL-6 amounts in NRCFB supernatants were determined by enzyme-linked immunosorbent assay (ELISA). Values shown are the means (± SEM) of three independent experiments. Statistical significance was calculated using a paired, two-tailed Student's t-test, * $p<0.05$, ** $p<0.01$.

As shown in figure 17A, mOSM and hIL-6/sIL-6R stimulations do not increase gp130 mRNA levels neither after 3 h nor 18 h stimulation, but mOSM contrariwise leads to a decrease of gp130 mRNA by approx. 25% after 3 h compared with the initial/basal mRNA level (Fig. 17A, upper left diagram). Moreover, IL-6R mRNA regulation in response to mOSM treatment cannot be observed (upper right diagram), while hIL-6/sIL-6R stimulation induces a slight IL-6R mRNA upregulation (2.17 ± 0.10-fold induction) that is rather transient and no longer detectable at later time points. Analogous to the results in NRCM, the OSMR mRNA levels are strongly, but transiently, increased after 3 h mOSM treatment (5.54 ± 1.04-fold induction). 18 h after cell treatment a significant increase of the OSMR mRNA cannot be observed (middle left diagram). In sharp contrast to the mOSM activity, hIL-6/sIL-6R treatment induces a clearly longer upregulation of the OSMR mRNA, that is even more elevated after 18 h (6.53 ± 1.17-fold induction after 3 h and 8.83 ± 1.86-fold induction after 18 h).

Moreover, the LIFR mRNA levels are elevated after 3 h stimulation with mOSM or hIL-6/sIL-6R (2.07 ± 0.14-fold induction after 3 h mOSM, 1.67 ± 0.14-fold induction after 3 h hIL-6/sIL-6R treatment), although no significant increases are detectable after 18 h cytokine treatment. While mOSM has no promoting effect on *Lif* transcription, hIL-6/sIL-6R treatment causes a 3.86 ± 0.58-fold increase of LIF mRNA levels after 3 h. The measurements for LIF mRNA after 18 h cytokine treatment are rather inhomogeneous, and no normal distribution of the values could be achieved (variation between 1.0 and 2.76-fold induction). In contrast to the IL-6 expression, however, the increased LIF expression seems to be rather transient.

Treatment with mOSM causes a clear upregulation of IL-6 mRNA levels after 3h (15.57 ± 4.33-fold induction), while hIL-6/sIL-6R stimulation mediates an enormous increase in *Il6* transcription after 3 h (203.56 ± 45.27-fold induction) and after 18 h (70.30 ± 12.90-fold induction). Detection of IL-6 protein by ELISA verified that the increase in mRNA is indeed translated into protein and furthermore that IL-6 is secreted by NRCFB and detectable in the cell supernatant (Fig. 17B). After 5 h mOSM or hIL-6/sIL-6R treatement, respectively, significantly increased rIL-6 amounts are not measurable. However, 20 h after the cytokines were added, we found rIL-6 concentrations of 131 (± 7) pg/ml in response to mOSM and of 265 (± 31) pg/ml in response to hIL-6/sIL-6R in the supernatants of NRCFB.

4.2.4 IL-6 and OSM perform cross-talk with the renin-angiotensin system in NRCFB

IL-6-type cytokines are not only able to induce the expression of their receptors or other cytokines of their own family, but also to mediate cross-talk with other ligand-receptor systems. Considering the proposed role of the renin-angiotensin system in cardiac hypertrophy and suspecting that it might be a system targeted by IL-6-type cytokines, the mRNA expression of angiotensin I converting enzyme (ACE) and angiotensin II receptor 1 alpha (AT1α) was analysed following mOSM and hIL-6/sIL-6R treatment. As shown in figure 18 (left diagram), hIL-6/sIL-6R as well as mOSM stimulation induces a clear and significant increase in ACE mRNA levels (3.02 ± 0.07-fold induction after 3 h mOSM and 1.78 ± 0.24-fold induction after 3 h hIL-6/sIL-6R treatment).

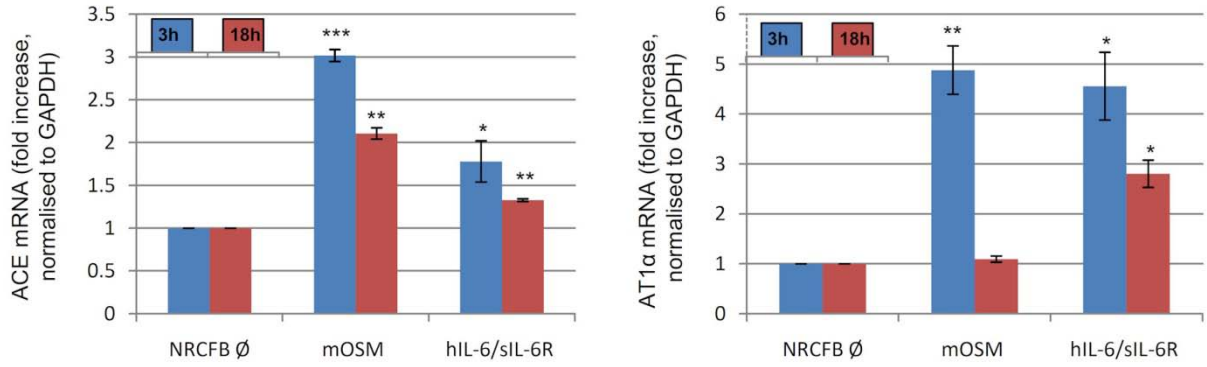

Figure 18: IL-6-type cytokines induce enhanced transcription of *Ace* and *At1α*
NRCFB (P1) were stimulated with 10 ng/ml mOSM or 20 ng/ml hIL-6 plus 0.5 µg/ml hsIL-6R for 3 h or 18 h, respectively. Afterwards total RNA was isolated and real time RT-PCR (reverse transcription, 40 cycles of denaturation, annealing, elongation) was performed. Values shown are the means (± SEM) of three (3 h values) or four (18 h values), respectively, independent experiments. Means represent x-fold mRNA induction, normalised to GAPDH mRNA levels. Statistical significance was calculated using a paired, two-tailed Student's t-test, * p<0.05, ** p<0.01, *** p<0.001.

In correlation with the strength of promoted transcription at early time points (3 h after cytokines were applied), both cytokines also mediate significant ACE mRNA increases after 18 h (2.11 ± 0.70-fold induction upon OSM and 1.33 ± 0.02-fold induction upon hIL-6/sIL-6R treatment).

The transcriptional increase of the important angiotensin receptor AT1α (Fig. 18, right diagram), which is known to be involved in hypertrophy development[263-266], is comparable in response to both stimuli (4.88 ± 0.48-fold induction after 3 h OSM treatment and 4.56 ± 0.68-fold induction after hIL-6/sIL-6R treatment). Interestingly,

as observed before for other targets (Fig. 17A), mOSM stimulation only leads to a transient increase in AT1α mRNA levels, whereas exposure of NRCFB to hIL-6/sIL-6R appears to maintain high AT1α mRNA levels at least up to 18 h (2.80 ± 0.27). This observation suggests that a similar mechanism might be responsible for the *At1α* gene induction as observed before for the *Osmr* and *Il6* transcription in NRCFB after IL-6 trans-signalling (see Fig. 17A).

4.3 Comparison of long time stimulation with hOSM and hIL-6 in NRCM and NRCFB: IL-6 induces prolonged C/EBP beta, C/EBP delta, IL-6 expression and signal transduction in NRCFB

The comparison of mOSM or hIL-6/sIL-6R induced IL-6 mRNA upregulation in NRCFB and NRCM reveals one obvious difference in the response of both primary cell types to these cytokines: In NRCM, mOSM as well as hIL-6/sIL-6R induce a clear, prolonged and comparable gene transcription resulting in elevated IL-6 mRNA levels up to 24 h or even 48 h (data not shown) past stimulation. In NRCFB, a completely different response can be observed. On the one hand, the potential of the mRNA induction is extremely different (ratio of hIL-6/sIL-6R to mOSM induced IL-6 mRNA expression is approximately 13:1 after 3 h, while it is 3:1 in NRCM). On the other hand, the kinetics of the regulated transcription of the *Il6* gene vary for both cytokines. While the IL-6/sIL-6R response is prolonged, OSM induces a very transient IL-6 mRNA upregulation which is completely shut down after 18 h. Taken together, this comparison suggests an additional factor in NRCFB that is activated or induced by IL-6, but not by mOSM. However, it is also possible that an already produced factor is more strongly activated or induced in NRCFB than in NRCM. In the following chapter the kinetics of signalling were analysed for both cytokines, and two potential candidate proteins facilitating the enormous IL-6 mRNA induction in NRCFB were introduced (C/EBPβ and C/EBPδ).

4.3.1 The short time kinetics of IL-6 and mOSM in NRCM and NRCFB are similar

To exclude the possibility that simple differences in the kinetics of signalling molecule activation contribute to the differences in gene transcription initiated by IL-6/sIL-6R or

OSM in NRCFB, we first performed short term (1-60 min) stimulations (Fig. 19). As previously described (compare sections 4.1.5 and 4.2.2), the hIL-6/sIL-6R stimulation is clearly stronger in NRCFB compared to NRCM, when mOSM serves as reference (Fig. 19, compare left panel with right panel).

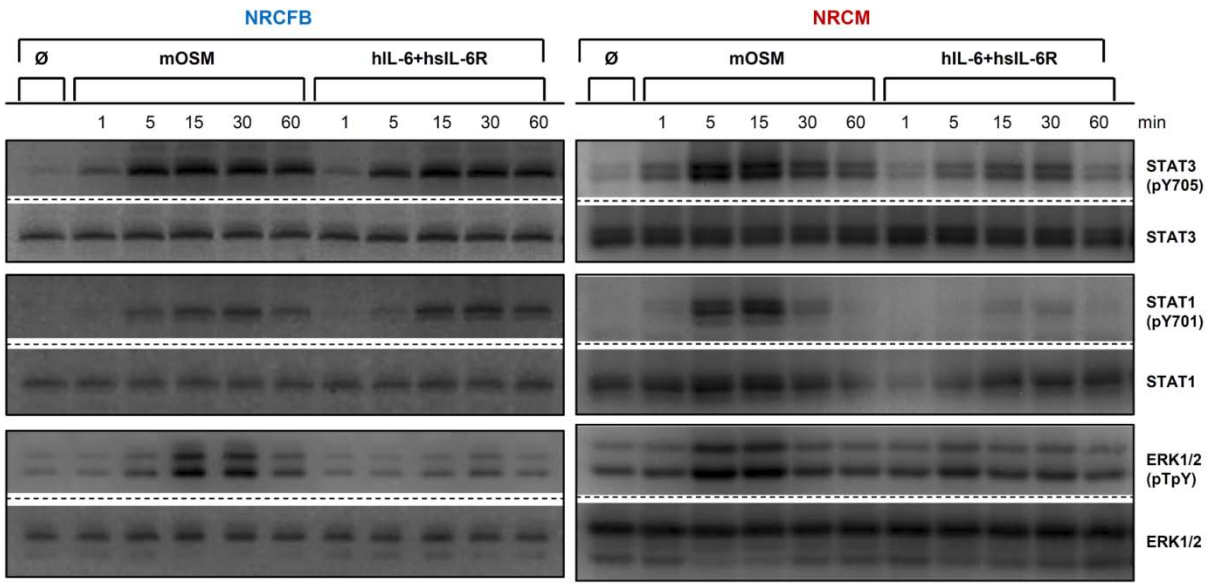

Figure 19: mOSM and hIL-6 induce similar short time kinetics of signalling in NRCFB and NRCM

Left panel of Western blots: NRCFB (P1) were stimulated with 10 ng/ml mOSM or 20 ng/ml hIL-6 plus 0.5 µg/ml hsIL-6R for the indicated time periods. Right panel of Western blots: NRCM (cultured for three days) were treated with 10 ng/ml mOSM or 20 ng/ml hIL-6 plus 0.5 µg/ml hsIL-6R for the indicated time periods. Phosphorylation levels of STAT3 (pY705) and STAT1 (pY701) as well as ERK1/2 (pT202/pY204) were detected via Western blot analysis. The blots were stripped and reprobed with antibodies recognising the proteins irrespective of their activation status (STAT3, STAT1 and ERK1/2). The Western blots shown are representative for three independent experiments.

As shown in the left Western blot panels representing mOSM and hIL-6/sIL-6R signalling kinetics on NRCFB, STAT3 and STAT1 phosphorylation is clearly induced via both cytokines. In contrast, a potent ERK1/2 phosphorylation is exclusively observed following mOSM treatment. The maxima of phosphorylations are reached after 15 min (quantification not shown), even though the 5 min, 15 min and 30 min values in NRCFB are rather similar. Interestingly, the signalling in NRCFB seems to be prolonged compared to NRCM, since strong STAT phosphorylations are still clearly detectable after 30 and 60 min. In contrast to this, after 60 min of cytokine treatment only small fractions of the initial STAT phosphorylations are detectable in NRCM (Fig. 19, right Western blots), when compared with the 15 min values. Thus, the short time kinetics cannot explain, why hIL-6/sIL-6R induces IL-6 mRNA

expression comparable to mOSM in NRCM, while it enforces much stronger and prolonged IL-6 mRNA upregulation in NRCFB. Furthermore, it is intriguing that *Il6* gene induction is rather constitutive in NRCM following treatment with either cytokine, although signalling pathways are mostly inhibited already after 60 min.

4.3.2 hIL-6/sIL-6R treatment causes prolonged signalling in NRCFB, but not in NRCM

To corroborate whether the trend towards prolonged STAT activation in NRCFB (Fig. 19, left panel) extends to increased phosphorylation levels even after several hours or days past stimulation, long time kinetics were performed. Therefore, NRCFB and NRCM were stimulated with mOSM or hIL-6/hsIL-6R for 3 h, 6 h, 12 h, 24 h and 48 h.

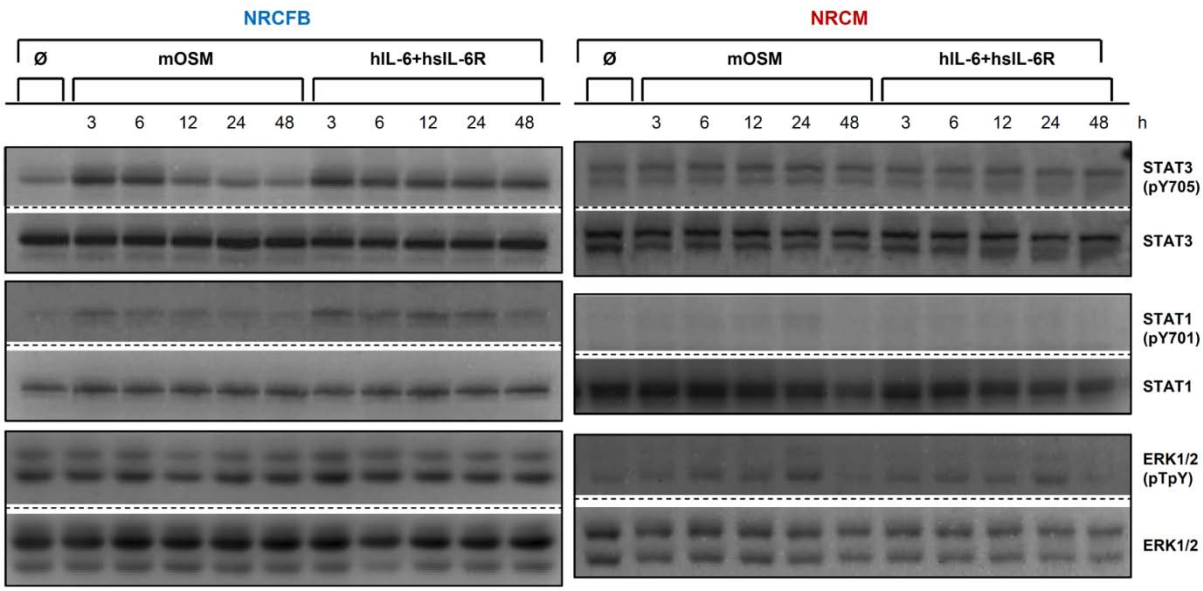

Figure 20: IL-6 signalling is clearly more prolonged in NRCFB than in NRCM
Left panel of Western blots: NRCFB (P1) were stimulated with 10 ng/ml mOSM or 20 ng/ml hIL-6 plus 0.5 µg/ml hsIL-6R for the indicated times. Right panel of Western blots: NRCM (cultured for three days) were treated with 10 ng/ml mOSM or 20 ng/ml hIL-6 plus 0.5 µg/ml hsIL-6R for the indicated duartions. Phosphorylation levels of STAT3 (pY705) and STAT1 (pY701) as well as ERK1/2 (pT202/pY204) were detected via Western blot analysis. The blots were stripped and reprobed with antibodies recognising the proteins irrespective of their activation status (STAT3, STAT1 and ERK1/2). Depicted blots are representative for three independent experiments.

The resulting Western blots are shown in figure 20. Again, the phosphorylation status of STAT3, STAT1 and ERK1/2 was used as readout for IL-6-type cytokine signalling. In NRCFB, STAT1 and STAT3 phosphorylations in response to OSM and IL-6/sIL-6R can still be detected even 3-6 h after stimulation. However, while OSM induced

signalling is mainly ceased between 6 and 12 h past stimulation, IL-6/sIL-6R induced STAT1 and STAT3 phosphorylations are maintained for at least 48 h (Fig. 20, left panel). This observation correlates with the prolonged *Il6* gene induction that was observed only in response to IL-6/sIL-6R stimulation (Fig. 17A). Aside from the induced ERK phosphorylation and the *Lif* transcription, this was the most significant difference we observed analysing these two cytokines on NRCFB. In NRCM, however, no increased phosphorylation of STATs was detectable at any time point between 3 h and 48 h (Fig. 20, right panel).

4.3.3 The IL-6 driven induction of the CCAAT/enhancer binding proteins (C/EBP) might be responsible for the strong induction of IL-6 and prolonged signalling in NRCFB

To identify potential proteins involved in the prolonged IL-6 expression in NRCFB, we decided to analyse the important IL-6 associated transcription factors C/EBPβ and C/EBPδ. C/EBPβ and δ are potent inducers of IL-6 expression[231-233]. On the other hand, as already described in the introduction, their expression is directly inducible by IL-6 treatment[232, 239-241]. To corroborate a potential involvement of these transcription factors in *Il6* transcription in NRCFB and NRCM, freshly isolated cells were stimulated for the same time periods as before with mOSM or hIL-6/shIL-6R (3 h, 12 h and 24 h for NRCM, 3 h and 18 h for NRCFB). Total RNA was isolated and mRNA levels of C/EBPβ, C/EBPδ and IL-6 were detected by quantitative real time RT-PCR (Fig. 21). Indeed, the induced C/EBP mRNA levels in NRCM are rather low (Fig. 21A, upper and middle diagram; approximately 1.8-fold C/EBPβ and 2.1-fold C/EBPδ mRNA increase after 3 h hIL-6/sIL-6R stimulation) compared with those observed in NRCFB (Fig. 21B, upper and middle diagram; 3.9-fold C/EBPβ and 14.9-fold C/EBPδ mRNA increase after 3 h hIL-6/sIL-6R treatment). However, particularly upon OSM stimulation the induction of both C/EBP mRNAs appears to be preserved for at least 24 h which correlates well with the weak, but persistent transcription of *Il6* in NRCM (Fig. 21A). Altogether, in NRCM mOSM, hLIF or hIL-6/sIL-6R induce very similar mRNA amounts of IL-6 and both C/EBPs.

Vice versa, in NRCFB the type of stimulus determines the fate of C/EBP and IL-6 expression. The *Cebpd* transcription following 3 h mOSM stimulation is potently elevated (7.4 ± 1.0-fold mRNA induction). Furthermore, C/EBP β expression is

weakly induced in response to 3 h mOSM stimulation (1.7 ± 0.2-fold mRNA induction), but only basal levels remain at later time points.

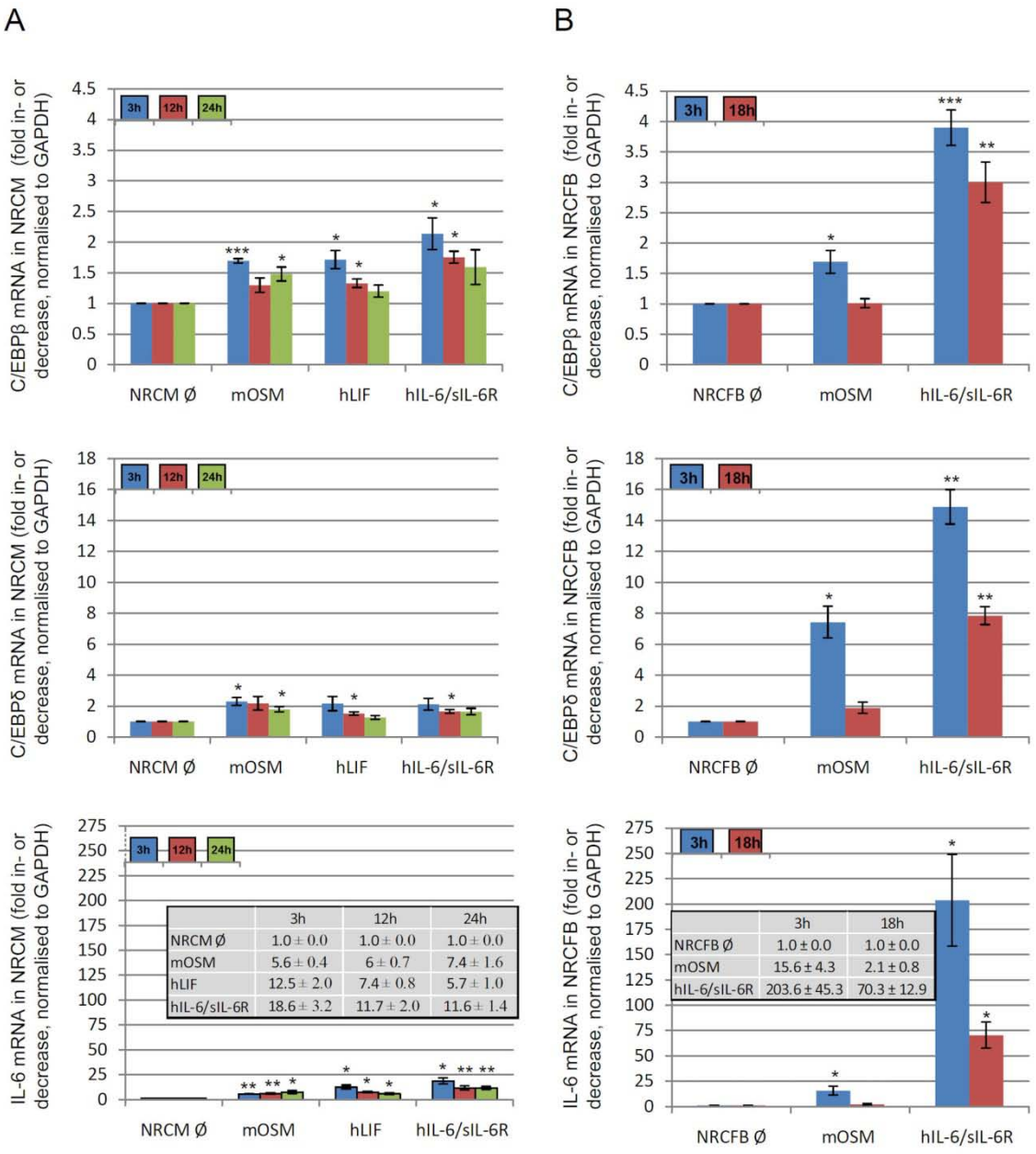

Figure 21: Enhanced C/EBPβ and δ mRNA expression in response to IL-6 correlates with the increased transcription of *Il6*

A, NRCM (cultured for three days) were treated with 10 ng/ml mOSM, hLIF or 20 ng/ml hIL-6 plus 0.5 µg/ml hsIL-6R for the indicated time periods (3 h, 12 h and 24 h). Total RNA was isolated and used for real time RT-PCR (reverse transcription, 40 cycles of denaturation, annealing and elongation). Shown are means (± SEM) of three or more independent experiments. Means represent x-fold mRNA increase or decrease, respectively, normalised to GAPDH mRNA levels. **B**, NRCFB (P1) were stimulated with 10 ng/ml mOSM or 20 ng/ml hIL-6 plus 0.5 µg/ml hsIL-6R for 3 h or 18 h. Afterwards total RNA was isolated and real time RT-PCR (reverse transcription, 40 cycles of denaturation, annealing and elongation) was performed. Shown are means (± SEM) of three or more independent experiments. Means represent x-fold mRNA inductions, normalised to GAPDH mRNA levels. Statistical significance was calculated using a paired, two-tailed Student's t-test, * p<0.05, ** p<0.01, *** p<0.001.

The nearly basal values of both C/EBPs after 18 h mOSM treatment are in line with the completely decreased IL-6 expression. In contrast, in response to hIL-6/sIL-6R treatment a stronger and more prolonged induction of C/EBP β (3.9 ± 0.3 after 3 h treatment, 3.0 ± 0.3 after 18 h treatment) and C/EBP δ (14.9 ± 1.1 after 3 h treatment, 7.8 ± 0.6 after 18 h treatment) transcription can be observed. This strongly corresponds to the much more prominent induction of *Il6* transcription in response to IL-6/sIL-6R stimulation after 3 h (203.6 ± 45.3-fold induction) and 18 h (70.3 ± 12.9-fold increase).

4.4 A comparison of hOSM, mOSM and the recently cloned rOSM: Signalling pathway induction and receptor usage

Several studies from the last two decades have clearly shown that human and murine OSM signal in a different manner. While human OSM uses two receptor complexes on human cells, the type I (gp130/LIFR) or the type II (gp130/OSMR) receptor complex [26, 73], murine OSM exclusively signals via the type II receptor complex in murine cells[74, 75]. In addition, it has been determined that human OSM activates only the type I receptor complex (LIFR/gp130) in mouse cells. However, murine OSM absolutely fails to activate signal transduction in human cells[74]. In chapters 4.1 - 4.3 the receptor preferences of mOSM and hOSM on cells from rat origin (NRCFB and NRCM) were described. These experiments indicated that hOSM and mOSM appear to use the same receptor complexes on rat cells as on murine cells. None of both cytokines is therefore able to correctly mimic the situation on human cells treated with hOSM. On the other hand, it could not be excluded that the OSMs of murine and rat origin share the same receptor preferences.

Since OSM from rat origin was not available in the past, an analysis of the receptor usage and induced signalling pathways was not performed previously. The most important question in this context has been, if the rat homologue equals the human or the murine cytokine. Therefore, an approach has been chosen, by which the receptor usage and the induced signalling pathways of human, murine and the recently available rat OSM were analysed in hepatoma cells from rat (JTC-27), human (HepG2) and murine (Hepa1c1c7) origin. All three cell lines express gp130, LIFR and OSMR (data not shown) and are capable of being stimulated by LIFR/gp130 and OSMR/gp130 activation.

4.4.1 Rat OSM induces the typical OSM mediated signalling pathways

To analyse the signalling capacities of the recently cloned rOSM, JTC-27 rat hepatoma cells were stimulated with 10, 20, 50, 100 and 200 ng/ml cytokine for 15 min.

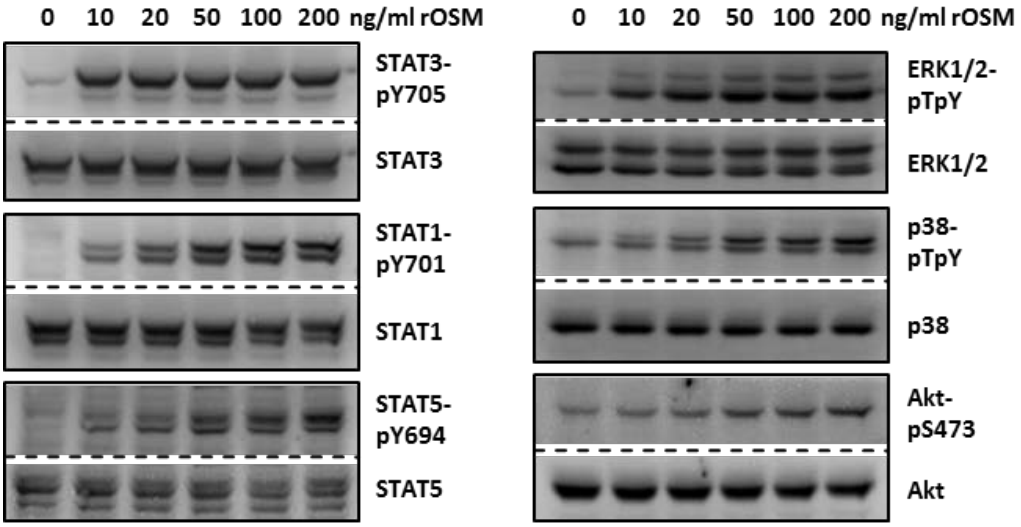

Figure 22: rOSM induces phosphorylation of STAT3, STAT1, STAT5, ERK1/2, p38 and Akt

JTC-27 cells were treated with 10, 20, 50, 100 or 200 ng/ml rOSM for 15 min. Phosphorylation levels of STAT3 (pY705), STAT1 (pY701), STAT5 (pY694), ERK1/2 (pT202/pY204), p38 (pT180/pY182) and Akt (pS473) were detected via Western blot analysis. The blots were stripped and reprobed with antibodies recognising the proteins irrespective of their phosphorylation status (STAT3, STAT1, STAT5, ERK1/2, p38 and Akt). Depicted blots are representative for three independent experiments.

The cells were lysed and SDS-PAGE followed by Western blotting was performed analysing the tyrosine phosphorylation sites of STAT3, STAT1 and STAT5 (Fig. 22). Moreover, double phosphorylation motifs of the MAPKs (ERK1/2 and p38) and the important serine (pS473) phosphorylation of Akt were analysed.

As already observed using other IL-6-type cytokines, the intensity of STAT3 phosphorylation is already maximal, when cells are treated with 10 ng/ml rOSM. Clear phosphorylations of STAT1, STAT5, ERK1/2 and p38 are already detectable at this cytokine concentration (10 ng/ml), but an rOSM induced Akt phosphorylation requires higher concentrations of the polypeptide (≥50 ng/ml). While the serine phosphorylation of Akt cannot be detected using lower concentrations of rOSM, STAT1, STAT5, ERK1/2 and p38 phosphorylation levels are even more elevated with increasing cytokine levels. Especially the levels of phospho-STAT5 and phospho-p38 are continuously augmented by increasing rOSM concentrations. Taken together,

rOSM mimics the human homologue by activating each of the analysed signalling pathways (compare chapter 4.4.2).

4.4.2 Rat OSM is able to initiate cell signalling in rat, human and murine cells

After determining the rOSM induced pathways in rat cells, its signalling capacities and cross-species activities in comparison to hLIF, hOSM and mOSM have been analysed. Therefore hepatoma cell lines from human, mouse and rat origin (HepG2, Hepa1c1c7, JTC-27) were utilised. All three cell lines were stimulated with human, murine or rat OSM (10 ng/ml) as well as human LIF (10 ng/ml) for 15 min (Fig. 23). The applied OSMs are able to induce individual signalling pattern in cells of their own species. Comparable to hLIF, hOSM, mOSM and rOSM induce the phosphorylation of STAT3, STAT1 and ERK1/2 in JTC-27 cells (Fig. 23, left panel) with partially different intensities. An activation of p38 or Akt in JTC-27 has not been observed upon stimulation with the indicated cytokine concentrations (data not shown, compare Fig. 22). As also shown previously in rat cardiac myocytes and fibroblasts, mOSM can indeed induce signal transduction on rat cells. Interestingly, the mOSM and rOSM induced STAT3 and ERK1/2 phosphorylations in JTC-27 cells show very similar strength, but rOSM mediates a clearly stronger STAT1 phosphorylation (Fig. 23, compare lanes 4 and 5). In murine cells (Hepa1c1c7, middle panel) hLIF and hOSM initiate STAT3, STAT1 and ERK1/2 phosphorylation with similar potentials, while mOSM and rOSM induce a much stronger ERK1/2 phosphorylation. However, compared with other cells STAT1 and ERK1/2 phosphorylation levels are rather weak in Hepa1c1c7 cells.

In sharp contrast to murine OSM, rat OSM is able to stimulate the human hepatoma cell line HepG2 (right panel). It induces clear tyrosine phosphorylation of STAT3, and a weak phosphorylation of STAT1 is also initiated. However, rOSM fails to distinctly activate ERK1/2. Notably, hLIF also fails to induce ERK1/2 phosphorylation and strongly mimics rOSM behaviour in human cells. Regarding these aspects, rOSM shows more similarity to hLIF than to hOSM on human cells (Fig. 23, compare lanes 12, 13 and 15). In contrast, rOSM and mOSM behave identically on murine cells (lanes 9 and 10). Taken together, rOSM can stimulate rat, murine and human cells. On rat cells, it activates similar pathways as hOSM on human cells (STAT3, STAT1, STAT5, ERK1/2 and at higher concentrations p38 and Akt, see Fig. 22). The

additional hOSM induced phosphorylations of STAT5, p38 and Akt in HepG2 cells are shown in figure 23B. Interestingly, hLIF is not able to induce p38 and Akt phosphorylation in these cells (an extremely weak STAT5 phospho-signal can be detected). Rat OSM also does not induce any of these pathways in HepG2 cells (data not shown).

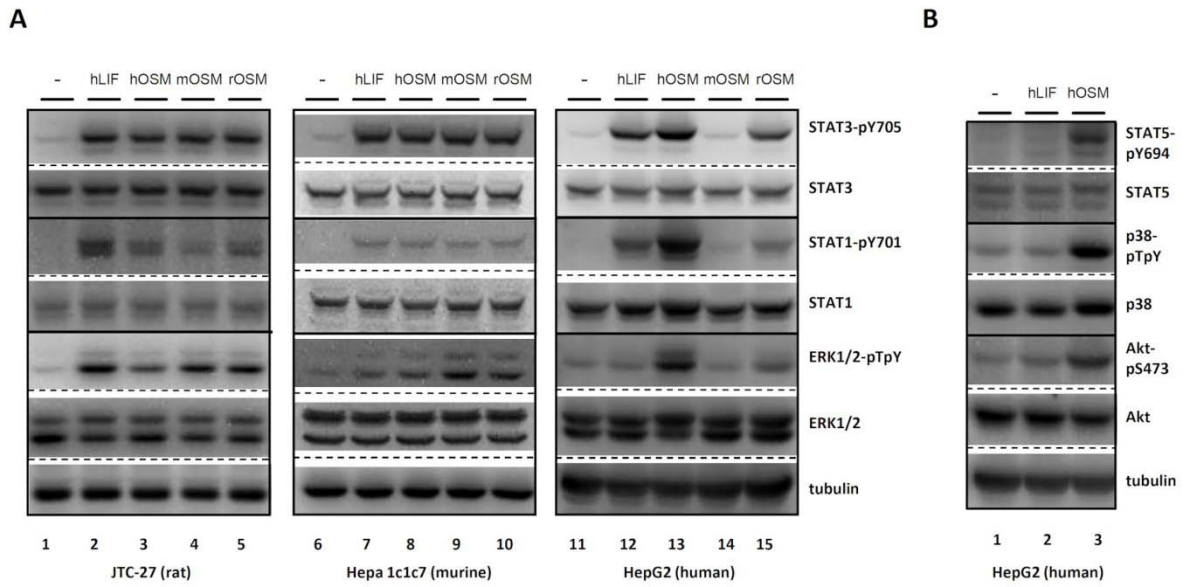

Figure 23: rOSM induces distinct signalling pathways on rat, murine and human cells

A, JTC-27 (left panel), Hepa1c1c7 (middle panel) and HepG2 (right panel) cells were stimulated with 10 ng/ml hLIF, hOSM, mOSM or rOSM for 15 min. Phosphorylation levels of STAT3 (pY705), STAT1 (pY701) and ERK1/2 (pT202/pY204) were detected via Western blot analysis. The blots were stripped and reprobed with antibodies recognising the proteins irrespective of their activation status (STAT3, STAT1, ERK1/2 and tubulin). Depicted blots are representative for three independent experiments. **B**, HepG2 cells were stimulated with 10 ng/ml hLIF, hOSM, mOSM or rOSM for 15 min. Phospho-levels of STAT5 (pY694), p38 (pT180/pY182) and Akt (pS473) were detected via Western blot analysis. After stripping, the membranes were reprobed with the respective, total protein recognising antibodies (STAT5, p38, Akt and tubulin). Western blots shown are representative for three independent experiments.

4.4.3 Rat OSM signals via the LIFR/gp130 (type I) and the OSMR/gp130 (type II) receptor complex on rat cells

After determining the signalling pathways induced by hOSM, mOSM and rOSM on rat, murine and human hepatoma cells, the used receptor complexes were characterised. To analyse the participation of the rLIFR for rOSM signalling, the LIFR was blocked by the antagonist LIF-05. This protein represents a mutated variant of human LIF in which the binding site for the LIFR (site 3) is unmodified, while the

binding site for gp130 (site 2) is destroyed. LIF-05 still binds to the LIFR, but acts as a strong LIF antagonist by preventing gp130-LIFR-heterodimerisation[254]. The antagonistic activity of LIF-05 is presented in figure 24. The induced signalling of hLIF (lanes 3 and 4) and hOSM (lanes 5 and 6) is strongly reduced in the presence of the LIFR antagonist.

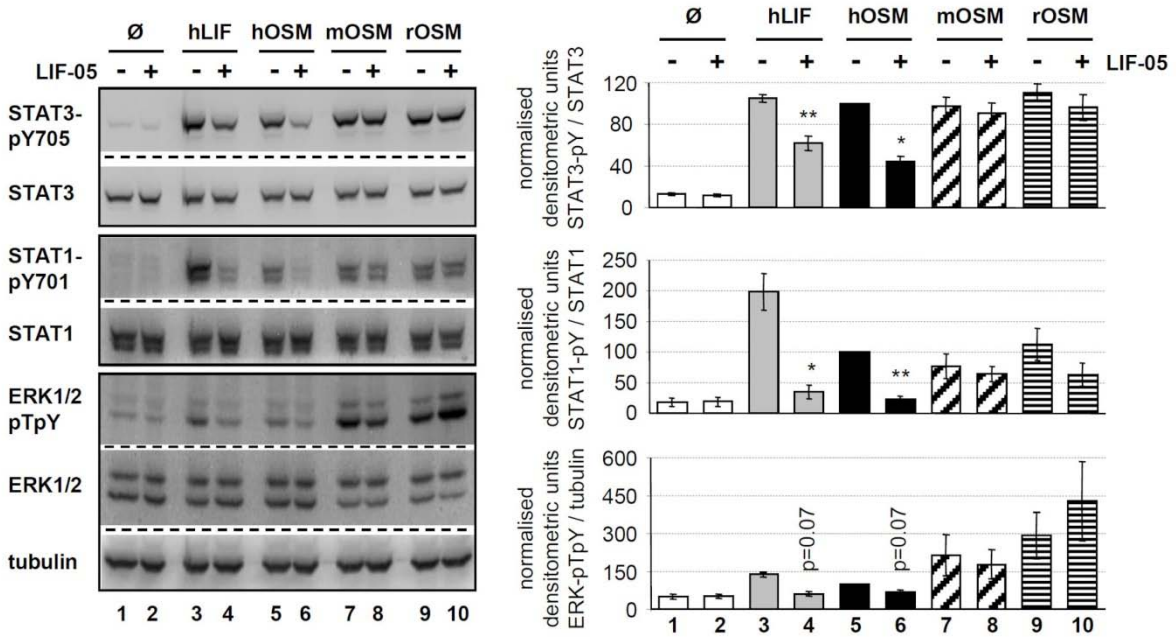

Figure 24: rOSM signals through LIFR/gp130 and OSMR/gp130 complexes: Blockade of the rLIFR through LIF-05

JTC-27 were preincubated with LIF-05 (50 ng/ml, 30 min) and subsequently stimulated with 10 ng/ml hLIF, hOSM, mOSM and rOSM for 15 min. The phosphorylation intensities of the indicated proteins were detected via Western blot analysis. The membranes were stripped and reprobed with antibodies recognising the proteins irrespective of their activation status (STAT3, STAT1, ERK1/2 and tubulin). Phosphorylation intensities were quantified by chemiluminescence analysis (right panel) and normalisation to loading controls. Shown are the means (n=3) with standard error of mean (SEM). * p<0.05, ** p<0.01 untreated vs. LIF-05-pretreated sample.

The dramatic decrease indicates that, equivalent to hOSM behaviour on murine cells, hOSM exclusively utilises the rLIFR/rgp130 (type I) receptor complex. In contrast, the activation of STAT3 and STAT1 following rOSM stimulation is barely decreased in the presence of LIF-05 (Fig. 24, lanes 9 and 10) supporting the hypothesis, that rOSM is able to signal via the gp130/OSMR complex. Surprisingly the rOSM mediated ERK1/2 activation is even increased in the presence of LIF-05. According to the results of the NRCM and NRCFB, no inhibitory effect of LIF-05 can be

observed, when JTC-27 were treated with mOSM indicating an exclusive rOSMR/rgp130 (type II receptor complex) activation by the murine cytokine.

Furthermore, RNA interference studies using siRNA specifically silencing the rat OSMR were performed in JTC-27 cells (Fig. 25A and B). Transient siRNA transfection of JTC-27 rat hepatoma cells targeting the rat OSMR resulted in 80% reduction of OSMR mRNA expression (Fig. 25A).

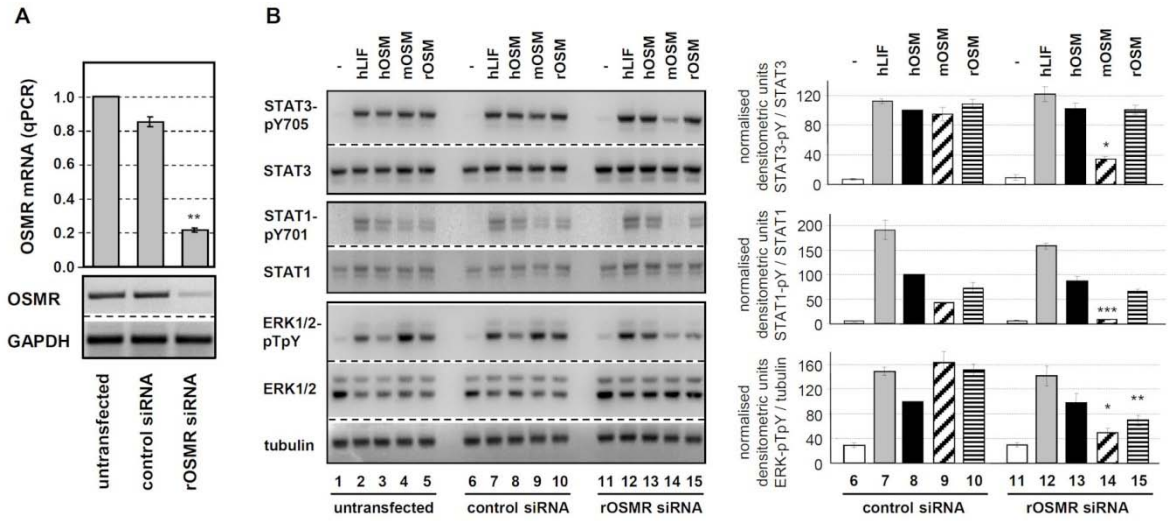

Figure 25: rOSM signals through LIFR/gp130 and OSMR/gp130 complexes: Silencing the rOSMR through use of siRNA

A, JTC-27 were transfected with control or rOSMR siRNA or left untransfected. Transfection efficiencies were analysed by semiquantitative RT-PCR (bottom) and quantitative real time RT-PCR (top). **B**, Untransfected, control siRNA and rOSMR siRNA transfected JTC-27 were treated with 10 ng/ml hLIF, hOSM, mOSM and rOSM for 15 min. Lysates were subjected to Western blot analysis using antibodies specific for the indicated proteins. The blots were stripped and reprobed with antibodies recognising the proteins irrespective of their phosphorylation status and with an α-tubulin antibody. Phosphorylation intensities were quantified by chemiluminescence analysis and normalisation to loading controls. hOSM activation level was set to 100%. Shown are the means (n=3) with standard error of mean (SEM). * p<0.05, ** p<0.01, *** p<0.001 OSMR siRNA vs. control siRNA.

Stimulation with hLIF guaranteed the specificity of the rOSMR knockdown, because LIFR/gp130 signalling is not impaired by rOSMR siRNA. LIF induces similar phosphorylation levels of STAT1, STAT3 and ERK1/2 in OSMR siRNA transfected, control siRNA transfected or untransfected cells (Fig. 25B, compare lanes 2, 7 and 12). An interesting result was observed in OSMR siRNA transfected JTC-27 cells treated with rOSM: the phosphorylation of STAT3 and STAT1 in response to rOSM is not significantly affected by rOSMR knockdown (Fig. 25B, lanes 5, 10, 15 and quantification). However, a clear reduction in ERK1/2 phosphorylation intensity

(approximately 50%) is observed in OSMR knockdown cells (Fig. 25B, lanes 5, 10 and 15). In sharp contrast, all mOSM induced signalling pathways (STAT3, STAT1, ERK1/2) are impaired by approx. 80% in JTC-27 transfected with rOSMR siRNA in comparison to untransfected cells (lanes 4, 9 and 14, quantification). This exactly correlates with the knockdown efficiency of the rOSMR (reduction of 80%, Fig. 25A). In contrast, hOSM signalling is not attenuated by the knockdown of the rat OSMR (lanes 3, 8 and 13). Taken together, these results strongly suggest that rOSM, unlike mOSM, but similar to hOSM, is able to utilise two receptor complexes, the type I (LIFR/gp130) and the type II (OSMR/gp130) receptor complex on rat cells. OSM from murine origin exclusively uses the type II receptor complex, while human OSM signals via the type I receptor complex on rat cells.

4.4.4 Rat OSM on murine cells: Higher preference for the type II OSMR receptor

Next, the signalling preferences of rOSM on murine hepatoma cells (Hepa1c1c7) were determined. As previously shown in figure 23, rOSM is able to induce signal transduction in Hepa1c1c7. Human OSM also mediates signalling on murine cells, but is known to exclusively use the type I (mLIFR/mgp130) receptor complex on mouse cells[74, 75]. To analyse, if rOSM only uses the type I receptor complex on murine cells too, LIFR mediated signalling was again blocked using the mutein LIF-05 (see 4.4.3, Fig. 24). As shown in figure 26, the blockade of LIFR strongly reduces the LIFR/gp130 induced phosphorylation of STAT3, STAT1 and ERK1/2 by hLIF and hOSM (Fig. 26, lanes 3, 4, 5 and 6). In contrast, no decrease of the mOSM or rOSM induced phosphorylations can be observed in the presence of LIF-05 (lanes 7, 8, 9 and 10). This is a clear proof that rOSM based signalling in mouse cells, in contrast to hOSM mediated signalling, does not exclusively rely on the type I receptor complex (gp130/LIFR).

Hepa1c1c7 cells were additionally treated with siRNA targeting murine OSMR mRNA. Thereby similar knockdown efficiencies as in rat JTC-27 (Fig. 25A) cells were achieved (Fig. 27A, panel 4, mOSMR protein, Fig. 27B, quantification of mOSMR levels). Equivalent reductions were determined for the mOSMR mRNA by semi-quantitative RT-PCR (data not shown). The analysis of the cytokine initiated signalling pathways in presence or absence of mOSMR siRNA clearly shows, that phosphorylations induced by hLIF as well as hOSM are not significantly reduced in

the presence of the mOSMR siRNA (Fig. 27A, compare lanes 2, 7 and 12 for hLIF, lanes 3, 8 and 13 for hOSM). However, mOSM and rOSM induced ERK1/2 phosphorylation is almost completely abrogated by the knockdown of the mOSMR (Fig. 27A, third panel, lanes 4, 5, 9, 10, 14 and 15). Moreover, the mOSM induced STAT1 tyrosine phosphorylation also seems to be mostly/exclusively mediated by the type II receptor complex since it is severely impaired upon mOSMR knockdown (Fig. 27A, second panel, lanes 4, 9 and 14).

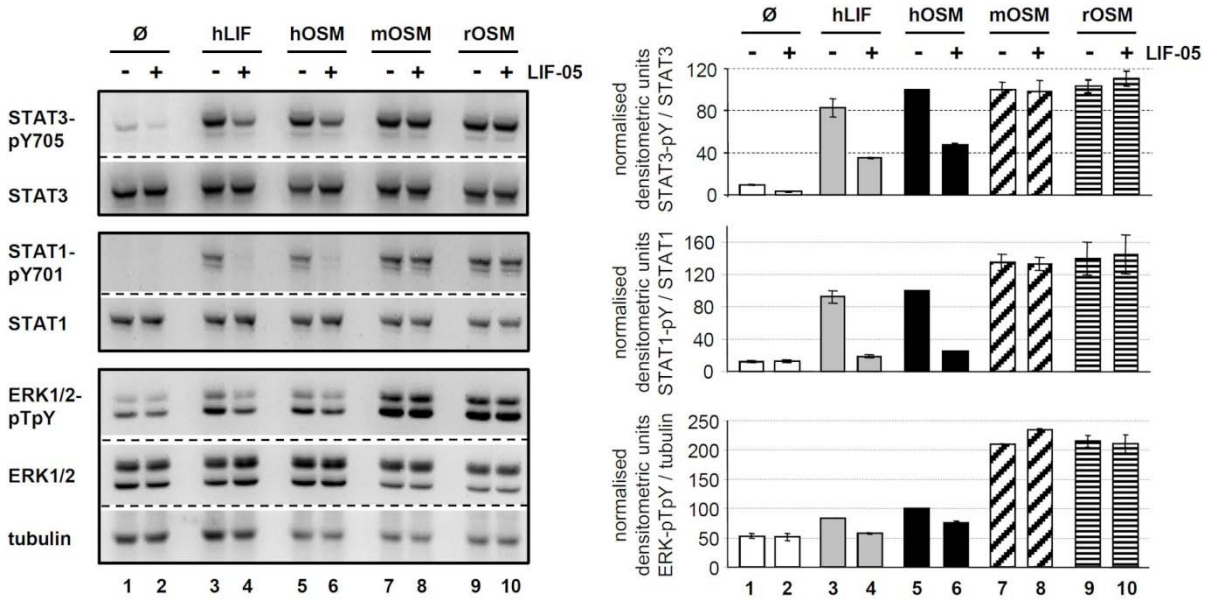

Figure 26: rOSM mainly signals via the type II receptor complex in murine cells: LIFR blockade using LIF-05

Murine hepatoma cells (Hepa1c1c7) were preincubated with 50 ng/ml LIF-05 for 30 min and subsequently treated with 1 ng/ml hLIF, 10ng/ml hOSM, 10ng/ml mOSM or 10ng/ml rOSM for further 15 min. The phosphorylation intensities of the indicated proteins were detected via Western blot analysis. The membranes were stripped and reprobed with antibodies recognising the proteins irrespective of their activation status (STAT3, STAT1, ERK1/2 and tubulin). Phosphorylation intensities were quantified by chemiluminescence analysis (right panel) and normalisation to loading controls. hOSM activation level was set to 100%. Shown are the means (n=2) with standard error of mean (SEM).

The results of STAT1 phosphorylation upon rOSM stimulation are rather ambiguous, as a partial, but not significant decrease of the already weak phospho-signal is observed in the presence of the mOSMR siRNA. Part of the STAT1 signal seems to be mediated by LIFR/gp130 heterodimers, although rOSM actually does not potently induce STAT1 phosphorylation in these cells. Similar to the results of the STAT1 activation, the STAT3 tyrosine phosphorylation following mOSM treatment is strongly

reduced in mOSMR siRNA transfected Hepa1c1c7 (Fig. 27A, lanes 4, 9 and 14, first panel). The rOSM induced STAT3 phosphorylation is also partly abrogated in mOSMR siRNA transfected Hepa1c1c7 cells, but clearly stronger STAT3 phosphorylation is maintained than after mOSM stimulation (lanes 5, 10 and 15 of the first panel) indicating that both receptor complexes might potentially be involved.

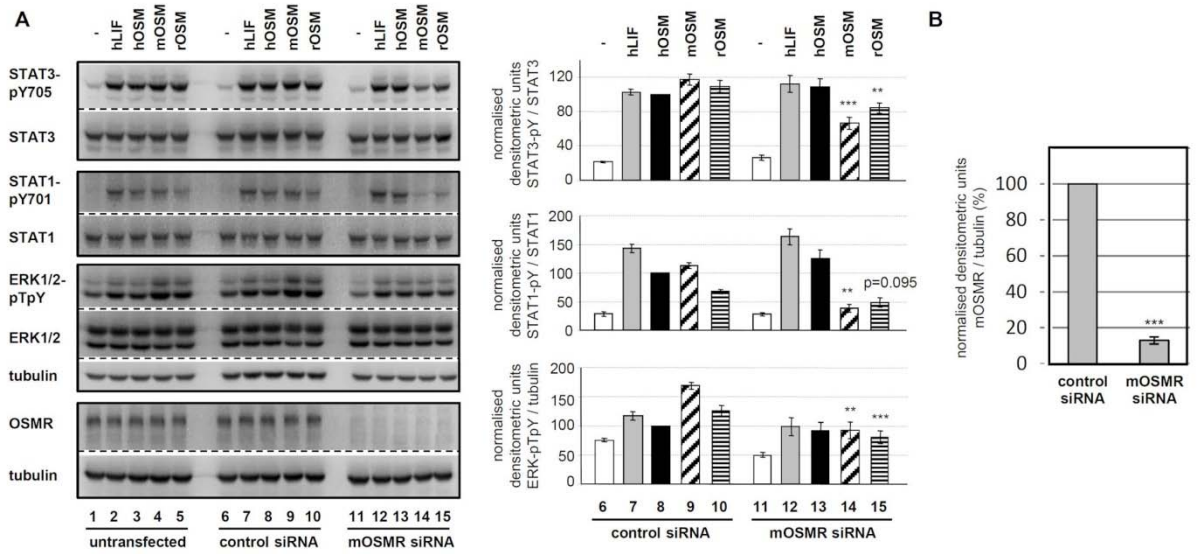

Figure 27: rOSM mainly signals via the type II receptor complex in murine cells: Silencing the murine OSMR using specific siRNA

A, Hepa1c1c7 were transfected with control or mOSMR siRNA or left untransfected. Untransfected, control and mOSMR siRNA transfected Hepa1c1c7 cells were treated with 10 ng/ml hLIF, hOSM, mOSM and rOSM for 15 min. Lysates were subjected to Western blot analysis using antibodies specific for the detection of STAT3 (pY705), STAT1 (pY701), ERK1/2 (pT202/pY204) and protein levels of the OSMR. The blots were stripped and reprobed with antibodies recognising the proteins irrespective of their phosphorylation status and with an α-tubulin antibody. Phosphorylation intensities were quantified by chemiluminescence analysis and normalisation to loading controls. hOSM activation level was set to 100%. Shown are the means (n=4) with standard error of mean (SEM). * p<0.05, ** p<0.01 and *** p<0.001 OSMR siRNA vs. control siRNA. **B**, Corresponding quantification of mOSMR protein levels normalised to tubulin. Control siRNA was set to 100%. Shown are the means (n=4) with standard error of mean (SEM). *** p<0.001 OSMR siRNA vs. control siRNA.

4.4.5 Rat OSM utilises the type I receptor complex on human cells

After characterizing the rOSM receptor preferences on rat and murine cells, human HepG2 hepatoma cells were used to determine the receptor usage of the cytokine on human cells. Therefore, equivalent experiments as performed before in Hepa1c1c7 and JTC-27 cells (4.4.4 and 4.4.3) have been carried out. Again, the LIFR based

signalling was suppressed using LIF-05. Blockade of the human LIFR by LIF-05 completely inhibits the rOSM induced STAT3 and STAT1 tyrosine phosphorylation (Fig. 28, lanes 9 and 10). Unlike hOSM that is known to signal via both human receptor complexes, no rescue of the rOSM and the hLIF mediated signalling occurs, if the LIFR is blocked (Fig. 28A, compare lanes 3, 4, 5, 6, 9 and 10). As described above, murine OSM is not able to elicit signalling on human cells. Unlike the situation in rat or murine cells, rat OSM exclusively signals via the type I receptor complex on human cells. There is no hint for any hOSMR activation by rOSM. In chapter 4.4.6 the clear evidence for this hypothesis is shown by using Ba/F3 cells expressing only hOSMR/hgp130.

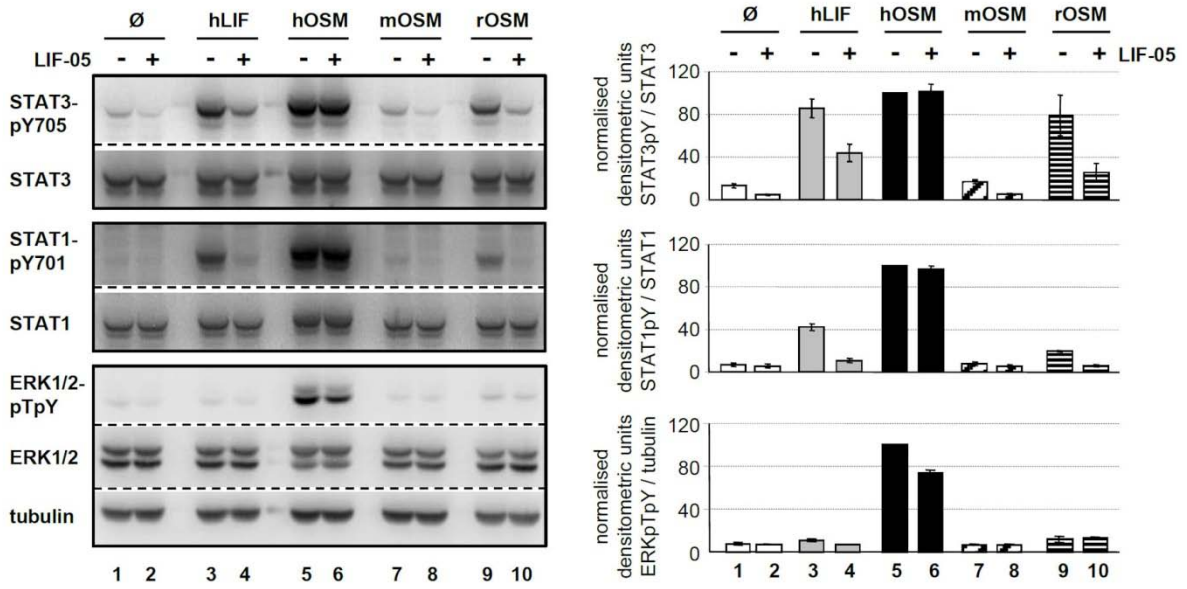

Figure 28: rOSM signals via the type I receptor complex in human cells: Blockade of the hLIFR via LIF-05

Human hepatoma cells (HepG2) were preincubated with LIF-05 (50ng/ml, 30 min). Afterwards the cells were treated with 10 ng/ml hLIF, hOSM, mOSM or rOSM for 15 min. The phosphorylation intensities of the indicated proteins were detected via Western blot analysis. The membranes were stripped and reprobed with antibodies recognising the proteins irrespective of their activation status (STAT3, STAT1, ERK1/2 and tubulin). Phosphorylation intensities were quantified by chemiluminescence analysis and normalisation to loading controls. hOSM activation level was set to 100%. Shown are the means (n=2) with standard error of mean (SEM).

Vice versa, silencing the human OSMR using specific hOSMR siRNA (Fig. 29A, panel 4, hOSMR protein, Fig. 29B, quantification of hOSMR levels) does not negatively influence rOSM induced signalling (Fig. 29A, lanes 5, 10 and 15 of panel 1 and 2). In contrast STAT1 and ERK1/2 phosphorylations in response to hOSM are

strongly decreased in the presence of OSMR siRNA confirming that LIFR/gp130 based signalling alone is not able to maintain the activation of these pathways. The phosphorylation of STAT3 is also significantly decreased in OSMR siRNA transfected cells, but the degree of inhibition is less severe compared to STAT1 and ERK1/2. Taken together, rOSM exclusively utilises the hLIFR/hgp130 type I receptor complex on human cells, thereby mimicking neither murine nor human OSM.

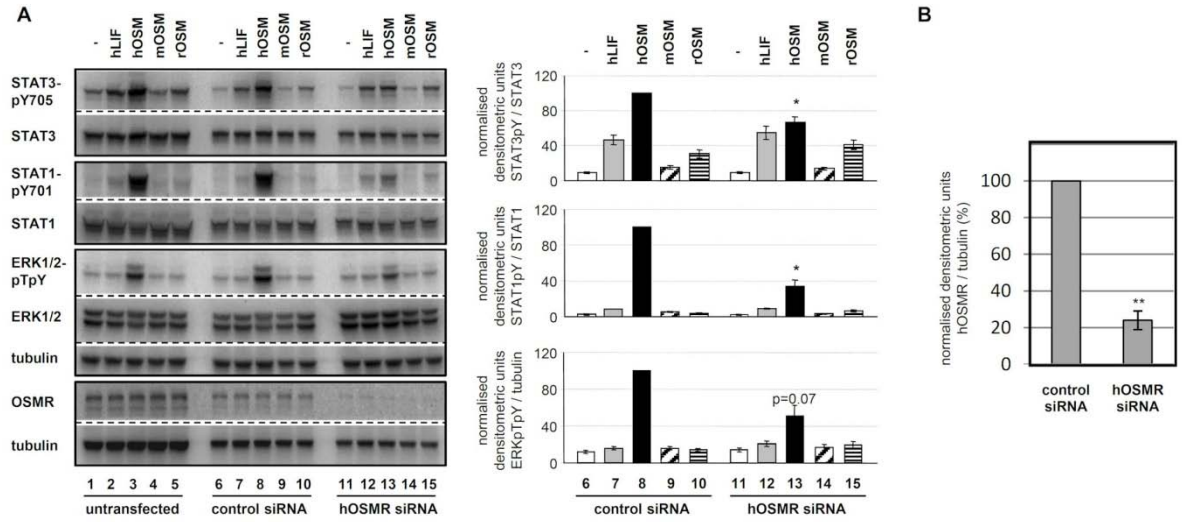

Figure 29: rOSM signals via the type I receptor complex in human cells: Silencing the hOSMR via specific OSMR siRNA

A, HepG2 were transfected with control or hOSMR siRNA or left untransfected. Untransfected, control and hOSMR siRNA transfected HepG2 cells were exposed to 10 ng/ml hLIF, hOSM, mOSM or rOSM for 15 min. Cell lysates were used for Western blot analysis and phosphorylation levels of STAT3 (pY705), STAT1 (pY701), ERK1/2 (pT202/pY204) and protein levels of the OSMR were detected. After stripping membranes were reprobed with antibodies recognising the proteins irrespective of their phosphorylation status and with an α-tubulin antibody. Phosphorylation intensities were quantified by chemiluminescence analysis and normalisation to loading controls. hOSM activation level was set to 100%. Shown are the means (n=3) with standard error of mean (SEM). * $p<0.05$, ** $p<0.01$ and *** $p<0.001$ OSMR siRNA vs. control siRNA. **B**, Corresponding quantification of hOSMR protein levels normalised to tubulin. Control siRNA was set to 100%. Shown are the means (n=3) with standard error of mean (SEM). ** $p<0.01$ OSMR siRNA vs. control siRNA.

4.4.6 Confirmation of the rat OSM receptor usage on human cells using stably transfected Ba/F3-hOSMR/hgp130 cells

To corroborate the rather surprising finding that rOSM might solely use the LIFR/gp130 type I receptor complex on human cells, proliferation assays were carried out in stably transfected Ba/F3 cells expressing only hOSMR and hgp130. For this purpose, the cells were treated with different concentrations of hOSM and rOSM

for 48 h. As shown in figure 30, Ba/F3 cells expressing hOSMR and hgp130 (type II receptor complex) proliferate in a dose dependent manner in response to hOSM. Already concentrations of 0.8 ng/ml hOSM are sufficient to induce measurable Ba/F3 proliferation. At concentrations of 20 to 100 ng/ml hOSM the proliferation response is saturated (Fig. 30, red curve).

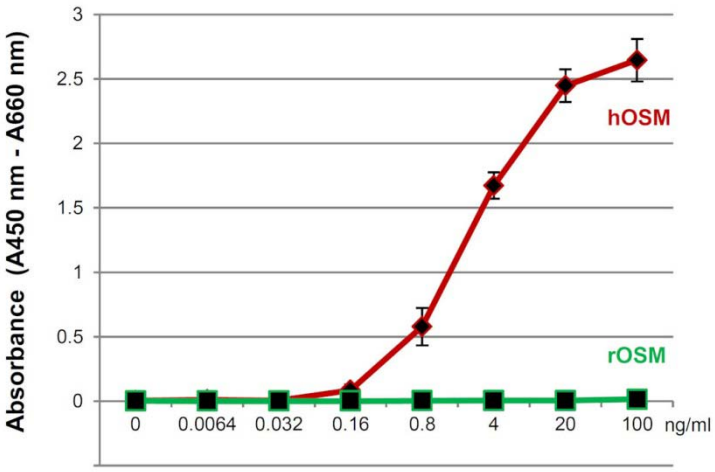

Figure 30: rOSM is not able to induce proliferation of hOSMR/hgp130 expressing Ba/F3 cells

Stably transfected Ba/F3 cells expressing hOSMR and hgp130 were treated with different concentrations of hOSM and rOSM (0.0064 – 100 ng/ml cytokine) for 48 h. To evaluate the proliferation rate, the WST-1 reagent was subsequently added to the cell suspension and Ba/F3 cells were incubated for additional 4 h. The shown values represent means (± SEM) of the measured absorbance at 450 nm minus absorbance at 660 nm. The means with SEM were calculated from three independent experiments.

In sharp contrast to hOSM, rOSM is unable to induce proliferation of the cells even at a concentration as high as 100 ng/ml which is ten times the amount used in experiments before (Fig. 30, green line). This clearly proves that the human type I receptor complex is activated by the cytokine, while the human type II receptor complex is not.

4.4.7 Confirmation of the finding that rOSM signals through the rat type I and the rat type II receptor complex using stably transfected Ba/F3 cells

Since LIF-05 or rat OSMR siRNA were not able to fully abrogate LIFR based signalling or OSMR transcription, respectively, in rat JTC-27 cells (see section 4.4.3), we decided to additionally analyse the receptor usage of rOSM on stably transfected

Ba/F3 cells. In contrast to cells naturally expressing rgp130, rOSMR and rLIFR, these cells have the clear advantage of synthesising only the desired receptor combination (rLIFR-rgp130 or rOSMR-rgp130). Therefore, rOSMR, rLIFR and rgp130 were cloned from total RNA isolated from the rat hepatoma cell line JTC-27 and subcloned into a vector containing a bidirectional tet-responsive promoter upstream of two multiple cloning sites (pBO)[255]. After inserting either the rOSMR and rgp130 combination or the rLIFR and rgp130 combination, the sequenced vectors (@164: pBO-rgp130-rOSMR and @166: pBO-rgp130-rLIFR) were singly electroporated into Ba/F3 cells already expressing the doxycycline inducible reverse tet-responsive transcriptional activator (rtTA). After selecting the cells with hygromycin and geneticin (G418), the expression of the respective receptor combination was induced by 0.5 µg/ml doxycycline (24 h). RNA was isolated and upon stimulation the cells were lysed to analyse the cytokine induced pathways. The resulting RNAs were used to confirm the expression of rgp130, rOSMR, rLIFR, while mGAPDH served as control (Fig. 31A). All transfected cells express rgp130 mRNA independent of the doxycycline induction, what might result from a leakiness of the promoter. The Ba/F3-rgp130-rOSMR cells additionally express rOSMR mRNA, however, similarly independent of doxycycline. The LIFR expression in Ba/F3-rgp130-rLIFR seems to be slightly increased upon doxycycline treatment, since more LIFR mRNA is produced in the presence of the antibiotic. However, the leakiness of the promoters is completely irrelevant for the analysed receptor preferences. As a precautionary measure, all induced signalling pathways were determined in the presence of doxycycline. For Western blot analyses, the cells were treated with 10 ng/ml hLIF, 20 ng/ml hOSM, mOSM or rOSM, respectively, for 15 min. The cell lysates were examined performing quantitative Western blot analysis detecting STAT3 (pY705), STAT1 (pY701) and ERK1/2 (pT202/pY204) phosphorylation levels. As shown in Fig. 31B (upper panel), in Ba/F3 cells expressing rgp130 and rOSMR STAT3, STAT1 and ERK1/2 are exclusively phosphorylated in response to mOSM or rOSM stimulation. Human LIF or hOSM fail to activate any analysed pathway. This is the clear proof that only mOSM and rOSM can utilise the rat OSMR/gp130 (type II) receptor complex among the analysed cytokines (Fig. 31B, lanes 4 and 5 of the upper panel). In sharp contrast, in Ba/F3 cells expressing rgp130 and rLIFR STAT3, STAT1 and ERK1/2 are exclusively phosphorylated in response to hLIF, hOSM and rOSM, while mOSM fails to induce any signalling pathway (Fig. 31B, lower panel, lanes 2, 3 and 5). Thus rOSM, just like

hLIF and hOSM, is able to signal via the rLIFR/rgp130 (type I) receptor complex. Comparable to the results shown in 4.4.3 (hOSM, mOSM and rOSM stimulation of JTC-27 cells), OSM from murine origin is not capable of utilising the rat OSM type I receptor complex.

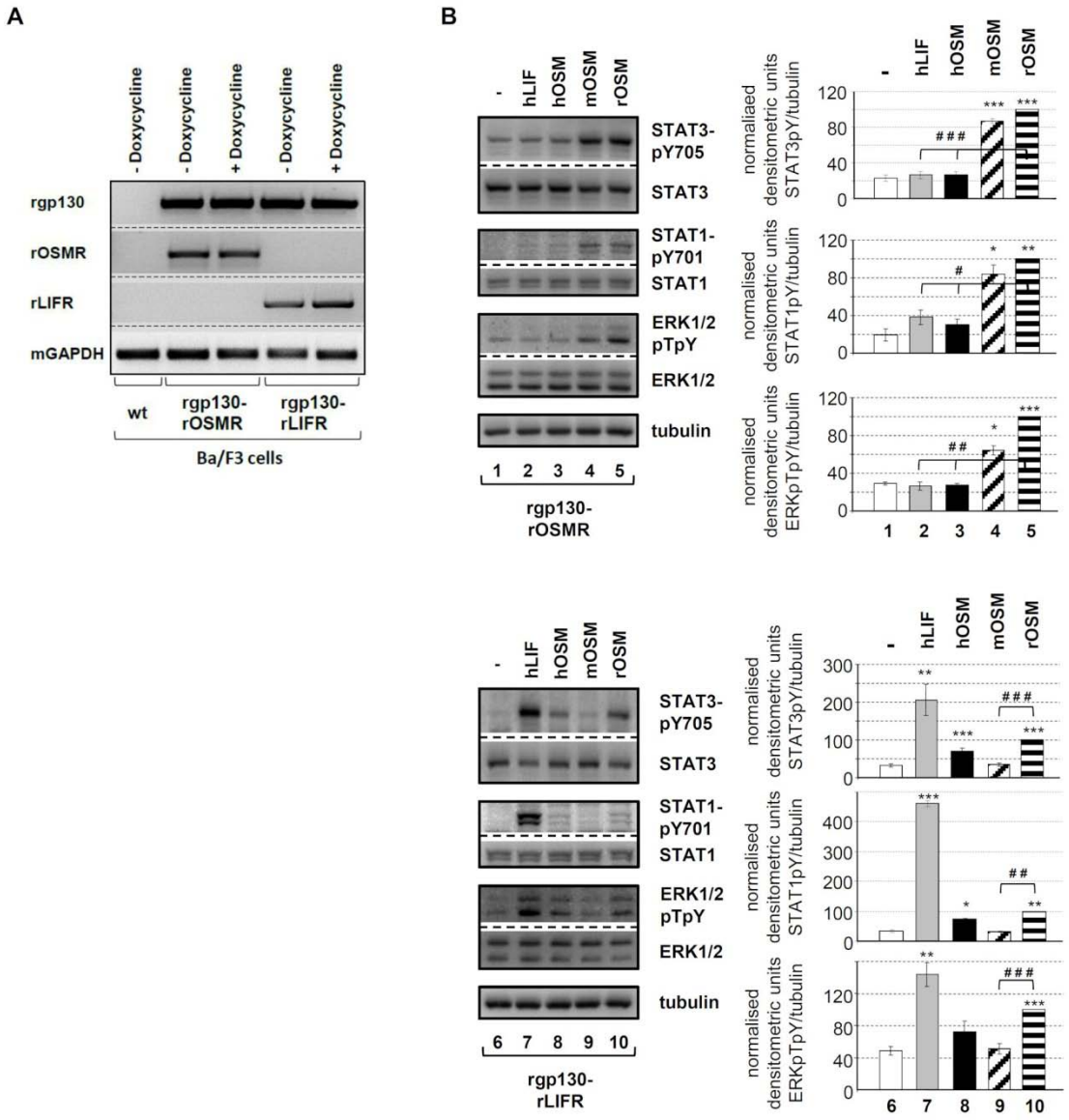

Figure 31: rOSM signals via the cloned rat type I and type II receptor complex

A, Ba/F3 cells (wt (wildtype), selected pool of cells expressing rgp130/rOSMR or rgp130/rLIFR) were cultured on 6 well plates (conditions, see 3.3.1). After reaching 80% confluency, one well of Ba/F3-rgp130-rOSMR and Ba/F3-rgp130-rLIFR each was treated with 0.5 µg/ml doxycycline for 24 h. Total RNA was isolated using the RNeasy Mini Kit. RT-PCR was performed using the indicated primers and the Verso 1-Step RT-PCR Kit. **B**, Ba/F3 cells expressing either rOSMR/rgp130 or rLIFR/rgp130 were cultured on 24 well plates to a density of 2 x 10^5 cells per well. The expression of the respective receptors was induced 24 h before addition of the cytokines. The cells were treated with 10 ng/ml hLIF or 20 ng/ml hOSM, mOSM or rOSM for 15 min. The phosphorylation intensities of the indicated proteins were detected via Western blot analysis. The membranes were stripped and reprobed with antibodies recognising the proteins irrespective of their activation status (STAT3, STAT1, ERK1/2 and tubulin). Activation determined for rOSM was set to 100%. Shown are the means (n=3 for STAT1 and ERK, n=6 for STAT3) with standard error of mean (SEM). * p<0.05, ** p<0.01, *** p<0.001 untreated vs. cytokine-treated sample, # p<0.05, ## p<0.01, ### p<0.001 for rOSM vs. either hLIF/hOSM or mOSM.

The results from Ba/F3 cells expressing the rat type I or type II OSM receptor complex provide clear evidence that rOSM is able to signal through both receptor complexes in a human OSM-like manner, that is clearly divergent from the murine homologue.

5 Discussion

5.1 Classification of the hypertrophic potential of IL-6-type cytokines

Cardiac hypertrophy is a crucial element of the protective cardiac remodelling upon pathological insults. However, in some cases cardiac hypertrophy can result in the development of a severe heart insufficiency. Initial processes of cardiac hypertrophy cause an increase of muscular mass as a compensatory reaction to altered conditions. The long term growth of cardiac myocytes, however, has rather harmful side effects. Such modifications contribute to a loss of myocardial contractility and primary plasticity, a scenario in which the primary compensatory response converts to a maladaptive reaction[267]. The experiments performed within this study highlight the hypertrophic influence of oncostatin M (OSM) in comparison to related IL-6-type cytokines on neonatal rat cardiac myocytes (NRCM). Within the first part of the results it has been shown that hOSM and mOSM as their related IL-6-type cytokines hLIF, hCT-1 and hIL-6 combined with hsIL-6R are able to induce an elongated phenotype (eccentric hypertrophy) of NRCM which results in cell growth of approximately twice the size of untreated cells. Although overexpression of STAT3 in transgenic mice has been shown to be sufficient to initiate cardiomyocyte hypertrophy *in vitro*[227] and *in vivo*[268], IL-6-type cytokines so far have not been considered as therapeutic targets in anti-hypertrophy approaches. To analyse, if different IL-6-type cytokines induce diverse kinds of hypertrophy based on their property to initiate not only redundant STAT3 phosphorylation, but also activation of different sets of MAPKs, further STATs, Akt and additional proteins involved in other hypertrophic pathways, we decided to perform a comparison of the hypertrophic potentials, the induced signalling pathways and the induction of hypertrophy enhancing mRNAs. The role of OSM was of central importance, as no publications determining the hypertrophic potential of the cytokine existed at that time. In contrast, several studies were already available showing the hypertrophic potential of LIF, IL-6 and CT-1[194-197, 199-205, 210]. In addition to NRCM, we also analysed the same signalling pathways and hypertrophy enhancing mRNAs in neonatal rat cardiac fibroblasts (NRCFB) to determine the involvement of this second cardiac cell type in the development of cardiac hypertrophy.

It has to be mentioned that the hypertrophic network comprises several ligand-receptor interactions and downstream pathways. Besides the IL-6-type cytokine-gp130-axis, Na^+/H^+ channels, Na^+/Ca^{2+} channels, insulin-like growth factor receptors, L-type Ca^{2+} channels and G protein coupled receptors like adrenergic receptors, angiotensin receptors and endothelin receptors play important roles in the development of cardiac hypertrophy[269]. The functions of many of these participating proteins have been analysed in recent years. In this study a potential interaction between IL-6-type cytokines and the renin-angiotensin system has been corroborated in more detail.

5.1.1 Hypertrophic potential of oncostatin M in relation to different heart relevant IL-6-type cytokines

Primary neonatal rat cardiomyocytes represent the most common and most frequently used *in vitro* model to determine cardiomyocytic hypertrophy. The primary culture of NRCM was already established 30 years before, in 1982[270], and until today it is the routinely used cell based system for basic cardiovascular research. The difficulties of NRCM preparation are to achieve high purity of myocyte cultures and to maintain the quality of such cultures by exact standardisation of preparation and culture conditions. Especially the analysis of induced signalling pathways places high demands on a freshly isolated primary cell culture. A number of cardiomyocyte cell lines (H2C9[271], HL-1[272] or AC16[273]) have been established within the past four decades which express specific cardiomyocyte markers (e.g. sarcomeric α-actinin or cardiac myosin heavy chain)[271-273] and seem to display a comparable hypertrophic potential as their primary counterparts[274, 275]. However, these cell lines have been described to develop the tendency to dedifferentiate[272, 276] rendering them inappropriate for reproducible results. We therefore decided to work with primary NRCM.

Supported by the group of Prof. Dr. Stefan Engelhardt (until October 2008 RVZ, Würzburg, now TU Munich), we have analysed cytokine induced cardiac hypertrophy using their established high content screening (HCS) technique[257]. This approach was originally developed to screen pools of siRNA or miRNA transfected cardiomyocytes on a multiwell plate format in an automated way[277-280]. The great advantage of the technique is the exclusion of remaining non-cardiomyocytes from

the cell size analysis, while cardiomyocytes are fully included, based on the criterion "expression of sarcomeric α-actinin"[257]. Therefore, cellular contaminants like cardiac fibroblasts are not counted, thus clearly increasing the quality of the results. The second advantage of the HCS is the automation of cell size analysis allowing the investigation of high numbers of NRCM (up to 3 x 10^3 cells per 96 well) within a few hours, while almost every cell on each well is acquired by the analysis. Jentzsch *et al.* have plausibly demonstrated that experimentally induced cell size alterations are comparably detectable by a manual microscopy/quantification method and the HCS method[257, 281-283]. As a positive control we have used the α_1-adrenergic ligand PE, which is well known as a classic hypertrophy inducing adrenergic agonist. The results shown in figure 6 of the presented thesis display that PE serves as appropriate positive control for NRCM hypertrophy. Although the HCS method allows the generation of unbiased and highly reproducible data sets, the method still needs to be strictly controlled. Hence, all segmentation data have been visually compared to the pure microscopy data to exclude any errors made by the software (e.g. two cells that are wrongly considered as one big cell).

After adapting the HCS method from the Engelhardt group, we first analysed the hypertrophic potential of OSM in relation to hLIF, hCT-1 and hIL-6 (± hsIL-6R). As shown in figure 6, hOSM and mOSM have hypertrophic potentials comparable to those of hLIF, hCT-1 and hIL-6/hsIL-6R. Slight differences, however, can be observed between the various IL-6-type cytokines indicating that the analysed cytokines partially stimulate different receptor complexes. A direct comparison between OSM, LIF, CT-1 and IL-6 regarding hypertrophic responses of NRCM has never before been published, but some studies analysing the hypertrophic potential and/or induced pathways of single cytokine(s) exist. First, our data regarding LIF emphasize the strong hypertrophy inducing role of this cytokine and confirm its ability to initiate the activation of the STAT3/STAT1, Akt and ERK1/2 pathways in NRCM (Fig. 7, 10). This is perfectly in line with previous studies, that have shown that LIF induces gp130, STAT3 and STAT1 tyrosine phosphorylation resulting in hypertrophic responses of rodent cardiomyocytes[284, 285]. Matsui *et al.* further suggested an autocrine/paracrine role of this IL-6-type cytokine in the heart, as they found LIF mRNA to be expressed by cardiomyocytes as well as by non-cardiomyocytes[285]. Our own data also demonstrate that LIF mRNA expression is induced by hLIF and IL-6/sIL-6R activity in NRCM (Fig. 13) and NRCFB (Fig. 17A). The observation that LIF

was the strongest hypertrophic stimulus among the tested IL-6-type cytokines might be due to the fact that STAT3 as well as Akt and ERK1/2 are phosphorylated in response to LIF. As previously mentioned, each of these phosphorylations is involved in the hypertrophic response of cardiomyocytes[146-148]. Another aspect that has to be discussed in this context is the high affinity of human LIF to the murine and obviously also to the rat LIFR. For rat cells this phenomenon has not been shown in previous studies, however, it is well known that hLIF binds the mLIFR with 100-500-fold higher affinity compared to mLIF[36]. Due to this affinity difference Huyton *et al.* might have preferred to use human LIF instead of murine LIF to crystallise the cytokine in complex with the mLIFR (D1-D5)[286]. This strong affinity also seems to be true for the interaction between hLIF and the rLIFR/rgp130 complex and might therefore be an accurate explanation for the observed differences between hLIF and hOSM induced signalling (Fig. 7 and 10).

As already mentioned, hOSM can only activate the type I receptor complex (LIFR/gp130) of murine cells[74], thus precisely mimicking LIF. Within the presented thesis we have shown in several experiments (Fig. 9, 15, 24, 31 and additional, not presented data) that the same receptor use (rLIFR/rgp130 type I complex) is also true for rat cells. Moreover, we could exclude any participation of the rat OSMR in hOSM signalling (Fig. 9, 15, 24 and 31). Since hLIF and hOSM induce signalling using the same rat receptor complex, the stronger phosphorylations of STAT3, STAT1, STAT5, ERK1/2, p38 and Akt in response to hLIF compared with hOSM, shown in figure 10, indicate that only hLIF but not hOSM has an extremely high affinity for the rat LIF receptor. Dose-response experiments comparing hLIF and hOSM might clarify this hypothesis in the future. Although the observed phosphorylations of the hypertrophy relevant proteins STAT1, ERK1/2 and Akt are clearly weaker in response to hOSM than to hLIF, the third strongest NRCM hypertrophy inducer among the analysed IL-6-type cytokines, however, is hOSM. This might be due to the strong STAT3 tyrosine phosphorylation probably representing the most important IL-6-type cytokine induced pro-hypertrophic pathway[191]. This hypothesis is strengthened by the findings that hCT-1 potently promotes NRCM hypertrophy, which - as also shown in older studies[195, 227, 287] - mainly induces the phosphorylation of STAT3 and only to a minor extent of STAT1 and ERK1/2 (Fig. 8). Taken together, all analysed LIFR/gp130 heterodimer activating cytokines induce hypertrophy, mainly through STAT3 phosphorylation.

The activation of OSMR/gp130 heterodimers through mOSM also causes NRCM hypertrophy (Fig. 6). Although the hypertrophic potential of murine OSM seems to be milder than the LIFR based hypertrophy, the mOSM induced phosphorylations of STAT3, STAT1, ERK1/2 and Akt rank between the hOSM and hLIF induced phosphorylation intensities (Fig. 10). This is an interesting finding, because the mOSM associated induction of NRCM hypertrophy is less severe than the one induced by hLIF or hOSM (Fig. 6). One might therefore anticipate that mOSM cannot activate additionally required, but here not analysed, signalling pathways or that it simultaneously induces hypertrophy antagonising signals. For example, it has been shown that the association of SHP2/Gab1 and the resulting ERK5 activation play a major role in LIF induced hypertrophy[217, 288, 289]. Takahashi *et al.* contend that ERK5 is even the major hypertrophy causing pathway induced by CT-1[218]. However, in our hands the activation of ERK5, at least in response to LIF or OSM, could not be detected (data not shown). Moreover, the observed differences cannot be explained by differential initiation of feedback inhibitors like SOCS1, SOCS3 or SHP2, because hLIF, but not mOSM, even induces the highest mRNA expression levels of SOCS1 and SOCS3 as well as the strongest SHP2 tyrosine phosphorylation of all tested cytokines (Fig. 14). Although it has recently been shown that OSM is able to induce myocyte hypertrophy and is an important mediator of cardiomyocyte dedifferentiation and remodelling[198, 290], the entirety of OSM induced signalling pathways in cardiomyocytes was not analysed or shown in these studies. Notably, we have determined that mOSM is able to induce STAT3, STAT1, STAT5, ERK1/2, Akt and p38 phosphorylation in a hLIF-like manner, though STAT1 and STAT5 tyrosine phosphorylations are clearly weaker (Fig. 10). Anyway, STAT5 phosphorylation is not considered to directly mediate cardiomyocyte hypertrophy, although it has been shown that STAT5a is activated in ischemia/reperfusion experiments and mediates the mRNA expression of angiotensinogen[291]. As described in the next sections, the link between the IL-6-type cytokines and the renin-angiotensin system is considered to be one of the most cardiomyocyte hypertrophy promoting cellular networks. Nevertheless, also STAT3 phosphorylation (in response to CT-1) has been shown to induce angiotensinogen expression in NRCM[292], what might partially relativise the exclusiveness of the STAT5 mediated expression of angiotensinogen. Why the hypertrophic response following mOSM stimulation is weaker than the hypertrophic responses to hOSM or hCT-1 remains unclear, however. Most likely the less

pronounced pro-hypertrophic character of mOSM is closely connected with the comparatively weak induction of IL-6 mRNA and the negative regulation of LIF mRNA expression (Fig. 13). In contrast to mOSM, hLIF induces an increase of LIF mRNA and provokes higher IL-6 mRNA levels (particularly at early time points) in NRCM. Both of the endogenously synthesised cytokines (especially LIF) are likely able to maintain previously induced (exogenic) NRCM hypertrophy. Furthermore, the different effects of mOSM and hOSM cannot be explained by the additionally detected mOSM mediated p38 phosphorylation, because this signalling pathway seems to be more pro-hypertrophic than anti-hypertrophic[293], and hLIF also mediates the phosphorylation of this MAPK (Fig. 10).

Contrary to the rLIFR ligands hLIF, hCT-1 and hOSM, classical IL-6 signalling via the membrane-bound IL-6R and gp130[11] is not capable of inducing hypertrophy (Fig. 6) or the related, typical signalling pathways in NRCM (e.g. STAT3, see Fig. 10). This is a rather interesting finding, because many studies have focused on the hypertrophic actions of pure IL-6 (classical IL-6 signalling[294]). As shown by Sano *et al.* the upregulation of IL-6 (induced by ATII activity), that actually activates cardiomyocytes to hypertrophy, is based on a complex regulatory network. Cardiac fibroblasts seem to be involved in this process, since cardiac myocytes only express marginal levels of AT-1 receptors, rendering them rather unresponsive to ATII[260]. The same is also true for the IL-6R[260]. Therefore, Sano *et al.* postulate that the described ATII induced hypertrophic effects might be mainly mediated by parallel LIF and CT-1 induction. These observations lead to the conclusion, that the abundantly expressed LIFR and gp130 are responsive mediators for the fibroblast-cardiomyocyte-ATII-IL-6-type cytokine hypertrophy promoting interplay. As shown in our results, IL-6 without its soluble α-receptor, the IL-6R, is indeed not able to signal on NCRM or to induce measurable NRCM hypertrophy (Fig. 10 and 6).

Notably, IL-6 trans-signalling (mimicked through stimulation with hIL-6/hsIL-6R, see Fig. 10) is required and leads to cardiomyocyte hypertrophy (Fig. 6 and 7). In this we clearly agree with Hirota *et al.* who have shown several years ago, that only the stimulation with IL-6 and sIL-6R induces hypertrophy in cardiomyocytes[199]. As described above the hypertrophic effects of IL-6 trans-signalling seem to be mainly mediated via STAT3 activation, since the activations of STAT1 and ERK1/2 are rather weak and Akt phosphorylation cannot be detected (Fig. 10). IL-6/sIL-6R thereby closely resembles the activities of CT-1. It has to be noted that the induction

of endogenous IL-6 and LIF likely contributes to the pro-hypertrophic phenotype of hIL-6/sIL-6R treatment (Fig. 8). Moreover, the participation of regulatory miRNAs and further hypertrophy supporting proteins cannot be excluded.

5.1.2 The analysis of IL-6-type cytokine target genes in NRCM suggests a potential autocrine amplification loop

NRCM treated with mOSM, hLIF and hIL-6/hsIL-6R transcribe a specific pattern of target genes that can possibly contribute to the development and persistence of cardiomyocyte hypertrophy. As shown in figure 13, analysis of a selected panel of potential target genes revealed that mOSM, hLIF and hIL-6/sIL-6R mediate varyingly strong, persistent IL-6 mRNA induction. Moreover, hIL-6/hsIL-6R or LIF stimulation of NRCM cultures causes the upregulation of endogenous LIF mRNA, an attribute of these two cytokines that is not shared by mOSM. In sharp contrast, mOSM signalling negatively influences LIF mRNA levels, a regulation that is even intensified after 12 or 24 h, respectively. The observation that cardiac myocytes (and fibroblasts) are able to produce LIF and IL-6 (partially by an autoinductive process and without any additional stimulus), and that this secretion causes hypertrophy, was initially described by Ancey and colleagues[197, 295]. Furthermore, there are several studies showing that IL-6 secretion is induced by ATII, adrenergic receptor activation (e.g. by isoproterenol) or IL-1β treatment[260, 296-298]. Moreover, Ng *et al.* have shown that IL-1β induces a delayed STAT3 activation in NRCM causing a LIF-like hypertrophic phenotype. They could show that this secondary STAT3 phosphorylation (already appearing after 60 min) occurs via ERK/p38 involvement, but it was not clear, if any intermediate IL-6-type cytokine expression was induced or not[299].

However, it has not been shown until now that IL-6-type cytokines can induce their own expression in cardiomyocytes. This is indeed a finding with far reaching consequences for the IL-6-type cytokine exposed heart. Once induced, LIF or IL-6 are likely able to maintain the hypertrophic actions of the primarily applied stimulus. On the other hand, mOSM shares the capacity of inducing *Il6* transcription with the related cytokines IL-6 and LIF (Fig. 13). The induction of the IL-6 expression is a feature of OSM that was already observed previously in other cell types. Several groups have described that OSM is able to promote IL-6 secretion of hepatocytes via C/EBP activation[8, 300, 301]. This induction was also described for murine fibroblasts[302], human synovial fibroblasts[303], vascular smooth muscle cells[304], human endothelial

cells[305], human astrocytes[306-309] and murine mammary epithelial cells[237, 310]. Our own data from rat hepatoma cells (JTC-27) that were stimulated with mOSM show also a strong upregulation of IL-6 and the IL-6R (data not shown), completely in line with the published data. In contrast to our findings in JTC-27 hepatoma cells, NRCM do not significantly upregulate the IL-6R expression in response to mOSM, hLIF or IL-6 (data not shown). As already mentioned, under basal conditions NRCM do also not express sufficient IL-6R molecules to directly respond to pure IL-6 (Fig. 6 and 10). These data are in line with the study of Sano *et al.*[260], in which they have demonstrated that NRCM express no significant amounts of the IL-6R. This fact is unfortunately ignored by many groups and complicates the understanding of the IL-6 expression and its impact on hypertrophy. It can, however, not be excluded that the low levels of the receptor are sufficient to promote or maintain hypertrophy over time. Nonetheless, we believe that in NRCM the actions of LIF and OSM might be more important for the development/persistence of hypertrophy. This hypothesis is supported by a study of Fuchs *et al.* demonstrating that deletion of the *Il6* gene in mice has neither a beneficial nor a harmful influence on left ventricular remodelling, function or infarct size[209].

A further induced target that likely contributes to the pro-hypertrophic actions of the analysed cytokines is the OSMR. All tested cytokines, mOSM, hLIF and hIL-6/sIL-6R cause the significant upregulation of the rat *Osmr* gene transcription (Fig. 13).

Intriguingly, this is a prolonged activity that leads to elevated rOSMR mRNA levels also after 12 or 24 h of stimulation. So far, the upregulation of the OSMR has only been described for OSM itself in human kidney tissue samples[311] and pulmonary fibroblasts[165].

Nevertheless, it has to be mentioned that -unlike the IL-6R- the OSMR mRNA levels under basal conditions are sufficient to allow clearly detectable mOSM mediated signalling. This can be read off the activated signalling pathways, induction of target gene transcription and initiation of hypertrophy. Since it is known that OSM stimulation results in a ligand dependent internalisation of the OSMR/gp130 receptor complex[165], the OSM-induced enhanced transcription of the OSMR might play a role in restoring the internalised OSMR molecules. Nevertheless, it is possible that the observed OSMR upregulation prepares the cells for later OSM impacts by increasing the sensitivity of the cells to the cytokine. Notably, so far we could not detect the induction of OSM mRNA following hIL-6/sIL-6R, hLIF or mOSM stimulation of NRCM

or NRCFB (data not shown) indicating that a mOSM induced hypertrophy is not the result of an autocrine OSM loop. Which stimulus might lead to OSM secretion remains to be determined. It is, however, well known that OSM is released by neutrophils, monocytes and T-cells[43, 58, 65, 66], which can be found in the heart in pathophysiological conditions such as ischemia/reperfusion or myocardial infarction[312, 313]. Moreover, Kubin *et al.* have demonstrated that patients suffering from dilated cardiomyopathy show strongly elevated OSM levels and resulting signalling. Interestingly, this cytokine seems to mediate the dedifferentiation of cardiomyocytes and an upregulation of stem cell markers thus initially improving cardiac function after myocardial infarction, what was also shown in a mouse model of myocardial infarction. While the first phase of OSM induced cardiac remodelling seems to be beneficial for the cardiac function, the extended dedifferentiation of cardiomyocytes by OSM clearly impairs the cardiac performance[198].

5.1.3 The response of NRCFB to IL-6-type cytokines: a contribution to hypertrophy

As described before for NRCM, mOSM or hIL-6/hsIL-6R stimulation strongly increases the transcription of the *Il6* gene in NRCFB. The induction mediated by IL-6 trans-signalling (i.e. via IL-6/sIL-6R, in contrast to classical IL-6 signalling via IL-6 binding to the membrane bound IL-6R) is, however, unequally stronger than the mOSM initiated upregulation of the cytokine's mRNA levels (16-fold mRNA induction after 3 h mOSM vs. 204-fold mRNA induction after 3 h hIL-6/hsIL-6R, Fig. 17A). Notably, this observed disparity is not described in literature until now. Additionally, the cardiac *Il6* transcription in response to OSM or IL-6/sIL-6R has not yet been shown. Fredj *et al.* have established a cardiac myocyte/fibroblast co-culture model, where they could clearly show, that ATII (produced from cardiac myocytes) induces IL-6 secretion by cardiac fibroblast subsequently causing hypertrophy of myocytes in a paracrine manner[314]. However, it is completely unclear whether pathological cardiac hypertrophy mediated/maintained by IL-6-type cytokines is always initiated by ATII or other non-IL-6-type cytokine family members.

In line with the mRNA induction, we have observed increased rIL-6 concentrations in the supernatants of mOSM and hIL-6/hsIL-6R stimulated NRCFB (Fig. 17B) demonstrating that the cytokine is truly secreted from these cells. It has to be

mentioned again, that it is unlikely that IL-6 is the major mediator of hypertrophy in this scenario, as cardiac myocytes express only marginal IL-6R levels. The same is true for NRCFB (Fig. 15 and 16). Therefore, other family members have to be involved in the hypertrophic response, because the application of antagonising anti-gp130 antibodies decreases the observed hypertrophy much stronger than the application of respective anti-IL-6 antibodies[314]. Furthermore, it cannot be excluded that the inhibitory influence of antagonising IL-6 antibodies is dependent on sIL-6R in the fetal calf serum used for the culture medium.

In equivalent co-culture systems, it was shown that cardiac myocytes/fibroblasts are able to produce CT-1[287], and exogenous CT-1 treatment can induce cardiac fibroblast proliferation via cross-talk with the endothelin system[315]. Therefore, besides IL-6, CT-1 might also play a major role in cardiac fibroblast proliferation/fibrosis development and transmission of hypertrophic signals to cardiomyocytes.

Our own data suggest that besides IL-6 and CT-1, LIF might be secreted by NRCFB, since we observed an upregulation of LIF mRNA levels in response to 3 h hIL-6/sIL-6R stimulation. However, induction of *Lif* transcription appears to be rather transient, because this upregulation was mostly aborted after 18 h of hIL-6/sIL-6R treatment (Fig. 17A). In contrast to cardiomyocytes, not much is known about the role of LIF in cardiac fibroblasts. Wang *et al.* have shown that LIF stimulation can inhibit the differentiation of cardiac fibroblasts into myofibroblasts, along with a decrease of collagen production and matrix metalloproteinase (MMP) activity[316]. Moreover, it has been shown that cardiac fibroblasts in co-cultures with myocytes produce LIF (and endothelin simultaneously) and that LIF, just like CT-1, can act *in trans* on cardiomyocytes inducing a typical IL-6-type cytokine induced hypertrophic phenotype[317]. Logically, the production of LIF by NRCFB can consequently induce *Lif* and *Il6* gene transcription in NRCM (Fig. 13). While mOSM decreases the transcription of *Lif* in NRCM (Fig. 13), it has no effect on LIF mRNA levels in NRCFB (Fig. 17A).

Besides regulating the expression of their own gene (e.g. IL-6) or that of a related family cytokine gene (LIF), IL-6 trans-signalling and mOSM signalling additionally mediate the gene expression of some of the IL-6-type cytokine receptors. Particularly the OSMR expression is strongly elevated (Fig. 17A). While the induction of OSMR mRNA following mOSM stimulation is transient and almost terminated after 18 h, the

OSMR mRNA induction in response to IL-6/sIL-6R stimulation is even increased after 18 h.

In addition to the OSMR mRNA induction through mOSM or hIL-6/sIL-6R, that was previously observed in NRCM too (chapter 5.1.2), we have detected a statistically significant twofold increase of IL-6R mRNA after 3 h IL-6 trans-signalling in NRCFB (Fig. 17A). This is in line with data from hepatocytes that were also described to upregulate the IL-6R in response to IL-6 stimulation[301]. In contrast to HepG2 cells that additionally elevate the IL-6R expression in response to OSM[300], however, we could not detect any augmented IL-6R levels in NRCFB after mOSM stimulation indicating that this might be a cell type specific regulation. The enhanced *Il6r* transcription in NRCFB in response to IL-6/sIL-6R might be of increased interest since –in case the increase is sufficient to allow translation into IL-6R protein- it would make NRCFB responsive to IL-6 signalling in the absence of soluble alpha-receptor, i.e. classical signalling in contrast to trans-signalling could occur. Unfortunately, we were unable to investigate IL-6R protein expression since no rat specific IL-6R-antibody was available and the antibodies detecting murine or human IL-6R did not cross-react with the rat protein.

Under pathological conditions, however, two possibilities exist maybe allowing IL-6 signalling and IL-6 induced hypertrophy, respectively, in these cells: 1) sIL-6R, delivered from serum or produced by a third cell type (e.g. invading leukocytes), does complete the trans-signalling requirements for IL-6, 2) very low membrane bound IL-6R protein levels still exist which, upon long term stimulation by secreted IL-6, might be sufficient to promote hypertrophic response over time. As already mentioned, the C_T-values of the IL-6R in both cell types, NRCM and NRCFB, are extraordinarily high and therefore not on a typical “expression level”, but also not on a comparable “no expression level”. Hirota *et al*. have shown several years earlier how harmful a strong parallel expression of IL-6 and the IL-6R can be. Mice transgenic for IL-6 and the membrane-bound IL-6R and therefore overexpressing both proteins develop a strong myocardial hypertrophy, while none of the mice transgenic either for IL-6 or the IL-6R alone has a comparable phenotype[199]. This indicates that indeed IL-6 trans-signalling is required for the induction of cardiac hypertrophy.

In addition to the OSMR and IL-6R, a transient upregulation of the LIFR can be detected in response to IL-6 trans-signalling and mOSM stimulation (Fig. 17A). Upon availability of specific antibodies future studies will have to clarify whether appropriate

increase in LIFR protein expression takes place allowing stronger or more sensitive signalling of cardiac fibroblasts under pathological conditions. The induction of the LIFR in response to OSM has previously been shown only in human pulmonary fibroblasts and epithelial cells[165].

As the renin-angiotensin system is a major mediator of hypertension and known to cross-talk with IL-6-type cytokines in cardiac hypertrophy[318], we decided to corroborate this cross-talk in more detail. Angiotensin II is a potent vasoconstrictor and, as already mentioned, plays an important role in the development of cardiac hypertrophy by initiating the expression of IL-6 by cardiac fibroblasts[260, 296].

In this study we could show that reciprocally, IL-6 or OSM induce a clear prolonged upregulation of the angiotensin I converting enzyme (ACE I) mRNA in NRCFB (Fig. 18). ACE I is the key enzyme for the ATII synthesis catalysing the conversion of the decapeptide angiotensin I into the active octapeptide angiotensin II[319, 320]. Therefore, IL-6-type cytokines induce critical components of the renin-angiotensin system that additionally amplify hypertrophic effects. While ATII induces IL-6 secretion of cardiac fibroblasts[226], IL-6 or OSM probably initiate the upregulation of cardiac ACE I that increases the local concentrations of bioactive ATII. In the presence of exogenous ATI and sIL-6R this cross-talk could possibly result in an enclosed autocrine IL-6-ATII loop.

What accessorily fits into this idea is the observed strong upregulation of the important ATII utilised angiotensin II receptor 1 alpha (AT1α) in response to mOSM or hIL-6/sIL-6R stimulation of NRCFB (Fig. 18). Contrary to the ACE I expression, a prolonged *Agtr1a* gene (encoding for the AT1α protein) induction was only observed in response to IL-6 trans-signalling. Indeed, it was shown several years ago that cardiomyocyte specific overexpression of the human AT1α is sufficient to induce cardiac hypertrophy and remodelling in mice[263]. These findings are consistent with results from hypertensive rats that also develop cardiac hypertrophy. In such rats the AT1α mRNA and protein levels have been found to be significantly upregulated[264], while the angiotensin II receptor type 2 (AT2) levels have not been significantly altered[265]. Moreover, AT1α has been shown to be upregulated after myocardial infarction allowing ATII to promote ventricular remodelling in the infarcted heart[266]. The simultaneous upregulation of AT1α and ACE I represents a crucial cardiac event that is connecting the hypertrophic side of the IL-6-type cytokines with the hypertensive/hypertrophic axis of the renin-angiotensin system.

5.1.4 Kinetics of IL-6/sIL-6R and mOSM regulated gene expression differs substantially in NRCFB

Comparison of OSM and IL-6 mediated signalling and gene expression in NRCM and NRCFB clearly shows that the duration of their stimulatory potential differs strongly. The IL-6 trans-signalling induced expression of the OSMR and IL-6 itself in NRCFB is clearly more prolonged than upon mOSM stimulation (Fig. 17A, OSMR and IL-6 mRNA levels). As already mentioned in the results section, the obvious decrease in IL-6 expression upon IL-6/sIL-6R stimulation after 18h stimulation is only due to the fact that the –fold increase is related to the corresponding untreated control. Since IL-6 is apparently constitutively released by NRCFB in culture[295], also the C_T values for untreated NRCFB decrease (higher IL-6 mRNA levels). Interestingly, the variation in signalling persistence upon IL-6 vs. OSM was not observed in NRCM, in which both target mRNAs are induced and remain expressed on a significantly increased level even after 12 and 24 h, irrespective of the used stimulus (Fig. 13).

To further scrutinise the differences in signalling persistence, we compared the short time (1-60 min) signalling and the long time (2-48 h) signalling with focus on phospho-STAT3, phospho-STAT1 and phospho-ERK1/2. While in NRCM no significant differences in signalling duration between both stimuli exist (Fig. 19, 1-60 min and Fig. 20, 1-48 h), a definite difference between mOSM and hIL-6/sIL-6R induced STAT3 and STAT1 phosphorylation is observed between 12 and 48 h in NRCFB. Interestingly, hIL-6 trans-signalling induces a clearly prolonged activation of STAT1 and STAT3, in contrast to mOSM. This is either due to an intermediate cytokine expression or due to a less efficient initiation of the feedback inhibition machinery in response to IL-6. However, Stross *et al.* have shown that classic IL-6 signalling is even more sensitive to SOCS3 inhibition than OSM signalling in human HepG2 and murine embryonic fibroblast[321]. Moreover, it has already been described that SOCS3 induction has a much stronger negative influence on IL-6-type cytokine signalling than SOCS1[322]. As mOSM induces slightly stronger STAT1 and STAT3 tyrosine phosphorylation (Fig. 16 and 19) and SOCS3 is a direct target of activated STAT3 as well as SOCS1 of activated STAT1[323], a more potent activation of the inhibition machinery after mOSM is rather comprehensible. This discrepancy could potentially explain the faster signalling shutdown upon mOSM stimulation.

Nevertheless, the differential SOCS3 induction is most likely not the only reason for the observed prolonged IL-6 trans-signalling in NRCFB.

In this study we identified C/EBPβ (formerly known as nuclear factor for IL-6, NF-IL6) and C/EBPδ as potential candidates for the differential induction of *Il6* transcription by IL-6 and OSM. The mRNA levels of both transcription factors are strongly upregulated in NRCFB correlating with the induced levels of IL-6 mRNA (Fig. 21). The C/EBP transcription factors are known to play important roles in cell proliferation, cell differentiation, inflammation and metabolism, but a hypertrophy stimulating role of C/EBPβ and C/EBPδ, as indicated in this thesis, is rather novel. Until now, the induction of members of this transcription family in response to IL-6-type cytokines was mainly observed in epithelial cells, hepatocytes, adipocytes and haematopoietic cells[231-233, 240, 241, 324, 325]. C/EBPβ and C/EBPδ are capable of inducing IL-6[232, 233] potentially mediating an autocrine IL-6-STAT3-C/EBP-IL-6-loop. The potential occurrence of an autocrine IL-6 loop demonstrates how important the cellular inhibition machinery is. Represented by SOCS proteins, PIAS proteins, phosphatases (e.g. SHP2) and receptor internalisation, these molecular brakes play important roles in the prevention of overshooting signalling. The prolonged induction of C/EBPδ might be an indirect result of an inefficient signalling inhibition. Previous studies have already shown that the initial C/EBPδ induction is driven by STAT3 activity, while a prolonged and constitutive induction is mainly mediated by autoregulation[235, 239-241, 326]. Regarding the results from NRCFB (Fig. 19, 20 and 21), it is obvious that mOSM, compared with hIL-6/sIL-6R, induces lower levels of both C/EBP mRNAs (Fig. 21). Therefore, it might fail to reach a threshold to activate the already mentioned C/EBP autoregulation necessary to induce prolonged IL-6 transcription. Importantly, we have found no upregulated OSM mRNA levels in NRCFB. Thus, any participation of newly synthesised OSM can certainly be excluded.

What might also play a role for the strong difference between both cytokines is the fact that IL-6 induces LIF mRNA upregulation, while mOSM does not regulate *Lif* transcription in these cells (Fig. 17A). As shown in Fig. 16, LIF is indeed able to mediate signalling in NRCFB, however, not with the potential observed in NRCM. This is the result of the low LIFR expression in NRCFB (Fig. 15). In NRCM, LIF induces a similar C/EBPβ and C/EBPδ mRNA upregulation as OSM (Fig. 21). Due to the comparable C/EBP mRNA induction and the stronger STAT3 activation, LIF is

even able to mediate higher initial IL-6 mRNA levels than mOSM. Interestingly, the downregulation of *Il6* transcription in NRCM following hLIF treatment occurs synchronously to the decrease of C/EBPβ and δ levels indicating a direct correlation. Furthermore, this downregulation seems to be in line with the strong initial SOCS1 and SOCS3 upregulation in response to hLIF (Fig. 14). Intriguingly, mOSM that initially induces less IL-6 mRNA expression in NRCM (also correlating with C/EBP levels) promotes a longer maintenance of IL-6 and C/EBP mRNA levels than hLIF, likely via less SOCS induction and weaker SHP2 activation (Fig. 14).

In contrast to NRCFB, in NRCM hIL-6 trans-signalling is only able to induce slightly higher C/EBPβ and C/EBPδ mRNA levels than OSM or LIF (Fig. 21). However, the hIL-6/hsIL-6R mediated upregulation of both transcription factors (in combination with other transcription factors) is sufficient to allow the strongest *Il6* gene induction, compared to all other used IL-6-type cytokines. This is a rather surprising finding, since hIL-6 plus sIL-6R clearly represents the weakest stimulus on signalling level among all tested IL-6-type cytokines in NRCM. So far, we have no substantiated explanation for the differential regulation of C/EBP gene expression by various IL-6-type cytokines in NRCM and NRCFB. One possible mechanism explaining the observed discrepancy is a differential methylation status of the C/EBP promoters in both cell types leading to a partial reduction of gene expression. This mechanism was previously described in cancer cells and can be responsible for different transcription efficiencies[241, 327]. Besides promoter methylation, additional mechanisms can be involved in the regulation of C/EBPs. The levels of C/EBP regulation include: Translation of either active or inactive C/EBPβ versions (LAP and LIP)[231], phosphorylation at various phospho-sites[231] and the promoter binding of additional transcription factors like CREB[236, 328] or Runx[329]. Nevertheless, it has been published that the transcriptional induction (primarily via STAT3 activity at the nucleus) of the C/EBPs is the most important regulatory level in controlling the activity of these transcription factors[231]. It remains to be elucidated, if the intense IL-6 mRNA induction in NRCFB is only the result of the high level *Cebpb* and *Cebpd* gene induction (maybe in combination with weak SOCS expression), or if further mechanisms are involved.

When comparing NRCM and NRCFB one obvious result attracts attention: While induced C/EBPβ mRNA levels were approximately comparable in both cardiac cell types, the transcriptional upregulation of C/EBPδ in NRCFB is unequally higher than

in NRCM. This is not only true for IL-6 trans-signalling, but also for mOSM induced C/EBPδ expression. The underlying molecular mechanism that is responsible for this difference remains to be defined. However, this imbalance could serve as further explanation for the differential IL-6 induction since both transcription factors might form heterodimeric complexes potentiating their transcriptional activity. Nonetheless, this hypothesis has to be substantiated in future. Several studies have shown that, with exception of C/EBPζ, all other C/EBP family members can form such heterodimeric complexes with a respective other family member[232, 233, 330-339]. As also described for STAT heterodimers, this mechanism provides the opportunity to expand and diversify the amount of responsive target genes.

Altogether, these results suggest that hIL-6 trans-signalling in NRCFB strongly initiates C/EBPβ and C/EBPδ expression causing IL-6 upregulation, which in turn induces C/EBP upregulation and thereby potentially initiates a vicious circle. In the context of cardiomyocyte hypertrophy this regulation exhibits a rather harmful mechanism that can be considered to maintain hypertrophy for an indefinite time. As noted before, NRCFB slightly upregulate their IL-6R expression as well, a result that was exclusively observed upon IL-6/sIL-6R treatment (Fig. 17A). Unfortunately, secondary stimulation experiments in NRCFB failed, within which we tried to confirm IL-6 binding to the newly synthesised IL-6R by secondary pure rat IL-6 stimulation of IL-6/sIL-6R pretreated NRCFB.

5.2 Characterisation of the rat OSM receptor complex

As previously mentioned, human OSM and murine OSM significantly differ in the usage of their receptors. While hOSM is able to bind and signal via the human type I (LIFR/gp130) and type II (OSMR/gp130) receptor complex[26, 27, 73], mOSM is only capable of binding to the murine type II (OSMR/gp130) complex, because it lacks specific affinity sites for the LIFR[74]. Moreover, cross-species experiments from human cells using mOSM and from murine cells treated with hOSM have shown that mOSM is not able to initiate any signalling on human cells, while hOSM exclusively utilises the murine type I (LIFR/gp130) receptor complex[74, 75]. Solid information on receptor usage of the OSM variants on rat cells has not been published so far. Since our previous studies on the hypertrophic potential of IL-6-type cytokines were performed using rat cardiac cells treated with hOSM or mOSM, we first analysed the

receptor usage of hOSM and mOSM on these cells using the LIFR specific antagonist LIF-05[254]. Later on, when rat OSM became available two years ago, first experiments with the new cytokine on human and rat hepatoma cells demonstrated clear differences between rOSM and the closely related mOSM. For this reason, we decided to characterise the receptor binding and signalling properties of rOSM. More specifically, we analysed the receptor usage by classic stimulation experiments in hepatoma cells from rat, murine and human origin, LIFR blockade experiments by the use of LIF-05, RNA interference experiments targeting the respective OSMR and finally by generation of stably transfected Ba/F3 cells either expressing gp130/OSMR or gp130/LIFR.

5.2.1 Only rat OSM signals through the rat LIFR/gp130 (type I) and the rat OSMR/gp130 (type II) receptor complex

So far, only one research group had made the effort to use OSM from rat origin for their experiments with rat cells[51]. Even in recent studies, within which the role of OSM in rat models of human diseases has been determined, OSM from human[340-342] or murine[343-346] origin has been used.

First, we analysed the receptor usage of both OSM variants in NRCM (Fig. 9) and NRCFB (Fig. 14). Using the specific LIFR antagonist LIF-05, we clearly could show that, analogously to murine cells, hOSM exclusively signals through the rat LIFR/gp130 type I complex, while mOSM uses the rat type II OSMR/gp130 receptor complex, as it does in murine cells too. In NRCFB, which barely express LIFR, the obtained results are absolutely unambiguous: Pretreatment with LIF-05 completely abrogates hOSM (and hLIF) signalling in NRCFB, while the antagonist has no influence on mOSM induced signalling pathways. Experiments in NRCM indicate that mOSM might have a very low affinity for the rLIFR since pretreatment of the cells with LIF-05 leads to a slightly reduced STAT3 and STAT1 tyrosine phosphorylation (chapter 4.1.4, Fig. 9). This hypothesis might be supported by experiments by Walker *et al.* showing that mOSM stimulates bone formation in *Osmr*$^{-/-}$ mice[347]. Consequently, the authors postulate that mOSM utilises the mLIFR in osteoblasts. However, the presented data regarding the activated signalling pathways are not entirely convincing. Furthermore, with focus on all experiments in rat hepatoma cells (JTC-27), reduction of mOSM mediated signalling upon LIF-05 treatment was never

observed (Fig. 24). Therefore, an alternative and more likely explanation is a detectable LIF-05 induced downregulation of signalling pathways activated by continuously secreted cytokines (Fig. 9, compare lane 1 and 2). As already described, NRCM are able to produce IL-6-type cytokines like LIF, CT-1 and IL-6 that are important for cell survival and functionality of these cells, thus serving as myokines[295]. Out of these only LIF and CT-1 signal via the LIFR and, therefore, might be responsible for the activation of signalling pathways under basal culture conditions. Indeed, the existence of this continuous stimulation by endogenous cytokines only becomes apparent when LIF-05 is used, since untreated cells normally serve as negative control. Moreover, the decrease of basal signalling can be observed in all LIF-05 experiments performed with NRCM. Our data from NRCM, NRCFB, JTC-27, Hepa1c1c7 and Ba/F3 cells expressing either rgp130/rOSMR or rgp130/rLIFR clearly demonstrate the exclusive type II receptor usage of mOSM and its inability to bind to the type I receptor (at least in the concentration used). This is completely in line with a study of Lindberg *et al*. who also attested that mOSM has no affinity to the LIFR/gp130 receptor complex[74]. Moreover, it is possible that, upon binding to the LIFR, the antagonist induces internalisation and maybe also co-internalisation of other receptors in close vicinity (e.g. gp130), independent of the typical ligand induced mechanism. This hypothesis would also explain the difference between NRCM and NRCFB, because NRCFB clearly express more gp130 (compare Fig. 11 and 15), therefore remaining unaffected by this effect. Notably, the strong negative influence of LIF-05 on hOSM signalling is comparable in both cardiac cell types indicating that hOSM exclusively signals through the rat LIFR/gp130 type I complex. Moreover, OSMR siRNA experiments in JTC-27 cells served as second line of evidence for the definition of the OSM receptor usage. In these cells the reduction of OSMR expression levels to 20% by siRNA knockdown results in total inhibition of mOSM induced signalling, while hOSM mediated STAT3, STAT1 and ERK phosphorylation remains completely unaffected (Fig. 25). Therefore, it can be concluded that mOSM utilises the OSMR/gp130 type II receptor complex on cells from rat origin.

With the availability of commercially produced rOSM in 2010, we have set out to characterise the receptor usage of this OSM variant. First, the LIFR blockade experiments in JTC-27 cells have clearly demonstrated that rOSM does not exclusively signal via the rat type I (rLIFR/rgp130) receptor complex, since STAT3

and STAT1 phosphorylations are almost completely unaffected upon LIF-05 treatment (Fig. 24). Notably, we observe an even increased ERK1/2 phosphorylation in the presence of LIF-05 what might indicate that the rOSMR/rgp130 complex has more potential to initiate MAPK signalling. In contrast, JTC cells expressing only 20% of the OSMR after siRNA transfection show a strong decrease of rOSM induced ERK1/2 activation, while STAT1 and STAT3 phosphorylations remain mostly unaffected (Fig. 25). On the one hand, this clearly implies that rOSM is able to utilise the type I and the type II receptor complex, since blocking the LIFR or knocking down the OSMR has almost no influence on the rOSM induced STAT3/STAT1 phosphorylations. On the other hand, both experiments argue for a higher ERK activation potential of the OSMR/gp130 receptor complex in comparison to the LIFR/gp130 complex. This might be due to the ability of the type II receptor complex to recruit SHP2 to gp130[137] and Shc to the OSMR[141]. In contrast, the type I receptor complex is only able to recruit SHP2, since the LIFR also recruits SHP2[138]. However, this correlation has to be verified in further studies.

The final evidence confirming our hypothesis, that rOSM uses both receptor complexes, has been obtained from Ba/F3 cells expressing either the type I (rgp130/rLIFR) receptor complex or the type II (rgp130/rOSMR) receptor complex (Fig. 31). While mOSM is exclusively able to signal via the rat type II receptor complex, and hOSM solely utilises the rat type I receptor complex, the rat ortholog mediates the phosphorylation of STAT3, STAT1 and ERK1/2 via both receptor complexes. This is analogous to the receptor usage of human OSM in human cells[26, 73] and differs strongly from murine OSM[74]. A fourth OSM variant was cloned several years ago, namely bovine OSM. While this cytokine has been shown to activate the type I (LIFR/gp130) receptor complex in murine cells[348], no characterisation of the cytokine was performed using bovine cells. Thus, it is not clear whether the protein is able to bind the type I and/or the type II receptor complex on bovine cells.

5.2.2 Rat OSM predominantly signals via the type II receptor complex on murine cells and via the type I receptor complex on human cells

As previously mentioned, hOSM is capable of inducing signalling in murine cells through binding to LIFR/gp130 heterodimers[74], while mOSM utilises the murine type II receptor complex[74, 75]. This is completely in line with our data from murine

Hepa1c1c7 hepatoma cells (and murine Hepa1-6 hepatoma cells, data not presented), shown in figure 26 and 27.

Since the mode of action and receptor usage of rOSM on murine cells were completely unknown, Hepa1c1c7 cells were stimulated with the cytokine, with or without LIF-05 pretreatment (Fig. 26), or after transfection with siRNA targeting the mOSMR (Fig. 27). Similarly to our observations in JTC-27 cells, LIF-05 pretreatment has no negative influence on rOSM mediated signalling in Hepa1c1c7. This indicates that, in Hepa1c1c7 cells, the OSMR/gp130 type II complex is able to rescue the LIF-05 caused blockade of the LIFR/gp130 type I receptor complex. In contrast to JTC-27, a clear decrease of the STAT3 phosphorylation in response to rOSM was observed upon OSMR silencing in Hepa1c1c7. Nevertheless, this reduction is not as strong as in response to mOSM. Moreover, the rOSM induced STAT1 phosphorylation, that is already weak in untreated cells, is not significantly decreased in the presence of OSMR siRNA indicating that the murine type I receptor complex might be utilised by rat OSM too. Ba/F3 cells expressing the murine type I or type II OSM receptor complex, respectively, would provide the ultimate evidence for the receptor usage of rOSM on murine cells.

In line with data from previous publications[23, 73], the results from human HepG2 hepatoma cells indicate that mOSM has no signalling potential on human cells (Fig. 28 and 29), while hOSM uses the human type I and type II receptor complex (Fig. 28-30). Interestingly, OSM from rat origin is indeed able to stimulate human cells, but exclusively utilises the human type I receptor complex on HepG2 cells (Fig. 28 and 29). Experiments, in which we used Ba/F3 cells expressing the human type II (OSMR/gp130) receptor complex, have clearly shown that rOSM is not able to induce proliferation of these cells by activating the type II receptor complex (Fig. 30). Thus, the receptor usage of rOSM on human cells represents the exact reverse cross-species specificity to the receptor usage of hOSM on rat cells, since both OSM variants only utilise the type I receptor complex on cells from the respective foreign species.

5.2.3 Possible reasons for the human OSM-like receptor usage by rat OSM

To our surprise, rOSM represents itself more homologous to hOSM than to mOSM with regard to its receptor preference. This fact is even more astonishing, when the

sequence identities of murine, rat and human OSM are compared. While rOSM and mOSM share approximately 60% identical amino acids, the alignment of rOSM and hOSM highlights only 49% sequence identity (EBLOSUM62 Matrix, Gap penalty: 10.0, Extension penalty: 0.5). The described difference in receptor preferences, however, would have suggested a higher homology of rOSM to hOSM than to mOSM.

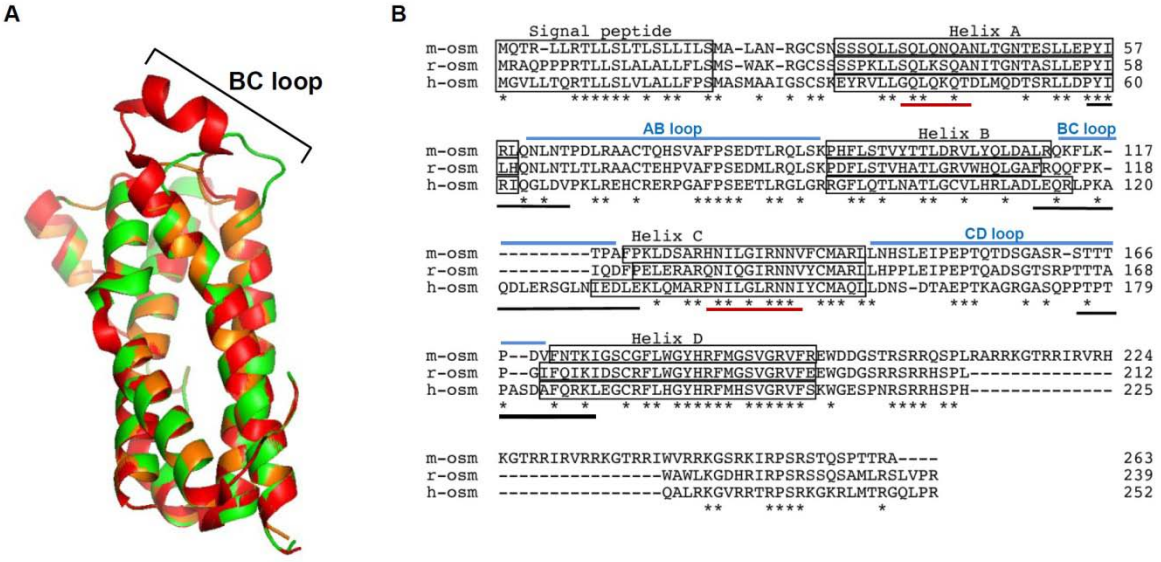

Figure 32: Differences in the BC loop of human, murine and rat OSM might be responsible for the unequal receptor usage.

A, Structures of mOSM (amino acids 25-205 of NP_001013383.1, orange) and rOSM (amino acids 26-207 of NP_001006962.1, green) were modelled using the solved crystal structure of human OSM (PDB entry code: 1EVS, red) as template. SWISS-MODEL-Server[349-351] was used for molecular modelling and PyMOL (DeLano, W.L. (2002) The PyMOL Molecular Graphics System. DeLano Scientific, San Carlos, CA, USA) for graphical presentation and structural overlay. **B**, Sequence alignment of murine, rat and human OSM. The sequential alignment was generated using a fold algorithm (ProHit package, ProCeryon Biosciences GmbH, Salzburg, Austria). Asterisks indicate identical amino acid residues in all three species. Helical regions are accentuated through black boxes, and interhelical loops are marked by blue bars. Black bars illustrate amino acids/regions that are part of the site 3 (binding site for the LIFR/OSMR)[42, 256, 286, 352] in the human cytokine, while red bars highlight amino acids/regions that are important for gp130 binding (site 2)[256].

Nevertheless, sheer sequence alignments frequently fail to explain protein differences or similarities and are thereby not suitable to interpret the found phenomenon. A study analysing the binding sites of CNTF to the LIFR has indicated that there are rather large interfaces between the LIFR and the LIFR binding cytokine (CNTF)[352]. This interacting region of the cytokine, the so-called site 3, consists of three structural entities: 1) Amino acid residues of the C-terminal A helix extending into the N-terminus of the AB loop, 2) amino acid residues of the BC loop and 3) amino acid residues of the C-terminal end of the CD loop reaching into the N-terminus of the D helix (Fig. 32B, amino acids contributing to the site 3 are marked by

black bars). Moreover, the crystal structure of hLIF in complex with the mLIFR identified the following residues as essential for LIF-LIFR binding: Pro-51 and Phe-52 (C-terminus of helix A), Phe-156 and Lys-159 (N-terminus of the D helix)[286]. While corresponding amino acids to Pro-51 and Phe-52 are completely absent in all OSM variants, Phe-156 and Lys-159 are not only present in all OSM (including mOSM) variants, but can be found in every potential LIFR interacting IL-6-type cytokine (LIF, OSM, CT-1, NP, CNTF and CLC). By combining this information with sequence comparisons of all three OSM variants, we conclude that differences in the BC loop might be responsible for the observed species divergence. As shown in figure 32A (hOSM, red structure), the BC loop of crystallised hOSM seems to contain a unique feature, a short inter-BC-helix.

Structural modelling of mOSM and rOSM on the basis of the crystal structure of hOSM as template using the SWISS-MODEL-Server[349-351] as well as overlaying the proposed structures using PyMOL (DeLano, W.L. (2002) The PyMOL Molecular Graphics System. DeLano Scientific, San Carlos, CA, USA) revealed important findings: First, neither mOSM nor rOSM seem to feature such an inter-BC-helix. Second, mOSM has been found to contain an extremely short BC loop, while this loop is substantially longer in hOSM and rOSM (Fig. 32A and B). Whether this region is definitely essential to allow high affinity binding of OSM to the LIFR has to be verified in future by performing mutagenesis experiments (e.g. insertion of the rat OSM BC loop into murine OSM). Successful identification of the important residues and mutagenesis of mOSM into a human- or rat-like variant would finally allow a reliable use of murine cells or mice as adequate model systems. Only a type I and II receptor complex binding OSM is accurate to mimic hOSM activity, a fact that should no longer be neglected.

5.2.4 Consequences of the use of non-human-like OSM model organisms

As already described, murine OSM lacks the ability to signal via both OSM receptor complexes. This difference to human or rat OSM does not remain without consequences. OSM is mostly expressed by neutrophils, macrophages, dendritic cells and activated T-cells[43, 58, 65, 66]. High expression levels of the cytokine were found in various inflammatory diseases[54-57], and the receptor complexes of OSM, LIFR/gp130 (type I receptor complex) and OSMR/gp130 (type II receptor complex),

are widely expressed. However, up to date the physiological function of OSM is still controversially discussed. Hence, pro- as well as anti-inflammatory activities have been attributed to the cytokine. For example, administration of recombinant human OSM to LPS treated mice induces a strong decrease of LPS mediated TNFα secretion, and a prolonged survival of the animals can be observed. In accordance with the suppressed inflammatory progress, the degree of joint destruction in these mice is reduced, indicative of an anti-inflammatory activity of OSM[353]. On the other hand, intra-articular injection of adenovirus encoded murine OSM mediates a rheumatoid arthritis-like phenotype in mice[354], clearly representing a pro-inflammatory effect of the cytokine. Furthermore, administration of murine OSM neutralising antibodies strongly attenuates the symptoms of collagen and pristane induced arthritis[355] also arguing for a strong pro-inflammatory role of the protein. Similar information was collected in a study showing that the inhalation of adenoviral particles encoding for murine OSM results in exacerbated infiltration of eosinophils into the lung tissue of infected mice[60]. One possible explanation for these highly controversial findings might originate from the fact that OSM from different species was used, while all experiments were performed utilising mouse cells or mice, respectively. Interestingly, in the study attributing an anti-inflammatory role to OSM, recombinant human OSM was injected into mice[353]. In contrast, the studies arguing for a more pro-inflammatory role of OSM made use of recombinant murine OSM[60, 354, 355]. As already mentioned, human OSM exclusively binds to the type I (gp130/LIFR) receptor complex on murine cells, while murine OSM exclusively activates the murine type II (gp130/OSMR) receptor system. Indeed, a recently published study describing the phenotypes of mice overexpressing bovine, human and murine OSM after retroviral gene transfer confirms this receptor usage and demonstrates that mice overexpressing bovine or human OSM display a LIF-like phenotype. On the other hand, it has been shown that mice overexpressing murine OSM develop a completely different phenotype[348]. Astonishingly, and in contrast to all previously published *in vivo* studies using retro- or adenovirally encoded murine OSM[60, 354], these mice display a rather mild phenotype including lymph node enlargement, splenic white pulp atrophy and thymic atrophy[348]. Nevertheless, it cannot be excluded that this rather mild phenotype is due to the cloning or expression strategy, respectively, used by Juan *et al.* in their study. In contrast to the two studies from Langdon *et al.* who used processed mOSM (Ala24-Arg206) lacking

the N-terminal signal peptide and the C-terminal propeptide[27, 59, 354], Juan and colleagues overexpressed mOSM, bOSM and hOSM as entire proteins (e.g. Met1-Ala263 of mOSM) by using respective primers to generate cDNA[348]. Interestingly, Linsley *et al.* have shown several years ago that the non-processed hOSM form has the same receptor binding activity as the processed hOSM, but is 5- to 60-fold less active in growth inhibition assays[68]. In sharp contrast, mOSM that still contains the C-terminal propeptide seems to have no measurable activity, since supernatants of COS cells secreting C-terminally untruncated mOSM have no growth stimulatory effect on DA-1 cells, while C-terminally truncated mOSM strongly mediates the growth of DA-1 cells[356]. Thus, it is possible that these mOSM overexpressing mice produce an fully or partially inactive form of the cytokine, what finally might explain the rather mild phenotype of these mice. Notably, all *in vitro* studies within which human primary cells as well as human cell lines were treated with hOSM indicate exacerbated inflammatory gene expression[56, 59-64]. Because of such divergent results and given by the fact that mOSM (on murine cells) cannot correctly reflect the human situation, the newly characterised rat OSM offers a more accurate and human-like alternative.

6 Future Prospects

6.1 Analysis of the hypertrophic potential of rat OSM

As shown in the result section (4.4), on cells of rat origin rOSM is the only OSM variant able to correctly mimic the signalling potential of hOSM on human cells. This is due to the capability of rOSM to utilise the rat type I and type II receptor complex, just as hOSM on human cells. Furthermore, mOSM exclusively utilises the rat type II (gp130/OSMR) receptor complex, while hOSM signals through the exclusive use of the rat type I (gp130/LIFR) complex. However, when the hypertrophy project started, within which the hypertrophic potential of several IL-6-type cytokines in heart cells was analysed, rOSM was not yet commercially produced and the differential receptor usage of the OSM orthologs was still unknown. Therefore, the experiments in neonatal rat cardiomyocytes and fibroblasts were initially performed using mOSM and hOSM. Preliminary data (not shown) comparing the mRNA levels of IL-6, OSMR and AT1α upon mOSM and rOSM stimulation indeed indicate that rOSM induces a stronger upregulation of these hypertrophy supporting target genes in comparison to mOSM. Therefore, hypertrophy assays in response to rOSM treatment will show, whether rOSM is a stronger hypertrophy inducer compared to other IL-6-type cytokines. Since hLIF/hOSM induce hypertrophy of NRCM utilising LIFR/gp130 heterodimers and mOSM mediates hypertrophic responses via OSMR/gp130 heterodimers, the double receptor complex binding cytokine rOSM is considered to mediate even stronger myocardial hypertrophy. Additional preliminary data (not shown) indicate that rOSM is able to mediate IL-6 expression in NRCFB. Notably, the IL-6 protein levels after 5 and 20 h cytokine treatment (data not shown) suggest, that IL-6 expression in response to rOSM treatment is highly induced and occurs earlier than the mOSM induced IL-6 secretion. Further experiments are required to confirm these preliminary data, but it is likely that rOSM has the strongest hypertrophy supporting influence on NRCM and NRCFB among LIFR and OSMR utilising cytokines, because both receptor complexes are activated.

6.2 Analysing the influence of AT1α and ACE induction

The results shown in 4.2.4 demonstrate that mOSM as well as hIL-6/sIL-6R induce increased mRNA levels of AT1α and ACE in NRCFB. Since AT1α represents the important angiotensin II receptor mediating cardiac hypertrophy, vasoconstriction and aldosterone synthesis[357], its upregulation by IL-6-type cytokines might be of increased interest. Furthermore, the overexpression of this receptor is sufficient to induce cardiac hypertrophy[263]. First, it has to be verified in future experiments, whether NRCFB have a higher responsiveness to ATII due to the finding that AT1α expression is increased by OSM or IL-6. In addition, this elevated AT1α expression might be crucial for maintaining cross-talk with IL-6-type cytokines. As already mentioned, ATII seems to be able to induce the secretion of IL-6 in heart tissue which, as an effector, mediates cardiac hypertrophy[296]. Therefore, we might observe an increased IL-6 secretion of NRCFB after prestimulating the cells with OSM or IL-6/sIL-6R, respectively, and later treatment with ATII. This would confirm the increased ATII responsiveness of these cells and also indicate that the expression levels of AT1α are crucial for the described cross-talk.

ACE represents a further potential protein of the renin-angiotensin system that seems to contribute to IL-6 type cytokine induced hypertrophy. The enzyme catalyses the conversion of the mostly inactive angiotensin I to the highly active angiotensin II. Whether ACE is truly released from NRCFB has to be confirmed in future experiments. The experimental setup to analyse the expression of ACE on protein level will be as follows: Stimulation of NRCFB with OSM or IL-6/sIL-6R in the presence of angiotensin I. Meanwhile, ACE can be directly detected via ELISA. In addition, it is possible to detected the enzymatic conversion to ATII by ELISA. Thereby, the amount of produced ATII serves as indirect readout of the existing ACE concentrations.

Furthermore, we want to analyse, if other components of the renin-angiotensin system such as angiotensinogen and renin are upregulated by IL-6-type cytokines in heart cells at later time points. Already performed experiments determining mRNA levels of angiotensinogen and renin upon 18 h stimulation with OSM, LIF or IL-6/sIL-6R did not show a significant upregulation in NRCFB. On the other hand, it has been shown that the cardiac-restricted expression of renin, angiotensinogen and resulting ATII can be induced under special conditions (e.g. stretch induced adaptive

responses in cardiac fibroblasts and myocytes)[358]. This local availability of all important renin-angiotensin components in the heart is called intracardiac renin-angiotensin system. This local system can generate active ATII without participation of the liver (produces angiotensinogen) or kidney (synthesises renin). Further analyses at different time points are required to verify whether some other components of the renin-angiotensin system are upregulated upon IL-6-type cytokine treatment. Interestingly, mOSM and hIL-6 were already described to potently suppress the renin transcription in the murine kidney and in immortalised renin producing renal tumor cells of murine origin[359, 360]. Regarding OSM, one of central questions will be whether this transcriptional regulation is only true for mOSM exlusively utilising the murine/rat type II receptor complex or also for rOSM signalling through the rat/murine type I and the type II receptor complex. Since our corresponding experiments in NRCFB and NRCM were performed using mOSM, the regulation of renin also will be analysed upon rOSM stimulation. It will be interesting if the renin expression is suppressed in the heart as well, because this decrease would finally cause attenuation of the ATII synthesis and the described IL-6-ATII-cross-talk. Furthermore, the examination of alternatively spliced angiotensin receptors and respective enzymes will complete the analyses. The exact expression analysis of angiotensinogen and renin in NRCFB or NRCM would be of great interest, since an enclosed ATII-IL-6-type cytokine-loop would probably explain the rather harmful longterm effects of the cytokine family during development of heart failure.

6.3 Validating the hypertrophic potential of IL-6 *in vivo*

One of the most important questions in future studies will be, if systemic sIL-6R levels are sufficient to allow prolonged IL-6 trans-signalling in the heart. Since we could demonstrate that neither NRCM hypertrophy nor the typical signalling pathways are induced by pure IL-6 treatment (classic IL-6 signalling), it would be interesting, if sIL-6R serum levels are partly responsible for cardiac hypertrophy *in vivo*. Hirota *et al.* have shown several years ago that mice overexpressing hIL-6 and hIL-6R develop myocardial hypertrophy, while mice exclusively overexpressing hIL-6 or hIL-6R do not[199]. These data are fully consistent with our *in vitro* data. However, it cannot be excluded that e.g. intravenous application of murine IL-6 has similar effects as those observed in the double transgenic mice. Systemic overrepresentation of IL-6 might

have a completely different phenotype than the locally restricted cardiospecific overexpression of IL-6, because sIL-6R would be continuously present in the serum. Since IL-6 binds to the IL-6R with very low affinity (K_d = 5.5 nM), it is possible that local overexpression of hIL-6 alone is not sufficient to induce hypertrophy (a local event), while circulating sIL-6R together with increased concentrations of IL-6 would allow the induction of myocardial hypertrophy under pathophysiological conditions. Therefore, it might be of special interest to determine the hypertrophic role of IL-6, OSM and LIF in an *in vivo* model in the presence and absence of soluble gp130 or an IL-6R neutralising antibody (equivalent to tocilizumab used to antagonise the hIL-6R). As tocilizumab is already used for the treatment of rheumatoid arthritis and systemic juvenile idiopathic arthritis, this antibody would possibly be beneficial for the treatment of cardiac hypertrophy. Indeed, recent publications studying polymorphisms of the human IL-6R in patients also postulate a beneficial effect of tocilizumab application to treat coronary heart disease[361, 362].

Furthermore, the generation of a conditional cardiomyocyte and/or cardiofibroblast specific gp130 (membrane bound and soluble) knockout mouse or rat would be an ambitious goal in the future. Unfortunately, the conditional gp130 knockout mice described by Betz *et al.* only showed about 20-30% effectiveness of the knockout in the heart and high levels of soluble gp130 were generated by floxing the exon encoding for the transmembrane region[363]. The gp130 knockout mice described by Hirota *et al.* are ventricular myocyte specific, but still produce sgp130[214]. Thus, the observed myocardial abnormalities that interestingly share similarities to IL-6 type cytokine induced hypertrophy (thinning of the ventricular walls, decreased myocyte diameter and dilated cardiomyopathy in response to pressure overload), are difficult to assess.

6.4 Determining the roles of C/EBPs during hypertrophy

Our results shown in 4.3 suggest the participation of C/EBPβ and C/EBPδ in prolonging the IL-6/sIL-6R induced hypertrophy. This might be due to an autocrine/paracrine loop of IL-6, STAT3 and C/EBPs between NRCFB and NRCM. Interestingly, the strong induction of IL-6 mRNA and protein levels obviously correlates with the previously mediated upregulation of C/EBPβ and C/EBPδ. The different levels of C/EBPβ and C/EBPδ might also explain why mOSM treatment is

not able to induce an equivalent prolonged IL-6 secretion in NRCFB in comparison to hIL-6 trans-signalling. Further experiments are required to finally prove the correlation of C/EBP levels and IL-6 levels. RNA silencing will be the appropriate method to determine the participation of both transcription factors in future. Furthermore, since several phosphorylation sites of C/EBP are known to increase or decrease the transcriptional activity, we will have to examine the phosphorylation status of the proteins by Western Blot or mass spectrometry. In the case of C/EBPβ, the ratio of LIP and LAP has to be analysed additionally, as LAP is the active form of C/EBPβ, while LIP decreases the transcription of C/EBPβ target genes.

6.5 Cloning of a human- and rat-like murine OSM

As demonstrated in 4.4 and discussed in 5.2, mOSM/mOSMR complexes cannot correctly mimic the interaction of hOSM with its two receptor complexes. While mOSM cannot utilise any receptor complex on human cells, it exclusively signals via the type II receptor complex on murine and rat cells. Depending on the LIFR and OSMR expression of a respective cell, the consequences of the different receptor usage can strongly alter the cell's response to OSM. Preliminary data of OSM induced hypertrophic genes in rat neonatal cardiomyocytes and initiated antiviral target genes in rat fibroblasts (data not shown) already indicate that the double receptor usage of rOSM truly increases activation of some signalling pathways (STAT1, STAT5, p38 and Akt) resulting in transgression of threshold levels required to induce gene transcription[364] (and not presented data). In both cell types the observed differences in mOSM and rOSM responses are much more significant than in JTC-27 (see 4.2) indicating that the expression levels of LIFR, OSMR and gp130 might be different.

For these reasons and to further analyse the pathophysiological effects of OSM *in vivo*, the cloning of a murine OSM variant utilising the type I and type II receptor is indispensable. We therefore recommend the replacement of the mOSM BC loop by that of rat OSM and human OSM. These altered mOSM variants could be used for stimulation of Ba/F3 cells stably expressing either the murine type I or type II receptor complex. As we consider the BC loop of hOSM and rOSM to be the critical region contributing to site III (site of LIFR binding), these muteins are expected to bind to

both receptor complexes. In contrast to native mOSM or hOSM, they could serve as adequate cytokines in murine models of human diseases.

7 Summary

Interleukin-6 (IL-6), oncostatin M (OSM), leukaemia inhibitory factor (LIF) and cardiotrophin-1 (CT-1) are members of the IL-6-type cytokine family that is characterised by sharing the common receptor subunit gp130. While the involvement of these polypeptides in cell differentiation, cell survival, proliferation, apoptosis, inflammation, haematopoiesis, immune response and acute phase reaction has already been demonstrated, the description of their role in development and progression of cardiac hypertrophy is still rather limited and partially controversial. For OSM, its modulatory functions on cells of cardiac origin were completely unclear at the time this study was initiated. A model has been postulated that declares the transient expression of IL-6-type cytokines as protective (e.g. an after myocardial infarction), while a continuous cardiac secretion of these proteins seems to be rather harmful for the heart.

Within the first part of the study (results 4.1, 4.2 and 4.3) it was shown that OSM induces hypertrophy of primary neonatal rat cardiomyocytes (NRCM), just as its related cytokines LIF, CT-1 and hIL-6/hsIL-6R (hsIL-6R, human soluble IL-6 receptor). Regarding the hypertrophic potentials the LIFR/gp130 utilising cytokines (hLIF, hOSM and hCT-1) are stronger inducers than the OSMR/gp130 utilising mOSM. Human IL-6/hsIL-6R which signals via a gp130 homodimer has the weakest hypertrophic effect. The thorough analysis of typical signalling pathways initiated by IL-6-type cytokines revealed that STAT3 phosphorylation at Y705 seems to be the most important hypertrophy promoting pathway, since it is the only activated signalling molecule common to all analysed cytokines. In addition and in contrast to published work, we clearly demonstrate that classical IL-6 signalling (upon pure IL-6 treatment) has no hypertrophic effect on cardiomyocytes, because they lack sufficient amounts of the membrane-bound IL-6R. This is also true for neonatal rat cardiac fibroblasts (NRCFB). Since these cells can also influence cardiac hypertrophy, signalling pathways and target genes were additionally examined in NRCFB in response to OSM, LIF and IL-6/sIL-6R. One of the key findings of this thesis is the selective change in expression of cytokines and receptors of the IL-6 family in both cell types upon IL-6-type cytokine stimulation. Out of the analysed receptor mRNA

levels, particularly the OSMR expression is promoted by OSM, LIF and IL-6/sIL-6R. Only minor changes occurred in mRNA levels of gp130, LIFR and IL-6R. Analysis of the cytokine genes revealed that IL-6 expression is strongly enhanced in NRCM and NRCFB, most notably upon IL-6/sIL-6R stimulation. Furthermore, LIF mRNA is upregulated by IL-6/sIL-6R and LIF stimulation. OSM, however, suppresses the transcription of *Lif*. A striking difference between NRCM and NRCFB is the fact that the target gene induction in NRCM is of similar duration upon mOSM and hIL-6/hsIL-6R treatment, while hIL-6/hsIL-6R is capable of promoting the induction of OSMR and IL-6 significantly longer in NRCFB.

By searching for transcription factors or intermediate cytokines which could be responsible for this difference, a strong correlation between increased *Il6* transcription and amount of mRNA levels for C/EBPβ and C/EBPδ was observed in response to IL-6/sIL-6R stimulation. Interestingly, mOSM also mediates the induction of C/EBPβ and δ, but the initiation is significantly less efficient than in response to IL-6/sIL-6R. Therefore, we assume that mOSM stimulation fails to reach threshold values required for a prolonged IL-6 secretion. Since we additionally observe a slight IL-6R mRNA upregulation in NRCFB, we assume that the combination of IL-6, LIF, C/EBPβ, C/EBPδ and IL-6R expression might be responsible for the observed different kinetics with which IL-6 and OSM stimulate NRCFB.

In addition to the aforementioned proteins, members of the renin-angiotensin system seem to support the IL-6-type cytokine mediated hypertrophy. While we did not find any of these genes to be significantly regulated in cardiomyocytes upon IL-6-type cytokine stimulation, we were able to show a significant increase of the angiotensin converting enzyme (ACE) and the angiotensin II (ATII) receptor type 1α (AT1α) mRNA in NRCFB upon OSM or IL-6/sIL-6R treatment. Since it has already been shown that angiotensin II vice versa induces IL-6 expression in NRCM and NRCFB, this enhanced expression of AT1α and ACE could be of crucial interest for the hypertrophy supporting phenotype.

The second part of the presented work (results 4.4) dealt with the characterisation of the receptor complexes of rat OSM that became available as recombinant protein at this time. The central question of this analysis was, whether rOSM, just like mOSM, only binds the type II (OSMR/gp130) receptor complex or is able to utilise the type II and type I (LIFR/gp130) receptor complex, exactly as hOSM. Using different

experimental approaches (knock-down of the OSMR expression by RNA interference, blocking of the LIFR by LIF-05, an antagonistic LIF variant, and generation of stably transfected Ba/F3 cells expressing the newly cloned rat OSMR/gp130 or LIFR/gp130 receptor complex) we can clearly show that rat OSM surprisingly utilises both, the type I and type II receptor complex. Therefore it closely mimics the human situation. Furthermore, rOSM displays cross-species activities and stimulates cells of human (HepG2) as well as murine origin (Hepa1c1c7). Its signaling capacities closely mimic those of human OSM in cell types of different origin in the way that strong activation of the JAK/STAT, the MAP kinase as well as the PI3K/Akt pathways can be observed. Therefore, the results obtained in the last section of this thesis clearly suggest that rat disease models would allow evaluation of the relevance of OSM for human biology much better than murine models.

8 Zusammenfassung

Interleukin-6 (IL-6), Oncostatin M (OSM), Leukämie inhibierender Faktor (LIF) und Cardiotrophin-1 (CT-1) sind Mitglieder der IL-6-Typ Zytokin-Familie, welche durch die gemeinsame Nutzung der Rezeptoruntereinheit gp130 charakterisiert ist. Während eine Beteiligung dieser Polypeptide bei Zelldifferenzierung, Zellüberleben, Proliferation, Apoptose, Entzündung, Hämatopoese, Immunantwort und Akut-Phase-Reaktion bereits gezeigt wurde, ist die Beschreibung ihrer Rolle bei der Entstehung und dem Fortschreiten der kardialen Hypertrophie deutlich limitierter und teilweise auch kontrovers. Die Wirkungsweise von OSM auf Zellen kardialen Ursprungs war zu jener Zeit, in welcher diese Arbeit begonnen wurde, noch gänzlich unklar. Es wurde bereits ein Modell postuliert, nach dem die kurzzeitige Expression dieser Zytokine (z.B. nach einem Herzinfarkt) schützend wirkt, während eine andauernde kardiale Sekretion dieser Proteine eher schädlich für das Herz zu sein scheint.

Innerhalb des ersten Teils der Arbeit (Ergebnisse 4.1, 4.2 und 4.3) konnte gezeigt werden, dass OSM wie auch seine verwandten Zytokine LIF, CT-1 und hIL-6/hsIL-6R (hsIL-6R, humaner löslicher IL-6 Rezeptor) Hypertrophie-induzierend auf primäre neonatale Ratten-Kardiomyozyten (NRCM) wirkt. Hinsichtlich ihres hypertrophen Potentials sind die Zytokine, welche über LIFR/gp130 signalisieren (hLIF, hOSM und hCT-1), die stärkeren Induktoren im Vergleich zu mOSM, welches den OSMR/gp130 Rezeptorkomplex bindet. Die Stimulation mit humanem IL-6/hsIL-6R, welches mit Hilfe von gp130 Homodimeren signalisiert, hatte hingegen die schwächste hypertrophe Wirkung. Unsere genaue Analyse der typischen IL-6-Typ Zytokin vermittelten Signalwege enthüllte die Phosphorylierung von STAT3 an Y705 als offenkundig wichtigsten Hypertrophie-fördernden Weg, da es das einzige Signalmolekül ist, das von allen analysierten Zytokine aktiviert wird. Zusätzlich dazu konnten wir auch zeigen, dass klassisches IL-6 *signalling* (nach purem IL-6) keinen hypertrophen Einfluss auf NRCM hat, da diesen Zellen ausreichende Mengen des membranständigen IL-6R fehlen. Diese Beobachtung steht in klarem Kontrast zu bereits publizierten Arbeiten. In den ebenfalls untersuchten neonatalen Ratten-Kardiofibroblasten (NRCFB) verhält es sich, was den IL-6R angeht, genauso wie in NRCM. Da auch diese Zellen eine kardiale Hypertrophie mit beeinflussen können,

wurden in ihnen die gleichen Signalwege und Zielgene nach Stimulation mit OSM, LIF und IL-6/sIL-6R untersucht. Die selektive Expressionsregulation von Zytokinen und Rezeptoren der IL-6-Familie in beiden Zelltypen nach IL-6-Typ Zytokin Stimulation ist hierbei einer unserer wichtigsten Befunde. Innerhalb der untersuchten Rezeptor-mRNAs wird speziell die OSMR Expression von OSM, LIF und IL-6/sIL-6R induziert. Bezüglich der gp130, LIFR und IL-6R Level waren hingegen nur geringe Veränderungen zu detektieren. Innerhalb der Analyse der Zytokin-Gene konnten wir in NRCM und NRCFB eine starke IL-6-Expression beobachten, welche besonders nach IL-6/sIL-6R Stimulation induziert wird. Des Weiteren regulieren LIF und IL-6/sIL-6R auch die LIF mRNA Level hoch. OSM supprimiert die *Lif* Transkription hingegen. Ein gravierender Unterschied zwischen NRCM und NRCFB besteht darin, dass die mOSM und hIL-6/hsIL-6R vermittelte Geninduktion in NRCM von vergleichbarer Dauer ist, wohingegen hIL-6/hsIL-6R die OSMR und IL-6 Expression in NRCFB deutlich länger induziert.

Bei der Suche nach Transkriptionsfaktoren oder intermediären Zytokinen, welche für diesen Unterschied verantwortlich sein könnten, beobachteten wir nach IL-6/sIL-6R Stimulation eine deutliche Korrelation zwischen der *Il6*-Transkription und den mRNA Mengen von C/EBPβ und C/EBPδ. Auch OSM ist in der Lage beide Transkriptionsfaktoren zu induzieren, jedoch viel ineffizienter als IL-6/sIL-6R. Wir vermuten deshalb, dass mOSM einen bestimmten Schwellenwert, der für die verlängerte IL-6 Sekretion benötigt wird, nicht erreicht. Da wir zusätzlich noch eine schwache Zunahme der IL-6R mRNA in NRCFB beobachten konnten, gehen wir davon aus, dass die Expression von IL-6, LIF, C/EBPβ, C/EBPδ und IL-6R für die unterschiedlichen Kinetiken, mit denen IL-6 und OSM NRCFB stimulieren, verantwortlich sein dürfte.

Zusätzlich zu den erwähnten Proteinen scheinen auch Mitglieder des Renin-Angiotensin-Systems die IL-6-Typ Zytokin vermittelte Hypertrophie zu unterstützen. Während in NRCM keines dieser Gene durch IL-6-Typ Zytokin-Stimulation reguliert wurde, konnten wir in NRCFB eine deutlich gesteigerte mRNA Induktion des Angiotensin konvertierenden Enzyms (ACE) und des Angiotensin II (ATII) Typ 1α Rezeptors (AT1α) detektieren. Da schon gezeigt wurde, dass Angiotensin II reziprok die IL-6 Expression in NRCM und NRCFB induziert, könnte diese verstärkte Synthese von AT1α und ACE von größter Bedeutung für den Hypertrophie-unterstützenden Phänotyp sein.

Der zweite Teil der Arbeit (4.4) beschäftigte sich mit der Charakterisierung der Rezeptorkomplexe des Ratten-OSM, das damals erstmals als rekombinantes Protein erhältlich wurde. Die zentrale Frage hierbei bestand darin, ob rOSM wie mOSM nur den Typ II (OSMR/gp130) Rezeptorkomplex bindet, oder wie das hOSM sowohl den Typ II als auch den Typ I (LIFR/gp130) Rezeptorkomplex benutzen kann. Mit Hilfe unterschiedlicher experimenteller Strategien (*knock-down* der OSMR Expression durch RNA-Interferenz, LIFR-Blockade durch die antagonistische LIF-Variante LIF-05, und die Generierung von stabil transfizierten Ba/F3-Zellen, welche die hierzu klonierten OSMR/gp130 oder LIFR/gp130 Rezeptorkomplexe der Ratte exprimieren) konnten wir eindeutig zeigen, dass Ratten-OSM überraschenderweise beide Rezeptorkomplexe benutzt. In dieser Hinsicht verhält sich das Zytokin also wie das humane Homolog. Des Weiteren besitzt Ratten-OSM Kreuz-Spezies-Aktivität und stimuliert humane (HepG2) und murine Zellen (Hepa1c1c7). Das Signal-Potential von rOSM ist dem von humanem OSM auf Zellen unterschiedlichen Ursprungs sehr ähnlich. Das Zytokin ist befähigt JAK/STAT, MAP Kinase und PI3K/Akt Signalwege potent zu aktivieren. Deshalb deuten die Daten des zweiten Teils dieser Arbeit darauf hin, dass Krankheitsmodelle in Ratten die Evaluierung der Relevanz des OSM für die humane Biologie deutlich besser widerspiegeln würden als murine Modelle.

9 References

1. Heinrich, P.C., Behrmann, I., Muller-Newen, G., Schaper, F. & Graeve, L. Interleukin-6-type cytokine signalling through the gp130/Jak/STAT pathway. *Biochem J* **334 (Pt 2)**, 297-314 (1998).
2. Derouet, D., Rousseau, F., Alfonsi, F., Froger, J., Hermann, J., Barbier, F., Perret, D., Diveu, C., Guillet, C., Preisser, L. *et al.* Neuropoietin, a new IL-6-related cytokine signaling through the ciliary neurotrophic factor receptor. *Proc Natl Acad Sci U S A* **101**, 4827-4832 (2004).
3. Pflanz, S., Timans, J.C., Cheung, J., Rosales, R., Kanzler, H., Gilbert, J., Hibbert, L., Churakova, T., Travis, M., Vaisberg, E. *et al.* IL-27, a heterodimeric cytokine composed of EBI3 and p28 protein, induces proliferation of naive CD4(+) T cells. *Immunity* **16**, 779-790 (2002).
4. Senaldi, G., Varnum, B.C., Sarmiento, U., Starnes, C., Lile, J., Scully, S., Guo, J., Elliott, G., McNinch, J., Shaklee, C.L. *et al.* Novel neurotrophin-1/B cell-stimulating factor-3: a cytokine of the IL-6 family. *Proc Natl Acad Sci U S A* **96**, 11458-11463 (1999).
5. Baumann, H. & Wong, G.G. Hepatocyte-stimulating factor III shares structural and functional identity with leukemia-inhibitory factor. *J Immunol* **143**, 1163-1167 (1989).
6. Castell, J.V., Gomez-Lechon, M.J., David, M., Fabra, R., Trullenque, R. & Heinrich, P.C. Acute-phase response of human hepatocytes: regulation of acute-phase protein synthesis by interleukin-6. *Hepatology* **12**, 1179-1186 (1990).
7. Peters, M., Roeb, E., Pennica, D., Meyer zum Buschenfelde, K.H. & Rose-John, S. A new hepatocyte stimulating factor: cardiotrophin-1 (CT-1). *FEBS Lett* **372**, 177-180 (1995).
8. Richards, C.D., Brown, T.J., Shoyab, M., Baumann, H. & Gauldie, J. Recombinant oncostatin M stimulates the production of acute phase proteins in HepG2 cells and rat primary hepatocytes in vitro. *J Immunol* **148**, 1731-1736 (1992).
9. Schooltink, H., Stoyan, T., Roeb, E., Heinrich, P.C. & Rose-John, S. Ciliary neurotrophic factor induces acute-phase protein expression in hepatocytes. *FEBS Lett* **314**, 280-284 (1992).
10. White, U.A. & Stephens, J.M. The gp130 receptor cytokine family: regulators of adipocyte development and function. *Curr Pharm Des* **17**, 340-346 (2011).
11. Heinrich, P.C., Behrmann, I., Haan, S., Hermanns, H.M., Muller-Newen, G. & Schaper, F. Principles of interleukin (IL)-6-type cytokine signalling and its regulation. *Biochem J* **374**, 1-20 (2003).
12. Collison, L.W., Delgoffe, G.M., Guy, C.S., Vignali, K.M., Chaturvedi, V., Fairweather, D., Satoskar, A.R., Garcia, K.C., Hunter, C.A., Drake, C.G. *et al.* The composition and signaling of the IL-35 receptor are unconventional. *Nat Immunol* **13**, 290-299 (2012).
13. Bazan, J.F. Structural design and molecular evolution of a cytokine receptor superfamily. *Proc Natl Acad Sci U S A* **87**, 6934-6938 (1990).
14. Davis, S., Aldrich, T.H., Valenzuela, D.M., Wong, V.V., Furth, M.E., Squinto, S.P. & Yancopoulos, G.D. The receptor for ciliary neurotrophic factor. *Science* **253**, 59-63 (1991).
15. Pflanz, S., Hibbert, L., Mattson, J., Rosales, R., Vaisberg, E., Bazan, J.F., Phillips, J.H., McClanahan, T.K., de Waal Malefyt, R. & Kastelein, R.A. WSX-1 and glycoprotein 130 constitute a signal-transducing receptor for IL-27. *J Immunol* **172**, 2225-2231 (2004).
16. Hibi, M., Murakami, M., Saito, M., Hirano, T., Taga, T. & Kishimoto, T. Molecular cloning and expression of an IL-6 signal transducer, gp130. *Cell* **63**, 1149-1157 (1990).
17. Yamasaki, K., Taga, T., Hirata, Y., Yawata, H., Kawanishi, Y., Seed, B., Taniguchi, T., Hirano, T. & Kishimoto, T. Cloning and expression of the human interleukin-6 (BSF-2/IFN beta 2) receptor. *Science* **241**, 825-828 (1988).
18. Murakami, M., Hibi, M., Nakagawa, N., Nakagawa, T., Yasukawa, K., Yamanishi, K., Taga, T. & Kishimoto, T. IL-6-induced homodimerization of gp130 and associated activation of a tyrosine kinase. *Science* **260**, 1808-1810 (1993).
19. Ward, L.D., Howlett, G.J., Discolo, G., Yasukawa, K., Hammacher, A., Moritz, R.L. & Simpson, R.J. High affinity interleukin-6 receptor is a hexameric complex consisting of two molecules each of interleukin-6, interleukin-6 receptor, and gp-130. *J Biol Chem* **269**, 23286-23289 (1994).
20. Paonessa, G., Graziani, R., De Serio, A., Savino, R., Ciapponi, L., Lahm, A., Salvati, A.L., Toniatti, C. & Ciliberto, G. Two distinct and independent sites on IL-6 trigger gp 130 dimer formation and signalling. *EMBO J* **14**, 1942-1951 (1995).

21. Hilton, D.J., Hilton, A.A., Raicevic, A., Rakar, S., Harrison-Smith, M., Gough, N.M., Begley, C.G., Metcalf, D., Nicola, N.A. & Willson, T.A. Cloning of a murine IL-11 receptor alpha-chain; requirement for gp130 for high affinity binding and signal transduction. *EMBO J* **13**, 4765-4775 (1994).
22. Karow, J., Hudson, K.R., Hall, M.A., Vernallis, A.B., Taylor, J.A., Gossler, A. & Heath, J.K. Mediation of interleukin-11-dependent biological responses by a soluble form of the interleukin-11 receptor. *Biochem J* **318 (Pt 2)**, 489-495 (1996).
23. Gearing, D.P., VandenBos, T., Beckmann, M.P., Thut, C.J., Comeau, M.R., Mosley, B. & Ziegler, S.F. Reconstitution of high affinity leukaemia inhibitory factor (LIF) receptors in haemopoietic cells transfected with the cloned human LIF receptor. *Ciba Found Symp* **167**, 245-255; discussion 255-249 (1992).
24. Zhang, J.G., Owczarek, C.M., Ward, L.D., Howlett, G.J., Fabri, L.J., Roberts, B.A. & Nicola, N.A. Evidence for the formation of a heterotrimeric complex of leukaemia inhibitory factor with its receptor subunits in solution. *Biochem J* **325 (Pt 3)**, 693-700 (1997).
25. Hilton, D.J. & Nicola, N.A. Kinetic analyses of the binding of leukemia inhibitory factor to receptor on cells and membranes and in detergent solution. *J Biol Chem* **267**, 10238-10247 (1992).
26. Gearing, D.P., Comeau, M.R., Friend, D.J., Gimpel, S.D., Thut, C.J., McGourty, J., Brasher, K.K., King, J.A., Gillis, S., Mosley, B. *et al.* The IL-6 signal transducer, gp130: an oncostatin M receptor and affinity converter for the LIF receptor. *Science* **255**, 1434-1437 (1992).
27. Ichihara, M., Hara, T., Kim, H., Murate, T. & Miyajima, A. Oncostatin M and leukemia inhibitory factor do not use the same functional receptor in mice. *Blood* **90**, 165-173 (1997).
28. Vlotides, G., Zitzmann, K., Stalla, G.K. & Auernhammer, C.J. Novel neurotrophin-1/B cell-stimulating factor-3 (NNT-1/BSF-3)/cardiotrophin-like cytokine (CLC)--a novel gp130 cytokine with pleiotropic functions. *Cytokine Growth Factor Rev* **15**, 325-336 (2004).
29. White, U.A. & Stephens, J.M. Neuropoietin activates STAT3 independent of LIFR activation in adipocytes. *Biochem Biophys Res Commun* **395**, 48-50 (2010).
30. Pennica, D., Shaw, K.J., Swanson, T.A., Moore, M.W., Shelton, D.L., Zioncheck, K.A., Rosenthal, A., Taga, T., Paoni, N.F. & Wood, W.I. Cardiotrophin-1. Biological activities and binding to the leukemia inhibitory factor receptor/gp130 signaling complex. *J Biol Chem* **270**, 10915-10922 (1995).
31. Robledo, O., Fourcin, M., Chevalier, S., Guillet, C., Auguste, P., Pouplard-Barthelaix, A., Pennica, D. & Gascan, H. Signaling of the cardiotrophin-1 receptor. Evidence for a third receptor component. *J Biol Chem* **272**, 4855-4863 (1997).
32. Villarino, A.V. & Hunter, C.A. Biology of recently discovered cytokines: Discerning the pro- and anti-inflammatory properties of interleukin-27. *Arthritis Res Ther* **6**, 225-233 (2004).
33. Ghilardi, N., Li, J., Hongo, J.A., Yi, S., Gurney, A. & de Sauvage, F.J. A novel type I cytokine receptor is expressed on monocytes, signals proliferation, and activates STAT-3 and STAT-5. *J Biol Chem* **277**, 16831-16836 (2002).
34. Dillon, S.R., Sprecher, C., Hammond, A., Bilsborough, J., Rosenfeld-Franklin, M., Presnell, S.R., Haugen, H.S., Maurer, M., Harder, B., Johnston, J. *et al.* Interleukin 31, a cytokine produced by activated T cells, induces dermatitis in mice. *Nat Immunol* **5**, 752-760 (2004).
35. Bazan, J.F. Haemopoietic receptors and helical cytokines. *Immunol Today* **11**, 350-354 (1990).
36. Owczarek, C.M., Zhang, Y., Layton, M.J., Metcalf, D., Roberts, B. & Nicola, N.A. The unusual species cross-reactivity of the leukemia inhibitory factor receptor alpha-chain is determined primarily by the immunoglobulin-like domain. *J Biol Chem* **272**, 23976-23985 (1997).
37. Hammacher, A., Richardson, R.T., Layton, J.E., Smith, D.K., Angus, L.J., Hilton, D.J., Nicola, N.A., Wijdenes, J. & Simpson, R.J. The immunoglobulin-like module of gp130 is required for signaling by interleukin-6, but not by leukemia inhibitory factor. *J Biol Chem* **273**, 22701-22707 (1998).
38. Kurth, I., Horsten, U., Pflanz, S., Dahmen, H., Kuster, A., Grotzinger, J., Heinrich, P.C. & Muller-Newen, G. Activation of the signal transducer glycoprotein 130 by both IL-6 and IL-11 requires two distinct binding epitopes. *J Immunol* **162**, 1480-1487 (1999).
39. Timmermann, A., Pflanz, S., Grotzinger, J., Kuster, A., Kurth, I., Pitard, V., Heinrich, P.C. & Muller-Newen, G. Different epitopes are required for gp130 activation by interleukin-6, oncostatin M and leukemia inhibitory factor. *FEBS Lett* **468**, 120-124 (2000).
40. Pflanz, S., Kurth, I., Grotzinger, J., Heinrich, P.C. & Muller-Newen, G. Two different epitopes of the signal transducer gp130 sequentially cooperate on IL-6-induced receptor activation. *J Immunol* **165**, 7042-7049 (2000).
41. Rousseau, F., Basset, L., Froger, J., Dinguirard, N., Chevalier, S. & Gascan, H. IL-27 structural analysis demonstrates similarities with ciliary neurotrophic factor (CNTF) and leads

to the identification of antagonistic variants. *Proc Natl Acad Sci U S A* **107**, 19420-19425 (2010).
42. Skiniotis, G., Lupardus, P.J., Martick, M., Walz, T. & Garcia, K.C. Structural organization of a full-length gp130/LIF-R cytokine receptor transmembrane complex. *Mol Cell* **31**, 737-748 (2008).
43. Zarling, J.M., Shoyab, M., Marquardt, H., Hanson, M.B., Lioubin, M.N. & Todaro, G.J. Oncostatin M: a growth regulator produced by differentiated histiocytic lymphoma cells. *Proc Natl Acad Sci U S A* **83**, 9739-9743 (1986).
44. Broxmeyer, H.E., Bruns, H.A., Zhang, S., Cooper, S., Hangoc, G., McKenzie, A.N., Dent, A.L., Schindler, U., Naeger, L.K., Hoey, T. *et al.* Th1 cells regulate hematopoietic progenitor cell homeostasis by production of oncostatin M. *Immunity* **16**, 815-825 (2002).
45. Tanaka, M., Hirabayashi, Y., Sekiguchi, T., Inoue, T., Katsuki, M. & Miyajima, A. Targeted disruption of oncostatin M receptor results in altered hematopoiesis. *Blood* **102**, 3154-3162 (2003).
46. Clegg, C.H., Rulffes, J.T., Wallace, P.M. & Haugen, H.S. Regulation of an extrathymic T-cell development pathway by oncostatin M. *Nature* **384**, 261-263 (1996).
47. Boileau, C., Houde, M., Dulude, G., Clegg, C.H. & Perreault, C. Regulation of extrathymic T cell development and turnover by oncostatin M. *J Immunol* **164**, 5713-5720 (2000).
48. Kinoshita, T., Nagata, K., Sorimachi, N., Karasuyama, H., Sekiguchi, T. & Miyajima, A. Oncostatin M suppresses generation of lymphoid progenitors in fetal liver by inhibiting the hepatic microenvironment. *Exp Hematol* **29**, 1091-1097 (2001).
49. Kinoshita, T., Sekiguchi, T., Xu, M.J., Ito, Y., Kamiya, A., Tsuji, K., Nakahata, T. & Miyajima, A. Hepatic differentiation induced by oncostatin M attenuates fetal liver hematopoiesis. *Proc Natl Acad Sci U S A* **96**, 7265-7270 (1999).
50. Kamiya, A., Kinoshita, T., Ito, Y., Matsui, T., Morikawa, Y., Senba, E., Nakashima, K., Taga, T., Yoshida, K., Kishimoto, T. *et al.* Fetal liver development requires a paracrine action of oncostatin M through the gp130 signal transducer. *EMBO J* **18**, 2127-2136 (1999).
51. Okaya, A., Kitanaka, J., Kitanaka, N., Satake, M., Kim, Y., Terada, K., Sugiyama, T., Takemura, M., Fujimoto, J., Terada, N. *et al.* Oncostatin M inhibits proliferation of rat oval cells, OC15-5, inducing differentiation into hepatocytes. *Am J Pathol* **166**, 709-719 (2005).
52. Nakamura, K., Nonaka, H., Saito, H., Tanaka, M. & Miyajima, A. Hepatocyte proliferation and tissue remodeling is impaired after liver injury in oncostatin M receptor knockout mice. *Hepatology* **39**, 635-644 (2004).
53. Vasse, M., Pourtau, J., Trochon, V., Muraine, M., Vannier, J.P., Lu, H., Soria, J. & Soria, C. Oncostatin M induces angiogenesis in vitro and in vivo. *Arterioscler Thromb Vasc Biol* **19**, 1835-1842 (1999).
54. Hui, W., Bell, M. & Carroll, G. Detection of oncostatin M in synovial fluid from patients with rheumatoid arthritis. *Ann Rheum Dis* **56**, 184-187 (1997).
55. Bonifati, C., Mussi, A., D'Auria, L., Carducci, M., Trento, E., Cordiali-Fei, P. & Ameglio, F. Spontaneous release of leukemia inhibitory factor and oncostatin-M is increased in supernatants of short-term organ cultures from lesional psoriatic skin. *Arch Dermatol Res* **290**, 9-13 (1998).
56. Gazel, A., Rosdy, M., Bertino, B., Tornier, C., Sahuc, F. & Blumenberg, M. A characteristic subset of psoriasis-associated genes is induced by oncostatin-M in reconstituted epidermis. *J Invest Dermatol* **126**, 2647-2657 (2006).
57. Albasanz-Puig, A., Murray, J., Preusch, M., Coan, D., Namekata, M., Patel, Y., Dong, Z.M., Rosenfeld, M.E. & Wijelath, E.S. Oncostatin M is expressed in atherosclerotic lesions: a role for Oncostatin M in the pathogenesis of atherosclerosis. *Atherosclerosis* **216**, 292-298 (2011).
58. Grenier, A., Combaux, D., Chastre, J., Gougerot-Pocidalo, M.A., Gibert, C., Dehoux, M. & Chollet-Martin, S. Oncostatin M production by blood and alveolar neutrophils during acute lung injury. *Lab Invest* **81**, 133-141 (2001).
59. Hohensinner, P.J., Kaun, C., Rychli, K., Niessner, A., Pfaffenberger, S., Rega, G., Furnkranz, A., Uhrin, P., Zaujec, J., Afonyushkin, T. *et al.* The inflammatory mediator oncostatin M induces stromal derived factor-1 in human adult cardiac cells. *FASEB J* **23**, 774-782 (2009).
60. Langdon, C., Kerr, C., Tong, L. & Richards, C.D. Oncostatin M regulates eotaxin expression in fibroblasts and eosinophilic inflammation in C57BL/6 mice. *J Immunol* **170**, 548-555 (2003).
61. Hintzen, C., Haan, C., Tuckermann, J.P., Heinrich, P.C. & Hermanns, H.M. Oncostatin M-induced and constitutive activation of the JAK2/STAT5/CIS pathway suppresses CCL1, but not CCL7 and CCL8, chemokine expression. *J Immunol* **181**, 7341-7349 (2008).
62. Hintzen, C., Quaiser, S., Pap, T., Heinrich, P.C. & Hermanns, H.M. Induction of CCL13 expression in synovial fibroblasts highlights a significant role of oncostatin M in rheumatoid arthritis. *Arthritis Rheum* **60**, 1932-1943 (2009).

63. Lee, M.J., Song, H.Y., Kim, M.R., Sung, S.M., Jung, J.S. & Kim, J.H. Oncostatin M stimulates expression of stromal-derived factor-1 in human mesenchymal stem cells. *Int J Biochem Cell Biol* **39**, 650-659 (2007).
64. Yao, L., Pan, J., Setiadi, H., Patel, K.D. & McEver, R.P. Interleukin 4 or oncostatin M induces a prolonged increase in P-selectin mRNA and protein in human endothelial cells. *J Exp Med* **184**, 81-92 (1996).
65. Brown, T.J., Lioubin, M.N. & Marquardt, H. Purification and characterization of cytostatic lymphokines produced by activated human T lymphocytes. Synergistic antiproliferative activity of transforming growth factor beta 1, interferon-gamma, and oncostatin M for human melanoma cells. *J Immunol* **139**, 2977-2983 (1987).
66. Suda, T., Chida, K., Todate, A., Ide, K., Asada, K., Nakamura, Y., Suzuki, K., Kuwata, H. & Nakamura, H. Oncostatin M production by human dendritic cells in response to bacterial products. *Cytokine* **17**, 335-340 (2002).
67. Malik, N., Kallestad, J.C., Gunderson, N.L., Austin, S.D., Neubauer, M.G., Ochs, V., Marquardt, H., Zarling, J.M., Shoyab, M., Wei, C.M. *et al.* Molecular cloning, sequence analysis, and functional expression of a novel growth regulator, oncostatin M. *Mol Cell Biol* **9**, 2847-2853 (1989).
68. Linsley, P.S., Kallestad, J., Ochs, V. & Neubauer, M. Cleavage of a hydrophilic C-terminal domain increases growth-inhibitory activity of oncostatin M. *Mol Cell Biol* **10**, 1882-1890 (1990).
69. Malik, N., Haugen, H.S., Modrell, B., Shoyab, M. & Clegg, C.H. Developmental abnormalities in mice transgenic for bovine oncostatin M. *Mol Cell Biol* **15**, 2349-2358 (1995).
70. Hara, T., Ichihara, M., Yoshimura, A. & Miyajima, A. Cloning and biological activity of murine oncostatin M. *Leukemia* **11 Suppl 3**, 449-450 (1997).
71. Rose, T.M. & Bruce, A.G. Oncostatin M is a member of a cytokine family that includes leukemia-inhibitory factor, granulocyte colony-stimulating factor, and interleukin 6. *Proc Natl Acad Sci U S A* **88**, 8641-8645 (1991).
72. Jeffery, E., Price, V. & Gearing, D.P. Close proximity of the genes for leukemia inhibitory factor and oncostatin M. *Cytokine* **5**, 107-111 (1993).
73. Mosley, B., De Imus, C., Friend, D., Boiani, N., Thoma, B., Park, L.S. & Cosman, D. Dual oncostatin M (OSM) receptors. Cloning and characterization of an alternative signaling subunit conferring OSM-specific receptor activation. *J Biol Chem* **271**, 32635-32643 (1996).
74. Lindberg, R.A., Juan, T.S., Welcher, A.A., Sun, Y., Cupples, R., Guthrie, B. & Fletcher, F.A. Cloning and characterization of a specific receptor for mouse oncostatin M. *Mol Cell Biol* **18**, 3357-3367 (1998).
75. Tanaka, M., Hara, T., Copeland, N.G., Gilbert, D.J., Jenkins, N.A. & Miyajima, A. Reconstitution of the functional mouse oncostatin M (OSM) receptor: molecular cloning of the mouse OSM receptor beta subunit. *Blood* **93**, 804-815 (1999).
76. Metcalf, D. The unsolved enigmas of leukemia inhibitory factor. *Stem Cells* **21**, 5-14 (2003).
77. Lust, J.A., Donovan, K.A., Kline, M.P., Greipp, P.R., Kyle, R.A. & Maihle, N.J. Isolation of an mRNA encoding a soluble form of the human interleukin-6 receptor. *Cytokine* **4**, 96-100 (1992).
78. Narazaki, M., Yasukawa, K., Saito, T., Ohsugi, Y., Fukui, H., Koishihara, Y., Yancopoulos, G.D., Taga, T. & Kishimoto, T. Soluble forms of the interleukin-6 signal-transducing receptor component gp130 in human serum possessing a potential to inhibit signals through membrane-anchored gp130. *Blood* **82**, 1120-1126 (1993).
79. Müllberg, J., Schooltink, H., Stoyan, T., Gunther, M., Graeve, L., Buse, G., Mackiewicz, A., Heinrich, P.C. & Rose-John, S. The soluble interleukin-6 receptor is generated by shedding. *Eur J Immunol* **23**, 473-480 (1993).
80. Matthews, V., Schuster, B., Schütze, S., Bussmeyer, I., Ludwig, A., Hundhausen, C., Sadowski, T., Saftig, P., Hartmann, D., Kallen, K.-J. *et al.* Cellular Cholesterol Depletion Triggers Shedding of the Human Interleukin-6 Receptor by ADAM10 and ADAM17 (TACE). *J Biol Chem* **278**, 38829-38839 (2003).
81. Baumann, H., Wang, Y., Morella, K.K., Lai, C.F., Dams, H., Hilton, D.J., Hawley, R.G. & Mackiewicz, A. Complex of the soluble IL-11 receptor and IL-11 acts as IL-6-type cytokine in hepatic and nonhepatic cells. *J Immunol* **157**, 284-290 (1996).
82. Davis, S., Aldrich, T.H., Ip, N.Y., Stahl, N., Scherer, S., Farruggella, T., DiStefano, P.S., Curtis, R., Panayotatos, N., Gascan, H. *et al.* Released form of CNTF receptor alpha component as a soluble mediator of CNTF responses. *Science* **259**, 1736-1739 (1993).
83. Kamiguchi, H., Yoshida, K., Sagoh, M., Sasaki, H., Inaba, M., Wakamoto, H., Otani, M. & Toya, S. Release of ciliary neurotrophic factor from cultured astrocytes and its modulation by cytokines. *Neurochem Res* **20**, 1187-1193 (1995).

84. Hashimoto, Y., Kurita, M. & Matsuoka, M. Identification of soluble WSX-1 not as a dominant-negative but as an alternative functional subunit of a receptor for an anti-Alzheimer's disease rescue factor Humanin. *Biochem Biophys Res Commun* **389**, 95-99 (2009).
85. Diveu, C., Venereau, E., Froger, J., Ravon, E., Grimaud, L., Rousseau, F., Chevalier, S. & Gascan, H. Molecular and Functional Characterization of a Soluble Form of Oncostatin M/Interleukin-31 Shared Receptor. *J Biol Chem* **281**, 36673-36682 (2006).
86. Layton, M.J., Cross, B.A., Metcalf, D., Ward, L.D., Simpson, R.J. & Nicola, N.A. A major binding protein for leukemia inhibitory factor in normal mouse serum: identification as a soluble form of the cellular receptor. *Proc Natl Acad Sci U S A* **89**, 8616-8620 (1992).
87. Zhang, J.-G., Zhang, Y., Owczarek, C.M., Ward, L.D., Moritz, R.L., Simpson, R.J., Yasukawa, K. & Nicola, N.A. Identification and Characterization of Two Distinct Truncated Forms of gp130 and a Soluble Form of Leukemia Inhibitory Factor Receptor α-Chain in Normal Human Urine and Plasma. *J Biol Chem* **273**, 10798-10805 (1998).
88. Jostock, T., Müllberg, J., Özbek, S., Atreya, R., Blinn, G., Voltz, N., Fischer, M., Neurath, M.F. & Rose-John, S. Soluble gp130 is the natural inhibitor of soluble interleukin-6 receptor transsignaling responses. *Eur J Biochem* **268**, 160-167 (2001).
89. Montero-Julian, F.A. The soluble IL-6 receptors: serum levels and biological function. *Cell Mol Biol (Noisy-le-grand)* **47**, 583-597 (2001).
90. Gaillard, J.P., Bataille, R., Brailly, H., Zuber, C., Yasukawa, K., Attal, M., Maruo, N., Taga, T., Kishimoto, T. & Klein, B. Increased and highly stable levels of functional soluble interleukin-6 receptor in sera of patients with monoclonal gammopathy. *Eur J Immunol* **23**, 820-824 (1993).
91. Garbers, C., Thaiss, W., Jones, G.W., Waetzig, G.H., Lorenzen, I., Guilhot, F., Lissilaa, R., Ferlin, W.G., Grötzinger, J., Jones, S.A. *et al.* Inhibition of Classic Signaling Is a Novel Function of Soluble Glycoprotein 130 (sgp130), Which Is Controlled by the Ratio of Interleukin 6 and Soluble Interleukin 6 Receptor. *J Biol Chem* **286**, 42959-42970 (2011).
92. Wilks, A.F., Harpur, A.G., Kurban, R.R., Ralph, S.J., Zurcher, G. & Ziemiecki, A. Two novel protein-tyrosine kinases, each with a second phosphotransferase-related catalytic domain, define a new class of protein kinase. *Mol Cell Biol* **11**, 2057-2065 (1991).
93. Harpur, A.G., Andres, A.C., Ziemiecki, A., Aston, R.R. & Wilks, A.F. JAK2, a third member of the JAK family of protein tyrosine kinases. *Oncogene* **7**, 1347-1353 (1992).
94. Takahashi, T. & Shirasawa, T. Molecular cloning of rat JAK3, a novel member of the JAK family of protein tyrosine kinases. *FEBS Lett* **342**, 124-128 (1994).
95. Firmbach-Kraft, I., Byers, M., Shows, T., Dalla-Favera, R. & Krolewski, J.J. tyk2, prototype of a novel class of non-receptor tyrosine kinase genes. *Oncogene* **5**, 1329-1336 (1990).
96. Ghoreschi, K., Laurence, A. & O'Shea, J.J. Janus kinases in immune cell signaling. *Immunol Rev* **228**, 273-287 (2009).
97. Rane, S.G. & Reddy, E.P. JAK3: a novel JAK kinase associated with terminal differentiation of hematopoietic cells. *Oncogene* **9**, 2415-2423 (1994).
98. Duhe, R.J. & Farrar, W.L. Structural and mechanistic aspects of Janus kinases: how the two-faced god wields a double-edged sword. *J Interferon Cytokine Res* **18**, 1-15 (1998).
99. O'Shea, J.J., Gadina, M. & Schreiber, R.D. Cytokine signaling in 2002: new surprises in the Jak/Stat pathway. *Cell* **109 Suppl**, S121-131 (2002).
100. Ungureanu, D., Wu, J., Pekkala, T., Niranjan, Y., Young, C., Jensen, O.N., Xu, C.F., Neubert, T.A., Skoda, R.C., Hubbard, S.R. *et al.* The pseudokinase domain of JAK2 is a dual-specificity protein kinase that negatively regulates cytokine signaling. *Nat Struct Mol Biol* **18**, 971-976 (2011).
101. Haan, C., Is'harc, H., Hermanns, H.M., Schmitz-Van De Leur, H., Kerr, I.M., Heinrich, P.C., Grotzinger, J. & Behrmann, I. Mapping of a region within the N terminus of Jak1 involved in cytokine receptor interaction. *J Biol Chem* **276**, 37451-37458 (2001).
102. Zhou, Y.J., Chen, M., Cusack, N.A., Kimmel, L.H., Magnuson, K.S., Boyd, J.G., Lin, W., Roberts, J.L., Lengi, A., Buckley, R.H. *et al.* Unexpected effects of FERM domain mutations on catalytic activity of Jak3: structural implication for Janus kinases. *Mol Cell* **8**, 959-969 (2001).
103. Radtke, S., Hermanns, H.M., Haan, C., Schmitz-Van De Leur, H., Gascan, H., Heinrich, P.C. & Behrmann, I. Novel role of Janus kinase 1 in the regulation of oncostatin M receptor surface expression. *J Biol Chem* **277**, 11297-11305 (2002).
104. Murakami, M., Narazaki, M., Hibi, M., Yawata, H., Yasukawa, K., Hamaguchi, M., Taga, T. & Kishimoto, T. Critical cytoplasmic region of the interleukin 6 signal transducer gp130 is conserved in the cytokine receptor family. *Proc Natl Acad Sci U S A* **88**, 11349-11353 (1991).
105. Haan, C., Hermanns, H.M., Heinrich, P.C. & Behrmann, I. A single amino acid substitution (Trp(666)-->Ala) in the interbox1/2 region of the interleukin-6 signal transducer gp130

abrogates binding of JAK1, and dominantly impairs signal transduction. *Biochem J* **349**, 261-266 (2000).
106. Haan, C., Heinrich, P.C. & Behrmann, I. Structural requirements of the interleukin-6 signal transducer gp130 for its interaction with Janus kinase 1: the receptor is crucial for kinase activation. *Biochem J* **361**, 105-111 (2002).
107. Radtke, S., Haan, S., Jorissen, A., Hermanns, H.M., Diefenbach, S., Smyczek, T., Schmitz-Vandeleur, H., Heinrich, P.C., Behrmann, I. & Haan, C. The Jak1 SH2 domain does not fulfill a classical SH2 function in Jak/STAT signaling but plays a structural role for receptor interaction and up-regulation of receptor surface expression. *J Biol Chem* **280**, 25760-25768 (2005).
108. Velazquez, L., Mogensen, K.E., Barbieri, G., Fellous, M., Uze, G. & Pellegrini, S. Distinct domains of the protein tyrosine kinase tyk2 required for binding of interferon-alpha/beta and for signal transduction. *J Biol Chem* **270**, 3327-3334 (1995).
109. Saharinen, P., Takaluoma, K. & Silvennoinen, O. Regulation of the Jak2 tyrosine kinase by its pseudokinase domain. *Mol Cell Biol* **20**, 3387-3395 (2000).
110. Saharinen, P., Vihinen, M. & Silvennoinen, O. Autoinhibition of Jak2 tyrosine kinase is dependent on specific regions in its pseudokinase domain. *Mol Biol Cell* **14**, 1448-1459 (2003).
111. Darnell, J.E., Kerr, I.M. & Stark, G.R. Jak-STAT pathways and transcriptional activation in response to IFNs and other extracellular signaling proteins. *Science* **264**, 1415-1421 (1994).
112. Berger, L.C., Hawley, T.S., Lust, J.A., Goldman, S.J. & Hawley, R.G. Tyrosine phosphorylation of JAK-TYK kinases in malignant plasma cell lines growth-stimulated by interleukins 6 and 11. *Biochem Biophys Res Commun* **202**, 596-605 (1994).
113. Lutticken, C., Wegenka, U.M., Yuan, J., Buschmann, J., Schindler, C., Ziemiecki, A., Harpur, A.G., Wilks, A.F., Yasukawa, K., Taga, T. *et al.* Association of transcription factor APRF and protein kinase Jak1 with the interleukin-6 signal transducer gp130. *Science* **263**, 89-92 (1994).
114. Stahl, N., Farruggella, T.J., Boulton, T.G., Zhong, Z., Darnell, J.E., Jr. & Yancopoulos, G.D. Choice of STATs and other substrates specified by modular tyrosine-based motifs in cytokine receptors. *Science* **267**, 1349-1353 (1995).
115. Matsuda, T., Yamanaka, Y. & Hirano, T. Interleukin-6-induced tyrosine phosphorylation of multiple proteins in murine hematopoietic lineage cells. *Biochem Biophys Res Commun* **200**, 821-828 (1994).
116. Guschin, D., Rogers, N., Briscoe, J., Witthuhn, B., Watling, D., Horn, F., Pellegrini, S., Yasukawa, K., Heinrich, P., Stark, G.R. *et al.* A major role for the protein tyrosine kinase JAK1 in the JAK/STAT signal transduction pathway in response to interleukin-6. *EMBO J* **14**, 1421-1429 (1995).
117. Rodig, S.J., Meraz, M.A., White, J.M., Lampe, P.A., Riley, J.K., Arthur, C.D., King, K.L., Sheehan, K.C., Yin, L., Pennica, D. *et al.* Disruption of the Jak1 gene demonstrates obligatory and nonredundant roles of the Jaks in cytokine-induced biologic responses. *Cell* **93**, 373-383 (1998).
118. Akira, S., Nishio, Y., Inoue, M., Wang, X.J., Wei, S., Matsusaka, T., Yoshida, K., Sudo, T., Naruto, M. & Kishimoto, T. Molecular cloning of APRF, a novel IFN-stimulated gene factor 3 p91-related transcription factor involved in the gp130-mediated signaling pathway. *Cell* **77**, 63-71 (1994).
119. Fujitani, Y., Hibi, M., Fukada, T., Takahashi-Tezuka, M., Yoshida, H., Yamaguchi, T., Sugiyama, K., Yamanaka, Y., Nakajima, K. & Hirano, T. An alternative pathway for STAT activation that is mediated by the direct interaction between JAK and STAT. *Oncogene* **14**, 751-761 (1997).
120. Fujitani, Y., Nakajima, K., Kojima, H., Nakae, K., Takeda, T. & Hirano, T. Transcriptional activation of the IL-6 response element in the junB promoter is mediated by multiple Stat family proteins. *Biochem Biophys Res Commun* **202**, 1181-1187 (1994).
121. Zhong, Z., Wen, Z. & Darnell, J.E., Jr. Stat3: a STAT family member activated by tyrosine phosphorylation in response to epidermal growth factor and interleukin-6. *Science* **264**, 95-98 (1994).
122. Lai, C.F., Ripperger, J., Morella, K.K., Wang, Y., Gearing, D.P., Horseman, N.D., Campos, S.P., Fey, G.H. & Baumann, H. STAT3 and STAT5B are targets of two different signal pathways activated by hematopoietin receptors and control transcription via separate cytokine response elements. *J Biol Chem* **270**, 23254-23257 (1995).
123. Nakajima, K., Matsuda, T., Fujitani, Y., Kojima, H., Yamanaka, Y., Nakae, K., Takeda, T. & Hirano, T. Signal transduction through IL-6 receptor: involvement of multiple protein kinases, stat factors, and a novel H7-sensitive pathway. *Ann N Y Acad Sci* **762**, 55-70 (1995).
124. Gerhartz, C., Heesel, B., Sasse, J., Hemmann, U., Landgraf, C., Schneider-Mergener, J., Horn, F., Heinrich, P.C. & Graeve, L. Differential Activation of Acute Phase Response

Factor/STAT3 and STAT1 via the Cytoplasmic Domain of the Interleukin 6 Signal Transducer gp130. *J Biol Chem* **271**, 12991-12998 (1996).
125. Hermanns, H.M., Radtke, S., Haan, C., Schmitz-Van de Leur, H., Tavernier, J., Heinrich, P.C. & Behrmann, I. Contributions of Leukemia Inhibitory Factor Receptor and Oncostatin M Receptor to Signal Transduction in Heterodimeric Complexes with Glycoprotein 130. *J Immunol* **163**, 6651-6658 (1999).
126. Kuropatwinski, K.K., De Imus, C., Gearing, D., Baumann, H. & Mosley, B. Influence of subunit combinations on signaling by receptors for oncostatin M, leukemia inhibitory factor, and interleukin-6. *J Biol Chem* **272**, 15135-15144 (1997).
127. Wang, Y., Robledo, O., Kinzie, E., Blanchard, F., Richards, C., Miyajima, A. & Baumann, H. Receptor subunit-specific action of oncostatin M in hepatic cells and its modulation by leukemia inhibitory factor. *J Biol Chem* **275**, 25273-25285 (2000).
128. Hintzen, C., Evers, C., Lippok, B.E., Volkmer, R., Heinrich, P.C., Radtke, S. & Hermanns, H.M. Box 2 Region of the Oncostatin M Receptor Determines Specificity for Recruitment of Janus Kinases and STAT5 Activation. *J Biol Chem* **283**, 19465-19477 (2008).
129. Kaptein, A., Paillard, V. & Saunders, M. Dominant negative stat3 mutant inhibits interleukin-6-induced Jak-STAT signal transduction. *J Biol Chem* **271**, 5961-5964 (1996).
130. Shuai, K., Stark, G.R., Kerr, I.M. & Darnell, J.E., Jr. A single phosphotyrosine residue of Stat91 required for gene activation by interferon-gamma. *Science* **261**, 1744-1746 (1993).
131. Uddin, S., Sassano, A., Deb, D.K., Verma, A., Majchrzak, B., Rahman, A., Malik, A.B., Fish, E.N. & Platanias, L.C. Protein kinase C-delta (PKC-delta) is activated by type I interferons and mediates phosphorylation of Stat1 on serine 727. *J Biol Chem* **277**, 14408-14416 (2002).
132. Haq, R., Halupa, A., Beattie, B.K., Mason, J.M., Zanke, B.W. & Barber, D.L. Regulation of erythropoietin-induced STAT serine phosphorylation by distinct mitogen-activated protein kinases. *J Biol Chem* **277**, 17359-17366 (2002).
133. Abe, K., Hirai, M., Mizuno, K., Higashi, N., Sekimoto, T., Miki, T., Hirano, T. & Nakajima, K. The YXXQ motif in gp 130 is crucial for STAT3 phosphorylation at Ser727 through an H7-sensitive kinase pathway. *Oncogene* **20**, 3464-3474 (2001).
134. Jain, N., Zhang, T., Fong, S.L., Lim, C.P. & Cao, X. Repression of Stat3 activity by activation of mitogen-activated protein kinase (MAPK). *Oncogene* **17**, 3157-3167 (1998).
135. Wen, Z. & Darnell, J.E., Jr. Mapping of Stat3 serine phosphorylation to a single residue (727) and evidence that serine phosphorylation has no influence on DNA binding of Stat1 and Stat3. *Nucleic Acids Res* **25**, 2062-2067 (1997).
136. Wen, Z., Zhong, Z. & Darnell, J.E., Jr. Maximal activation of transcription by Stat1 and Stat3 requires both tyrosine and serine phosphorylation. *Cell* **82**, 241-250 (1995).
137. Wegrzyn, J., Potla, R., Chwae, Y.J., Sepuri, N.B., Zhang, Q., Koeck, T., Derecka, M., Szczepanek, K., Szelag, M., Gornicka, A. *et al.* Function of mitochondrial Stat3 in cellular respiration. *Science* **323**, 793-797 (2009).
138. Fukada, T., Hibi, M., Yamanaka, Y., Takahashi-Tezuka, M., Fujitani, Y., Yamaguchi, T., Nakajima, K. & Hirano, T. Two signals are necessary for cell proliferation induced by a cytokine receptor gp130: involvement of STAT3 in anti-apoptosis. *Immunity* **5**, 449-460 (1996).
139. Takahashi-Tezuka, M., Yoshida, Y., Fukada, T., Ohtani, T., Yamanaka, Y., Nishida, K., Nakajima, K., Hibi, M. & Hirano, T. Gab1 acts as an adapter molecule linking the cytokine receptor gp130 to ERK mitogen-activated protein kinase. *Mol Cell Biol* **18**, 4109-4117 (1998).
140. Schiemann, W.P., Bartoe, J.L. & Nathanson, N.M. Box 3-independent signaling mechanisms are involved in leukemia inhibitory factor receptor alpha- and gp130-mediated stimulation of mitogen-activated protein kinase. Evidence for participation of multiple signaling pathways which converge at Ras. *J Biol Chem* **272**, 16631-16636 (1997).
141. Hermanns, H.M., Radtke, S., Schaper, F., Heinrich, P.C. & Behrmann, I. Non-redundant signal transduction of interleukin-6-type cytokines. The adapter protein Shc is specifically recruited to the oncostatin M receptor. *J Biol Chem* **275**, 40742-40748 (2000).
142. Schaper, F., Gendo, C., Eck, M., Schmitz, J., Grimm, C., Anhuf, D., Kerr, I.M. & Heinrich, P.C. Activation of the protein tyrosine phosphatase SHP2 via the interleukin-6 signal transducing receptor protein gp130 requires tyrosine kinase Jak1 and limits acute-phase protein expression. *Biochem J* **335 (Pt 3)**, 557-565 (1998).
143. Avruch, J., Zhang, X.F. & Kyriakis, J.M. Raf meets Ras: completing the framework of a signal transduction pathway. *Trends Biochem Sci* **19**, 279-283 (1994).
144. Pearson, G., Robinson, F., Beers Gibson, T., Xu, B.E., Karandikar, M., Berman, K. & Cobb, M.H. Mitogen-activated protein (MAP) kinase pathways: regulation and physiological functions. *Endocr Rev* **22**, 153-183 (2001).

145. Calleja, V., Alcor, D., Laguerre, M., Park, J., Vojnovic, B., Hemmings, B.A., Downward, J., Parker, P.J. & Larijani, B. Intramolecular and intermolecular interactions of protein kinase B define its activation in vivo. *PLoS Biol* **5**, e95 (2007).
146. Milburn, C.C., Deak, M., Kelly, S.M., Price, N.C., Alessi, D.R. & Van Aalten, D.M. Binding of phosphatidylinositol 3,4,5-trisphosphate to the pleckstrin homology domain of protein kinase B induces a conformational change. *Biochem J* **375**, 531-538 (2003).
147. Sarbassov, D.D., Guertin, D.A., Ali, S.M. & Sabatini, D.M. Phosphorylation and Regulation of Akt/PKB by the Rictor-mTOR Complex. *Science* **307**, 1098-1101 (2005).
148. Negoro, S., Oh, H., Tone, E., Kunisada, K., Fujio, Y., Walsh, K., Kishimoto, T. & Yamauchi-Takihara, K. Glycoprotein 130 regulates cardiac myocyte survival in doxorubicin-induced apoptosis through phosphatidylinositol 3-kinase/Akt phosphorylation and Bcl-xL/caspase-3 interaction. *Circulation* **103**, 555-561 (2001).
149. Jee, S.H., Chiu, H.C., Tsai, T.F., Tsai, W.L., Liao, Y.H., Chu, C.Y. & Kuo, M.L. The phosphotidyl inositol 3-kinase/Akt signal pathway is involved in interleukin-6-mediated Mcl-1 upregulation and anti-apoptosis activity in basal cell carcinoma cells. *J Invest Dermatol* **119**, 1121-1127 (2002).
150. Shi, Y., Hsu, J.H., Hu, L., Gera, J. & Lichtenstein, A. Signal pathways involved in activation of p70S6K and phosphorylation of 4E-BP1 following exposure of multiple myeloma tumor cells to interleukin-6. *J Biol Chem* **277**, 15712-15720 (2002).
151. Hsu, J.H., Shi, Y., Hu, L., Fisher, M., Franke, T.F. & Lichtenstein, A. Role of the AKT kinase in expansion of multiple myeloma clones: effects on cytokine-dependent proliferative and survival responses. *Oncogene* **21**, 1391-1400 (2002).
152. Hideshima, T., Nakamura, N., Chauhan, D. & Anderson, K.C. Biologic sequelae of interleukin-6 induced PI3-K/Akt signaling in multiple myeloma. *Oncogene* **20**, 5991-6000 (2001).
153. Kortylewski, M., Feld, F., Kruger, K.D., Bahrenberg, G., Roth, R.A., Joost, H.G., Heinrich, P.C., Behrmann, I. & Barthel, A. Akt modulates STAT3-mediated gene expression through a FKHR (FOXO1a)-dependent mechanism. *J Biol Chem* **278**, 5242-5249 (2003).
154. Eulenfeld, R. & Schaper, F. A new mechanism for the regulation of Gab1 recruitment to the plasma membrane. *J Cell Sci* **122**, 55-64 (2009).
155. Boulton, T.G., Stahl, N. & Yancopoulos, G.D. Ciliary neurotrophic factor/leukemia inhibitory factor/interleukin 6/oncostatin M family of cytokines induces tyrosine phosphorylation of a common set of proteins overlapping those induced by other cytokines and growth factors. *J Biol Chem* **269**, 11648-11655 (1994).
156. Hof, P., Pluskey, S., Dhe-Paganon, S., Eck, M.J. & Shoelson, S.E. Crystal structure of the tyrosine phosphatase SHP-2. *Cell* **92**, 441-450 (1998).
157. Lechleider, R.J., Sugimoto, S., Bennett, A.M., Kashishian, A.S., Cooper, J.A., Shoelson, S.E., Walsh, C.T. & Neel, B.G. Activation of the SH2-containing phosphotyrosine phosphatase SH-PTP2 by its binding site, phosphotyrosine 1009, on the human platelet-derived growth factor receptor. *J Biol Chem* **268**, 21478-21481 (1993).
158. Sugimoto, S., Wandless, T.J., Shoelson, S.E., Neel, B.G. & Walsh, C.T. Activation of the SH2-containing protein tyrosine phosphatase, SH-PTP2, by phosphotyrosine-containing peptides derived from insulin receptor substrate-1. *J Biol Chem* **269**, 13614-13622 (1994).
159. Pluskey, S., Wandless, T.J., Walsh, C.T. & Shoelson, S.E. Potent stimulation of SH-PTP2 phosphatase activity by simultaneous occupancy of both SH2 domains. *J Biol Chem* **270**, 2897-2900 (1995).
160. Lu, W., Gong, D., Bar-Sagi, D. & Cole, P.A. Site-specific incorporation of a phosphotyrosine mimetic reveals a role for tyrosine phosphorylation of SHP-2 in cell signaling. *Mol Cell* **8**, 759-769 (2001).
161. Lehmann, U., Schmitz, J., Weissenbach, M., Sobota, R.M., Hortner, M., Friederichs, K., Behrmann, I., Tsiaris, W., Sasaki, A., Schneider-Mergener, J. *et al.* SHP2 and SOCS3 contribute to Tyr-759-dependent attenuation of interleukin-6 signaling through gp130. *J Biol Chem* **278**, 661-671 (2003).
162. Starr, R., Willson, T.A., Viney, E.M., Murray, L.J., Rayner, J.R., Jenkins, B.J., Gonda, T.J., Alexander, W.S., Metcalf, D., Nicola, N.A. *et al.* A family of cytokine-inducible inhibitors of signalling. *Nature* **387**, 917-921 (1997).
163. Endo, T.A., Masuhara, M., Yokouchi, M., Suzuki, R., Sakamoto, H., Mitsui, K., Matsumoto, A., Tanimura, S., Ohtsubo, M., Misawa, H. *et al.* A new protein containing an SH2 domain that inhibits JAK kinases. *Nature* **387**, 921-924 (1997).
164. Narazaki, M., Fujimoto, M., Matsumoto, T., Morita, Y., Saito, H., Kajita, T., Yoshizaki, K., Naka, T. & Kishimoto, T. Three distinct domains of SSI-1/SOCS-1/JAB protein are required for its suppression of interleukin 6 signaling. *Proc Natl Acad Sci U S A* **95**, 13130-13134 (1998).

165. Blanchard, F., Wang, Y., Kinzie, E., Duplomb, L., Godard, A. & Baumann, H. Oncostatin M regulates the synthesis and turnover of gp130, leukemia inhibitory factor receptor alpha, and oncostatin M receptor beta by distinct mechanisms. *J Biol Chem* **276**, 47038-47045 (2001).
166. Naka, T., Narazaki, M., Hirata, M., Matsumoto, T., Minamoto, S., Aono, A., Nishimoto, N., Kajita, T., Taga, T., Yoshizaki, K. *et al.* Structure and function of a new STAT-induced STAT inhibitor. *Nature* **387**, 924-929 (1997).
167. Magrangeas, F., Boisteau, O., Denis, S., Jacques, Y. & Minvielle, S. Negative cross-talk between interleukin-3 and interleukin-11 is mediated by suppressor of cytokine signalling-3 (SOCS-3). *Biochem J* **353**, 223-230 (2001).
168. Matsumoto, A., Masuhara, M., Mitsui, K., Yokouchi, M., Ohtsubo, M., Misawa, H., Miyajima, A. & Yoshimura, A. CIS, a cytokine inducible SH2 protein, is a target of the JAK-STAT5 pathway and modulates STAT5 activation. *Blood* **89**, 3148-3154 (1997).
169. Verdier, F., Chretien, S., Muller, O., Varlet, P., Yoshimura, A., Gisselbrecht, S., Lacombe, C. & Mayeux, P. Proteasomes regulate erythropoietin receptor and signal transducer and activator of transcription 5 (STAT5) activation. Possible involvement of the ubiquitinated Cis protein. *J Biol Chem* **273**, 28185-28190 (1998).
170. Yasukawa, H., Misawa, H., Sakamoto, H., Masuhara, M., Sasaki, A., Wakioka, T., Ohtsuka, S., Imaizumi, T., Matsuda, T., Ihle, J.N. *et al.* The JAK-binding protein JAB inhibits Janus tyrosine kinase activity through binding in the activation loop. *EMBO J* **18**, 1309-1320 (1999).
171. Masuhara, M., Sakamoto, H., Matsumoto, A., Suzuki, R., Yasukawa, H., Mitsui, K., Wakioka, T., Tanimura, S., Sasaki, A., Misawa, H. *et al.* Cloning and characterization of novel CIS family genes. *Biochem Biophys Res Commun* **239**, 439-446 (1997).
172. Sasaki, A., Yasukawa, H., Shouda, T., Kitamura, T., Dikic, I. & Yoshimura, A. CIS3/SOCS-3 suppresses erythropoietin (EPO) signaling by binding the EPO receptor and JAK2. *J Biol Chem* **275**, 29338-29347 (2000).
173. Sasaki, A., Yasukawa, H., Suzuki, A., Kamizono, S., Syoda, T., Kinjyo, I., Sasaki, M., Johnston, J.A. & Yoshimura, A. Cytokine-inducible SH2 protein-3 (CIS3/SOCS3) inhibits Janus tyrosine kinase by binding through the N-terminal kinase inhibitory region as well as SH2 domain. *Genes Cells* **4**, 339-351 (1999).
174. Schmitz, J., Weissenbach, M., Haan, S., Heinrich, P.C. & Schaper, F. SOCS3 exerts its inhibitory function on interleukin-6 signal transduction through the SHP2 recruitment site of gp130. *J Biol Chem* **275**, 12848-12856 (2000).
175. Nicholson, S.E., De Souza, D., Fabri, L.J., Corbin, J., Willson, T.A., Zhang, J.G., Silva, A., Asimakis, M., Farley, A., Nash, A.D. *et al.* Suppressor of cytokine signaling-3 preferentially binds to the SHP-2-binding site on the shared cytokine receptor subunit gp130. *Proc Natl Acad Sci U S A* **97**, 6493-6498 (2000).
176. Eyckerman, S., Broekaert, D., Verhee, A., Vandekerckhove, J. & Tavernier, J. Identification of the Y985 and Y1077 motifs as SOCS3 recruitment sites in the murine leptin receptor. *FEBS Lett* **486**, 33-37 (2000).
177. Bjorbak, C., Lavery, H.J., Bates, S.H., Olson, R.K., Davis, S.M., Flier, J.S. & Myers, M.G., Jr. SOCS3 mediates feedback inhibition of the leptin receptor via Tyr985. *J Biol Chem* **275**, 40649-40657 (2000).
178. Hortner, M., Nielsch, U., Mayr, L.M., Johnston, J.A., Heinrich, P.C. & Haan, S. Suppressor of cytokine signaling-3 is recruited to the activated granulocyte-colony stimulating factor receptor and modulates its signal transduction. *J Immunol* **169**, 1219-1227 (2002).
179. Hortner, M., Nielsch, U., Mayr, L.M., Heinrich, P.C. & Haan, S. A new high affinity binding site for suppressor of cytokine signaling-3 on the erythropoietin receptor. *Eur J Biochem* **269**, 2516-2526 (2002).
180. Johnston, J.A. Are SOCS suppressors, regulators, and degraders? *J Leukoc Biol* **75**, 743-748 (2004).
181. Chung, C.D., Liao, J., Liu, B., Rao, X., Jay, P., Berta, P. & Shuai, K. Specific inhibition of Stat3 signal transduction by PIAS3. *Science* **278**, 1803-1805 (1997).
182. Liu, B., Liao, J., Rao, X., Kushner, S.A., Chung, C.D., Chang, D.D. & Shuai, K. Inhibition of Stat1-mediated gene activation by PIAS1. *Proc Natl Acad Sci U S A* **95**, 10626-10631 (1998).
183. Forrester, J.S., Wyatt, H.L., Da Luz, P.L., Tyberg, J.V., Diamond, G.A. & Swan, H.J. Functional significance of regional ischemic contraction abnormalities. *Circulation* **54**, 64-70 (1976).
184. Haghikia, A., Stapel, B., Hoch, M. & Hilfiker-Kleiner, D. STAT3 and cardiac remodeling. *Heart Fail Rev* **16**, 35-47 (2011).
185. Soonpaa, M.H. & Field, L.J. Survey of studies examining mammalian cardiomyocyte DNA synthesis. *Circ Res* **83**, 15-26 (1998).

186. Wakatsuki, T., Schlessinger, J. & Elson, E.L. The biochemical response of the heart to hypertension and exercise. *Trends Biochem Sci* **29**, 609-617 (2004).
187. Whelan, R.S., Kaplinskiy, V. & Kitsis, R.N. Cell death in the pathogenesis of heart disease: mechanisms and significance. *Annu Rev Physiol* **72**, 19-44 (2010).
188. Cokkinos, D.V. & Pantos, C. Myocardial remodeling, an overview. *Heart Fail Rev* **16**, 1-4 (2011).
189. Shahbaz, A.U., Sun, Y., Bhattacharya, S.K., Ahokas, R.A., Gerling, I.C., McGee, J.E. & Weber, K.T. Fibrosis in hypertensive heart disease: molecular pathways and cardioprotective strategies. *J Hypertens* **28 Suppl 1**, S25-32 (2010).
190. Sheng, Z., Pennica, D., Wood, W.I. & Chien, K.R. Cardiotrophin-1 displays early expression in the murine heart tube and promotes cardiac myocyte survival. *Development* **122**, 419-428 (1996).
191. Fischer, P. & Hilfiker-Kleiner, D. Survival pathways in hypertrophy and heart failure: the gp130-STAT axis. *Basic Res Cardiol* **102**, 393-411 (2007).
192. Hilfiker-Kleiner, D., Hilfiker, A. & Drexler, H. Many good reasons to have STAT3 in the heart. *Pharmacol Ther* **107**, 131-137 (2005).
193. Boengler, K., Hilfiker-Kleiner, D., Drexler, H., Heusch, G. & Schulz, R. The myocardial JAK/STAT pathway: from protection to failure. *Pharmacol Ther* **120**, 172-185 (2008).
194. Wollert, K.C. & Chien, K.R. Cardiotrophin-1 and the role of gp130-dependent signaling pathways in cardiac growth and development. *J Mol Med (Berl)* **75**, 492-501 (1997).
195. Wollert, K.C., Taga, T., Saito, M., Narazaki, M., Kishimoto, T., Glembotski, C.C., Vernallis, A.B., Heath, J.K., Pennica, D., Wood, W.I. *et al.* Cardiotrophin-1 activates a distinct form of cardiac muscle cell hypertrophy. Assembly of sarcomeric units in series VIA gp130/leukemia inhibitory factor receptor-dependent pathways. *J Biol Chem* **271**, 9535-9545 (1996).
196. Wang, F., Seta, Y., Baumgarten, G., Engel, D.J., Sivasubramanian, N. & Mann, D.L. Functional significance of hemodynamic overload-induced expression of leukemia-inhibitory factor in the adult mammalian heart. *Circulation* **103**, 1296-1302 (2001).
197. Ancey, C., Menet, E., Corbi, P., Fredj, S., Garcia, M., Rucker-Martin, C., Bescond, J., Morel, F., Wijdenes, J., Lecron, J.C. *et al.* Human cardiomyocyte hypertrophy induced in vitro by gp130 stimulation. *Cardiovasc Res* **59**, 78-85 (2003).
198. Kubin, T., Poling, J., Kostin, S., Gajawada, P., Hein, S., Rees, W., Wietelmann, A., Tanaka, M., Lorchner, H., Schimanski, S. *et al.* Oncostatin M is a major mediator of cardiomyocyte dedifferentiation and remodeling. *Cell Stem Cell* **9**, 420-432 (2011).
199. Hirota, H., Yoshida, K., Kishimoto, T. & Taga, T. Continuous activation of gp130, a signal-transducing receptor component for interleukin 6-related cytokines, causes myocardial hypertrophy in mice. *Proc Natl Acad Sci U S A* **92**, 4862-4866 (1995).
200. Melendez, G.C., McLarty, J.L., Levick, S.P., Du, Y., Janicki, J.S. & Brower, G.L. Interleukin 6 mediates myocardial fibrosis, concentric hypertrophy, and diastolic dysfunction in rats. *Hypertension* **56**, 225-231 (2010).
201. Pennica, D., King, K.L., Shaw, K.J., Luis, E., Rullamas, J., Luoh, S.M., Darbonne, W.C., Knutzon, D.S., Yen, R., Chien, K.R. *et al.* Expression cloning of cardiotrophin 1, a cytokine that induces cardiac myocyte hypertrophy. *Proc Natl Acad Sci U S A* **92**, 1142-1146 (1995).
202. Rattazzi, M., Puato, M., Faggin, E., Bertipaglia, B., Zambon, A. & Pauletto, P. C-reactive protein and interleukin-6 in vascular disease: culprits or passive bystanders? *J Hypertens* **21**, 1787-1803 (2003).
203. Tsutamoto, T., Hisanaga, T., Wada, A., Maeda, K., Ohnishi, M., Fukai, D., Mabuchi, N., Sawaki, M. & Kinoshita, M. Interleukin-6 spillover in the peripheral circulation increases with the severity of heart failure, and the high plasma level of interleukin-6 is an important prognostic predictor in patients with congestive heart failure. *J Am Coll Cardiol* **31**, 391-398 (1998).
204. Buzas, K., Megyeri, K., Hogye, M., Csanady, M., Bogats, G. & Mandi, Y. Comparative study of the roles of cytokines and apoptosis in dilated and hypertrophic cardiomyopathies. *Eur Cytokine Netw* **15**, 53-59 (2004).
205. Roig, E., Orus, J., Pare, C., Azqueta, M., Filella, X., Perez-Villa, F., Heras, M. & Sanz, G. Serum interleukin-6 in congestive heart failure secondary to idiopathic dilated cardiomyopathy. *Am J Cardiol* **82**, 688-690, A688 (1998).
206. Maeda, K., Tsutamoto, T., Wada, A., Mabuchi, N., Hayashi, M., Tsutsui, T., Ohnishi, M., Sawaki, M., Fujii, M., Matsumoto, T. *et al.* High levels of plasma brain natriuretic peptide and interleukin-6 after optimized treatment for heart failure are independent risk factors for morbidity and mortality in patients with congestive heart failure. *J Am Coll Cardiol* **36**, 1587-1593 (2000).

207. Orus, J., Roig, E., Perez-Villa, F., Pare, C., Azqueta, M., Filella, X., Heras, M. & Sanz, G. Prognostic value of serum cytokines in patients with congestive heart failure. *J Heart Lung Transplant* **19**, 419-425 (2000).
208. Birks, E.J., Latif, N., Owen, V., Bowles, C., Felkin, L.E., Mullen, A.J., Khaghani, A., Barton, P.J., Polak, J.M., Pepper, J.R. *et al.* Quantitative myocardial cytokine expression and activation of the apoptotic pathway in patients who require left ventricular assist devices. *Circulation* **104**, I233-240 (2001).
209. Fuchs, M., Hilfiker, A., Kaminski, K., Hilfiker-Kleiner, D., Guener, Z., Klein, G., Podewski, E., Schieffer, B., Rose-John, S. & Drexler, H. Role of interleukin-6 for LV remodeling and survival after experimental myocardial infarction. *FASEB J* **17**, 2118-2120 (2003).
210. Hirota, H., Izumi, M., Hamaguchi, T., Sugiyama, S., Murakami, E., Kunisada, K., Fujio, Y., Oshima, Y., Nakaoka, Y. & Yamauchi-Takihara, K. Circulating interleukin-6 family cytokines and their receptors in patients with congestive heart failure. *Heart Vessels* **19**, 237-241 (2004).
211. Podewski, E.K., Hilfiker-Kleiner, D., Hilfiker, A., Morawietz, H., Lichtenberg, A., Wollert, K.C. & Drexler, H. Alterations in Janus kinase (JAK)-signal transducers and activators of transcription (STAT) signaling in patients with end-stage dilated cardiomyopathy. *Circulation* **107**, 798-802 (2003).
212. Zolk, O., Ng, L.L., O'Brien, R.J., Weyand, M. & Eschenhagen, T. Augmented Expression of Cardiotrophin-1 in Failing Human Hearts Is Accompanied by Diminished Glycoprotein 130 Receptor Protein Abundance. *Circulation* **106**, 1442-1446 (2002).
213. Hirano, T., Nakajima, K. & Hibi, M. Signaling mechanisms through gp130: a model of the cytokine system. *Cytokine Growth Factor Rev* **8**, 241-252 (1997).
214. Hirota, H., Chen, J., Betz, U.A., Rajewsky, K., Gu, Y., Ross, J., Jr., Muller, W. & Chien, K.R. Loss of a gp130 cardiac muscle cell survival pathway is a critical event in the onset of heart failure during biomechanical stress. *Cell* **97**, 189-198 (1999).
215. Funamoto, M., Fujio, Y., Kunisada, K., Negoro, S., Tone, E., Osugi, T., Hirota, H., Izumi, M., Yoshizaki, K., Walsh, K. *et al.* Signal transducer and activator of transcription 3 is required for glycoprotein 130-mediated induction of vascular endothelial growth factor in cardiac myocytes. *J Biol Chem* **275**, 10561-10566 (2000).
216. Oh, H., Fujio, Y., Kunisada, K., Hirota, H., Matsui, H., Kishimoto, T. & Yamauchi-Takihara, K. Activation of phosphatidylinositol 3-kinase through glycoprotein 130 induces protein kinase B and p70 S6 kinase phosphorylation in cardiac myocytes. *J Biol Chem* **273**, 9703-9710 (1998).
217. Nakaoka, Y., Nishida, K., Fujio, Y., Izumi, M., Terai, K., Oshima, Y., Sugiyama, S., Matsuda, S., Koyasu, S., Yamauchi-Takihara, K. *et al.* Activation of gp130 transduces hypertrophic signal through interaction of scaffolding/docking protein Gab1 with tyrosine phosphatase SHP2 in cardiomyocytes. *Circ Res* **93**, 221-229 (2003).
218. Takahashi, N., Saito, Y., Kuwahara, K., Harada, M., Tanimoto, K., Nakagawa, Y., Kawakami, R., Nakanishi, M., Yasuno, S., Usami, S. *et al.* Hypertrophic responses to cardiotrophin-1 are not mediated by STAT3, but via a MEK5-ERK5 pathway in cultured cardiomyocytes. *J Mol Cell Cardiol* **38**, 185-192 (2005).
219. Florholmen, G., Aas, V., Rustan, A.C., Lunde, P.K., Straumann, N., Eid, H., Odegaard, A., Dishington, H., Andersson, K.B. & Christensen, G. Leukemia inhibitory factor reduces contractile function and induces alterations in energy metabolism in isolated cardiomyocytes. *J Mol Cell Cardiol* **37**, 1183-1193 (2004).
220. Florholmen, G., Andersson, K.B., Yndestad, A., Austbo, B., Henriksen, U.L. & Christensen, G. Leukaemia inhibitory factor alters expression of genes involved in rat cardiomyocyte energy metabolism. *Acta Physiol Scand* **180**, 133-142 (2004).
221. Kurdi, M. & Booz, G.W. Evidence that IL-6-type cytokine signaling in cardiomyocytes is inhibited by oxidative stress: parthenolide targets JAK1 activation by generating ROS. *J Cell Physiol* **212**, 424-431 (2007).
222. Chin, B.S., Blann, A.D., Gibbs, C.R., Chung, N.A., Conway, D.G. & Lip, G.Y. Prognostic value of interleukin-6, plasma viscosity, fibrinogen, von Willebrand factor, tissue factor and vascular endothelial growth factor levels in congestive heart failure. *Eur J Clin Invest* **33**, 941-948 (2003).
223. Negoro, S., Kunisada, K., Tone, E., Funamoto, M., Oh, H., Kishimoto, T. & Yamauchi-Takihara, K. Activation of JAK/STAT pathway transduces cytoprotective signal in rat acute myocardial infarction. *Cardiovasc Res* **47**, 797-805 (2000).
224. Yamauchi-Takihara, K. & Kishimoto, T. A novel role for STAT3 in cardiac remodeling. *Trends Cardiovasc Med* **10**, 298-303 (2000).
225. Jacoby, J.J., Kalinowski, A., Liu, M.G., Zhang, S.S., Gao, Q., Chai, G.X., Ji, L., Iwamoto, Y., Li, E., Schneider, M. *et al.* Cardiomyocyte-restricted knockout of STAT3 results in higher

sensitivity to inflammation, cardiac fibrosis, and heart failure with advanced age. *Proc Natl Acad Sci U S A* **100**, 12929-12934 (2003).
226. Hilfiker-Kleiner, D., Hilfiker, A., Fuchs, M., Kaminski, K., Schaefer, A., Schieffer, B., Hillmer, A., Schmiedl, A., Ding, Z., Podewski, E. *et al.* Signal transducer and activator of transcription 3 is required for myocardial capillary growth, control of interstitial matrix deposition, and heart protection from ischemic injury. *Circ Res* **95**, 187-195 (2004).
227. Kunisada, K., Tone, E., Fujio, Y., Matsui, H., Yamauchi-Takihara, K. & Kishimoto, T. Activation of gp130 Transduces Hypertrophic Signals via STAT3 in Cardiac Myocytes. *Circulation* **98**, 346-352 (1998).
228. Yajima, T., Yasukawa, H., Jeon, E.S., Xiong, D., Dorner, A., Iwatate, M., Nara, M., Zhou, H., Summers-Torres, D., Hoshijima, M. *et al.* Innate defense mechanism against virus infection within the cardiac myocyte requiring gp130-STAT3 signaling. *Circulation* **114**, 2364-2373 (2006).
229. Tanaka, T., Kanda, T., McManus, B.M., Kanai, H., Akiyama, H., Sekiguchi, K., Yokoyama, T. & Kurabayashi, M. Overexpression of interleukin-6 aggravates viral myocarditis: impaired increase in tumor necrosis factor-alpha. *J Mol Cell Cardiol* **33**, 1627-1635 (2001).
230. Matsushita, K., Iwanaga, S., Oda, T., Kimura, K., Shimada, M., Sano, M., Umezawa, A., Hata, J. & Ogawa, S. Interleukin-6/soluble interleukin-6 receptor complex reduces infarct size via inhibiting myocardial apoptosis. *Lab Invest* **85**, 1210-1223 (2005).
231. Ramji, D.P. & Foka, P. CCAAT/enhancer-binding proteins: structure, function and regulation. *Biochem J* **365**, 561-575 (2002).
232. Akira, S., Isshiki, H., Sugita, T., Tanabe, O., Kinoshita, S., Nishio, Y., Nakajima, T., Hirano, T. & Kishimoto, T. A nuclear factor for IL-6 expression (NF-IL6) is a member of a C/EBP family. *EMBO J* **9**, 1897-1906 (1990).
233. Poli, V., Mancini, F.P. & Cortese, R. IL-6DBP, a nuclear protein involved in interleukin-6 signal transduction, defines a new family of leucine zipper proteins related to C/EBP. *Cell* **63**, 643-653 (1990).
234. Descombes, P. & Schibler, U. A liver-enriched transcriptional activator protein, LAP, and a transcriptional inhibitory protein, LIP, are translated from the same mRNA. *Cell* **67**, 569-579 (1991).
235. Kinoshita, S., Akira, S. & Kishimoto, T. A member of the C/EBP family, NF-IL6 beta, forms a heterodimer and transcriptionally synergizes with NF-IL6. *Proc Natl Acad Sci U S A* **89**, 1473-1476 (1992).
236. Niehof, M., Streetz, K., Rakemann, T., Bischoff, S.C., Manns, M.P., Horn, F. & Trautwein, C. Interleukin-6-induced tethering of STAT3 to the LAP/C/EBPbeta promoter suggests a new mechanism of transcriptional regulation by STAT3. *J Biol Chem* **276**, 9016-9027 (2001).
237. Hutt, J.A., O'Rourke, J.P. & DeWille, J. Signal transducer and activator of transcription 3 activates CCAAT enhancer-binding protein delta gene transcription in G0 growth-arrested mouse mammary epithelial cells and in involuting mouse mammary gland. *J Biol Chem* **275**, 29123-29131 (2000).
238. Sabatakos, G., Davies, G.E., Grosse, M., Cryer, A. & Ramji, D.P. Expression of the genes encoding CCAAT-enhancer binding protein isoforms in the mouse mammary gland during lactation and involution. *Biochem J* **334 (Pt 1)**, 205-210 (1998).
239. Yamada, T., Tobita, K., Osada, S., Nishihara, T. & Imagawa, M. CCAAT/enhancer-binding protein delta gene expression is mediated by APRF/STAT3. *J Biochem* **121**, 731-738 (1997).
240. Cantwell, C.A., Sterneck, E. & Johnson, P.F. Interleukin-6-specific activation of the C/EBPdelta gene in hepatocytes is mediated by Stat3 and Sp1. *Mol Cell Biol* **18**, 2108-2117 (1998).
241. Ramji, D.P., Vitelli, A., Tronche, F., Cortese, R. & Ciliberto, G. The two C/EBP isoforms, IL-6DBP/NF-IL6 and C/EBP delta/NF-IL6 beta, are induced by IL-6 to promote acute phase gene transcription via different mechanisms. *Nucleic Acids Res* **21**, 289-294 (1993).
242. Yamada, T., Tsuchiya, T., Osada, S., Nishihara, T. & Imagawa, M. CCAAT/enhancer-binding protein delta gene expression is mediated by autoregulation through downstream binding sites. *Biochem Biophys Res Commun* **242**, 88-92 (1998).
243. O'Rourke, J.P., Hutt, J.A. & DeWille, J. Transcriptional regulation of C/EBPdelta in G(0) growth-arrested mouse mammary epithelial cells. *Biochem Biophys Res Commun* **262**, 696-701 (1999).
244. Zhu, S., Yoon, K., Sterneck, E., Johnson, P.F. & Smart, R.C. CCAAT/enhancer binding protein-beta is a mediator of keratinocyte survival and skin tumorigenesis involving oncogenic Ras signaling. *Proc Natl Acad Sci U S A* **99**, 207-212 (2002).
245. Nakajima, T., Kinoshita, S., Sasagawa, T., Sasaki, K., Naruto, M., Kishimoto, T. & Akira, S. Phosphorylation at threonine-235 by a ras-dependent mitogen-activated protein kinase

cascade is essential for transcription factor NF-IL6. *Proc Natl Acad Sci U S A* **90**, 2207-2211 (1993).
246. Trautwein, C., Caelles, C., van der Geer, P., Hunter, T., Karin, M. & Chojkier, M. Transactivation by NF-IL6/LAP is enhanced by phosphorylation of its activation domain. *Nature* **364**, 544-547 (1993).
247. Wegner, M., Cao, Z. & Rosenfeld, M.G. Calcium-regulated phosphorylation within the leucine zipper of C/EBP beta. *Science* **256**, 370-373 (1992).
248. Trautwein, C., van der Geer, P., Karin, M., Hunter, T. & Chojkier, M. Protein kinase A and C site-specific phosphorylations of LAP (NF-IL6) modulate its binding affinity to DNA recognition elements. *J Clin Invest* **93**, 2554-2561 (1994).
249. Ray, A. & Ray, B.K. Serum amyloid A gene expression under acute-phase conditions involves participation of inducible C/EBP-beta and C/EBP-delta and their activation by phosphorylation. *Mol Cell Biol* **14**, 4324-4332 (1994).
250. LeClair, K.P., Blanar, M.A. & Sharp, P.A. The p50 subunit of NF-kappa B associates with the NF-IL6 transcription factor. *Proc Natl Acad Sci U S A* **89**, 8145-8149 (1992).
251. Vallejo, M., Ron, D., Miller, C.P. & Habener, J.F. C/ATF, a member of the activating transcription factor family of DNA-binding proteins, dimerizes with CAAT/enhancer-binding proteins and directs their binding to cAMP response elements. *Proc Natl Acad Sci U S A* **90**, 4679-4683 (1993).
252. Hsu, W., Kerppola, T.K., Chen, P.L., Curran, T. & Chen-Kiang, S. Fos and Jun repress transcription activation by NF-IL6 through association at the basic zipper region. *Mol Cell Biol* **14**, 268-276 (1994).
253. Weiergraber, O., Hemmann, U., Kuster, A., Muller-Newen, G., Schneider, J., Rose-John, S., Kurschat, P., Brakenhoff, J.P., Hart, M.H., Stabel, S. *et al.* Soluble human interleukin-6 receptor. Expression in insect cells, purification and characterization. *Eur J Biochem* **234**, 661-669 (1995).
254. Vernallis, A.B., Hudson, K.R. & Heath, J.K. An antagonist for the leukemia inhibitory factor receptor inhibits leukemia inhibitory factor, cardiotrophin-1, ciliary neurotrophic factor, and oncostatin M. *J Biol Chem* **272**, 26947-26952 (1997).
255. Haan, C., Rolvering, C., Raulf, F., Kapp, M., Druckes, P., Thoma, G., Behrmann, I. & Zerwes, H.G. Jak1 has a dominant role over Jak3 in signal transduction through gammac-containing cytokine receptors. *Chem Biol* **18**, 314-323 (2011).
256. Deller, M.C., Hudson, K.R., Ikemizu, S., Bravo, J., Jones, E.Y. & Heath, J.K. Crystal structure and functional dissection of the cytostatic cytokine oncostatin M. *Structure* **8**, 863-874 (2000).
257. Jentzsch, C., Leierseder, S., Loyer, X., Flohrschutz, I., Sassi, Y., Hartmann, D., Thum, T., Laggerbauer, B. & Engelhardt, S. A phenotypic screen to identify hypertrophy-modulating microRNAs in primary cardiomyocytes. *J Mol Cell Cardiol* **52**, 13-20 (2012).
258. Pfaffl, M.W. A new mathematical model for relative quantification in real-time RT-PCR. *Nucleic Acids Res* **29**, e45 (2001).
259. Laemmli, U.K. Cleavage of structural proteins during the assembly of the head of bacteriophage T4. *Nature* **227**, 680-685 (1970).
260. Sano, M., Fukuda, K., Kodama, H., Pan, J., Saito, M., Matsuzaki, J., Takahashi, T., Makino, S., Kato, T. & Ogawa, S. Interleukin-6 family of cytokines mediate angiotensin II-induced cardiac hypertrophy in rodent cardiomyocytes. *J Biol Chem* **275**, 29717-29723 (2000).
261. Chiu, C.P., Moulds, C., Coffman, R.L., Rennick, D. & Lee, F. Multiple biological activities are expressed by a mouse interleukin 6 cDNA clone isolated from bone marrow stromal cells. *Proc Natl Acad Sci U S A* **85**, 7099-7103 (1988).
262. Pennica, D., Swanson, T.A., Shaw, K.J., Kuang, W.J., Gray, C.L., Beatty, B.G. & Wood, W.I. Human cardiotrophin-1: protein and gene structure, biological and binding activities, and chromosomal localization, in *Cytokine*, Vol. 8 183-189 (1996).
263. Paradis, P., Dali-Youcef, N., Paradis, F.W., Thibault, G. & Nemer, M. Overexpression of angiotensin II type I receptor in cardiomyocytes induces cardiac hypertrophy and remodeling. *Proc Natl Acad Sci U S A* **97**, 931-936 (2000).
264. Suzuki, J., Matsubara, H., Urakami, M. & Inada, M. Rat angiotensin II (type 1A) receptor mRNA regulation and subtype expression in myocardial growth and hypertrophy. *Circ Res* **73**, 439-447 (1993).
265. Fujii, N., Tanaka, M., Ohnishi, J., Yukawa, K., Takimoto, E., Shimada, S., Naruse, M., Sugiyama, F., Yagami, K., Murakami, K. *et al.* Alterations of angiotensin II receptor contents in hypertrophied hearts. *Biochem Biophys Res Commun* **212**, 326-333 (1995).
266. Nio, Y., Matsubara, H., Murasawa, S., Kanasaki, M. & Inada, M. Regulation of gene transcription of angiotensin II receptor subtypes in myocardial infarction. *J Clin Invest* **95**, 46-54 (1995).

267. Frey, N., Katus, H.A., Olson, E.N. & Hill, J.A. Hypertrophy of the heart: a new therapeutic target? *Circulation* **109**, 1580-1589 (2004).
268. Kunisada, K., Negoro, S., Tone, E., Funamoto, M., Osugi, T., Yamada, S., Okabe, M., Kishimoto, T. & Yamauchi-Takihara, K. Signal transducer and activator of transcription 3 in the heart transduces not only a hypertrophic signal but a protective signal against doxorubicin-induced cardiomyopathy. *Proc Natl Acad Sci U S A* **97**, 315-319 (2000).
269. Frey, N. & Olson, E.N. Cardiac hypertrophy: the good, the bad, and the ugly. *Annu Rev Physiol* **65**, 45-79 (2003).
270. Simpson, P., McGrath, A. & Savion, S. Myocyte hypertrophy in neonatal rat heart cultures and its regulation by serum and by catecholamines. *Circ Res* **51**, 787-801 (1982).
271. Kimes, B.W. & Brandt, B.L. Properties of a clonal muscle cell line from rat heart. *Exp Cell Res* **98**, 367-381 (1976).
272. Claycomb, W.C., Lanson, N.A., Jr., Stallworth, B.S., Egeland, D.B., Delcarpio, J.B., Bahinski, A. & Izzo, N.J., Jr. HL-1 cells: a cardiac muscle cell line that contracts and retains phenotypic characteristics of the adult cardiomyocyte. *Proc Natl Acad Sci U S A* **95**, 2979-2984 (1998).
273. Davidson, M.M., Nesti, C., Palenzuela, L., Walker, W.F., Hernandez, E., Protas, L., Hirano, M. & Isaac, N.D. Novel cell lines derived from adult human ventricular cardiomyocytes. *J Mol Cell Cardiol* **39**, 133-147 (2005).
274. Landstrom, A.P., Kellen, C.A., Dixit, S.S., van Oort, R.J., Garbino, A., Weisleder, N., Ma, J., Wehrens, X.H. & Ackerman, M.J. Junctophilin-2 expression silencing causes cardiocyte hypertrophy and abnormal intracellular calcium-handling. *Circ Heart Fail* **4**, 214-223 (2011).
275. Watkins, S.J., Borthwick, G.M. & Arthur, H.M. The H9C2 cell line and primary neonatal cardiomyocyte cells show similar hypertrophic responses in vitro. *In Vitro Cell Dev Biol Anim* **47**, 125-131 (2011).
276. Hescheler, J., Meyer, R., Plant, S., Krautwurst, D., Rosenthal, W. & Schultz, G. Morphological, biochemical, and electrophysiological characterization of a clonal cell (H9c2) line from rat heart. *Circ Res* **69**, 1476-1486 (1991).
277. Conrad, C. & Gerlich, D.W. Automated microscopy for high-content RNAi screening. *J Cell Biol* **188**, 453-461 (2010).
278. Krausz, E. High-content siRNA screening. *Mol Biosyst* **3**, 232-240 (2007).
279. Lam, L.T., Lu, X., Zhang, H., Lesniewski, R., Rosenberg, S. & Semizarov, D. A microRNA screen to identify modulators of sensitivity to BCL2 inhibitor ABT-263 (navitoclax). *Mol Cancer Ther* **9**, 2943-2950 (2010).
280. Santhakumar, D., Forster, T., Laqtom, N.N., Fragkoudis, R., Dickinson, P., Abreu-Goodger, C., Manakov, S.A., Choudhury, N.R., Griffiths, S.J., Vermeulen, A. *et al.* Combined agonist-antagonist genome-wide functional screening identifies broadly active antiviral microRNAs. *Proc Natl Acad Sci U S A* **107**, 13830-13835 (2010).
281. Zhang, C.G., Jia, Z.Q., Li, B.H., Zhang, H., Liu, Y.N., Chen, P., Ma, K.T. & Zhou, C.Y. beta-Catenin/TCF/LEF1 can directly regulate phenylephrine-induced cell hypertrophy and Anf transcription in cardiomyocytes. *Biochem Biophys Res Commun* **390**, 258-262 (2009).
282. Cao, D.J., Wang, Z.V., Battiprolu, P.K., Jiang, N., Morales, C.R., Kong, Y., Rothermel, B.A., Gillette, T.G. & Hill, J.A. Histone deacetylase (HDAC) inhibitors attenuate cardiac hypertrophy by suppressing autophagy. *Proc Natl Acad Sci U S A* **108**, 4123-4128 (2011).
283. Usui, S., Maejima, Y., Pain, J., Hong, C., Cho, J., Park, J.Y., Zablocki, D., Tian, B., Glass, D.J. & Sadoshima, J. Endogenous muscle atrophy F-box mediates pressure overload-induced cardiac hypertrophy through regulation of nuclear factor-kappaB. *Circ Res* **109**, 161-171 (2011).
284. Kodama, H., Fukuda, K., Pan, J., Makino, S., Baba, A., Hori, S. & Ogawa, S. Leukemia Inhibitory Factor, a Potent Cardiac Hypertrophic Cytokine, Activates the JAK/STAT Pathway in Rat Cardiomyocytes. *Circ Res* **81**, 656-663 (1997).
285. Matsui, H., Fujio, Y., Kunisada, K., Hirota, H. & Yamauchi-Takihara, K. Leukemia inhibitory factor induces a hypertrophic response mediated by gp130 in murine cardiac myocytes. *Res Commun Mol Pathol Pharmacol* **93**, 149-162 (1996).
286. Huyton, T., Zhang, J.G., Luo, C.S., Lou, M.Z., Hilton, D.J., Nicola, N.A. & Garrett, T.P. An unusual cytokine:Ig-domain interaction revealed in the crystal structure of leukemia inhibitory factor (LIF) in complex with the LIF receptor. *Proc Natl Acad Sci U S A* **104**, 12737-12742 (2007).
287. Kuwahara, K., Saito, Y., Harada, M., Ishikawa, M., Ogawa, E., Miyamoto, Y., Hamanaka, I., Kamitani, S., Kajiyama, N., Takahashi, N. *et al.* Involvement of cardiotrophin-1 in cardiac myocyte-nonmyocyte interactions during hypertrophy of rat cardiac myocytes in vitro. *Circulation* **100**, 1116-1124 (1999).

288. Nakaoka, Y., Shioyama, W., Kunimoto, S., Arita, Y., Higuchi, K., Yamamoto, K., Fujio, Y., Nishida, K., Kuroda, T., Hirota, H. *et al.* SHP2 mediates gp130-dependent cardiomyocyte hypertrophy via negative regulation of skeletal alpha-actin gene. *J Mol Cell Cardiol* **49**, 157-164 (2010).
289. Nicol, R.L., Frey, N., Pearson, G., Cobb, M., Richardson, J. & Olson, E.N. Activated MEK5 induces serial assembly of sarcomeres and eccentric cardiac hypertrophy. *EMBO J* **20**, 2757-2767 (2001).
290. Poling, J., Gajawada, P., Lorchner, H., Polyakowa, V., Szibor, M., Bottger, T., Warnecke, H., Kubin, T. & Braun, T. The Janus face of OSM-mediated cardiomyocyte dedifferentiation during cardiac repair and disease. *Cell Cycle* **11**, 439-445 (2012).
291. Mascareno, E., El-Shafei, M., Maulik, N., Sato, M., Guo, Y., Das, D.K. & Siddiqui, M.A. JAK/STAT signaling is associated with cardiac dysfunction during ischemia and reperfusion. *Circulation* **104**, 325-329 (2001).
292. Fukuzawa, J., Booz, G.W., Hunt, R.A., Shimizu, N., Karoor, V., Baker, K.M. & Dostal, D.E. Cardiotrophin-1 increases angiotensinogen mRNA in rat cardiac myocytes through STAT3 : an autocrine loop for hypertrophy. *Hypertension* **35**, 1191-1196 (2000).
293. Nemoto, S., Sheng, Z. & Lin, A. Opposing effects of Jun kinase and p38 mitogen-activated protein kinases on cardiomyocyte hypertrophy. *Mol Cell Biol* **18**, 3518-3526 (1998).
294. Rose-John, S., Waetzig, G.H., Scheller, J., Grotzinger, J. & Seegert, D. The IL-6/sIL-6R complex as a novel target for therapeutic approaches. *Expert Opin Ther Targets* **11**, 613-624 (2007).
295. Ancey, C., Corbi, P., Froger, J., Delwail, A., Wijdenes, J., Gascan, H., Potreau, D. & Lecron, J.C. Secretion of IL-6, IL-11 and LIF by human cardiomyocytes in primary culture. *Cytokine* **18**, 199-205 (2002).
296. Coles, B., Fielding, C.A., Rose-John, S., Scheller, J., Jones, S.A. & O'Donnell, V.B. Classic interleukin-6 receptor signaling and interleukin-6 trans-signaling differentially control angiotensin II-dependent hypertension, cardiac signal transducer and activator of transcription-3 activation, and vascular hypertrophy in vivo. *Am J Pathol* **171**, 315-325 (2007).
297. Kaminski, K.A., Dziemidowicz, M., Litvinovich, S., Bonda, T., Ptaszynska, K., Kozuch, M., Taranta, A., Musial, W.J. & Winnicka, M.M. Interleukin 6 is not necessary for STAT3 phosphorylation and myocardial hypertrophy following short term beta-adrenergic stimulation. *Adv Med Sci* **57**, 94-99 (2012).
298. Szabo-Fresnais, N., Lefebvre, F., Germain, A., Fischmeister, R. & Pomerance, M. A new regulation of IL-6 production in adult cardiomyocytes by beta-adrenergic and IL-1 beta receptors and induction of cellular hypertrophy by IL-6 trans-signalling. *Cell Signal* **22**, 1143-1152 (2010).
299. Ng, D.C., Long, C.S. & Bogoyevitch, M.A. A role for the extracellular signal-regulated kinase and p38 mitogen-activated protein kinases in interleukin-1 beta-stimulated delayed signal tranducer and activator of transcription 3 activation, atrial natriuretic factor expression, and cardiac myocyte morphology. *J Biol Chem* **276**, 29490-29498 (2001).
300. Cichy, J., Rose-John, S., Potempa, J., Pryjma, J. & Travis, J. Oncostatin M stimulates the expression and release of the IL-6 receptor in human hepatoma HepG2 cells. *J Immunol* **159**, 5648-5653 (1997).
301. Mackey, S.L. & Darlington, G.J. CCAAT enhancer-binding protein alpha is required for interleukin-6 receptor alpha signaling in newborn hepatocytes. *J Biol Chem* **279**, 16206-16213 (2004).
302. Smyth, D.C., Kerr, C. & Richards, C.D. Oncostatin M-induced IL-6 expression in murine fibroblasts requires the activation of protein kinase Cdelta. *J Immunol* **177**, 8740-8747 (2006).
303. Kiyoshi, M., Atsumasa, K., Takafumi, T., Yumi, M., Yasumori, I., Yuka, J., Taiichiro, M., Minoru, N., Satoru, M. & Hiromi, I. CP690,550 inhibits oncostatin M-induced JAK/STAT signaling pathway in rheumatoid synoviocytes. *Arthritis Res Ther* **13** (2011).
304. Bernard, C., Merval, R., Lebret, M., Delerive, P., Dusanter-Fourt, I., Lehoux, S., Créminon, C., Staels, B., Maclouf, J. & Tedgui, A. Oncostatin M Induces Interleukin-6 and Cyclooxygenase-2 Expression in Human Vascular Smooth Muscle Cells : Synergy With Interleukin-1ß. *Circ Res* **85**, 1124-1131 (1999).
305. Brown, T.J., Rowe, J.M., Liu, J.W. & Shoyab, M. Regulation of IL-6 expression by oncostatin M. *J Immunol* **147**, 2175-2180 (1991).
306. Van Wagoner, N.J., Choi, C., Repovic, P. & Benveniste, E.N. Oncostatin M regulation of interleukin-6 expression in astrocytes: biphasic regulation involving the mitogen-activated protein kinases ERK1/2 and p38. *J Neurochem* **75**, 563-575 (2000).
307. Van Wagoner, N.J. & Benveniste, E.N. Interleukin-6 expression and regulation in astrocytes. *J Neuroimmunol* **100**, 124-139 (1999).

308. Van Wagoner, N.J., Oh, J.W., Repovic, P. & Benveniste, E.N. Interleukin-6 (IL-6) production by astrocytes: autocrine regulation by IL-6 and the soluble IL-6 receptor. *J Neurosci* **19**, 5236-5244 (1999).
309. Oh, J.W., Van Wagoner, N.J., Rose-John, S. & Benveniste, E.N. Role of IL-6 and the soluble IL-6 receptor in inhibition of VCAM-1 gene expression. *J Immunol* **161**, 4992-4999 (1998).
310. Hutt, J.A. & DeWille, J.W. Oncostatin M induces growth arrest of mammary epithelium via a CCAAT/enhancer-binding protein delta-dependent pathway. *Mol Cancer Ther* **1**, 601-610 (2002).
311. Luyckx, V.A., Cairo, L.V., Compston, C.A., Phan, W.L. & Mueller, T.F. Oncostatin M pathway plays a major role in the renal acute phase response. *Am J Physiol Renal Physiol* **296**, F875-883 (2009).
312. Frangogiannis, N.G. Regulation of the Inflammatory Response in Cardiac Repair. *Circ Res* **110**, 159-173 (2012).
313. Liehn, E.A., Postea, O., Curaj, A. & Marx, N. Repair after myocardial infarction, between fantasy and reality: the role of chemokines. *J Am Coll Cardiol* **58**, 2357-2362 (2011).
314. Fredj, S., Bescond, J., Louault, C., Delwail, A., Lecron, J.C. & Potreau, D. Role of interleukin-6 in cardiomyocyte/cardiac fibroblast interactions during myocyte hypertrophy and fibroblast proliferation. *J Cell Physiol* **204**, 428-436 (2005).
315. Tsuruda, T., Jougasaki, M., Boerrigter, G., Huntley, B.K., Chen, H.H., D'Assoro, A.B., Lee, S.C., Larsen, A.M., Cataliotti, A. & Burnett, J.C., Jr. Cardiotrophin-1 stimulation of cardiac fibroblast growth: roles for glycoprotein 130/leukemia inhibitory factor receptor and the endothelin type A receptor. *Circ Res* **90**, 128-134 (2002).
316. Wang, F., Trial, J., Diwan, A., Gao, F., Birdsall, H., Entman, M., Hornsby, P., Sivasubramaniam, N. & Mann, D. Regulation of cardiac fibroblast cellular function by leukemia inhibitory factor. *J Mol Cell Cardiol* **34**, 1309-1316 (2002).
317. King, K.L., Lai, J., Winer, J., Luis, E., Yen, R., Hooley, J., Williams, P.M. & Mather, J.P. Cardiac fibroblasts produce leukemia inhibitory factor and endothelin, which combine to induce cardiac myocyte hypertrophy in vitro. *Endocrine* **5**, 85-93 (1996).
318. Calvieri, C., Rubattu, S. & Volpe, M. Molecular mechanisms underlying cardiac antihypertrophic and antifibrotic effects of natriuretic peptides. *J Mol Med (Berl)* **90**, 5-13 (2012).
319. Soffer, R.L., Das, M., Caldwell, P.R., Seegal, B.C. & Hsu, K.C. Biological and biochemical properties of angiotensin-converting enzyme. *Agents Actions* **6**, 534-537 (1976).
320. Caldwell, P.R., Seegal, B.C., Hsu, K.C., Das, M. & Soffer, R.L. Angiotensin-converting enzyme: vascular endothelial localization. *Science* **191**, 1050-1051 (1976).
321. Stross, C., Radtke, S., Clahsen, T., Gerlach, C., Volkmer-Engert, R., Schaper, F., Heinrich, P.C. & Hermanns, H.M. Oncostatin M receptor-mediated signal transduction is negatively regulated by SOCS3 through a receptor tyrosine-independent mechanism. *J Biol Chem* **281**, 8458-8468 (2006).
322. Croker, B.A., Krebs, D.L., Zhang, J.G., Wormald, S., Willson, T.A., Stanley, E.G., Robb, L., Greenhalgh, C.J., Forster, I., Clausen, B.E. *et al.* SOCS3 negatively regulates IL-6 signaling in vivo. *Nat Immunol* **4**, 540-545 (2003).
323. Alexander, W.S. Suppressors of cytokine signalling (SOCS) in the immune system. *Nat Rev Immunol* **2**, 410-416 (2002).
324. Sivko, G.S., Sanford, D.C., Dearth, L.D., Tang, D. & DeWille, J.W. CCAAT/Enhancer binding protein delta (c/EBPdelta) regulation and expression in human mammary epithelial cells: II. Analysis of activating signal transduction pathways, transcriptional, post-transcriptional, and post-translational control. *J Cell Biochem* **93**, 844-856 (2004).
325. Sivko, G.S. & DeWille, J.W. CCAAT/Enhancer binding protein delta (c/EBPdelta) regulation and expression in human mammary epithelial cells: I. "Loss of function" alterations in the c/EBPdelta growth inhibitory pathway in breast cancer cell lines. *J Cell Biochem* **93**, 830-843 (2004).
326. Alam, T., An, M.R. & Papaconstantinou, J. Differential expression of three C/EBP isoforms in multiple tissues during the acute phase response. *J Biol Chem* **267**, 5021-5024 (1992).
327. Tang, D., Sivko, G.S. & DeWille, J.W. Promoter methylation reduces C/EBPdelta (CEBPD) gene expression in the SUM-52PE human breast cancer cell line and in primary breast tumors. *Breast Cancer Res Treat* **95**, 161-170 (2006).
328. Niehof, M., Manns, M.P. & Trautwein, C. CREB controls LAP/C/EBP beta transcription. *Mol Cell Biol* **17**, 3600-3613 (1997).
329. McCarthy, T.L., Ji, C., Chen, Y., Kim, K.K., Imagawa, M., Ito, Y. & Centrella, M. Runt domain factor (Runx)-dependent effects on CCAAT/ enhancer-binding protein delta expression and activity in osteoblasts. *J Biol Chem* **275**, 21746-21753 (2000).

330. Descombes, P., Chojkier, M., Lichtsteiner, S., Falvey, E. & Schibler, U. LAP, a novel member of the C/EBP gene family, encodes a liver-enriched transcriptional activator protein. *Genes Dev* **4**, 1541-1551 (1990).
331. Chang, C.J., Chen, T.T., Lei, H.Y., Chen, D.S. & Lee, S.C. Molecular cloning of a transcription factor, AGP/EBP, that belongs to members of the C/EBP family. *Mol Cell Biol* **10**, 6642-6653 (1990).
332. Roman, C., Platero, J.S., Shuman, J. & Calame, K. Ig/EBP-1: a ubiquitously expressed immunoglobulin enhancer binding protein that is similar to C/EBP and heterodimerizes with C/EBP. *Genes Dev* **4**, 1404-1415 (1990).
333. Cao, Z., Umek, R.M. & McKnight, S.L. Regulated expression of three C/EBP isoforms during adipose conversion of 3T3-L1 cells. *Genes Dev* **5**, 1538-1552 (1991).
334. Williams, S.C., Cantwell, C.A. & Johnson, P.F. A family of C/EBP-related proteins capable of forming covalently linked leucine zipper dimers in vitro. *Genes Dev* **5**, 1553-1567 (1991).
335. Ron, D. & Habener, J.F. CHOP, a novel developmentally regulated nuclear protein that dimerizes with transcription factors C/EBP and LAP and functions as a dominant-negative inhibitor of gene transcription. *Genes Dev* **6**, 439-453 (1992).
336. Rorth, P. & Montell, D.J. Drosophila C/EBP: a tissue-specific DNA-binding protein required for embryonic development. *Genes Dev* **6**, 2299-2311 (1992).
337. Katz, S., Kowenz-Leutz, E., Muller, C., Meese, K., Ness, S.A. & Leutz, A. The NF-M transcription factor is related to C/EBP beta and plays a role in signal transduction, differentiation and leukemogenesis of avian myelomonocytic cells. *EMBO J* **12**, 1321-1332 (1993).
338. Kousteni, S., Kockar, F.T., Sweeney, G.E. & Ramji, D.P. Characterisation and developmental regulation of the Xenopus laevis CCAAT-enhancer binding protein beta gene. *Mech Dev* **77**, 143-148 (1998).
339. Chumakov, A.M., Grillier, I., Chumakova, E., Chih, D., Slater, J. & Koeffler, H.P. Cloning of the novel human myeloid-cell-specific C/EBP-epsilon transcription factor. *Mol Cell Biol* **17**, 1375-1386 (1997).
340. Xia, X., Li, Y., Huang, D., Wang, Z., Luo, L., Song, Y., Zhao, L. & Wen, R. Oncostatin M protects rod and cone photoreceptors and promotes regeneration of cone outer segment in a rat model of retinal degeneration. *PLoS One* **6**, e18282 (2011).
341. Sparks, J.D., Cianci, J., Jokinen, J., Chen, L.S. & Sparks, C.E. Interleukin-6 mediates hepatic hypersecretion of apolipoprotein B. *Am J Physiol Gastrointest Liver Physiol* **299**, 980-989 (2010).
342. Teerds, K.J., van Dissel-Emiliani, F.M., De Miguel, M.P., de Boer-Brouwer, M., Körting, L.M. & Rijntjes, E. Oncostatin-M inhibits luteinizing hormone stimulated Leydig cell progenitor formation in vitro. *Reprod Biol Endocrinol* **5**, 43 (2007).
343. David, E., Guihard, P., Brounais, B., Riet, A., Charrier, C., Battaglia, S., Gouin, F., Ponsolle, S., Bot, R.L., Richards, C.D. *et al.* Direct anti-cancer effect of oncostatin M on chondrosarcoma. *Int J Cancer* **128**, 1822-1835 (2011).
344. Brounais, B., David, E., Chipoy, C., Trichet, V., Ferre, V., Charrier, C., Duplomb, L., Berreur, M., Redini, F., Heymann, D. *et al.* Long term oncostatin M treatment induces an osteocyte-like differentiation on osteosarcoma and calvaria cells. *Bone* **44**, 830-839 (2009).
345. Brounais, B., Chipoy, C., Mori, K., Charrier, C., Battaglia, S., Pilet, P., Richards, C.D., Heymann, D., Rédini, F. & Blanchard, F. Oncostatin M Induces Bone Loss and Sensitizes Rat Osteosarcoma to the Antitumor Effect of Midostaurin In vivo. *Clinical Cancer Research* **14**, 5400-5409 (2008).
346. Pham Van, T., Couchie, D., Martin-Garcia, N., Laperche, Y., Zafrani, E.S. & Mavier, P. Expression of matrix metalloproteinase-2 and -9 and of tissue inhibitor of matrix metalloproteinase-1 in liver regeneration from oval cells in rat. *Matrix Biol* **27**, 674-681 (2008).
347. Walker, E.C., McGregor, N.E., Poulton, I.J., Solano, M., Pompolo, S., Fernandes, T.J., Constable, M.J., Nicholson, G.C., Zhang, J.G., Nicola, N.A. *et al.* Oncostatin M promotes bone formation independently of resorption when signaling through leukemia inhibitory factor receptor in mice. *J Clin Invest* **120**, 582-592 (2010).
348. Juan, T.S., Bolon, B., Lindberg, R.A., Sun, Y., Van, G. & Fletcher, F.A. Mice overexpressing murine oncostatin M (OSM) exhibit changes in hematopoietic and other organs that are distinct from those of mice overexpressing human OSM or bovine OSM. *Vet Pathol* **46**, 124-137 (2009).
349. Arnold, K., Bordoli, L., Kopp, J. & Schwede, T. The SWISS-MODEL workspace: a web-based environment for protein structure homology modelling. *Bioinformatics* **22**, 195-201 (2006).
350. Schwede, T., Kopp, J., Guex, N. & Peitsch, M.C. SWISS-MODEL: An automated protein homology-modeling server. *Nucleic Acids Res* **31**, 3381-3385 (2003).

351. Guex, N. & Peitsch, M.C. SWISS-MODEL and the Swiss-PdbViewer: an environment for comparative protein modeling. *Electrophoresis* **18**, 2714-2723 (1997).
352. Kallen, K.J., Grotzinger, J., Lelievre, E., Vollmer, P., Aasland, D., Renne, C., Mullberg, J., Myer zum Buschenfelde, K.H., Gascan, H. & Rose-John, S. Receptor recognition sites of cytokines are organized as exchangeable modules. Transfer of the leukemia inhibitory factor receptor-binding site from ciliary neurotrophic factor to interleukin-6. *J Biol Chem* **274**, 11859-11867 (1999).
353. Wallace, P.M., MacMaster, J.F., Rouleau, K.A., Brown, T.J., Loy, J.K., Donaldson, K.L. & Wahl, A.F. Regulation of inflammatory responses by oncostatin M. *J Immunol* **162**, 5547-5555 (1999).
354. Langdon, C., Kerr, C., Hassen, M., Hara, T., Arsenault, A.L. & Richards, C.D. Murine oncostatin M stimulates mouse synovial fibroblasts in vitro and induces inflammation and destruction in mouse joints in vivo. *Am J Pathol* **157**, 1187-1196 (2000).
355. Plater-Zyberk, C., Buckton, J., Thompson, S., Spaull, J., Zanders, E., Papworth, J. & Life, P.F. Amelioration of arthritis in two murine models using antibodies to oncostatin M. *Arthritis Rheum* **44**, 2697-2702 (2001).
356. Yoshimura, A., Ichihara, M., Kinjyo, I., Moriyama, M., Copeland, N.G., Gilbert, D.J., Jenkins, N.A., Hara, T. & Miyajima, A. Mouse oncostatin M: an immediate early gene induced by multiple cytokines through the JAK-STAT5 pathway. *EMBO J* **15**, 1055-1063 (1996).
357. Catt, K.J., Mendelsohn, F.A., Millan, M.A. & Aguilera, G. The role of angiotensin II receptors in vascular regulation. *J Cardiovasc Pharmacol* **6 Suppl 4**, S575-586 (1984).
358. Lijnen, P. & Petrov, V. Antagonism of the renin-angiotensin system, hypertrophy and gene expression in cardiac myocytes. *Methods Find Exp Clin Pharmacol* **21**, 363-374 (1999).
359. Baumann, H., Wang, Y., Richards, C.D., Jones, C.A., Black, T.A. & Gross, K.W. Endotoxin-induced renal inflammatory response. Oncostatin M as a major mediator of suppressed renin expression, in *J Biol Chem*, Vol. 275 22014-22019 (2000).
360. Pan, L., Wang, Y., Jones, C.A., Glenn, S.T., Baumann, H. & Gross, K.W. Enhancer-dependent inhibition of mouse renin transcription by inflammatory cytokines, in *Am J Physiol Renal Physiol*, Vol. 288 117-124 (2005).
361. Hingorani, A.D. & Casas, J.P. The interleukin-6 receptor as a target for prevention of coronary heart disease: a mendelian randomisation analysis, in *Lancet*, Vol. 379 1214-1224 (2012).
362. Sarwar, N., Butterworth, A.S., Freitag, D.F., Gregson, J., Willeit, P., Gorman, D.N., Gao, P., Saleheen, D., Rendon, A., Nelson, C.P. *et al.* Interleukin-6 receptor pathways in coronary heart disease: a collaborative meta-analysis of 82 studies, in *Lancet*, Vol. 379 1205-1213 (2012).
363. Betz, U.A., Bloch, W., van den Broek, M., Yoshida, K., Taga, T., Kishimoto, T., Addicks, K., Rajewsky, K. & Müller, W. Postnatally Induced Inactivation of gp130 in Mice Results in Neurological, Cardiac, Hematopoietic, Immunological, Hepatic, and Pulmonary Defects. *J Exp Med* **188**, 1955-1965 (1998).
364. Drechsler, J., Grötzinger, J. & Hermanns, H.M. Characterization of the Rat Oncostatin M Receptor Complex Which Resembles the Human, but Differs from the Murine Cytokine Receptor. *PLoS One* **7**, e43155 (2012).

Acknowledgements

Firstly, I take the opportunity to thank PD Dr. Heike Hermanns for giving me the chance to work in her group. I would not have achieved this degree without Heike who provided scientific and financial support, let me participate in her expertise and argumentation. Furthermore, presentation of my results on international conferences, initiation of cooperations, the OSM paper, correction of the thesis and generation of so many experiments only beared fruit, because Heike played a decisive role in discussing the data, initiating projects and pointing a way forward. I cannot abnegate that I have seen and learned so many important things during the last four years in this lab, for which I would like to extend my sincere thanks.

I also want to thank Prof. Dr. Stefan Engelhardt for supporting the early concept of the heart issue, for applying to be my second supervisor and for his interest in the stadium of the developing results.

I like to express my deep gratitude to Prof. Dr. Manfred Lutz for applying to be my third supervisor and for the beneficial and pleasant discussions during the annual reports.

I particularly want to thank all my present and former lab members and colleagues (Daniela Kraemer, Dr. Christine Mais, Dr. Christoph Hintzen, Carmen Schäfer, Sabine Walter, Julia Erb, Christiane Erb and Christoph Groß) for the support, the technical help, the joint ventures, the familiar atmosphere and particularly for the essential and helpful discussions. It was always a great pleasure to discuss our data, possible explanations and future plans with my colleagues.
Importantly, I like to thank Christine Mais for her great help with the cardiomyocytes, the receptor cloning, the thesis correction, all the smoking breaks and her patience.
Furthermore, I want to thank my Hiwi Anna Uri for doing so many experiments with such an extraordinary good performance.

A great word of thanks goes to the working group of Stefan Engelhardt. Claudia Jentzsch and Simon Leierseder, in particular, patiently supported me by developing and analysing the cardiomyocyte hypertrophy assays finally allowing the visualisation and quantification of the suggested/analysed effects. I also want to thank Nadine Yurdagül-Hemmrich for all the help with the cardiomyocyte preparation.

I want to thank Martin Busch, Miriam Koch und Dr. Helga Manthey for the kind lab neighbourhood and the evenings which we shared.

Additionally, I like to thank Dr. Ana Costa-Pereira and Nair Bonito from the Imperial College (London, UK) for the very interesting cooperation that highlights a complete new side of the ERK proteins, which ultimately might be of great interest for the scientific world of signal transduction.

In particular, I would like to express all my thanks to my girlfriend Christine. I truly believe that I would not have completed this path without her. She gave me all her patience and listened to me. Your love and positive attitude to life really improve each day. I wholeheartedly thank you for being as you are!

Last but not least, I like to thank my parents. Without supporting me from earliest childhood, encouraging me and trusting in me, this thesis and the corresponding work would not have been completed. I would like to sincerely thank you for your patience and love!

Danksagungen

Zu allererst möchte ich die Gelegenheit ergreifen, PD Dr. Heike Hermanns dafür zu danken, dass sie mir die Chance gab, in ihrer Gruppe zu arbeiten. Ohne Heike, die mir wissenschaftliche und finanzielle Unterstützung zukommen ließ, mich an ihrem wissenschaftlichen Sachverstand und ihren Schlussfolgerungen teilhaben ließ, hätte ich diesen Grad niemals erreichen können. Des Weiteren spielte Heike eine ganz entscheidende Rolle bei der Präsentation meiner Ergebnisse auf internationalen Konferenzen, dem Initiieren von Kooperationen, dem OSM *paper*, der Korrektur meiner Doktorarbeit und der Planung so vieler Experimente, indem sie die Daten mit mir diskutierte, Projekte auf den Weg brachte und mir stets einen möglichen Weg aufzeigte. Ich kann definitiv nicht leugnen, dass ich so viele wichtige Dinge, für die ich äußerst dankbar bin, in den letzten vier Jahren in diesem Labor gesehen und gelernt habe.

Außerdem möchte ich Prof. Dr. Stefan Engelhardt dafür danken, dass er die frühe Konzeption des Herz-Projekts nachhaltig unterstützt hat, sich als mein zweiter *supervisor* anbot und ferner stets großes Interesse an der Phase des sich entwickelnden Projekts zeigte.

Meinen tief empfundenen Dank möchte ich auch Prof. Dr. Manfred Lutz dafür aussprechen, dass er sich als mein dritter *supervisor* anbot und meine Arbeit durch seine hilfreiche und angenehme Art des Diskutierens positiv beeinflusste.

Besonders möchte ich meinen momentanen und ehemaligen Labor-Mitgliedern und Kollegen (Daniela Kraemer, Dr. Christine Mais, Dr. Christoph Hintzen, Carmen Schäfer, Sabine Walter, Julia Erb, Christiane Erb und Christoph Groß) für deren Unterstützung, technische Hilfe, gemeinsame Unternehmungen, die familiäre Atmosphäre und ganz speziell für die essentiellen und hilfreichen Diskussionen bedanken. Es war mir stets ein großes Vergnügen, unsere Ergebnisse, mögliche Erklärungsansätze und Zukunftspläne mit meinen Kollegen zu diskutieren.
Ganz besonders möchte ich mich bei Christine Mais für die riesige Hilfe mit den Kardiomyozyten, der Rezeptor-Klonierung, der Korrektur dieser Arbeit und ihrer Geduld mit mir bedanken.
Des Weiteren richte ich ein Wort des Dankes an meine Hiwi Anna Uri, welche so viele Experimente auf wirklich vortreffliche Weise durchgeführt hat.

Auch der Arbeitsgruppe von Stefan Engelhardt schulde ich großen Dank. Es waren im Besonderen Claudia Jentzsch und Simon Leierseder, die mich bei der Entwicklung und Analyse der Kardiomyozyten Hypertrophie Experimente, welche letztlich die Visualisierung und die Quantifizierung der vermuteten/analysierten Effekte ermöglichten, mit viel Geduld unterstützten. Ich möchte zusätzlich Nadine Yurdagül-Hemmrich für all die Mühe mit der Kardiomyozyten-Isolation danken.

Ich danke Martin Busch, Miriam Koch und Dr. Helga Manthey für die nette Labor-Nachbarschaft und die Abende, die wir miteinander verbringen durften.

Außerdem möchte ich mich bei Dr. Ana Costa-Pereira und Nair Bonito vom *Imperial College* (London, UK) für die äußerst interessante Kooperation bedanken, innerhalb welcher eine gänzlich neue Seite der ERK Proteine beleuchtet wurde, was schließlich in der Wissenschaftswelt der Signaltransduktion von größtem Interesse sein dürfte.

Besonderen Dank möchte ich meiner Freundin Christine aussprechen. Ich glaube in der Tat, dass ich diesen Weg ohne sie nicht hätte vollenden können. Sie hat mir stets ihre ganze Geduld und ihr Gehör entgegengebracht. Deine Liebe und deine positive Lebenseinstellung verschönern mir jeden Tag und ich danke dir von ganzem Herzen, dass du bist wie du bist!

Zum Schluss will ich meinen Eltern danken. Ohne euer Vertrauen, die Fähigkeit mich aufzubauen und die Förderung von Kindesbeinen an, würde es weder diese Doktorarbeit noch die dazugehörigen Studien geben. Ich danke euch von ganzem Herzen für eure Liebe und Geduld!

Affidavit

I hereby confirm that my thesis entitled “Determination of the hypertrophic potential of Oncostatin M on rat cardiac cells and the characterisation of the receptor complexes utilised by rat Oncostatin M“ is the result of my own work. I did not receive any help or support from commercial consultants. All sources and / or materials applied are listed and specified in the thesis.

Furthermore, I confirm that this thesis has not yet been submitted as part of another examination process neither in identical nor in similar form.

Würzburg, 11.09.12 _____

Eidesstattliche Erklärung

Hiermit erkläre ich an Eides statt, die Dissertation „Erforschung des hypertrophen Potentials von Oncostatin M auf Ratten-Herzzellen und die Charakterisierung der Rezeptorkomplexe, welche von Ratten-Oncostatin M genutzt werden“ eigenständig, d.h. insbesondere selbständig und ohne Hilfe eines kommerziellen Promotionsberaters, angefertigt und keine anderen als die von mir angegebenen Quellen und Hilfsmittel verwendet zu haben.

Ich erkläre außerdem, dass die Dissertation weder in gleicher noch in ähnlicher Form bereits in einem anderen Prüfungsverfahren vorgelegen hat.

Würzburg, 11.09.12 _____